A systematic revision of the genus *Prognathodon* (Squamata: Mosasauridae)

by

Sydney Rhode Mohr

A thesis submitted in partial fulfillment of the requirements for the degree of

Doctor of Philosophy

in

Systematics and Evolution

Department of Biological Sciences
University of Alberta

ABSTRACT

Mosasaurs are an extinct group of large aquatic lizards that swam the world's oceans during the late Cretaceous, approximately 94 to 66 million years ago. The genus *Prognathodon* is a diverse subgroup of medium to large-sized mosasaurs with a unique set of features that have made it difficult for researchers to classify amongst other major mosasaurs groups. Furthermore, multiple analyses attempting to classify *Prognathodon* typically find highly inconsistent patterns of relationship and often part of a poorly resolved clade comprising of other mosasaur genera. A critical examination of the historical conceptualization of *Prognathodon* finds a series of recurring issues in the diagnoses and descriptions of both the type species and referred taxa, underpinning the need for a broad systematic reassessment of the group. A detailed re-evaluation of type species, *Prognathodon solvayi*, recognizes several newly identified osteological characters and provided a precise diagnosis that established a well-defined and informative concept of the taxon. A comparison between the emended diagnosis and the morphological characteristics of six referred species forms hypotheses as to their validity as members within *Prognathodon*. A single species, *Prognathodon giganteus*, bears strong enough resemblance to warrant synonymizing it with the type species. All other taxa deviate from the generic diagnosis to a great enough degree that supported their exclusion from the group. A phylogenetic analysis further tests these assumptions by incorporating a set of updated and new data based on the morphological assessment of *Prognathodon*. The resulting trees both recover *Prognathodon solvayi* as the sole member of the genus *Prognathodon* and support the referral of *Prognathodon giganteus* to the type species. Informed by morphological comparisons, the remaining referred taxa that fell outside *Prognathodon* were assigned to different genera. Although precisely how *Prognathodon* fits into the larger context of other major mosasaur groups remains unclear, the

integration between a comprehensive morphological review and phylogenetic analysis nevertheless provided a coherent model of the genus and improved understanding of the internal systematic relationships of the group as a whole.

PREFACE

This thesis is an original work by Sydney Rhode Mohr. No portions of this document have been previously published.

ACKNOWLEDGEMENTS

Firstly, to my supervisor Michael Caldwell: thank you for taking me under your wing (or maybe, secondarily aquatic flipper), continually guiding me in my research and for coming up with brilliant solutions to every problem I encountered. Additionally, thank you for your patience as you sit eagerly awaiting the submission of this dissertation.

Thank you as well to my committee members C. Sullivan, and R. Nydam for their insightful comments and advice. A further thank you to C. Sullivan for providing a multitude of reference letters! J. Anderson and J. Acorn also offered numerous invaluable comments and recommendations that I am extremely grateful for.

I would also like to thank the following people: B. Strilisky (TMP), N. Fox (SDSMT), A. Folie and colleagues (IRSNB), N-E. Jalil (MNHN), J. Jagt and colleagues (NHMM) for their hospitality and assistance with specimen access, as well as E. Mulder, for his help in interpreting *P. saturator* and for his excellent, interesting conversations over lunch.

Thank you to my colleagues A. LeBlanc and T. Konishi for their mentoring, training, and advice. Thank you as well to my former and current lab mates, H. Sharpe, M. Campbell, T. Simoes, H. Street, and I. Paparella. A particular thank you to M. Powers and O. Vernygora for their assistance in my phylogenetic analyses.

To my very special friends, J. Acorn, who continues to provide the most amazing, thoughtful conversations and fantastic stories about interesting topic under the sun (although I've never been there…). I am forever looking forward to the next birding trip, maybe with some corixid-stopping along the way. To C. Charchuk, your friendship has kept me sane through some tumultuous times, and you make me a better, smarter, braver person. To C. Hales, the finest gent that ever gented, thank you for always being ready for a quick conversation, your wonderful

Christmas letters, sending me top quality Instagram reels that always managed to make me laugh, and for being my forever fren.

To my Mom and Dad, and my family and friends, thank you for always believing in me and supporting me every step of the way. A heartfelt thank you to C. and D. Evans for their unyielding support and belief in my abilities.

To C. Douglas, who means the absolute world to me. Thank you for being ready to help at a moment's notice, and for your constant reassurance. Also, thank you to Porter the Doggo, who sat by quietly as I did my candidacy exam on my couch, and for being my loving dog-shaped shadow; I'll miss you forever.

Finally, I would like to thank the various organizations who were instrumental in supporting me throughout my studies. These include NSERC, Alberta Lottery Fund, Alberta Historical Resources Foundation, and the University of Alberta.

TABLE OF CONTENTS

LIST OF TABLES

Chapter 5

LIST OF FIGURES

Chapter 2

Figure:

Chapter 3

Figure:

Chapter 4

Figure:

Chapter 5

Figure:

Chapter 6

Figure:

Chapter 7

INSTITUTIONAL ABBREVIATIONS

ALMNH PV, Alabama Museum of Natural History, Tuscaloosa, Alabama, USA;

AMNH, American Museum of Natural History, New York, USA

BMNH, British Museum of Natural History, London, UK;

CM, Canterbury Museum, Christchurch, New Zealand;

FMNH PR, Field Museum of Natural History, Chicago, Illinois, U.S.A.;

IRSNB, Institut Royal des Sciences Naturelles de Belgique, Brussels, Belgium;

KU, The University of Kansas Natural History Museum, Lawrence, Kansas, USA;

MGUAN, Museo Geológico da Universidade Agostino Neto, Luanda, Angola;

MNHN, Muséum National d'Histoire Naturelle, Paléontologie, Paris, France;

NHMM, Natuurhistorisch Museum Maastricht, Maastricht, The Netherlands;

OCP DEK/GE, Office Chérifien des Phosphates, Collection de Paléontologie, Centre Minier de Khouribga, Khouribga, Morocco;

SDSMT, South Dakota School of Mines and Technology, Rapid City, South Dakota, USA;

TMP, Royal Tyrrell Museum of Palaeontology, Drumheller, Alberta, Canada;

UALVP, University of Alberta Laboratory for Vertebrate Paleontology, Edmonton, Alberta, Canada

ANATOMICAL ABBREVIATIONS

Due to the large number of figures and figure labels, a list of anatomical abbreviations is provided within the figure captions.

CHAPTER 1. INTRODUCTION

INTRODUCTION TO *PROGNATHODON*

Mosasaurs were a diverse but relatively short-lived group of secondarily aquatic squamates that achieved a worldwide distribution before going extinct at the end of the Late Cretaceous (94 to 66 million years ago). The first mosasaur fossils were discovered near Maastricht, the Netherlands between the 1760's and 1780's (Cuvier, 1808) and were central to the early development of the initially radical notions of extinction. Today, there are roughly 60 recognized species, most of which are assigned to one of three major mosasaur groups. These include the Halisaurinae, Russellosaurina, and the Mosasaurinae (Bell, 1997; Bell and Polcyn, 2005; Simões et al. 2017a).

The genus *Prognathodon* Dollo, 1889a was a group of medium to large-sized mosasaurine mosasaurs typically characterized as having large, robust skulls; some of which reached well over a meter in length (Russell, 1967; Bell, 1997; Lingham-Soliar and Nolf, 1989; Dortangs et al. 2002, Christiansen and Bonde, 2002; Konishi et al. 2011). Currently including around a dozen species, *Prognathodon* occurred from the late Campanian to the late Maastrichtian and is derived from marine sediments in North America, Europe, New Zealand, Africa, and the Middle East (Lingham-Soliar and Nolf, 1989; Konishi et al. 2011). The type species, *Prognathodon solvayi*, was recovered from the Ciply Phosphatic Chalks in the Solvay quarry in Belgium. The type specimen consisted of a well-preserved skull, disarticulated vertebrae, and a partial pectoral girdle. A short description was provided soon after that emphasized its strongly procumbent teeth and lack of a predental rostrum, distinct features for which it was named (Dollo, 1889b). Curiously, the genus was renamed *Prognathosaurus* by Dollo (1889b) for unspecified reasons, which was maintained for decades until it was restored by Russell (1967). During this time,

Dollo (1904) provided no anatomical description but assigned an apt name to a newly discovered and much larger specimen from the Solvay quarry, *Prognathosaurus giganteus*. Apart from this newly assigned species, *P. giganteus* and *P. solvayi* would remain essentially untouched until Russell's (1967) broad systematic review of American mosasaurs. Neither *P. solvayi* nor *P. giganteus* were discussed in specific detail, as Russell (1967) instead based his generic diagnosis of *Prognathodon* on American taxa, namely *Brachysaurus overtoni* Williston, 1897; *Liodon crassartus* Cope, 1871b, and *Macrosaurus laevis*, Leidy, 1865, all of which he transferred to *Prognathodon*.

With this work Russell (1967) established the concept of the genus *Prognathodon* as it is understood today, with *Prognathodon overtoni, Prognathodon crassartus,* and *Prognathodon rapax* forming the basis the first generic diagnosis, with only fleeting reference to their European counterparts (Russell, 1967). They were assigned to the Prognathodontini and described as belonging to the Plioplatecarpinae, a large subgroup within the Russellosaurina , but were unique in having robust jaws and teeth. Shortly after this study, Welles and Gregg (1971) described a highly fragmented specimen from The Middle Waipara River in New Zealand and named it *Prognathodon waiparensis*, in large part due to the fusion between the suprastapedial and infrastapedial processes of the quadrate.

Lingham-Soliar and Nolf (1989), a century after *Prognathodon* was first named, provided the first detailed description of *P. solvayi* and *P. giganteus* and echoed Russell (1967) in recounting the massively built cranial elements in both taxa. *Prognathodon crassartus* was referred to the genus *Plioplatecarpus* in the same paper.

Prognathodon would remain as a plioplatecarpine until Bell (1997), wherein a broad phylogenetic analysis would firmly establish the major mosasaur subgroups as they are

understood today. Relying again solely on the North American species *Prognathodon overtoni* and *Prognathodon rapax* to represent the genus, Bell's (1997) analysis found the two species paraphyletic with respect to *Plesiotylosaurus crassidens*, with which they formed a sister clade to *Globidens*, a group of medium-sized mosasaurs with unique rounded and stout dentition seemingly specialized for durophagy (Leblanc et al. 2019). This group was referred to as the Globidensini, defined in large part by the presence of fused suprastapedial and infrastapedial processes of the quadrate.

Following this, three new large taxa were described and referred to the genus *Prognathodon* in quick procession: *Prognathodon stadtmani* Kass, 1999, *Prognathodon currii* Christiansen & Bonde, 2002; and *Prognathodon saturator* Dortangs et al. 2002. Despite having fused processes of the quadrate, *P. stadtmani* was otherwise dissimilar from and did not form a monophyletic clade with *Prognathodon*, eventually resulting in its referral to a new genus, *Gnathomortis* (Lively, 2020). *Prognathodon currii* and *P. saturator* were represented primarily by cranial material and were huge animals with robust teeth and massively built skulls reaching over a meter in length. Both have fused suprastapedial and infrastapedial processes of the quadrate, and both were found to be closely related to *P. solvayi* following phylogenetic analysis. The concept of the Globidensini was also supported by these results.

Prognathodon kianda Schulp et al. 2008 from Angola is one of the more recent species to be assigned to the genus but is currently known from mostly fragmentary cranial material–a common trend within the genus. Using features of the dentition and an aspect ratio analysis comparing tooth shape across the jaw, three species of *Liodon* (*L. compressidens* Gaudry, 1892, *L. mosasauroides* Gaudry, 1892, and *L. sectorius* Cope, 1871) were also transferred to *Prognathodon* because of reported similarities with *P. kianda*. Shortly after, *Prognathodon*

hashimi Kaddumi, 2009 and *Prognathodon hudae* Kaddumi, 2009 from Jordan were referred to the genus. *Prognathodon hashimi* was transferred from *Tenerasaurus* and is one of the few (if not the only) species in the genus to not have any associated cranial material. Its referral was instead largely based off other taxa that preserve large portions of their vertebral column, pectoral girdle, pelvic girdle, and hindlimbs (i.e. *P. overtoni*, Konishi et al. 2011). The specimen itself exhibits remarkable preservation, retaining soft tissue impressions throughout its length, including a caudal fin (Lindgren et al. 2018). *Prognathodon hudae,* on the other hand, is named from a right and left dentary, and may have been referred based on comparisons with *P. kianda* and *Liodon*. *Prognathodon lutugini* Yakovlev, 1901, a specimen even more fragmented than most representatives of *Prognathodon*, was transferred from *Dollosaurus* Yakovlev, 1901 by Grigoriev (2013) based on its pterygoid and previous reports that it had procumbent teeth and lacked a rostrum. Lastly, numerous isolated teeth attributed to *Prognathodon* have been reported from various locations in Europe and the Middle East (Bardet et al. 1997; Bardet et al. 2000; Bardet and Superbiola, 2002), although some of these identifications were questioned based on differences betwee to the type species (Lindgren 2005).

PURPOSE OF STUDY

All assigned members of *Prognathodon* that preserve a quadrate exhibit fused suprastapedial and infrastapedial processes, and a number have a large, robustly built skull with stout teeth. Despite these apparently shared characteristics, ingroup relationships within *Prognathodon* have become unstable since more taxa began to be included in the early to mid 2000's. In several recent studies, different species of *Prognathodon* often place separately alongside different genera, or forms an unresolved polytomy, rendering both the genus and

Globidensini as paraphyletic (LeBlanc et al. 2013, Street, 2017; Simões et al. 2017a; Lively, 2020; Strong et al. 2020; Longrich et al. 2022; Zietlow et al. 2023). *Prognathodon kianda* is consistently recovered in a separate, basal position relative to multiple other taxa, with the exception of *Clidastes* (LeBlanc et al. 2013, Simões et al. 2017a). Furthermore, purportedly diagnostic characters of the Globidensini, such as fused suprastapedial and infrastapedial processes of the quadrate, were described in taxa other than *Prognathdoon* and *Globidens*, including *Plesiotylosaurus* and *Eremisasaurus* (Lindgren, 2009; Leblanc et al. 2013), calling into question whether these traits have utility in defining more inclusive groups or providing resolution to problematic clades in phylogenetic analysis. Following these conflicting results, several workers have pointed out the need and called for a critical review of the genus *Prognathodon* (Leblanc et al. 2013, Konishi et al. 2011; Lively, 2020; Longrich et al. 2022).

The ultimate aim of this study is to provide a revised model and improved understanding of the evolutionary relationships of *Prognathodon* by determining which morphological traits define the group and how they are distributed across assigned species. This will involve a rigorous and critical evaluation of *Prognathodon* that includes detailed and direct comparisons between multiple species to specifically address the question of which belong to the genus. Detailed comparisons between referred taxa and a robust diagnosis of *Prognathodon* based on a set of discrete morphological features will assess the validity of assigned species and resolve their respective interrelationships, as well as potentially identify new characters that can better define the genus. With a primary focus on systematics and taxonomy, this study has particular significance for future work describing and assigning new fossil specimens, and ultimately has broader implications for understanding the evolutionary relationships and history of mosasaurs as a whole.

Notes on included taxa

Due to a variety of circumstances, several *Prognathodon* species were not observed directly in person. These include *Prognathodon currii,* Christiansen & Bonde, 2002, *Prognathodon hashimi* Kaddumi, 2009, *Prognathodon hudae* Kaddumi, 2009, *Prognathodon kianda,* Schulp et al. 2008, *Prognathodon lutugini* Yakovlev, 1901, *Prognathodon rapax* Hay, 1902, and *P. waiparensis* Welles & Gregg, 1971. Many were examined using photographs and notes taken by other colleagues, and/or their original descriptions, and are dealt with in more detail in Chapter 8.

INTRODUCTION TO THE CHAPTERS

Chapter 2

As the first of five anatomical chapters, this section provides a detailed redescription of the holotype of *Prognathodon solvayi*. An emended generic and species diagnosis is constructed based on the holotype and two referred specimens. This is followed by a review of historical interpretations of *P. solvayi* in attempt to identify potential root causes of the issues surrounding the genus, as well as an overview and assessment of the groups original referral to the Plioplatecarpinae.

Chapter 3

The second anatomical chapter details the first comparative assessment of a referred taxon, which involves the redescription of the holotype of *Prognathodon giganteus*. This is cross-referenced with the revised diagnoses formulated in Chapter 2 and compared to both the

holotype of *P. solvayi* and the two referred specimens. This information provides a taxonomic hypothesis concerning the validity of *P. giganetus*.

Chapter 4

This third anatomical chapter provides an extensive redescription of *P. saturator* that involves an evaluation of previous descriptions and the addition of previously undescribed elements of the braincase and postcranium. A direct comparison with the emended diagnosis from Chapter 2 informs taxonomic inferences made with respect to *Prognathodon*.

Chapter 5

This chapter describes a new specimen of *Prognathodon overtoni* and compares it to the holotype and referred material, and a performs a short analysis to assesses any osteological differences that may result from ontogeny. As with the previous two chapters, this description is used to briefly compare the anatomy of *P. overtoni* with the type species and emended diagnosis in order to evaluate its validity within the group.

Chapter 6

Liodon represents a collection of highly fragmentary named specimens and no clear consensus on their taxonomic affinities, despite recently being assigned to *Prognathodon.* The validity of these species and possible referrals are discussed following a detailed description of three specimens and a comparison against the revised diagnosis of *Prognathodon*.

Chapter 7

This chapter tests the taxonomic inferences formed from the preceding morphological comparisons. A character list compiled by previous workers is revised by correcting character scorings of multiple taxa and adding new characters based on morphological data derived from Chapters 2 through 6. A phylogenetic analysis assesses the in- and outgroup relationships of *Prognathodon*. The utility of characters typically used to define *Prognathodon*, namely the fusion of the suprastapedial and infrastapedial processes of the quadrate, is discussed within the context of these results.

Chapter 8

This chapter performs a broad systematic and taxonomic revision of the genus *Prognathodon* based on the combined results of the phylogenetic analysis and hypotheses generated from morphological comparisons in Chapters 2 through 6. Species removed from *Prognathodon* are assigned new generic and/or specific epithets, providing an amended and clearly defined concept of *Prognathodon*.

CHAPTER 2. REDESCRIPTION AND REDIAGNOSIS OF *PROGNATHODON SOLVAYI*

INTRODUCTION

The first account of *Prognathodon solvayi* appears in Dollo (1889a) in a list of fossil acquisitions to the Institut Royal des Sciences Naturelles de Belgique (IRSNB) in Bruxelles, Belgium. The holotype (IRSNB R33 (previously 4672)) came from the Solvay quarry at Mesvin (Lingham-Soliar and Nolf, 1989), which is dominated by the lower Maastrichtian Ciply Phosphatic Chalk (Robaszynski and Christensen, 1989). It is not known where in the section the specimen was recovered. Soon after, Dollo (1889b) provided a somewhat limited description of *Prognathodon solvayi*, focusing primarily on, and naming it for, its protruding front teeth and a premaxilla that was "absolutely deprived of a rostrum" (pp. 214). An account of certain elements present or missing from the specimen (e.g., preserved sclerotic ring, but lacking a sacrum and interclavicle), as well as a few largely uninformative features (e.g., a large triangular frontal, lateral orbits, prefrontal and postorbitofrontal forming the upper margin of the orbit, meeting at a point) were also incorporated into the description. Dollo (1889b) unofficially or mistakenly renamed the genus from *Prognathodon* to *Prognathosaurus*, which was repeated by Dollo (1890) and Kuhn (1939) who both made only brief mention of the genus in a list of known fossil taxa. The name *Prognathodon* was restored by Russell (1967), whose study was one of the first serious attempts at classifying the genus, although no formal description or diagnosis of *P. solvayi* was provided. He referred three North American taxa to the group, including *Prognathodon overtoni*, *Prognathodon crassartus,* and *Prognathodon rapax* (Russell, 1967). The resulting generic diagnosis consisted of a combination of characters derived from Dollo's

(1889b) description and those observed in the three referred North American taxa. At this time, the tribe Prognathodontini was erected and included within the Plioplatecarpinae (Russell, 1967).

No studies examined the type material of *P. solvayi* after Dollo's (1889) description for a century after its initial description, until Lingham-Soliar and Nolf (1989) published a comprehensive analysis of the holotype. They also recharacterize *Prognathodon giganteus*, IRSNB 0106, a large specimen named by Dollo (1904). The authors also cited two referred specimens of *P. solvayi* added to the IRSNB collections following the acquisition of the holotype. IRSNB 0107 was recovered from the same quarry as the holotype, whereas IRSNB 0108 was found a distance away in the Houzeau quarry at Spiennes. Both consist primarily of very fragmented cranial material and did not receive an in-depth evaluation at the time.

The inclusion of *Prognathodon* within the Plioplatecarpinae was maintained by Lingham-Solar and Nolf (1989). Although no direct morphological comparisons were provided, they suggested that *P. solvayi* was intermediate between *Platecarpus curtirostris* (now *Platecarpus tympaniticus*, Konishi et al. 2011) and younger *Prognathodon* species. This model persisted until Bell (1997) performed a taxonomic reassessment that resulted in the placement of *Prognathodon* within the Mosasaurinae. Like Russell (1967), Bell (1997) referenced North American representatives of the genus only, namely *P. overtoni* and *P. rapax* (two isolated quadrates) and did not discuss the holotype specimen. Conrad (2008) used the descriptions of *P. solvayi* as given by Russell (1967) and Lingham-Soliar and Nolf (1989), once again recovering *Prognathodon* within the Plioplatecarpinae. A subsequent comprehensive morphological evaluation by Konishi et al. (2011) found considerable support for the inclusion of *Prognathodon* within the Mosasaurinae, specifically the Globidensini. Several subsequent phylogenetic analyses found support for the same hypothesis (Schulp et al. 2008, Leblanc et al., 2012; Madzia

and Cau, 2017; Simoes et al. 2017; Lively, 2020; Longrich et al. 2022). However, some of these studies also cast doubt on the monophyly of the genus (Madzia and Cau, 2017; Simoes et al. 2017, Lively, 2020).

The historical and long-standing inconsistencies regarding the taxonomic relationships within *Prognathodon* and between the broader Mosasauridae underscores the need for an extensive reassessment of the type species. This study provides a revised description and diagnosis of *P. solvayi*, as well as a descriptive comparison between the holotype, IRSNB 0107, and IRSNB 0108 in order to confirm their referral to the species. Finally, the ramifications of the updated diagnosis and how they impact our current understanding of the genus as a whole are discussed with respect to previous conceptions and approaches towards *P. solvayi* in previous studies.

MATERIALS AND METHODS

IRSNB R33, IRSNB 0107, IRSNB 0108 were photographed using a Nikon D500 camera with a Nikkor AF-S 50 mm lens and a Google Pixel 2 smartphone. Photographs were processed and figures produced in Adobe Photoshop CS6 and Adobe Photoshop 24.6.0. Several cranial elements of IRSNB R33 could not easily be removed from the mount without potentially damaging both the mount itself and particularly thin, fragile bones; therefore, by necessity certain figures include parts of the mount and associated elements. Line drawings were traced from photographs and stippled using a Wacom Intuos pro pen tablet.

DESCRIPTION

Cranium

Skull—The skull is the most complete and well-preserved component of IRSNB R33 (Fig. 2.1). Laterally, the outer margins of the jaws are rounded in appearance and roughly 60 cm in length (Dollo, 1889b; Lingham-Soliar and Nolf, 1989). In dorsal aspect the skull is broad posteriorly with a short temporal arcade and a gradually tapering snout, which is also short relative to other taxa, such as *Mosasaurus* (Street and Caldwell, 2017). The orbits are proportionately large. The bone surface on most of the cranial elements appear worn or abraded, which Lingham-Soliar and Nolf (1989) observed as typical for mosasaur remains found in the Ciply Phosphatic Chalk. The left elements on the skull generally appear more weathered than those on the right.

Premaxilla—In IRSNB R33, a predental rostrum is virtually absent and instead terminates at the first set of premaxillary teeth (Fig. 2.1, Fig. 2.2A). In dorsal view, the anterior-most end is blunt and rounded. The dorsal surface is flat with lateral edges that slope shallowly from the first two tooth positions. The anterior section of the premaxillary-maxillary suture of *P. solvayi* is described by Konishi et al. (2011) as weakly sinusoidal, although the suture appears largely straight in lateral view in *P. solvayi* due to the anterior edge of the maxilla slightly overlapping the suture when viewed in articulation. Dorsally, the margins form a convexity, possibly to accommodate the alveoli, with a small constriction at the midpoint along the second tooth position, then taper posteriorly towards the internarial bar. The premaxillary-maxillary suture is short and angled at approximately 27 degrees, extending only to the third maxillary tooth position. Although most of the internarial bar is not preserved (Fig. 2.2D), the base of the bar and

a short fragment from the midsection are present in IRSNB R33 and are both shaped as an inverted triangle in cross-section.

The premaxillary teeth of IRSNB R33 are long, tapered, sinusoidal in outline, and highly procumbent, the crown tips of which protrude well beyond the rostrum (Fig. 2.2A-C). The first set of teeth preserve two prominent carinae on the mesial and distal edges of each crown. Small remnants of carinae are also visible in the same positions on the second set of teeth. No serrations are visible. Parts of the crowns preserve flutes on both inner and outer surfaces, particularly on the first set of teeth. The tips of two replacement teeth posterior to the second tooth set are visible on the ventral surface of the element. Flutes are present on the enamel surface of both replacement teeth (Fig. 2.2C).

Maxilla—Lingham-Soliar and Nolf (1989) describe the maxilla of IRSNB R33 as robust; however, the bone itself is thin, particularly along the dorsal margin, and only thick where the tooth row is housed (Fig. 2.2H, I). The ventral margin is slightly bowed dorsally rather than straight as reported in Lingham-Soliar and Nolf (1989) (Figs. 2.1, 2.2). The row of nutrient foramina above the tooth row on the lateral surface is also not straight, instead following the curvature of the dental margin. The maxillary margin along the premaxillary-maxillary suture is straight in lateral view in IRSNB R33 and extends posterodorsally at an angle of approximately 27 degrees until terminating at the third tooth position. Anteriorly, a shallow facet into which the premaxilla inserts occurs along the anterior-most border of the maxilla, narrowing as it reaches the anterodorsal process of the maxilla. The expanded region of the narial opening of IRSNB R33 spans three tooth positions, from the posterior edge of the third tooth to approximately the posterior edge of the sixth tooth. The anterodorsal process is oriented dorsally and therefore is

visible in lateral view. A faint, thin ridge oriented roughly towards the corresponding ridge and supraorbital process of the prefrontal extends from below the posterodorsal process and terminates posterior to the tip of the external nares (Figs. 2.1A, 2.3A). The posterodorsal process is oriented dorsally and extends farther dorsally than the anterodorsal process. Parts of the posterior edge of both maxillae appear to be broken off due to the thinness of the bone; the anterior margin of the left prefrontal is complete, and its shape suggests that the maxillary suture itself should contact the prefrontal at a shallow angle dorsally, then steepens 2/3 of the way along the edge of the prefrontal lamina. The maxilla also does not exclude the prefrontal from the border of the external naris. The posterior-most tip of the maxilla extends past the last maxillary tooth position by a little over 2 cm, forming a narrow triangle. A shallow depression into which the anterior ramus of the jugal is situated is angled anterodorsally along the lateral surface of the tip.

Twelve teeth are preserved along the tooth row in IRSNB R33, the roots of which are ankylosed to the jawbone. The first tooth is very weakly procumbent; less so than the premaxillary teeth. Posteriorly the teeth straighten along the vertical axis, but crown apices curve posterolingually. The labial surface of the crowns is convex whereas the lingual surface is largely straight, which creates an asymmetrical lenticular shape in basal or apical view (Fig. 2.2I). This may be what Lingham-Soliar and Nolf (1989) were referring to when they described bulbous or inflated bases of the teeth, but this applies strictly to the labial side. Conversely, inflated bases may instead refer to the large roots that expand below the base of the teeth, although this is not unique to *Prognathodon*. The asymmetrical shape and the weak sinusoidal curvature of the anterior crowns contribute to the appearance of a faintly splayed orientation, although this is more apparent in the dentary teeth. Lingually, crown shapes are weakly

heterodont: anteriorly the marginal teeth are proportionately long, tapered, and mostly uniform in shape, but broaden posteriorly in the jaw. The posterior-most teeth are short with a strongly curved apex, giving them an almost hooked appearance. Distinct fluting, characterized as thin longitudinal ridges separating narrow, shallow grooves, is present on the labial and lingual crown surfaces but are most pronounced at the base (Fig. 2.3). This feature is slightly reduced in the posterior teeth. The tips of multiple replacement teeth are visible in medial view and are likewise fluted. Lindgren (2005) described minute undulating striations near the crown apices, presumably on both the maxillary and dentary teeth. This feature is not immediately apparent on most crowns as many of the apices are worn away; however, very faint striations or crenulations can be seen on some unerupted replacement crowns particularly on the right maxilla (Fig. 2.3D). Carinae are present on both mesial and distal crown edges. Lingham-Soliar and Nolf (1989) make no mention of serrations, but Lindgren (2005) noted both that the carinae were not sharp and weak serrations were present. Serrations are very faint and only visible on unerupted crowns but are largely not observable on erupted crowns (Fig. 2.3D). The apparent lack of serrations on older teeth is consistent with the observation by Street et al. (2021) that mosasaur enamel and serrations by extension are comparatively thin and likely prone to wear (Street et al. 2021).

Frontal—The frontal of IRSNB R33 is broad and triangular in shape (Fig. 2.3A). A median ridge on the dorsal surface is absent, and the frontal table as a whole is largely featureless and planar. Anterolateral processes are absent, but two shoulder-like protrusions border the anteromedian process, creating a sinusoidal anterolateral margin. It is not possible to discern whether the anteromedian process is bifurcated, as only the base of the process is preserved. The posterolateral alae are rounded and project posterolaterally. Lingham-Soliar and Nolf (1989)

state that, while difficult to discern, the frontoparietal suture is mostly straight and is more visible on the ventral surface. However, overlap with the parietal makes this impossible to interpret with any certainty. A line transecting the pineal fenestra appears to be breakage as opposed to the frontoparietal suture, as the same crack occurs on the ventral surface of the frontal and both postorbitofrontals (Fig. 2.3B). Dorsally the suture in IRSNB R33 is clearly visible along the lateral edges, curving anteriorly where the postorbital processes of the parietal overlap the frontal (Fig. 2.3A). This curve is more pronounced than what is portrayed by Lingham-Soliar and Nolf (1989) in their reconstruction (see Fig. 2.6B). The suture dissipates near the pineal fenestra. There is potentially an outline of what might have been the posteromedial processes extending roughly two thirds of the way around the parietal foramen (Fig. 2.3A); however, this is extremely faint and makes it difficult to determine the shape of the outline with certainty.

Ventrally, the posterior length of the olfactory tract is narrow but broadens abruptly where the subolfactory processes expand laterally and form a curved medial border with the prefrontals. The posterior margin of the prefrontal is in close proximity to, but does not articulate with, the anterior edge of the postorbitofrontal. As a result, a small portion of the frontal is included within the orbital margin.

Prefrontal—The prefrontals are largely complete save for the ventral section of the lamina on the right element (Fig. 2.3C). The lateral face is concave but flattens anteriorly, and a lamina descends ventrally to form the anterior margin of the orbit. A series of fine striae originate posteriorly from under the supraorbital process, radiating outwards and extending to the margins of the anterior and descending laminae. Medially, a concave sheet of bone forms the posterior margin of the descending lamina. A broad, shallow and elongate depression or fossa with a

crescentic posterior end is located near the anteromedial tip of the prefrontal. Dorsally, the anteromedial margin is concave and follows the posterodorsal edge of the maxilla, delineating a substantial portion of the border of the external nares. A ridge demarcates the dorsal and lateral surface of the anterior corner of the prefrontal, gradually enlarging to form the prominent supraorbital process laterally overhanging the posterior-most portion. On the ventral side of the frontal, the posterior margin of the prefrontal approaches but does not contact the anterior margin of the postorbitofrontal. This condition is present in *Jormundgandr walhallensis*, although *P. solvayi* lacks the ridge separating the prefrontal and postorbitofrontal (Zietlow et al. 2023).

Postorbitofrontal—The postorbitofrontals are strongly affixed to the skull roof in IRSNB R33, although the jugal process is missing on the left element and only the base is preserved on the right (Figs. 2.1,2.3). Dorsally, the posterolateral edge expands to form a short, rounded overhanging process over the posterior edge of the orbit. The medial edge is strongly sinusoidal to accommodate both the blunt, rounded frontal alae and rounded lobes of the postorbital process of the parietal (Figs. 2.3, 2.7). A broad ramus projects posteriorly from the lateral edge of the postorbitofrontal and is firmly situated within a long, deep facet of the corresponding squamosal.

Parietal—The parietal in IRSNB R33 is in articulation with the entirety of the skull roof and is well preserved (Figs. 2.2A, B, 2.8A-C). The prominent postorbital processes form the posterodorsal surface of the skull roof. The processes extend to the posterolateral corners of the frontal, the sutures of which are emarginated. Although there is minor breakage along two sections of the anterior margin, the parietal foramen is large, oval in shape and at least 2/3 of its length is located in the parietal. Dollo (1889b) however described it as small, and it may well

have been small compared to other known taxa at the time. The foramen is also positioned in the center of a slightly raised triangular platform, the tip and lateral margins of which extend halfway onto the parietal table. The surface directly surrounding the foramen is depressed, likely due to compression of the skull roof. The parietal table is short and is a broad hourglass shape in dorsal view, largely due to the anterior extension of the triangular platform. The anterior-most lateral edges of the table run parallel to those of the triangular platform and slightly overhang the temporal fenestrae and descending processes of the parietal before slightly constricting midway along the table (Fig. 2.8A, C). In lateral view, the parietal table rises above the dorsal margin of the skull, but it is not known if this is its natural position or is the outcome of taphonomic processes (Fig. 2.1B). Posteriorly, the parietal table consists of a series of four ridges separated by three sulci; two outer ridges forming the lateral margins, and two inner ridges that appear to extend posteriorly from the triangular platform. The ridges flare laterally and terminate along the posteromedial edges of the suspensorial rami (supratemporal processes?), which are gently arched dorsally. The rami originate directly from the posterior edge of the postorbital processes, ventral to the anterior-most boundary of the parietal table. The bases of the rami are oriented horizontally and remain so throughout their length, diverging at an acute angle (slightly less than 90%) before curving ventrolaterally and forking to clasp the parietal process of the supratemporal dorsally and ventrally (Figs. 2.7A, 2.8A, C).

In ventral view, the anterior sutural outline is obscured by the postorbitofrontals and frontal, and a crack extends across nearly the entire length, transecting the parietal foramen. Two narrow ridges extend midway along the parietal foramen and converge posteriorly. Laterally, the broad descending processes extend posteroventrally from the parietal table to overlap the prootic. The suture is most visible on the right side and is semicircular in shape (Fig. 2.8C).

Jugal—The jugals of IRSNB R33 are relatively well preserved, only missing the tips on the anterior end of the horizontal rami (Fig. 2.4A, B). Nevertheless, a shallow facet to receive the posterior prong of the maxilla is preserved, extending a short distance along the medial face of the rami. The horizontal rami are slightly bowed, narrow, and twice as long as the vertical rami. A posteroventral process is virtually absent; the posterior margin of the horizontal ramus is instead smooth and curves slightly along the base of vertical ramus. The vertical ramus is broader laterally than the horizontal rami and tapers slightly towards the postorbitofrontal process. This section is flattened and a facet for the postorbital frontal is either not preserved or absent.

Sclerotic ossicles—Five overlapping ossicles are preserved on both sides, although the best example is the right sclerotic ring (Fig. 2.5C). Sub-rectangular in shape, there are at least two ossicle types preserved for certain (Yamashita et al. 2015): the plus type, which overlaps both neighbouring ossicles, and the imbricating type, in which one edge is overlapped and the other is overlapping its neighbouring ossicles. The remaining ventral border of the sclerotic ring indicates it likely would have been circular (Konishi et al. 2011).

Palatine and Vomer—Both palatines are preserved in IRSNB R33, although the right palatine is in better condition. The palatines and vomers are both disarticulated, but they could not be removed from the current mount (Fig. 2.6). It is difficult to see precisely where along the maxilla they would have been situated, although Lingham-Soliar and Nolf (1989) placed the anterior margin of the main body of the palatine at the seventh tooth position. Note as well that the

palatines are upside down and reversed in the current mount for the skull of IRSNB R33. The main body is a flat sheet of thin bone with a sinusoidal posterior margin into which the anterior border of the pterygoid inserts (Fig. 2.5A). The lateral edges are straight and run parallel to the medial walls of the maxillae, extending an elongate, triangular posterolateral process between the pterygoids and maxillae.

The medial border is punctuated by a shallow V-shaped embayment between the vomerine process and a broad rectangular medial process, the latter of which articulated with the opposite palatine. A posterior flange on this process curves laterally to clasp the anterior-most tip of the pterygoid. The vomerine process projects anteromedially but then curves abruptly to point anterolaterally. The process forms a raised ridge at its base that descends below the main body and is slender and laterally compressed along its length. Anteriorly the process would have contacted the narrow posterolateral edges of the vomers.

The vomers are thin walled, elongate and broaden anteriorly, and are longitudinally concave along their dorsal surface (Fig. 2.6).

Pterygoid—Lingham-Soliar and Nolf (1989) describe this element as notably "stout", despite the overall thin main body and lightly-built, narrow quadrate process (Fig. 2.7A-C). Viewed ventrally, the main body of the pterygoid is broad and flat with a pronounced convex curvature of the lateral margin. Unlike in many other mosasaurs, such as *Mosasaurus* (Street and Caldwell, 2017), the teeth do not descend ventrally from a tall ridge or flange, but instead erupt directly from the slightly thickened base of the main platform (Fig. 2.7A, C). Russell (1969) describes seven tooth positions as typical for *Prognathodon*, whereas Lingham-Soliar and Nolf (1989) states eight are present in *P. solvayi*. Six pterygoid tooth positions are identified, three of which

preserve teeth in the sockets (Fig. 2.7A, C). The pterygoid teeth are notably large relative to the pterygoid itself, and similar in size to the marginal teeth. The crowns are not well preserved and largely featureless, but there are traces of a small posterior carina on the first and third crowns. They resemble the shape of the anterior and middle marginal teeth in the maxillae and dentaries but are more strongly curved and subcircular to circular in cross-section. The tooth sockets decrease in diameter moving posteriorly, and despite only preserving the anterior three teeth, the length of the crowns likewise appear to slightly decrease posteriorly. A large foramen is positioned midway and near the convex lateral margin on the dorsal surface of the main platform (Fig. 2.7B). The ectopterygoid process extends roughly perpendicular to the dorsolateral surface of the main body of pterygoid. The process is roughly triangular in shape with a broad base, but curves posteriorly at its terminus. The posterior margin is strongly concave and bears a flattened, broad facet. The anterolateral surface is rugose where it would have articulated with the ectopterygoid.

Posteriorly, the main body narrows and curves laterally before terminating at the base of the basisphenoid process. Lingham-Soliar and Nolf (1989) described the basisphenoid process as being damaged but slender with a narrow base, although they may have been referring to the quadrate process instead. The former is similar in shape to the ectopterygoid process, but shorter and only slightly narrower. The tip of the process curves laterally slightly, following the slight curve of the main body, giving the element an overall sinusoidal shape in dorsal and ventral views. Although damaged, the quadrate ramus is distinctly narrow along its length with little variation in width. The articular surface with the quadrate, if complete, is blunt and rounded.

Ectopterygoid—Lingham-Soliar and Nolf (1989) describe a single thin, flattened triangular element originally mounted along the anterior margin of the orbit IRSNB R33 as the lacrimal. Instead, this element likely represents the proximal end of the right ectopterygoid (Fig. 2.7D, E) (Konishi et al. 2011). The hypothetical posterior edge is slanted and the lateral and medial prongs are inclined at an acute angle. The medial prong is shorter, broad and likely missing a corner of the tip that would contact the ectopterygoid process of the pterygoid. The lateral prong is likely missing much of its anterior portion, but is nevertheless longer and slightly narrower with a straight margin where it presumably would have articulated with the medial surface of the jugal ramus. The dorsal and ventral surfaces of the ectopterygoid are otherwise featureless.

Squamosal—The squamosals of IRSNB R33 are both preserved and are in articulation on their respective sides of the skull, although the right element is better preserved (Fig. 2.8). In lateral view the element is slightly bowed dorsally. In dorsal view, the anterior shaft is laterally compressed and a deep groove which receives the posterior process of the postorbitofrontal runs along nearly the entire length of the shaft, terminating at the articulation points for the supratemporal and quadrate. Ventrally the squamosal extends nearly to the articulation between the postorbitofrontal and parietal (Fig. 2.8B). The posterior shaft flattens and broadens slightly, partially due to the flared ledge of bone along the lateral margin that forms the posterolateral crest. The dorsal surface of the crest is lightly striated. Laterally, the outer border of the crest is sharp and forms a narrow shelf that follows the arc of the squamosal shaft. The posteromedial border curves abruptly into a large, broad, nearly rectangular-shaped parietal process (Fig. 2.8A, C). The parietal process overlaps the supratemporal but does not contact the supratemporal process of the parietal. The posterior-most end of the squamosal is broad and curves ventrally to

meet the suprastapedial process of the quadrate. A lateral fragment of the quadrate process extends ventrally, but most of the facet is not preserved.

Supratemporal—The right supratemporal of IRSNB R33 is more complete than the left; the right being a splint of bone connecting the supratemporal process of the parietal and the poorly preserved left squamosal (Figs. 2.4, 2.8, 2.9). The shape of the supratemporal is largely concealed dorsolaterally by the overlapping parietal process of the squamosal and ventrally by the paroccipital bar. Medially it is likewise clasped between the dorsal and ventral forks of the supratemporal process of the parietal.

Prootic—Much of the braincase of IRSNB R33, including the prootic, is distorted and slanted towards the right side of the skull (Figs. 2.4A, B, 2.8A, 2.9A, 2.10D). Despite this, much of the prootic is preserved in articulation with the parietal and basioccipital, although its ventral contribution to the ventral section of the paroccipital process is missing. As with the majority of the skull, the surface of the prootic is weathered and cranial nerve foramina are not visible. The ascending prootic process/alar wing is oriented medially relative to the descending process from the parietal, which broadly overlaps this contact in lateral view. A pedestal descends anteroventrally to contact the basisphenoid (Figs. 2.8B, 2.10D). Posteriorly, a dorsal process would have extended to articulate with the supraoccipital, although this region of the braincase surface is cracked and too heavily worn such that any trace of a suture is no longer apparent.

Opisthotic-Exoccipital—The exoccipitals of IRSNB R33 are missing or are too distorted to visualize. The right paroccipital process of the opisthotic forms the dorsal portion of the

paroccipital bar but is in poor condition; the ventral surface where the prootic would have extended is hollowed out. The bar projects dorsolaterally to contact the supratemporal (Figs. 2.8A, 2.10C). Only a short proximal segment of the left paroccipital bar is present. The quadrate articular facet is also missing on both sides.

Basisphenoid—Although compressed and slightly distorted, the basisphenoid of IRSNB R33 is the best-preserved element of the braincase (Fig. 2.10A-C). The parasphenoid process is V-shaped in cross-section and protrudes anteriorly from the midline of the main body, raised dorsally above the basipterygoid processes on a vertically oriented, thin wall of bone. Posteriorly, the dorsal margin ascends steeply towards the sella turcica, creating a deep recess situated on a ridge between the two dorsally open vidian canals incised into the lateral surface of the main body. The dorsal margin of the sella turcica is more poorly preserved and it is difficult to distinguish the dorsum sellae as a result. On the left face of the basisphenoid, a narrow sheet of bone originating from the base of the alar process extends over the canal midway along its length and connects ventrally to the lateral surface. Dorsally, the narrow, elongate alar processes are tilted laterally and the anterior tips are angled dorsally to contact the prootics. The articular surfaces are shallowly concave and heavily rugose. The alar processes converge posteriorly and form the lateral borders of a flat-bottomed triangular depression that represents the anterior termination of the basioccipital canal.

Well-developed and vertically compressed, the basipterygoid processes are positioned anteroventrally and serve as the contact point with the pterygoids (Fig. 2.10 A,B). Proximally the processes are constricted, whereas the articulating surfaces are expanded and slightly bulbous with a rugose texture. Although they currently project anteroventrally from the midline, this

orientation appears to be due to compression and were likely oriented anterolaterally. The main body of the basisphenoid constricts posterior to the basipterygoid processes, the bases of which are confluent with the posterior lobed processes in lateral view. The posterior processes project posterolaterally only a short distance from the main body. Similar in size and length to the basipterygoid processes, they are broad laterally and slightly compressed vertically. Along with the central constriction of the main body, this creates an X-shape in ventral view (Fig. 2.10B). The articular facets for the basioccipital tubera are long, very weakly concave, and angled posterodorsally. Ventrally, a narrow groove extends along the midline of the main body between the basipterygoid process and the posterior lobes.

Basioccipital—The basioccipital forms the posterior extent of the braincase, and in IRSNB R33 is in articulation with the prootic and paroccipital bars (Figs. 2.4B; 2.8, 2.11). Like the rest of the braincase, the basioccipital has been distorted by compression and is offset from the midline of the skull, and much of the right side is missing. The exoccipitals that would connect the dorsal basioccipital with the proximal end of the paroccipital processes are largely broken away. Anteriorly, the basioccipital tubera descend ventrally to contact the posterior processes of the corresponding basisphenoid. The basal tubera as presently preserved diverge ventrolaterally at an oblique angle of about 110 degrees and are notably broad and short, barely extending beyond the main body of the basioccipital. Posteriorly, the occipital condyle is reniform in shape. The articular surfaces for the vertebrae are smooth and rounded. The dorsal surface of the occipital condyle bears a shallow depression in which an opening of the basioccipital canal is situated (Fig. 2.11B). The canal opening is oriented vertically relative to the horizontal dorsal surface of the basioccipital. The ventral portion of the canal is largely concealed from view but overlain by

a thin, longitudinally concave roof of bone with thin outer ridges that taper dorsally near the occipital condyle.

Lower Jaw

Dentary—The dentary of *P. solvayi* is short relative to those of *Mosasaurus* (Lingham-Soliar, 2000; Konishi et al. 2014; Street and Caldwell 2017), and only slightly longer than the posterior mandibular unit (PMU, comprising of the angular, surangular, coronoid, and articular-prearticular); (Fig. 2.12A-C). Laterally, the upper and lower margins are strongly bowed. The slight tapering of the anterior dentary and its blunted tip may have contributed to a notion of robustness (Lingham-Soliar and Nolf, 1989); however, the dentary is otherwise not noticeably deep nor broad, and the bone itself is not remarkably thick. A row of large elongate nutrient foramina are present along the midline and become stacked and randomly interspersed at the anterior tip of the dentary. The Meckellian groove extends the entire length of the element in medial view, narrowing anteriorly as it follows along the ventral edge. The groove is open at the dentary tip.

There are thirteen tooth positions in IRSNB R33. Like in the premaxilla and maxilla, the dentary teeth are proportionately large and fluted from the base to the apex on both lingual and labial surfaces. The first two anterior teeth are strongly procumbent and extend beyond the tip of the dentary bone. The third and fourth teeth are also weakly procumbent but less than the first two, and the crowns straighten by the fifth tooth position. The anterior dentary teeth have a sinusoidal curvature and are more strongly splayed than the maxillary teeth. The lingual face is largely flat, whereas the base on the labial face is slightly convex and the crown apices are curved posterolingually. The crowns are likewise asymmetrical and lenticular in shape in dorsal view. As in the maxilla, the dentary teeth are weakly heterodont, with crowns broadening

posteriorly until the twelfth and thirteenth teeth, which are short and squat with strongly curved tips. Prominent flutes occur from the base to the apex of the crowns on both labial and lingual surfaces. This is most apparent on anterior and middle crowns but less pronounced in the posterior teeth; the enamel surface of the twelfth and thirteenth crowns appear largely featureless although this may be a result of wear. Carinae are present on the distal and medial edges of the anterior and middle teeth along the jaw. Much like the maxillary teeth, striations/crenulations on the apices and serrations on the carinae are largely only visible on replacement teeth, although the latter is more difficult to observe as only the apices are visible.

Splenial—Roughly half of the left splenial of IRSNB R33 is missing but most of the right splenial is preserved; they could not be removed from the mount (Fig. 2.12D, E). The splenial is an elongate wedge-shaped bone that when in articulation is mostly concealed by the dentary, with only a thin posteroventral section visible in lateral view. Like the dentary, the ventral margin is gently bowed. The left splenial preserves the anterior tip, which extends roughly to the 5th tooth position on the dentary. In cross-section the splenial has an asymmetric V shape, formed by thin lateral and medial wings extending dorsally from the thickened base. The lateral wing is short and bears a shallow sulcus that spans the lateral surface and descends anteriorly to follow the ventral margin of the splenial. Although portions of the medial wing are incomplete, it is taller than its lateral counterpart. The posterior edge of the medial wing rises anterodorsally from the splenial base further anterior than does the lateral wing, such that the posteroventral corner of the lateral wing is visible in medial view. The wing terminates abruptly midway along the splenial, and the remainder of the base is a long, narrow and gently tapered bar. A large and slightly elongate foramen is situated a quarter of the length from the posterior end at the juncture

between the medial wing and splenial base (Lingham-Soliar and Nolf, 1989: fig. 21B). A deeply concave U-shaped cotyle forms the posteroventral corner of the splenial and articulates with the convex face of the angular, creating a ball-and-socket joint that constitutes the ventral portion of the intermandibular joint. The cotyle is deepest at its center, and its ventral edge projects posteriorly slightly to meet the angular. Dorsally, an anterior segment from the base of the lateral wing curves medially and overhangs the cotyle.

Angular—Both angulars are preserved in IRSNB R33, although the posterior tips are broken away (Fig. 2.13). The angular is a long wedge-shaped bone that tapers posteriorly, with the anteroventral corner and ventral margin unobscured by the surangular in lateral view. The ventral border is straight and the medial and lateral faces are formed by thin plates that taper gradually before terminating posteriorly along a narrow, thin blade of bone. Viewed anteriorly the angular is a compressed V-shape in cross-section, although laterally there is a constriction between the base of element and the lateral wing directly posterior to the intramandibular joint. This forms a shelf running lengthwise along the ventrolateral face on which the ventral margin of the overlapping surangular rests (Fig. 2.13B, D). A narrow ledge spanning the ventromedial surface of the surangular likewise corresponds with a thin horizontal ridge situated midway along the medial face of the lateral wing on the angular (Fig. 2.13G). Despite minor breakage along the dorsal margins, preserved portions suggest the lateral and medial wings are shorter in height, barely extending above the anterior articular facet. Contact between the coronoid and angular has been previously scored as present (Schulp, 2006), but similar to *Globidens simplex* (Leblanc et al. 2019), the short medial wing in IRSNB R33 likely does not extend to meet the anteromedial wing of the coronoid. The angular foramen is difficult to discern as it has an incomplete dorsal

margin but is positioned along the dorsal border of the medial wing a short distance from the intramandibular joint. The articular surface of the angular compliments that of the splenial: the anteroventral corner that slots into the cotyle of the splenial is rounded and convex. Dorsally, a shallow, narrow concavity corresponds with the convex dorsal projection above the splenial cotyle.

Articular—The articular is a long, vertically oriented bone that contributes to the posteroventral region of the posterior mandibular unit (Fig. 2.13). Like other mosasaurs, the articular and prearticular were probably fused in *P. solvayi* and are not possible to differentiate. A middle section of the right articular is strongly laterally compressed and contacts the lateral face of the medial wing on the angular. Anteriorly, the articular is V-shaped with a deep, narrow sulcus to receive the posterior blade from the angular (Fig. 2.13F). Posterior to the sulcus, the articular forms the lateral and posterior borders of the glenoid fossa. The fossa is crescentic in shape and tilted medially. A small eminence emerges from the dorsal edge off the fossa posterior to the glenoid fossa, then slopes ventrally and forms the short, rounded posterior end of the retroarticular process. The retroarticular process is oriented posteriorly and angled largely parallel to the PMU, with only a slight medial rotation to the ventral margin. No foramina are preserved or visible on any surface of the left or right process.

Surangular—Large portions of both surangulars of IRSNB R33 are preserved, although sections of the anterior margin are missing (Fig. 2.14). This element represents the largest component of the posterior mandibular unit, overlapping most other associated elements in lateral view. The surangular is a long rhomboid-shape with flattened, nearly parallel dorsal and ventral margins

that taper only slightly posteriorly (the coronoids are currently affixed to the surangulars and obscure the dorsal margin, but Lingham-Soliar and Nolf (1989) shows the unarticulated right surangular in fig. 23). The posterolateral corner of the surangular is a pointed wedge that forms the anterolateral border with the glenoid fossa. Directly anterior to the glenoid fossa, a deep excavation or fossa with a smooth ventral border occurs on the upper posterior half of the lateral surface. The anterodorsal corner of the surangular projects anteriorly over the dorsal section of the intramandibular joint. Lingham-Soliar and Nolf (1989) make note of a U-shaped or crescentic depression situated along the lateral face of the right surangular (Fig. 2.14A, C), but conclude it results from taphonomic damage as the left surangular does not preserve this feature. However, most of the same region on the left surangular is missing in IRSNB R33 and numerous other mosasaurines preserve similarly shaped fossae that open anteriorly in the same location (i.e., *Globidens simplex*). It is therefore probable that this depression represents the anterior surangular fossa.

The medial face is deeply excavated by the adductor fossa, the ventral edge of which is bounded by a prominent shelf that slopes anteriorly from the glenoid fossa (Fig. 2.14). A slender ridge ventral to the shelf inserts against the medial wing of the angular. Beneath this the surangular tapers into a thin sheet that curves medially to sit against the lateral shelf of the angular. A large foramen piercing the anteromedial surface is figured by Lingham-Soliar and Nolf ((1989): fig. 23) but is otherwise obscured by the coronoid.

Coronoid—The coranoid is well represented for *Prognathodon solvayi*; in IRSNB R33, as with other mosasaurines, the coronoid is a complex, saddle-shaped bone that forms the dorsal section of the posterior mandibular unit, embracing the anterodorsal margin of the surangular via a series

of overlying processes (Fig. 2.14). Posteriorly, the coronoid process projects dorsally above the concave upper margin. The anterolateral margin of the process forms a broad, thickened lip that overhangs the shallowly excavated posterolateral face of the coronoid. A low, rounded protuberance visible on both coronoids is present midway along the medial surface of the process (Fig. 2.14B, D, F). In dorsal view this feature is aligned with the dorsal limit of the overhanging shelf on the lateral face. A series of fine ridges run parallel to each other along the dorsal margin from the peak of the coronoid process to the anterior wing, following the concave curvature of the dorsal margin. The coronoid process is medially deflected in dorsal view rather than aligned parallel to the PMU (Fig. 2.14D). Posterior to the coronoid process, the dorsal edge of the coronoid descends steeply towards the thin, wedge-shaped posterodorsomedial process. In articulation, a narrow sliver of the process projects posteriorly over the dorsal margin of the surangular and is visible in lateral view. A heavily striated fossa on the lateral face of the process articulates with the surangular.

Although broken in all specimens, the shape of the lateral wing is indicated by a shallow fossa on the lateral surface of the surangular in IRSNB R33. The posterior lateral wing is short and originates anteroventrally from the coronoid process. The shape of the surangular fossa indicates that midway along the coronoid the anterior lateral wing expanded ventrally and was fan-shaped with a curved outer edge (Fig. 2.14A). The anterior edge would have curved dorsally and terminated at the anterodorsal tip of the rounded coronoid ramus where it bifurcates from the anteromedial wing. The wing is a thin, fan-shaped sheet of bone with smooth posterior and ventral margins. The posterior extent originates at the base of the coronoid process, protruding anteromedially from the coronoid ramus. Although the edge extends further ventrally than the lateral wing, it likely did not contact the short medial wing of the angular (Fig. 2.14B). A narrow

ledge delimits a shallow articular facet for the surangular along the internal surface of the process (this is only visible when disarticulated, see Lingham-Soliar and Nolf, 1989: fig. 24).

Quadrate—Of all three specimens of *P. solvayi*, only the right and left quadrates of the holotype IRSNB R33 are preserved (Fig. 2.15). The posterior section of the right quadrate appears to be the most well-preserved, although much of the quadrate conch is missing. The left quadrate appears compressed and distorted, but the quadrate conch and ala are in better condition. On the right quadrate, the mandibular condyle is narrow, short, and angled anteriorly in lateral view. In ventral view the condyle is reniform in shape, although the shape may be obscured by compression. Schulp (2006) describes a dorsal deflection of the anterior mandibular condyle surface in *P. solvayi*, but this feature is not detectable beyond a slight anterior slant of the condyle itself, as the surfaces of both quadrates are abraded and detailed features are not readily discernible. The structure typically referred to as the infrastapedial process resembles the small, narrow posterior pillar-like process (ppp) of *Selmasaurus* described by Palci et al. (2021: fig. 3A). However, the authors stated that the process in *Selmasaurus* may instead be derived from the posterolateral process only, rather than the combination of both the posterolateral and posteromedial processes as suggested for other members of *Prognathodon.* Like *Selmasaurus*, the base of the process in *P. solvayi* originates on the lateral surface of the quadrate (Fig. 2.5C), indicating this structure is likely not the same as the posterior pillar-like process observed in other members of *Prognathodon*. This structure is instead more accurately referred to as the posterolateral process (plp) (Fig. 2.5). The dorsal margin of the process is largely straight in both quadrates of *P. solvayi*, ascending at an acute angle (slightly less than 90 degrees) from the posteroventral corner of the tympanic crest and mandibular condyle (Fig. 2.15A, F). In posterior view, the mandibular and cephalic condyles are in alignment with each other. Here the process

forms a slightly enlarged pedestal where it contacts horizontally with the distal tip of the suprastapedial process. The suture is oriented anteroposteriorly relative to the quadrate shaft (Fig. 2.15A-D). The suprastapedial process narrows at the sutural contact but broadens dorsally and is demarcated by a narrow groove along its lateral surface. The dorsomedial surface likewise bears an elongate excavation, creating a pinched appearance of the posterodorsal margin (Fig. 2.15B). Orienting this depression with the quadrate process of the squamosal indicates the quadrate, like in plioplatecarpines (Palci et al. 2021), was tilted posteroventrally when in articulation (Fig. 2.1B). Although the tympanic ala and tympanic crest is mostly broken and missing on the right quadrate, the left element preserves a small, straight crest that ascends to the cephalic condyle at a slightly obtuse angle. The cephalic condyle forms a small, flattened peak but does not extend above the dorsal margin of the quadrate ala. The posteromedial surface of the tympanic ala is longitudinally concave and bounded by a thin median ridge that extends dorsally from the mandibular condyle, forming the anterior border of the stapedial pit (Fig. 2.15C). The stapedial pit is tear-dropped shaped and overhung dorsally by the ventromedial edge of the suprastapedial process. A dorsomedial eminence is formed by the continuation of the median ridge on the dorsal border of the quadrate and at the proximal extent of the suprastapedial process (Fig. 2.15B, G). This structure may have functioned as a buttress against the quadrate process of the squamosal.

Axial Skeleton

The axial skeleton of *Prognathodon solvayi* is fragmentary; most of what remains are partial series of the vertebral column and ribs. Most, if not all, the vertebrae are compressed and/or deformed and missing large sections of the proximal structures that surround the centrum.

Atlas—The atlas of IRSNB R33 is comprised of four separate elements, most of which are present but weathered (Fig. 2.16). The left atlas neural arch is preserved and is a flattened triangle in lateral view. Only the rounded shape of the anterior articulation surface with the occipital condyle is discernible. The spinous process projects dorsally and is separated from the articular surface by a shallow notch (Russell, 1967). Posteriorly, the synapophyseal process is broad, flat, and extends posteroventrally.

Anteriorly, the atlas centrum is a square bone with a smooth, flat surface (Fig. 2.16C, D). A broad ridge situated in the center of the element between two shallow indentations is visible on the posterior surface. Although slightly compressed, in ventral view the centrum is concave and overall elliptical in shape.

The atlas intercentrum is largely featureless likely due to poor preservation; Lingham-Soliar and Nolf (1989) stated the hypapophysis is absent, but a smooth, low peak is present in the center on one surface (Fig. 2.16E). The intercentrum is an elongate oval shape, one edge of which has a longitudinally tapered edge. The opposite, broader edge bears a flat facet.

Axis—Most of the distal extremities of the axis in IRSNB R33 are broken (Fig. 2.17A,B). The anterior face is broad mediolaterally and bears two circular structures with flattened, ventrally angled surfaces that articulate with the synapophyseal processes of the atlas neural arch. A shallow vertically oriented groove is situated between these two articulations and recedes into the bone posteroventrally to receive the axis intercentrum. Dorsally, the neural spine is expanded anteroposteriorly across most of the surface of the axis. The dorsal margin of the spine is broken but likely descended steeply anteriorly as the point projecting just dorsal to the neural canal

appears largely undamaged. The anterior border of the neural canal is incomplete, but posteriorly the canal is large and oval in shape, although this may be due to distortion. The posterior surface of the axis, including much of the neural arch, is shorn away and preserves only the base of the postzygapophyses. There is no trace of the axis centrum remaining. The base of the transverse processes is anteroposteriorly broad but otherwise incomplete. Ventrally, only a very small anterior portion of the base of the hypapophysis is remaining.

Two isolated incomplete elements accompany the axis and likely represent the axis intercentrum and the second axis intercentrum/cervical intercentrum (see Konishi et al., 2007) (Fig. 2.17C, D). The possible axis intercentrum is dominated by a rectangular bone with a prominent, pointed apex in the center (Fig. 2.17C). A broken, double pronged protuberance with a small foramen in the center emerges from the long axis of the rectangle. The apex may have inserted into the deepest portion of the concave anterior facet of the axis, with the prongs oriented posteroventrally. The second element is a flattened and distorted sub-rectangular bone with a single small projection preserved along its edge (Fig. 2.17D), although this presumably would have been paired. The flat dorsal surface opposite the projection may have articulated with the axis hypophysis.

Cervical vertebrae—The cervical vertebra figured by Lingham-Soliar and Nolf ((1989): fig. 30)) does not appear to be currently with the other elements associated with IRSNB R33. In the remaining examples the neural spines are poorly preserved but are still tall and angled posteriorly in lateral view. The neural spine in the better-preserved specimen from Lingham-Soliar and Nolf (1989) is relatively broad anteroposteriorly and blade-like in shape. In some examples the anterior margin tapers to a narrow ridge on the midline of the spine (Fig. 2.18A, C). Anteriorly,

the centra are roughly circular and slightly notched along their dorsal surface, as well as constricted anterior to the condyle. The neural canal is large and circular. The transverse processes originate slightly dorsal to the dorsal border of the centra, and the synapophyseal processes are as tall as the centra and oriented laterally. In lateral view, the transverse processes are positioned anteriorly along the centra, and even in the most compressed examples, a sinuous, thin crest curves anteriorly from the ventral edge of the synapophyseal process to connect with the lateral border of the cotyle (Fig. 2.18B, E; see also Lingham-Soliar and Nolf, 1989: fig. 30B). The prezygapophyses are large with broad bases and tapered tips that point anterolaterally, although the facets are difficult to discern. The postzygapophyses are short with posteroventrally directed facets that project posterolaterally from the base of the neural spine. The zygosphenes are large, taper to a rounded point, and diverge slightly from their base at an acute angle. The zygantra on the posterior face are deep, oval in shape, and angled towards the midline of the vertebra.

Dorsal vertebrae—Lingham-Soliar and Nolf (1989) counted 30 dorsal vertebrae, but these are now removed from the mount and most are contorted and missing significant portions of key structures. The anterior-most examples are the best preserved (Fig. 2.19). The neural spines are mediolaterally compressed and oriented posteriorly. Lingham-Soliar and Nolf (1989) stated the dorsal neural spines are possibly shorter than those of the cervical vertebrae, but this is ambiguous as most of the spines are worn or missing. The centra are largely all distorted but were likely subcircular in anterior view. The dorsal margins are notched, as in the cervical vertebrae. The transverse processes originate well above the midline on the centrum, project dorsolaterally, and are dorsoventrally short but robust anteroposteriorly. Laterally, the transverse

processes are situated anteriorly along the centrum but the ventral margin is not continuous with the lateral edge of the cotyle. The synapophyseal processes are rounded, dorsally expanded, and angled slightly anteriorly. The prezygapophyses are long and narrow and seem to point anterolaterally. Most of the postzygapophyses are broken away but the remaining examples are short, pointed, and project posterolaterally. The zygosphenes are prominent and the zygantra are large and deep. Lingham-Soliar and Nolf (1989) recounted that these structures begin to reduce in size after the ninth dorsal vertebra and are non-functional after the fourteenth. However, one of the better-preserved posterior vertebrae appears to preserve the base of zygosphenes (Fig. 20B).

Most of the posterior dorsal vertebrae are dorsoventrally compressed and their features are either distorted or missing altogether (Fig. 2.20). Although mostly missing, the base of the neural spines are angled posteriorly, are thin, and anteroposteriorly broad. The cotyles and condyles are subcircular and proportionately large with a notched dorsal margin. The transverse processes are positioned along the midline of the centrum and oriented ventrolaterally and taper laterally towards rounded and narrow synapophyseal process. The prezygapophyses are generally poorly preserved but appear roughly similar in size to those on the anterior dorsal vertebrae. The postzygapophyses are likewise mainly broken but appear reduced in size relative to more anterior vertebrae.

Pygal vertebrae—The pygals have sub-rounded centra, some of which are circular and others that are taller than they are wide (Fig. 2.21). All examples have a notched dorsal margin. The borders of the neural canal are generally well-preserved and circular in shape. The neural spine is broad, thin, and angled posteriorly. Most of the transverse processes are incomplete, but they are

long and narrow in the best example and positioned anteriorly along the centrum (Lingham-Soliar and Nolf, 1989: fig. 34). The tips of the processes are oriented posterolaterally.

Ribs—A handful of cervical and dorsal ribs are preserved but most of the distal tips are missing. The larger, more posteriorly positioned ribs are a similar shape to the cervical ribs but have considerably longer shafts, although all the distal sections are incomplete (Fig. 2.22). The rib head is fan-shaped, sometimes preserving a flat articulating surface (Fig. 2.22B, D), and is only slightly broader than the diaphysis, but there is no constriction between the rib head and shaft. The proximal surface of the rib head is flattened in some examples, and the posterior surface is shallowly concave.

Appendicular Skeleton

Scapula and coracoid—Both the scapula and coracoids of IRSNB R33 are incomplete and missing most of their expanded distal margins (Fig. 2.23A, C, F), but are the only components of the appendicular skeleton to survive. A narrow ridge divides the articular facets on the proximal head of the left scapula (Fig. 2.23D). The largest facet is directed posterolaterally and forms a portion of the glenoid facet for the humerus, whereas the smaller is angled anteromedially to articulate with the coracoid. This facet is broken in the right scapula. The scapular neck is a similar width to the articular facet, but the margin expands abruptly as it transitions into the broad, fan-shaped distal sections of the scapula.

The coracoid is broadest at the articular facet and thins abruptly posterior to the neck (Fig. 2.23B). The foramen is large but its borders are weathered and may be exaggerated in size (Lingham-Soliar and Nolf, 1989). The articular facet of the coracoid would have been directed

posterolaterally when in articulation and is subcircular but heavily worn, such that any separation of the facet for the scapula and glenoid fossa is not visible.

Comparison of Referrred Specimens (IRSNB 0107, 0108) to IRSNB R33

IRSNB 0107 and IRSNB 0108 are primarily represented by sparse and highly fragmented cranial material. IRSNB 0108 is roughly half the size of IRSNB R33, whereas IRSNB 0107 appears to be similar in size, if not slightly larger. The precise proportions of IRSNB 0107 relative to the holotype are difficult to interpret due to the lack of complete elements.

Premaxilla—A fragment of the premaxilla is preserved in IRSNB 0107, which was erroneously placed along the posterior dentary on its mount (Fig. 2.24A) and not figured by Lingham-Soliar and Nolf (1989). The left lateral margin posterior to the teeth is intact and convex as in IRSNB R33. The dorsal surface is also similarly broad and flat; however, unlike IRSNB R33, a faint, shallow median sulcus extends anteroposteriorly along the anterior portion of the element of IRSNB 0107. It may have extended to the tip of the premaxillary rostrum, although this section is missing. The posterior extent of the sulcus is also not preserved. This feature is either not present or not preserved in IRSNB R33, possibly due to wear. In IRSNB 0107, a partial tooth is preserved in the second tooth position and is procumbent as in IRSNB R33. An empty alveolus is also preserved and strongly angled, appearing to match the inclination of the adjacent crown.

Maxilla—A small fragment of the anterior-most section of the maxilla is preserved in IRSNB 0107, and closely resembles that of IRSNB R33 in overall shape, possessing a short premaxillary-maxillary suture that extends to the third tooth position and remnants of the

anterodorsal process (Fig. 2.24B). The second maxillary tooth in IRSNB 0107 is poorly preserved, but the first tooth is complete and is similar to those in IRSNB R33, possessing flutes that are well-defined at the base of the crown and reduced towards the apex, mesial and distal carinae with small serrations visible on erupting teeth, and a distally curved apex that also points lingually in anterior view (Fig. 2.24B). A replacement tooth is preserved in the second position, which also possesses distinct flutes on its surface.

Frontal, Prefrontal, Postorbitofrontal—The frontal and associated orbital elements are partially preserved in two parts in IRSNB 0107, although the frontal fragments do not have any diagnosable characteristics (Fig. 2.24C). However, the ventral surface of the right fragment preserves the posterior and anterior margins of the prefrontal and postorbitofrontal, respectively. As in IRSNB R33, they are close to but not in direct contact with each other, and therefore do not entirely exclude the frontal from the orbital margin.

Pterygoid—A portion of the right pterygoid is preserved in IRSNB 0108, including the posterior-most end of the tooth-bearing platform, the ectopterygoid process, and quadrate ramus (Fig. 2.25A, B). The quadrate ramus is better preserved than in the holotype and is likewise thin and narrow, but in dorsal view is broadest midway along its length. The articular end of the ramus is small and rounded, as in the holotype. Like IRSNB R33, the main tooth-bearing platform appears to have been broad and flat with a strongly curved lateral margin. A single erupting crown is situated in a poorly preserved alveolus. Only the apex is visible, but like the holotype the crown surface appears smooth. The base of the ectopterygoid process is slightly narrower than in the holotype, but like IRSNB R33 has a curved posterior margin with a broad,

flat facet. The articulation for the ectopterygoid is an enlarged pedestal-shaped and heavily textured facet. Only the base of the basisphenoid process is preserved.

Squamosal—A disarticulated partial left and very small fragment of the right squamosal are preserved in IRSNB R 0108 (Fig. 2.25C-F). Like the holotype, the shaft is dorsally bowed. The inner surface of the dorsal groove for the posterior ramus of the postorbitofrontal is exposed and shows a series of small ridges running along its length. The groove is deeply incised, and its depth is maintained for most of the length of the squamosal. As in the holotype, the posterolateral crest is a narrow, arched ledge and its dorsal surface is weakly striated. Only a small anterior fragment of the parietal process is preserved, and the articular facet for the quadrate is broken.

Dentary—IRSNB 0107 preserves a fragment of the posterior-most and anterior right dentary and a middle section of the left dentary (Fig. 2.26A-C). In addition, a large but incomplete fragment of the left dentary is preserved in IRSNB 0108 (Fig. 2.27A-C). Both specimens bear strong resemblance to the dentaries the holotype. Although the dentary of IRSNB 0108 is slightly narrower than those of IRSNB R33, it is similar in having strongly bowed dorsal and ventral margins. In both specimens, the midline on the lateral face bears a row of elongate foramina, although the cluster of foramina visible on the anterolateral and ventral surface of the dentaries in IRSNB R33 are absent here. Medially, the Meckellian groove runs the length of the entire dentary along its ventral edge, narrowing anteriorly but remaining open, at the tip.

The teeth of both IRSNB 0107 and IRSNB 0108 also resemble those of IRSNB R33. In IRSNB 0107, the first tooth is missing but the anterior edge of the first alveolus is situated

directly against the edge of the dentary tip and steeply angled, suggesting it likely extended slightly beyond the jaw as in the holotype. The fourth tooth is also weakly procumbent, although the crowns seem to have straightened by the sixth tooth position. The first tooth in IRSNB 0108 is also procumbent, but this is less exaggerated than in IRSNB R33. The middle and posterior teeth that are preserved in both specimens have convex labial and straight lingual faces. The tooth crowns in both specimens also show a splayed orientation that is most evident in the anterior teeth of IRSNB 0108 (Fig. 2.27A, C). The roots and crowns of IRSNB 0108 are slightly inclined towards the labial face of the jaw (Fig. 2.26C). The enamel surfaces of the crowns in both specimens are strongly fluted from the base to the apex, and carinae are present on the medial and distal edges. Smaller features are difficult to observe on the erupting teeth of IRSNB 0108, but minute serrations and striations/crenulations near the crown apex are visible in IRSNB 0107 (Fig. 2.26C). Neither are visible on the fully erupted crowns.

Splenials—The left and right splenials of IRSNB 0108 are better preserved and identical to those of the holotype. Like the holotype, the lateral wing is shorter in height than the medial wing and tapers gradually posteriorly, whereas the tall medial wing terminates abruptly a little over halfway along the posterior bar (Fig. 2.27E-I). There is a weak indication of the elongate, curved sulcus on the face of the lateral wing, but this is less pronounced then in the holotype. The medial wing also bears a large, elongate foramen. The posterior articulating face with the angular is better preserved in IRSNB 0108, and like the holotype, bears a deep U-shaped cotyle overhung by a dorsal projection from the curved ventral tip of the lateral wing.

Coronoid—IRSNB 0108 and IRSNB 0107 both preserve mostly complete examples and are virtually identical to those of the holotype (Figs. 2.26D-E, 2.28A-F). Shared features are most visible in IRSNB 0108 and include the broad overhanging lip extending across the dorsal process and most of the lateral surface, fan-shaped lateral and anteromedial wings, and a wedge-shaped posterdorsomedial process, the internal surface of which is heavily striated (Fig. 2.28A). A sloped shelf on the internal ventral surface of the anteromedial process marks the border of a shallow articular facet with the surangular. The small, rounded protuberance on the medial surface of the dorsal process in the holotype is also visible on both coronoids of IRSNB 0108 (Fig. 2.28B, C, E). The dorsal processes of both referred specimens are also medially deflected, but this is most clear in IRSNB 0107 (Fig. 2.26C).

Cervical Vertebrae— IRSNB 0108 preserves three mostly complete and once highly fragmented cervical vertebrae. The first of the best two examples is dorsoventrally compressed but appears largely intact in lateral view (Fig. 2.29A-D), whereas the second is well-preserved across its mediolateral axis but heavily compressed anteroposteriorly (Fig. 2.29E-G). Like in the holotype, the centra are subcircular with notched dorsal borders, and a thin ventral crest from the synapophyseal processes curves towards and is continuous with the lateral margin of the cotyle. The prezygapophyses are similarly short and tapered, with the facets angled dorsomedially, the corresponding facets of the postzygapophyses slanted ventrolaterally. The hypapophyses are short and angled ventrally. The zygosphenes and zygantra are also large and particularly well-preserved.

DISCUSSION

The broad similarities shared between the holotype IRSNB R33 and IRSNB 0108 and IRSNB 0107 confirm that the latter two specimens are assignable to *Prognathodon solvayi*. This emended diagnosis likewise combines the description of all three specimens and finds several new characters with which to identify the taxon, including a low ridge on the lateral surface of the maxilla, horizontally oriented suspensorial rami originating proximally from the parietal, a flattened pterygoid lacking a ventral eminence for the tooth row, a medially deflected dorsal process of the coronoid, a vertically oriented and posteriorly projecting retroarticular process, an anteroposterior orientation of suture between the suprastapedial and posterolateral processes of the quadrate, a dorsomedial eminence of the quadrate, and a synapophyseal crest connecting with the lateral cotyle rim on the cervical vertebrae. While not visible on the holotype, the otherwise strong similarity of the premaxilla to the partial example from IRSNB 0107 suggests a shallow median dorsal sulcus of the premaxilla is also diagnostic for the species.

Notable changes from Lingham-Soliar and Nolf (1989) include: the reduction of the pterygoid teeth to six, the identification of a possible fragment of ectopterygoid, a curved rather than straight frontoparietal future with the addition of possible but largely ambiguous posteromedial flanges, and a more extensive description of the individual components of the dentition, cranium, and axial skeleton. This evaluation also reconsiders the characterization of multiple cranial elements as “robust”. The apparent shape and thickness of any given element is in many ways a matter of perception and entirely relative; however, there is little support for the notion that any element of *P. solvayi* (e.g., the maxilla, pterygoid, marginal dentition, etc.) is uniquely massively built. Notably, robustness as a character is not included in any of the initial diagnoses for the type species or genus (Dollo, 1889b), apart from the dentition (Russell, 1967; Lingham-Soliar and Nolf, 1967). Lindgren (2005) likewise noted the distinctiveness of the teeth

of *P. solvayi* compared to other assigned members of *Prognathodon*, specifically regarding their compressed shape, gently fluted surface, and blunted carinae. Despite this, the label has persisted and is considered effectively diagnostic of the group (Christiansen and Bond, 2002; Dortangs et al. 2002; Conrad, 2008; Bardet et al. 2000; Lindgren, 2005; Konishi et al. 2011). The concern with this interpretation of *Prognathodon* may on the surface appear trivial and semantical, but it effectively underscores the origin of the underlying issues surrounding the broader characterization of the group.

Much of the ongoing ambiguity surrounding *Prognathodon* appears to stem in large part from the initial paucity of a thorough description and the effective exclusion of the type species, *P. solvayi*, from early discussions of the genus, which set the benchmark for the later conception of the group (Russell, 1967; Bell, 1997). The key diagnostic features that were and are consistently carried forward from Dollo (1889b) center on the procumbent anterior marginal teeth and lack of a predental rostrum, the fusion of the suprastapedial and posterolateral/posterior pillar-like processes of the quadrate, and proportionately large pterygoid teeth. With only this available for reference and limited mention of the type specimen itself, Russell (1967) based much of the generic diagnosis of *Prognathodon* on the referred North American taxa (*P. crassartus*, *P. overtoni*, and *P. rapax*), seemingly resulting in the inclusion of several characters absent in *P. solvayi*, including a median dorsal ridge on the frontal, supraorbital wing of the prefrontal contacting the postorbitofrontal, small posteroventral process on jugal, seven pterygoid teeth, thick tympanic ala of the quadrate, medial coronoid wing contacting the angular, stout mandibular teeth, and small or absent zygosphenes and zygantra. In the diagnosis for the Prognathodontini, Russell (1967: pg. 162) also stated that *Prognathodon* was unique in having "…massive jaws with heavy dentition much more suited to crushing prey than that of members

of the Plioplatecarpini.”. However, the long, curved, and labiolingually compressed teeth of *P. solvayi* differ substantially from the rounded, blunt dentition in other *Prognathodon* taxa (Lindgren, 2005), as well as the stout and bulbous crowns of durophagous mosasaurs (Leblanc et al. 2019). Lingham-Soliar and Nolf (1989) later referred *P. crassartus* to *Plioplatecarpus* but maintained and contrasted *P. overtoni* and *P. rapax* with *P. solvayi*, effectively operating under Russell’s (1967) North American framework and ostensibly influencing the conceptualization of both the type species and genus as a whole. Much of the current paradigm surrounding *Prognathodon* as a taxon with massive jaws and teeth is therefore based less on the type specimen, and more so on later referred species, such as *Prognathodon overtoni*. This has resulted in the continuous referral of specimens with massively built skulls and/or robust dentition to the genus, particularly those with fused processes of the quadrate (Welles and Gregg, 1972; Christiansen and Bonde, 2002; Dortangs et al. 2002; Lindgren, 2005), but no consistent resolution of the groups’ phylogenetic interrelationships (Simoes et al. 2017; Lively, 2020).

Character evaluation of *Prognathodon solvayi*

The same issues that ostensibly produced the current concept of *Prognathodon* also affect the instability of its systematic relationships. Bell’s (1997) major revision of the major mosasaur groups omitted *P. solvayi* from the analysis, instead using Russell’s (1967) referred taxa, *P. overtoni* and *P. rapax.* This did not include *P. crassartus* as Lingham-Soliar and Nolf (1989) had since reassigned it to *Plioplatecarpus*. The revised trees contrasted strongly with Russell’s (1967) conclusions and resulted in *Prognathodon* maintaining its ingroup relationships but nesting within the Globidensini alongside *Globidens* and *Plesiotylosaurus*, switching from the Plioplatecarpinae to the Mosasaurinae. Bell (1997) made particular note of the fused processes of

the quadrate, horizontal inflection of the retroarticular process, roughly textured, anastomosing enamel surface of marginal tooth crowns, and inflated posterior crowns in *Prognathodon*; however, only the quadrate fusion and to a lesser degree the anastomosing texture is applicable to *P. solvayi*. Furthermore, Character 1 describing the absence or presence of a premaxillary rostrum was coded as present for both *P. overtoni* and *P. rapax* but would be absent in *P. solvayi*. Character 42 relating the elevation of the pterygoid tooth row coded *Prognathodon* as having a tooth row emanating from a ridge on the main body of pterygoid, but this ridge is also absent in *P. solvayi*. Conversely, while Christiansen and Bonde (2002) included the type specimen in their description of a new species, *Prognathodon currii*, and likewise recovered the genus within the Mosasaurinae, a subsequent analysis by Conrad (2008) referencing Dollo (1889b), Russell (1967), Bell (1997), and Christiansen and Bonde (2002) again recovered *Prognathodon* within the Plioplatecarpinae. Several synapomorphies supported this grouping, the notable ones including the presence of a basioccipital canal, procumbent anterior teeth, and broad postorbital processes of the parietal. However, there were several discrepancies with the scoring of *Prognathodon*. Although Christiansen and Bonde (2002) scored the predental rostrum as present in *P. overtoni* and absent in *P. solvayi*, this was scored as present in both *P. overtoni* and *P. solvayi* in Conrad (2008) (character 15). The retroarticular process is also erroneously coded as inflected in *P. solvayi* (character 210). Furthermore, a clade formed by *Ectenosaurus* and *Prognathodon* was supported by the presence of a tall and narrow coronoid process, unforked supratemporal processes of parietal contacting the supratemporal, and lack of contact between the prefrontal and postorbitofrontal. This grouping is tenuous as the relative size and shape of the coronoid overall are very different between the two taxa, *Ectenosaurus* lacking the large, fan-shaped medial and lateral processes that are present in *P. solvayi* (Lindgren et al. 2011;

Willam et al. 2021). The supratemporal is also clasped between the forked processes of the parietal in *Prognathodon*, and the prefrontal and postorbitofrontal are in contact and overlapping in *P. overtoni* (Russell, 1967; Konishi et al. 2011). In direct contrast to Conrad's (2008) findings, Christiansen and Bonde (2002) scored the latter character as overlapping for *P. solvayi* in character 30 but (?) for whether the postorbitofrontal overlapped the prefrontal ventrally or laterally (character 31). *Prognathodon solvayi* is also scored as having straight margins on the frontal (character 9), despite Lingham-Soliar and Nolf (1989) describing convex lateral margins that become concave anteriorly. The anterior projection of the dentary beyond the first tooth position was also scored as present (0) for *P. solvayi* (Character 69), although both Russell (1967) and Lingham-Soliar and Nolf (1989) included the lack of an anterior dentary projection in their generic diagnoses. Finally, several scorings in the descriptions of *Prognathodon saturator* contrast with our current observations (Dortangs et al. 2002; Schulp 2006), wherein *P. solvayi* was erroneously scored as lacking both serrations and flutes on the marginal teeth, having a rotated retroarticular process, contact between the coronoid and angular medial wings, and no coronoid posteromedial process.

The above selected examples demonstrate that, whether through its omission altogether or inconsistent character scorings amongst clade members across different studies, certain key diagnostic characters of *P. solvayi* have been continuously excluded from systematic analysis. Many characters are not shared with other referred members of the genus, such as the lack of a predental rostrum. These issues stem primarily from the prevailing conception of *Prognathodon* and have evidently played a crucial role in the resulting systematic relationships of the type species and the genus. Although *Prognathodon* is currently widely considered to be firmly nested within the Mosasaurinae (Schulp et al. 2008; Bell and Polcyn; Konishi et al. 2011;

Leblanc et al., 2012; Madzia and Cau, 2017; Simoes et al. 2017; Christiansen and Bonde, 2002; Dortangs et al. 2002; Simoes et al. 2017; Lively, 2020; Longrich et al. 2022), the fact that *Prognathodon* was originally considered a member of the Plioplatecarpinae emphasizes the comparative uniqueness of the type species and therefore warrants further examination.

Review of plioplatecarpine and mosasaurine characters

The short, broad posterior temporal arcade, short tapering jaws, and long, slender teeth of *P. solvayi* on initial inspection bears strong resemblance to certain plioplatecarpines, such as *Latoplatecarpus* (Konishi and Caldwell, 2011), *Plesioplatecarpus* (Konishi and Caldwell, 2011), *Plioplatecarpus* (Konishi and Caldwell, 2009), and *Selmasaurus* (Wright and Shannon, 1988; Polcyn and Everhart, 2008). Other similar but previously undescribed characters that *P. solvayi* shares include the medial inflection of the coronoid process, a vertically oriented retroarticular process, and a horizontal orientation of the base of the supratemporal processes (*cf.* *Latoplatecarpus* Konishi and Caldwell, 2009; *Plioplatecarpus* Konishi and Caldwell, 2009; *Selmasaurus* Polcyn and Everhart, 2008). These features generally differ in mosasaurines, which tend to have an uninflected coronoid process, rotated retroarticular processes relative to the PMU, and a vertically oriented base of the supratemporal processes (compare *Clidastes*, Lively, 2019; *Mosasaurus*, Konishi et al. 2014; *Plotosaurus*, Leblanc et al. 2013).

Despite the apparent similarities, *P. solvayi* shows subtle but unique differences in addition to numerous typically mosasaurine features that indicate purported plioplatecarpine characteristics are not homologous. Russell's (1967) diagnosis of the Plioplatecarpinae included several characters broadly applicable to *Prognathodon*, namely a small or absent rostrum of the premaxilla, a canal for the basilar artery penetrating the basioccipital and basisphenoid, rounded

(possibly meaning concave) and horizontally oriented dorsal margin of the surangular, and twelve or more teeth in the dentary. As evidence that *Prognathodon* belonged within the Plioplatecarpinae, Russell (1967) referenced the groove or canal located on the floor of the basioccipital and basisphenoid, smooth or faceted teeth that are elliptical in shape, and fused or unfused haemal arches of the caudal vertebrae. There are no caudals associated with any specimen of *P. solvayi* currently or at the time of Lingham-Soliar and Nolf's (1989) description, although the authors noted Dollo (1889b) stated the chevrons were both "free" and co-ossified with the haemal arches. Determinable characters for the type species include the short, blunt-ended premaxillary rostrum, which is also present in *Latoplatecarpus* (Konishi and Caldwell, 2011), *Plesioplatecarpus* (Konishi and Caldwell, 2011), *Plioplatecarpus* (Konishi and Caldwell, 2009), and *Selmasaurus* (Wright and Shannon, 1988; Polcyn and Everhart, 2008). Apart from *Plioplatecarpus*, *P. solvayi* is nevertheless largely distinct in altogether lacking a rostrum extending beyond the first tooth position. Similarly, the strongly procumbent premaxillary teeth for which *Prognathodon* is named occurs in *Latoplatecarpus* and *Plioplatecarpus*, albeit to a lesser extent (Holmes, 1996; Konishi and Caldwell, 2009; Konishi and Caldwell, 2011). The anterior-most dentary teeth in *Latoplatecarpus* and *Selmasaurus* are also procumbent (Konishi and Caldwell, 2011; Polcyn and Everhart, 2008), but this feature is more developed and present in a greater number of tooth positions in *P. solvayi*. Procumbence is also not limited to the Plioplatecarpinae: Although rarely noted and possibly influenced by taphonomy, weakly procumbent premaxillary teeth are present in some examples of *Mosasaurus*, including *Mosasaurus hoffmannii* (Lingham-Soliar and Nolf, 1995; compare Mulder, 1999: fig. 3), *Mosasaurus conodon* (Ikejiri and Lucas, 2004: fig. 3), *Mosasaurus glycys* (Street, 2016: formerly *M. hoffmannii* (Mulder, 1999: fig. 5), and *Mosasaurus lemonnieri* (Madzia, 2020: fig. 4).

Descriptions of the enamel ornamentation of the marginal dentition in *P. solvayi* have also varied heavily, often with different terms applied to the same enamel structure. The narrow grooves separated by thin, longitudinal ridges on the teeth of *P. solvayi* have been occasionally referred to as facets (Dollo, 1889b), flutes (Lingham-Soliar and Nolf, 1989), or striations (Russell, 1969; Lingham-Soliar and Nolf, 1989; Conrad, 2008). Street et al. (2021) found that tooth facets and flutes represent different ends of the same spectrum and should be treated as a single character in phylogenetic analysis. In *P. solvayi*, the grooves and ridges are more widely spaced and occur on the entire crown. It is therefore most accurate to refer to these features as flutes. Street et al. (2021) found striations differ developmentally from flutes and facets, are generally restricted to the base of the crown, and appear primarily in russellosaurines and/or plioplatecarpines. In contrast, flutes, facets, carinae, serrations, and anastomosing texture, most of which are present in *P. solvayi*, were shown to occur mainly within the Mosasaurinae. The faint ridges or crenulations restricted to the apices of the marginal teeth in *P. solvayi* have also been referred to as striations (Lindgren, 2005), although these are not comparable to the striations described in Street et al. (2021) and may instead represent very weakly developed anastomosing texture.

With regard to skeletal characters, the basioccipital canal featured heavily in several examinations of the genus following Russell's (1967) diagnosis (Bell, 1997; Christiansen and Bonde, 2002; Conrad, 2008). However, Cuthbertson et al. (2005) stated the basioccipital canal is paired and exits through both sides of the lateral walls of the basisphenoid in plioplatecarpines, which is not the case for *Prognathodon*. Conversely, Bell (1997) remarked that the canal in *Prognathodon* differed from those in plioplatecarpines in being a single, blind-ended chamber situated along the midline, and therefore likely not homologous. This view was shared by

Konishi et al. (2011), who nevertheless determined this character is diagnostic for *Prognathodon* and differentiates the group from other mosasaurines.

Other cranial characters purportedly linking *P. solvayi* to the Plioplatecarpinae included the surangular, the dorsal margin of which is largely straight in *P. solvayi*, rather than the concave or curved margin in plioplatecarpines (Konishi and Caldwell, 2009; Konishi and Caldwell, 2011; Polcyn and Everhart, 2008). While the surangular in many mosasaurines expands anteriorly and the posterodorsal margin forms a buttress against the posterior wing of the coronoid (e.g., *Mosasaurus*, *Eremiasaurus*, and *Globidens simplex*; Leblanc et al. 2012; Street and Caldwell, 2017; Leblanc et al. 2019), the surangular of the mosasaurine *Globidens schurmmani* (Martin, 2007) is shaped similarly to that of *P. solvayi*. The presence of the surangular fossa is also shared with *Globidens schurmmani*, and *Eremiasaurus* (Martin, 2007; Konishi et al. 2011; Leblanc et al. 2012). In addition, the coronoid of *P. solvayi* bears close semblance to those of mosasaurines in possessing an elaborate series of large lateral and medial wings and a deeply concave dorsal margin (compare *Eremiasaurus, Globidens*, *Mosasaurus* Martin, 2007; Leblanc et al. 2012; Konishi et al. 2014; Street and Caldwell, 2017; Leblanc et al. 2019). The presence of the prominent supraorbital process on the prefrontal and postorbitofrontal is also a typically mosasaurine feature (Bell, 1997; Konishi et al. 2011).

CONCLUDING STATEMENTS

This extensive reassessment underscores the morphological peculiarities present in *P. solvayi*, particularly its distinct combination of both typically mosasaurine and seemingly plioplatecarpine characteristics. A survey of these features nevertheless demonstrates that many of the apparent similarities between *P. solvayi* and plioplatecarpines are superficial and instead

likely constitute a series of homoplastic characters. In accordance with the preponderance of mosasaurine characters, *P. solvayi* therefore represents a unique member of the Mosasaurinae. Although these findings agree with the broader consensus on the classification of *Prognathodon*, a review of the conceptualization of the genus finds a series of recurring issues that continue to play a role in the broader taxonomic classification of the group. This redescription and emended diagnosis provide a refined definition of *Prognathodon* with several new characters that further identify the type species and challenges the long-held notion that the genus constitutes a group of massively built mosasaurs with robust crania and dentition. This recharacterization of the type species indicates further investigation and a comprehensive review of referred taxa is required to resolve the longstanding and complex controversies regarding the evolutionary relationships of this genus.

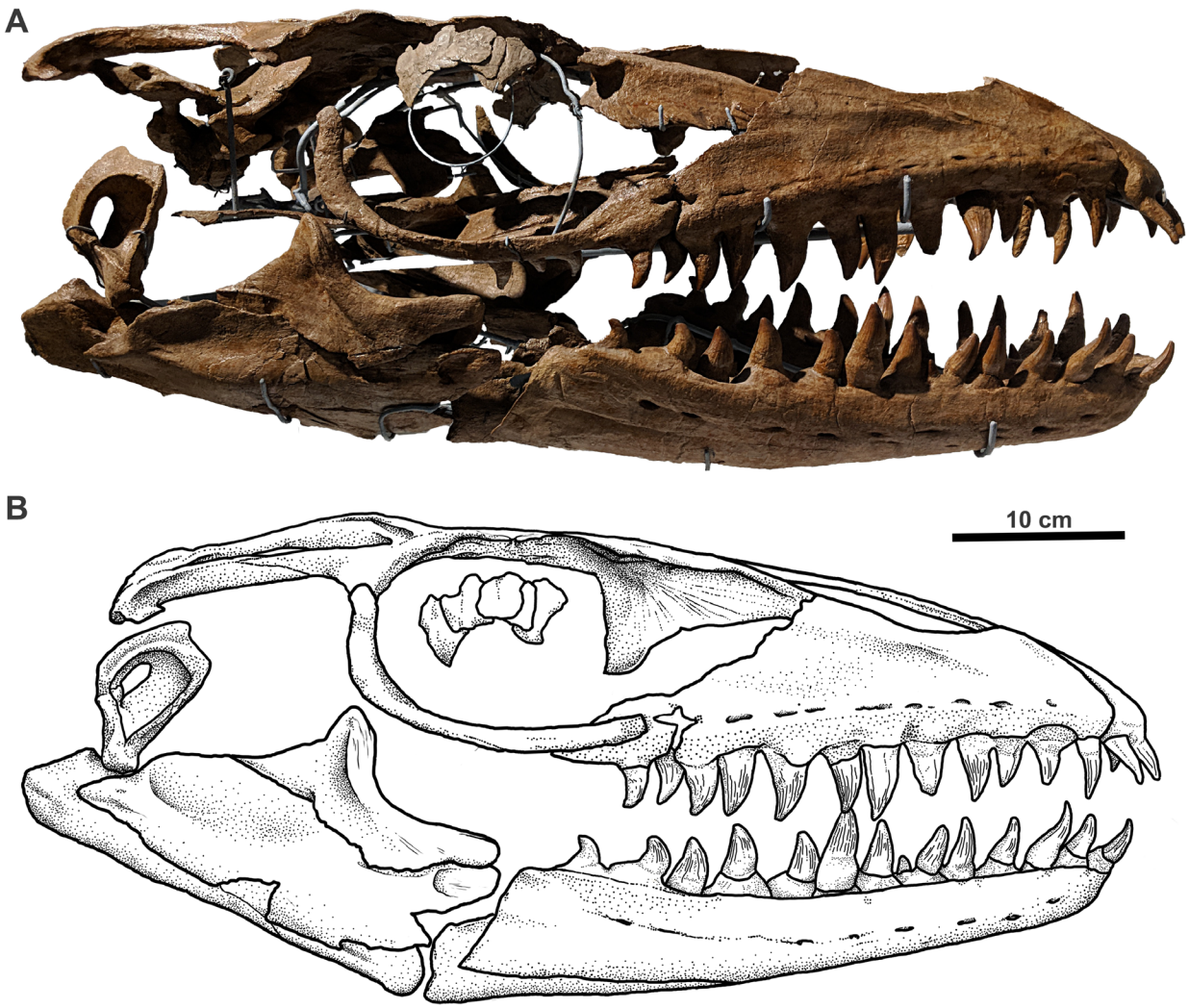

Figure 2.1. (A) mounted skull of IRSNB R33; (B) reconstruction of dermatocranium and quadrate of *Prognathdon solvay*i with elements moved into hypothetical life positions.

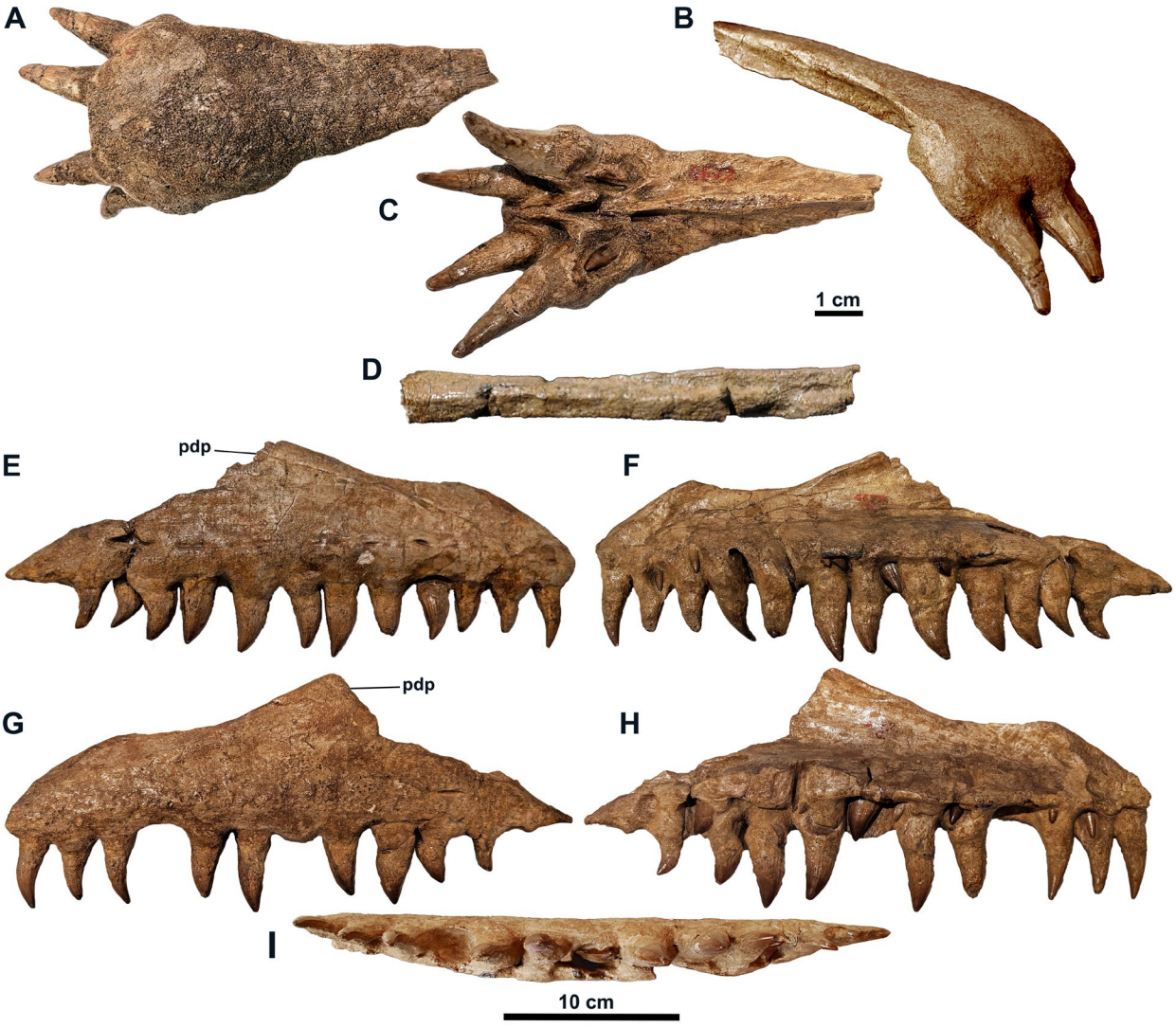

Figure 2.2. IRSNB R33 premaxilla in (A) dorsal, (B) lateral, and (C) ventral views; fragment of internarial bar in (D) dorsolateral view; right maxilla in (E) lateral and (F) medial views; left maxilla in (G) lateral, (H) medial, (I) dorsal views. Abbreviations: pdp: posterodorsal process.

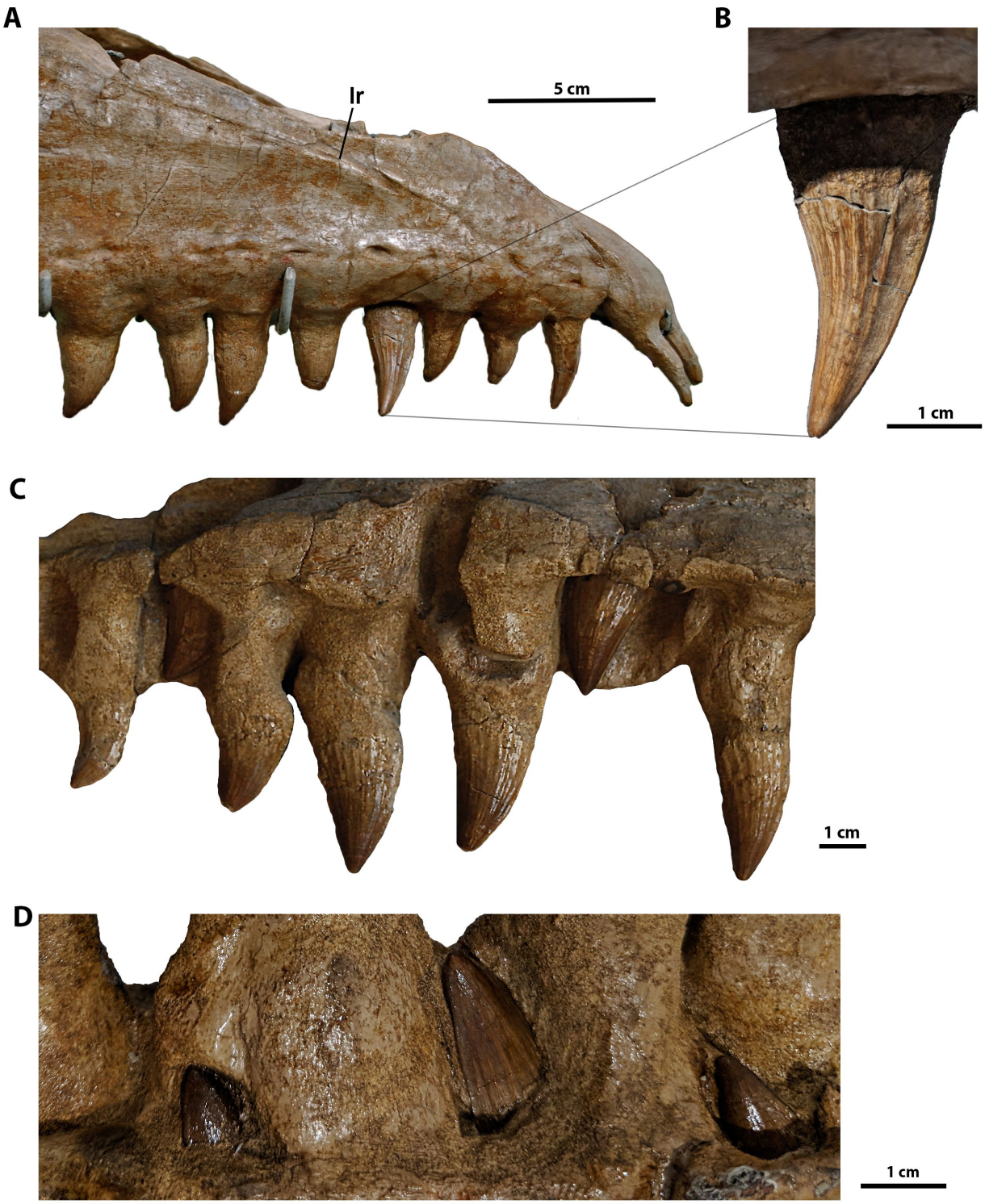

Figure 2.3. Premaxillary and maxillary dentition of IRSNB R33 in (A) lateral view, right maxilla; (B) closeup of flutes and unserrated carinae, 4th tooth position; (C) medial view of posterior maxillary dentition on left maxilla, including replacement teeth; (D) Replacement teeth on right maxilla. Abbreviations: lr, lateral ridge.

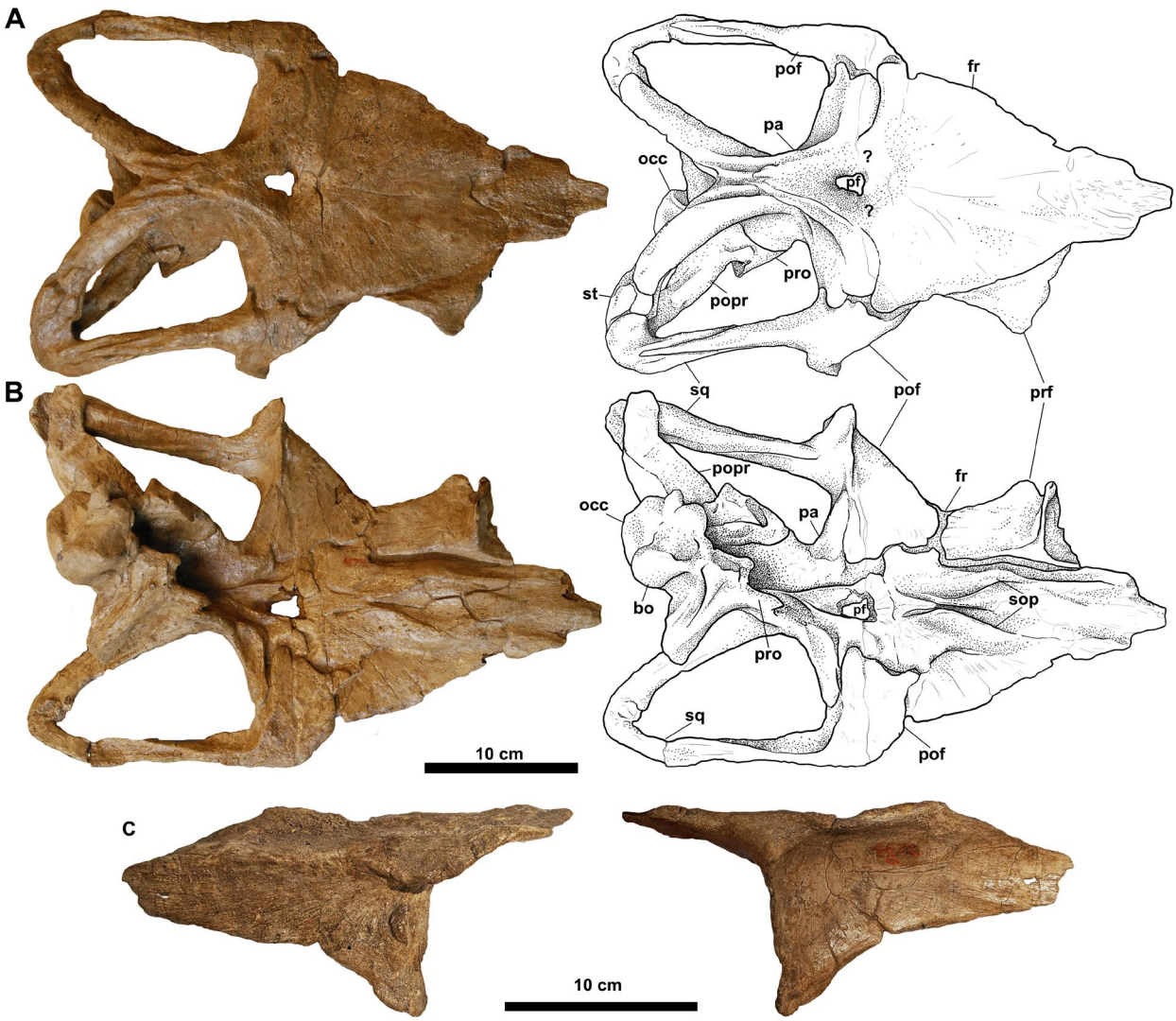

Figure 2.4. Skull roof of IRSNB R33 in (A) dorsal and (B) ventral views; left prefrontal in (C) lateral and medial views. Abbreviations: bo, basioccipital process; fr, frontal; occ, occipital condyle; pf, parietal foramen; pof, postorbitofrontal; popr, paroccipital process; prf, prefrontal; pro, prootic; sop, subolfactory processes; sq, squamosal.

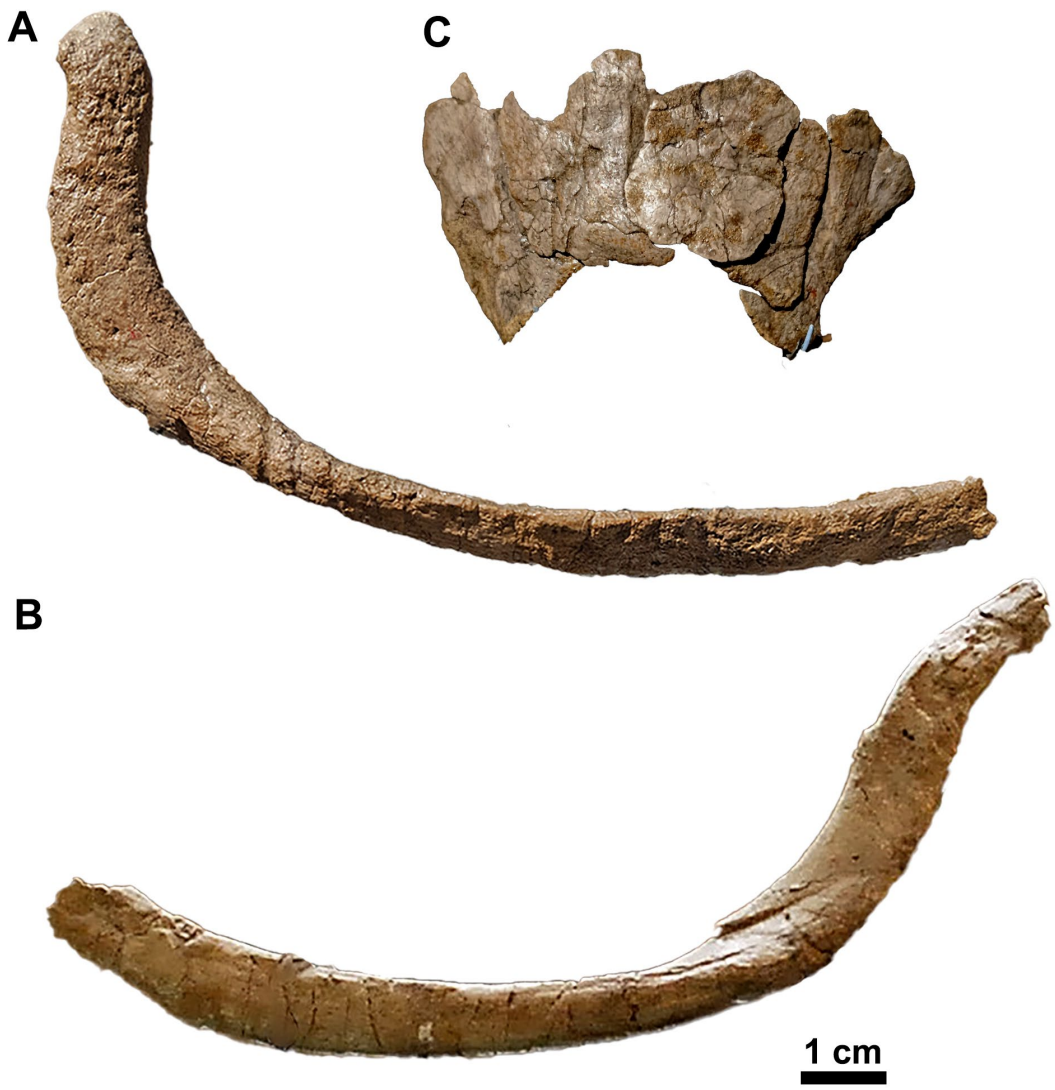

Figure 2.5. IRSNB R33 right jugal in (A) lateral view; left jugal in (B) lateral view. Fragment of right sclerotic ring in (C) lateral view.

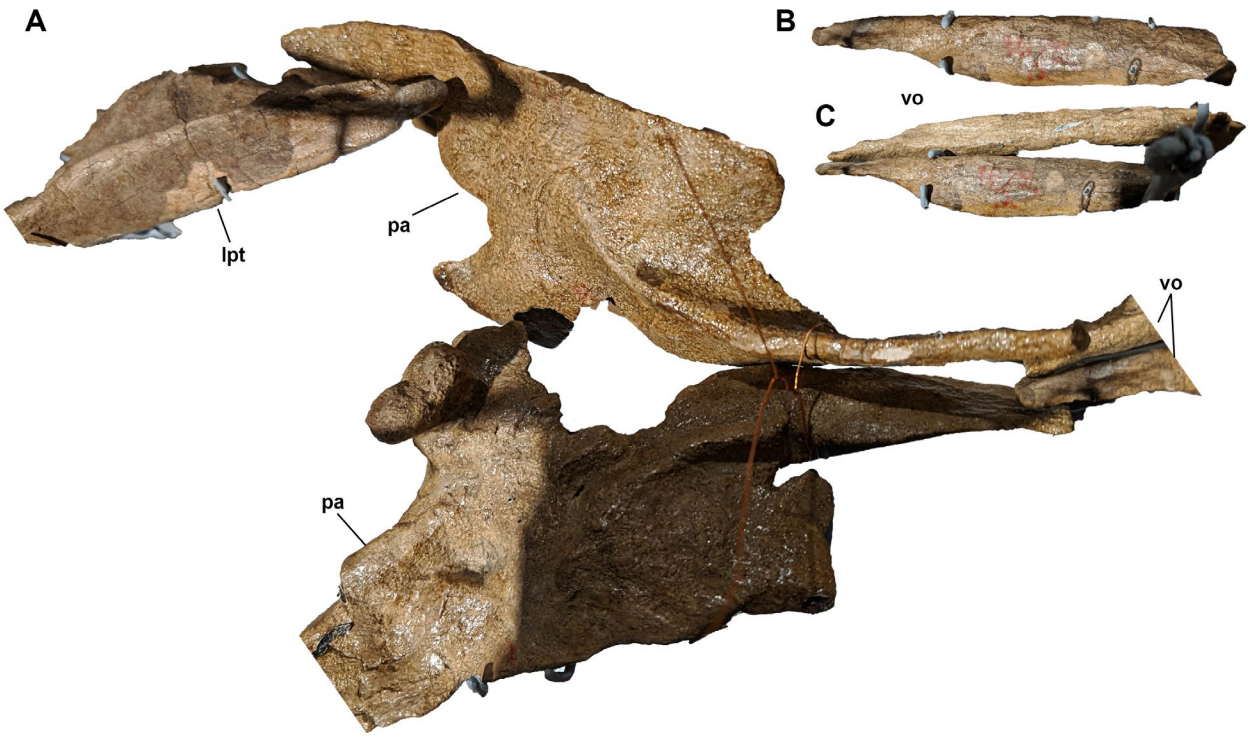

Figure 2.6. Palatines and vomers of IRSNB R33. (A) left and right palatines with anterior fragment of pterygoid and posterior segment of vomers; (B) vomer in dorsal view; (C) vomers in lateral view. Abbreviations: lpt, left pertgoid; lpa, left palatine; rpa, right palatine; vo, vomer(s).

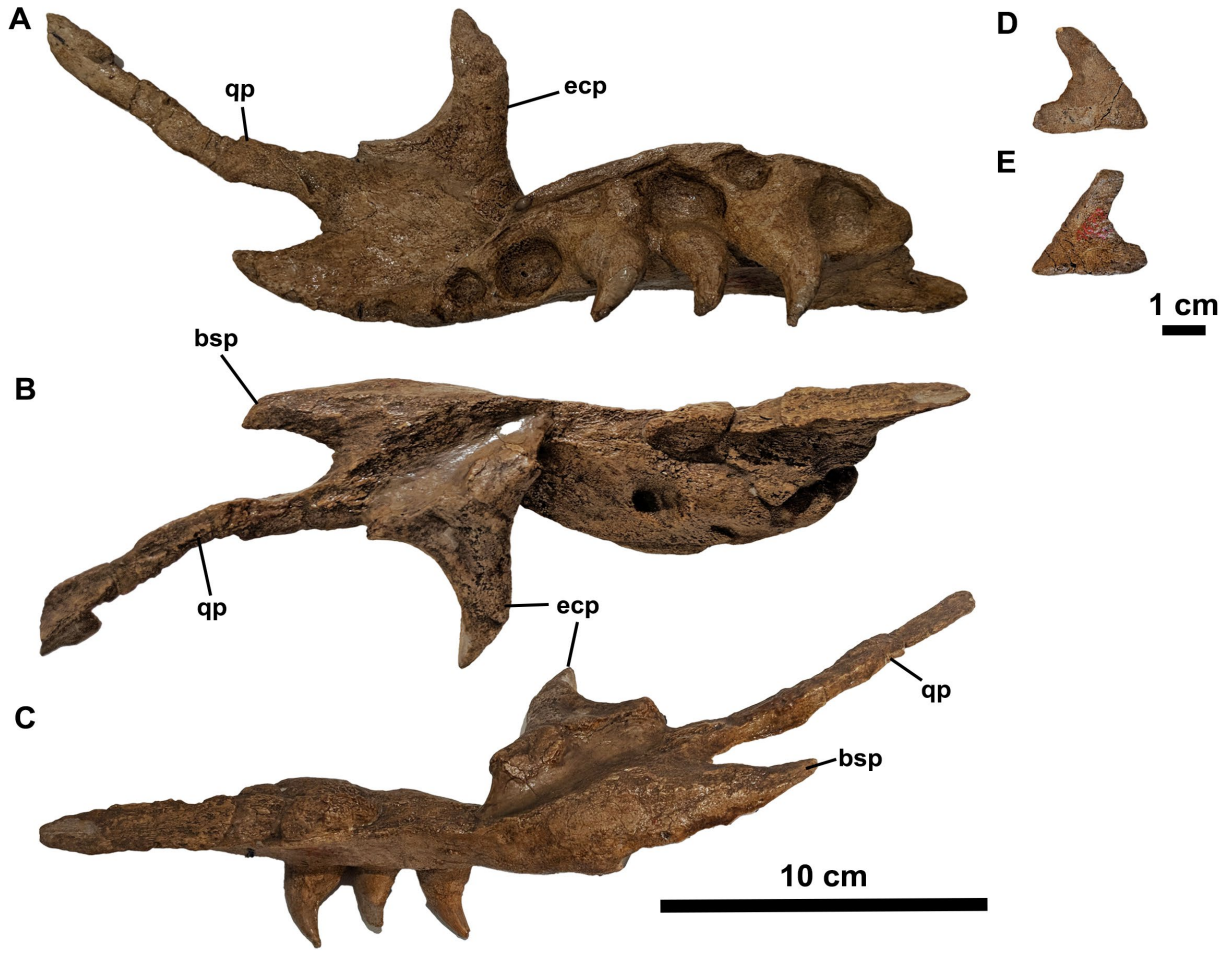

Figure 2.7. Pterygoid of IRSNB R33 in (A) ventral, (B) dorsal, and (C) medial views; Ectopterygoid(?) in (D) dorsal(?) and (E) ventral(?) views. Abbreviations: bsp, basisphenoid process; ecp, ectopterygoid process; qp, quadrate process.

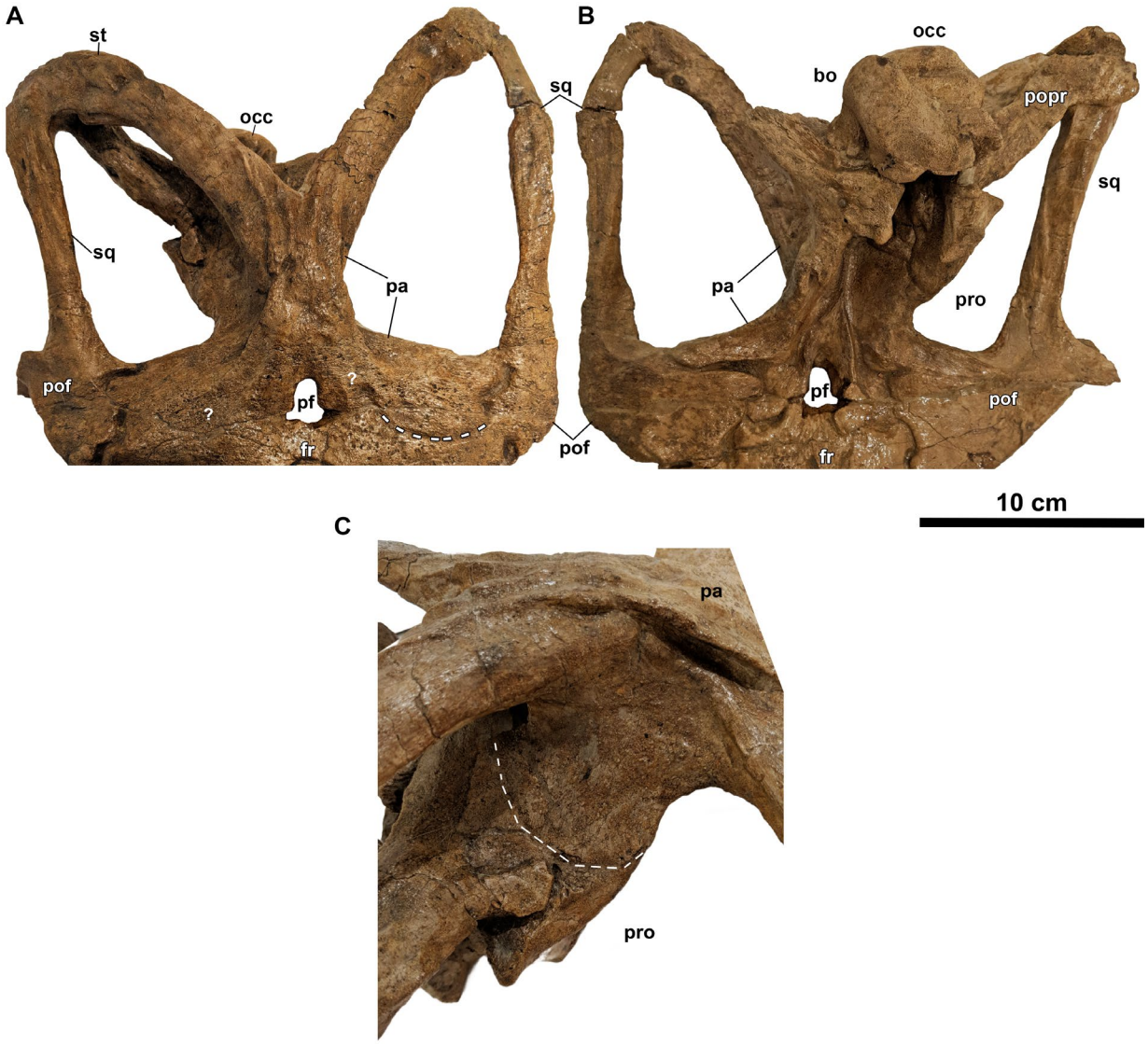

Figure 2.8. Parietal of IRSNB R33 in (A), dorsal, (B), ventral, and (C), right lateral views. Dotted line in (A) indicates visible anterior border on left postorbital process of parietal, and "?" indicates where the border is less clear or not visible. Dotted line in (C) indicates border of descending process of parietal. Abbreviations: bo, basioccipital; fr, frontal; occ, occipital condyle; pa, parietal, including supratemporal processes; pof, postorbitofrontal; popr, paroccipital process; pro, prootic; sq, squamosal, st, supratemporal.

Figure 2.9. Squamosal of IRSNB R33 in (A) dorsal, (B) ventral, and (C) lateral views. Dotted line in (B) approximates the ventral borders of the squamosal and postorbitofrontal. Abbreviations: pa, parietal; plc, posterolateral crest; pof, postorbitofrontal; popr, paroccipital process of the opisthotic; qp, quadrate process; pro, prootic; sq, squamosal; stp, supratemporal processes of parietal.

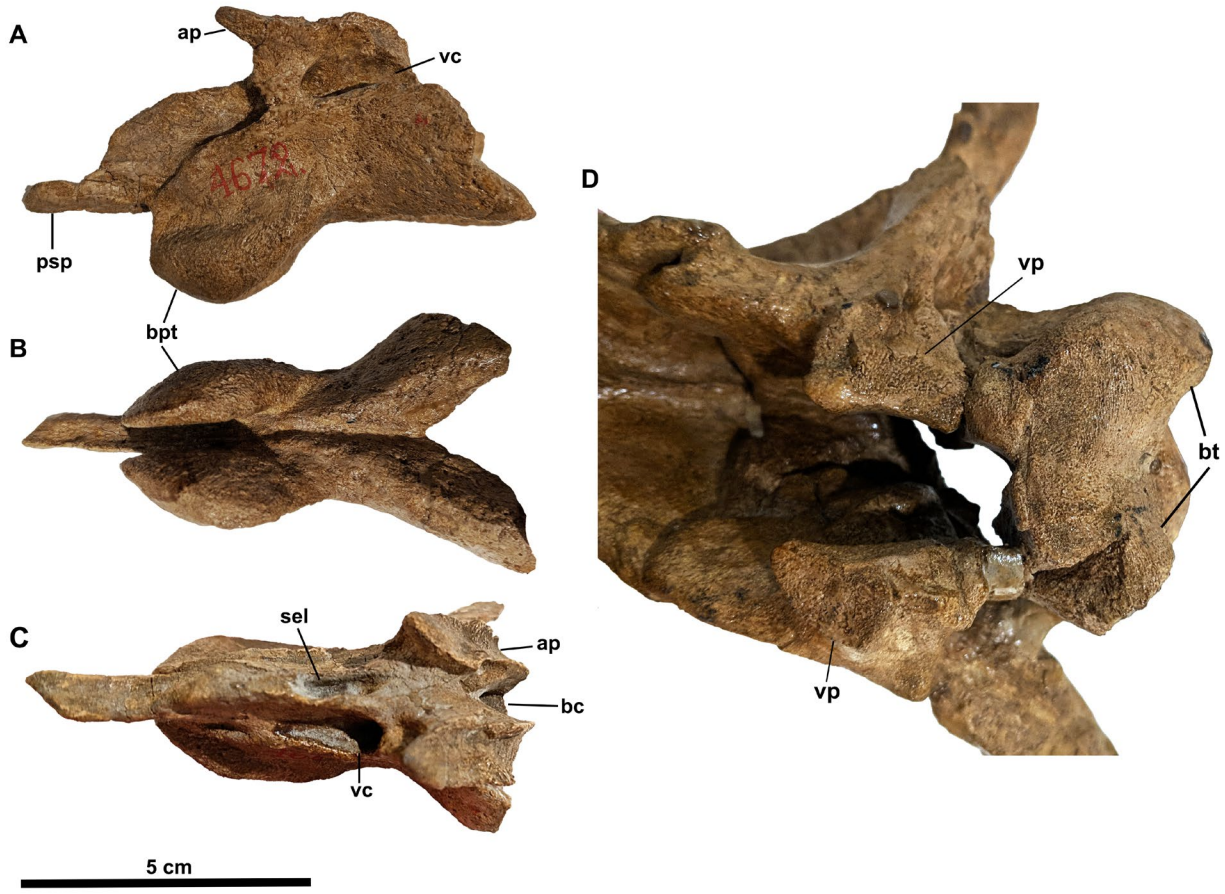

Figure 2.10. Basisphenoid of IRSNB R33 in (A), lateral, (B), ventral and (C), dorsal views; (D) ventral view of skull roof, including the articulation sites of the prootic and basioccipital with the basisphenoid. Abbreviations: ap, alar process; bc, basioccipital canal; bpt, basipterygoid processes; bt, basioccipital tubera; psp, parasphenoid process; sel, sella turcica; vc, vidian canal; vp, ventral pedestals of prootic.

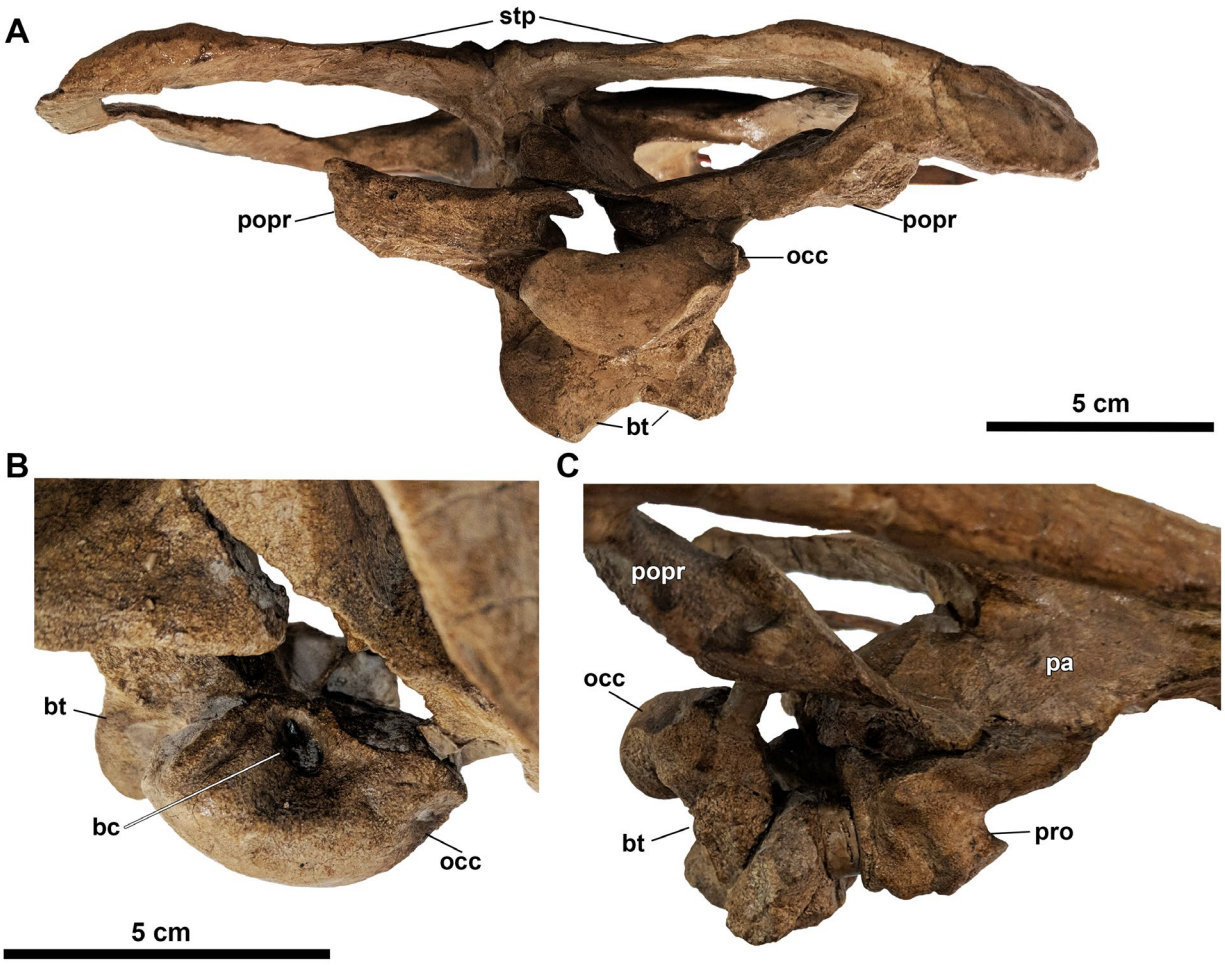

Figure 2.11. Basioccipital and associated braincase and skull roof elements of IRSNB R33 in (A) posterior, (B) dorsal, and (C) right lateral views. Abbreviations: bc, basioccipital canal; bt, basioccipital tubera, occ, occipital condyle; pa, parietal; popr, paroccipital process of the opisthotic; pro, prootic; stp, supratemporal processes of parietal.

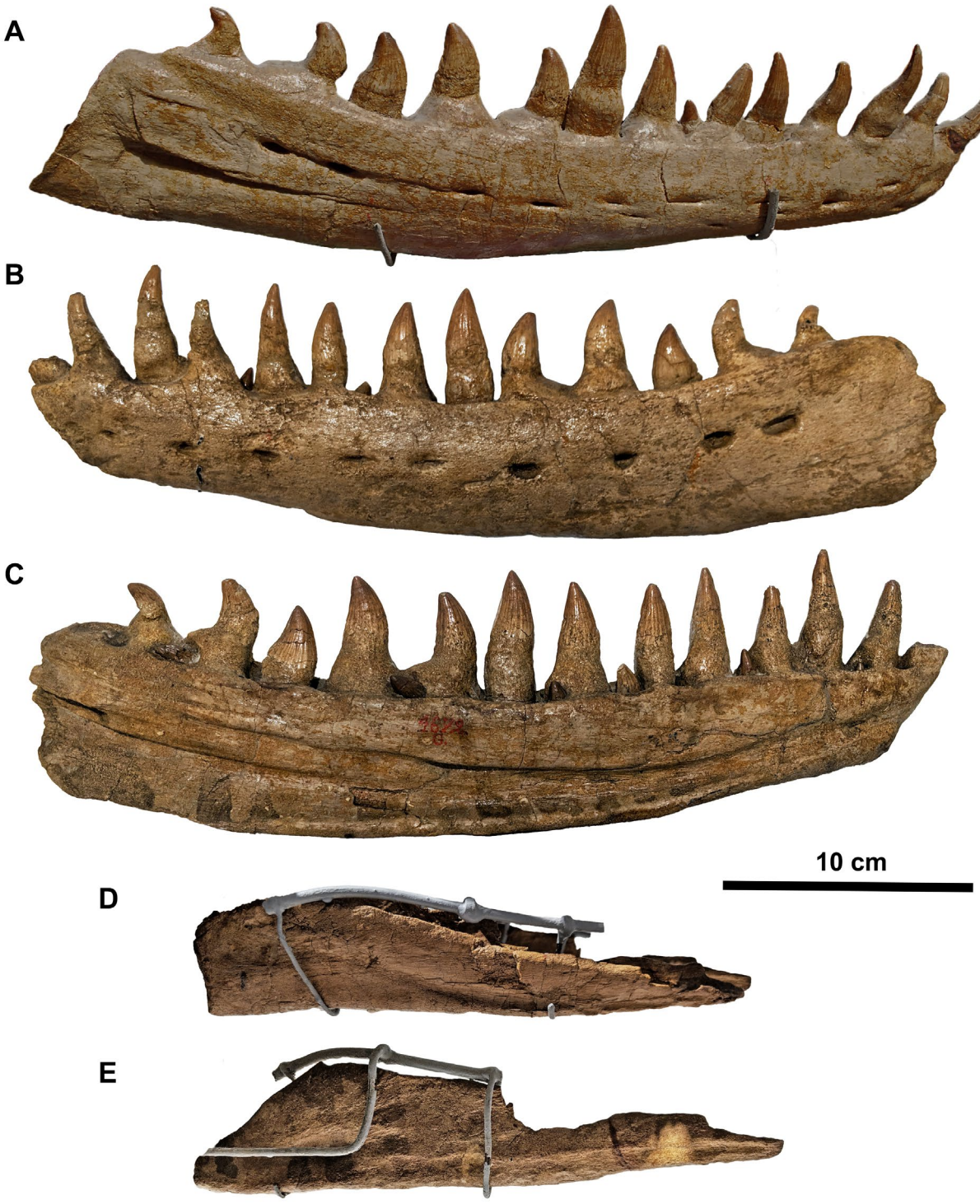

Figure 2.12. Right dentary of IRSNB R33 in (A) lateral view; left dentary in (B) lateral and (C) medial views; mounted right splenial IRSNB R33 in (D) lateral view; mounted left splenial in (E) medial view.

Figure 2.13. Ventral section of posterior mandibular unit (PMU) of IRSNB R33. Left articular/prearticular and angular in (A) medial, (B) lateral, and (C) dorsal views; right articular/prearticular in (D) lateral and (E) dorsal views; right angular in (F) lateral, (G) medial, and (H) dorsolateral views. Abbreviations: ang, angular; art, articular; gf, glenoid fossa; rep, retroarticular process.

Figure 2.14. Dorsolateral section of posterior mandibular unit (PMU) of IRSNB R33. Right surangular and coronoid in (A) lateral, (B) medial, (C) dorsolateral views. Right coronoid in (D) dorsal view; left surangular and coronoid in (E) lateral and (F) medial views. Abbreviations: adf, adductor fossa; am, anteromedial process; cp, coronoid (dorsal) process; gf, anterolateral border for glenoid fossa; lw, lateral wing; suf, surangular fossa.

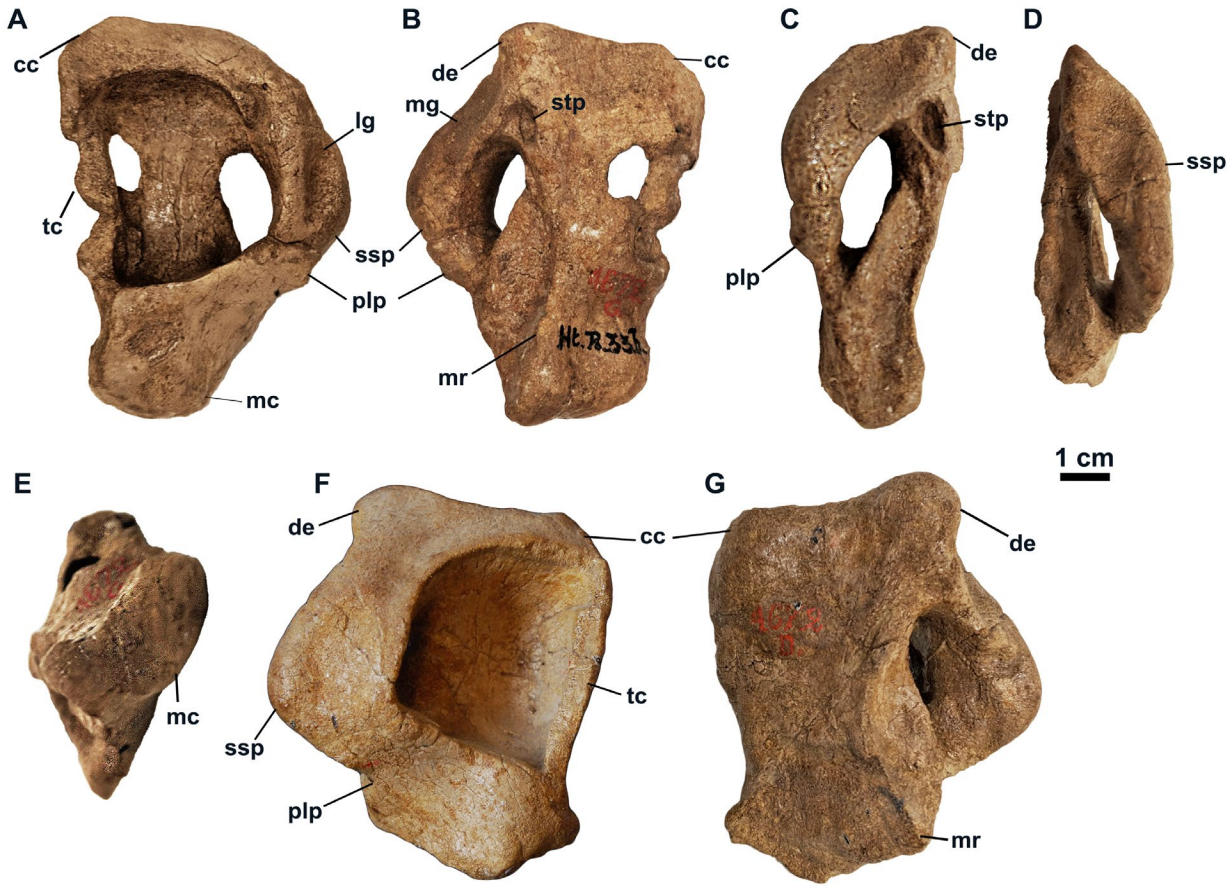

Figure 2.15. IRSNB R33 left quadrate in (A) lateral, (B) medial, (C) posterior, (D) dorsal, and (E) ventral views; right quadrate in (F) lateral and (G) medial views. Abbreviations: cc, cephalic condyle; de, dorsomedial eminence; lg, lateral groove; mc, mandibular condyle; mg, medial groove; mr, median ridge; plp, posterolateral process; ssp, suprastapedial process; stp, stapedial pit, tc, tympanic crest.

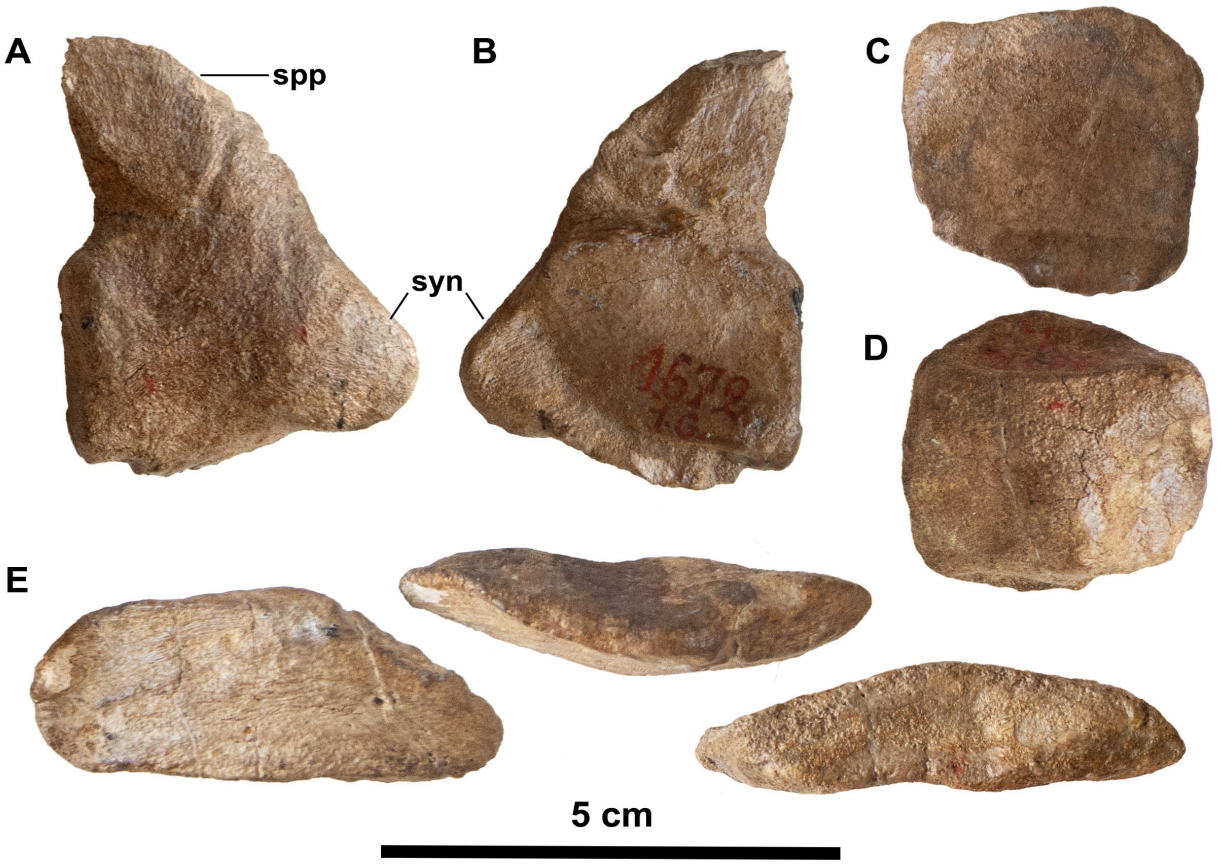

Figure 2.16. Atlantal elements of IRSNB R33. Left atlas neural arch in (A) lateral and (B) medial views; atlas centrum in (C) anterior and (D) posterior views; (E) various views of atlas intercentrum. Abbreviations: spp, spinous process; syn, synapophyseal process.

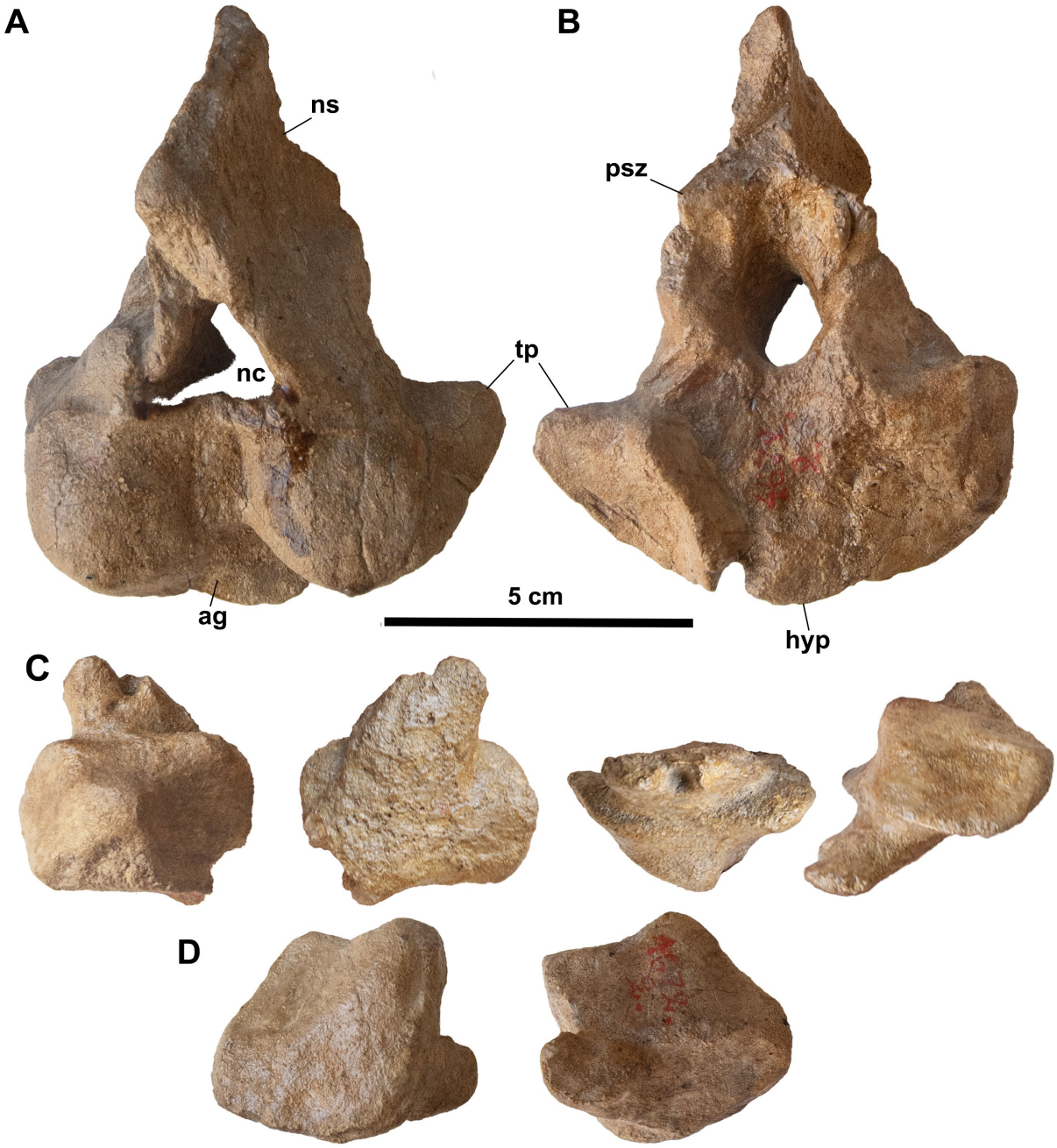

Figure 2.17. Axis elements of IRSNB R33 in (A) anterior and (B) posterior views; (C) posterior axis intercentrum in anterodorsal, ventral, posterior, and lateral views; (D) second axis/ cervical intercentrum in dorsolateral and ventral views. Abbreviations: ag, anterior groove; hyp, base of hypapophysis; nc, neural canal; ns, neural spine; psz, base of postzygapophysis; tp, transverse process.

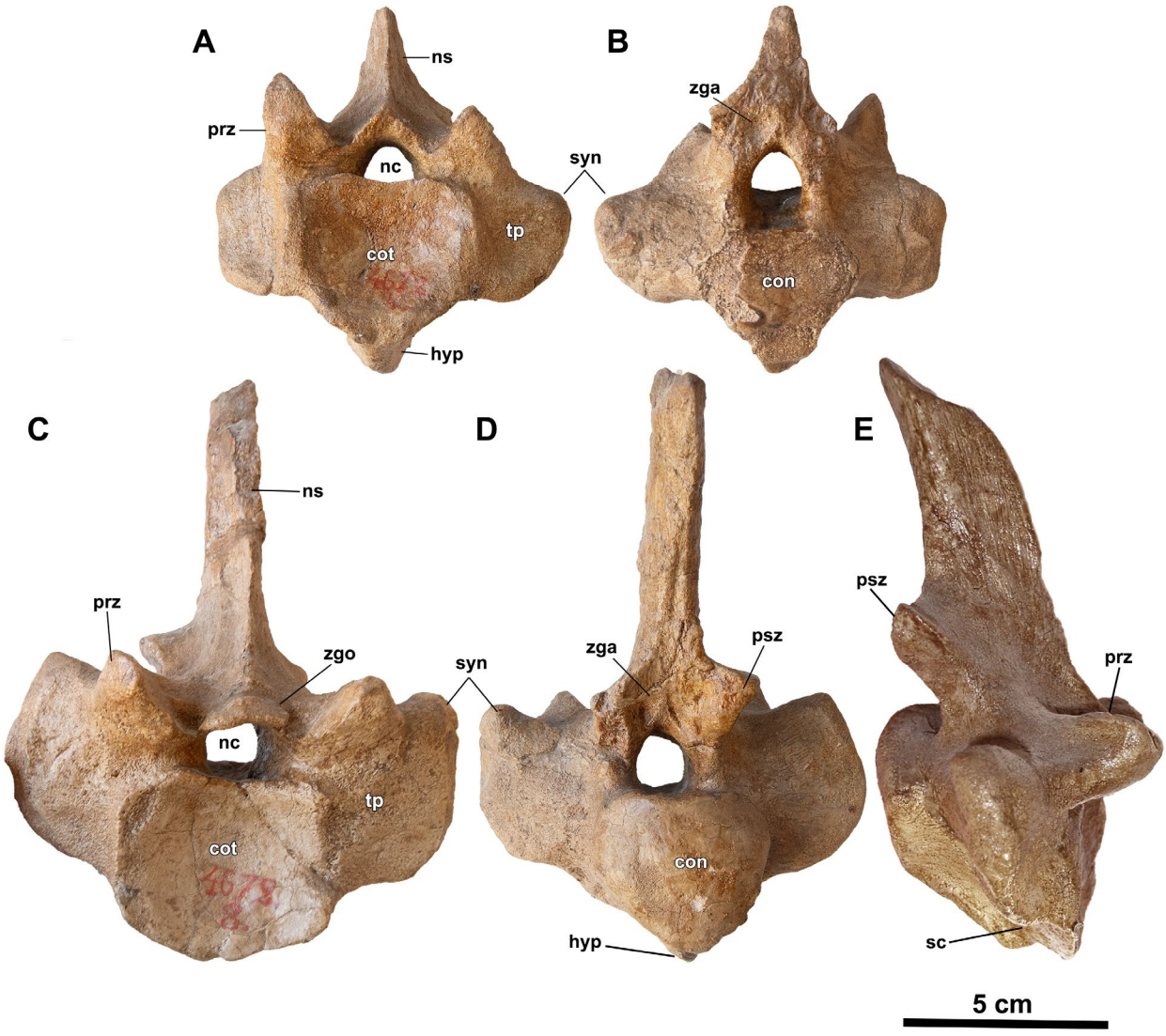

Figure 2.18. Select cervical vertebrae of IRSNB R33 in (A) anterior, (B) posterior, (C) anterior, (D) lateral, and (E) posterior views. Note that (E) represents a different element from (C) and (D) and was included as it best preserves the synapophyseal crest. Abbreviations: cot, cotyle; con, condyle; hyp, posterior fragment of hypapophysis; nc, neural canal; ns, neural spine; prz, prezygapophysis; psz, postzygapophysis; sc; synapophyseal crest; syn, synapophyseal process; tp, transverse process; zga; zygantra, zgo, zygosphene.

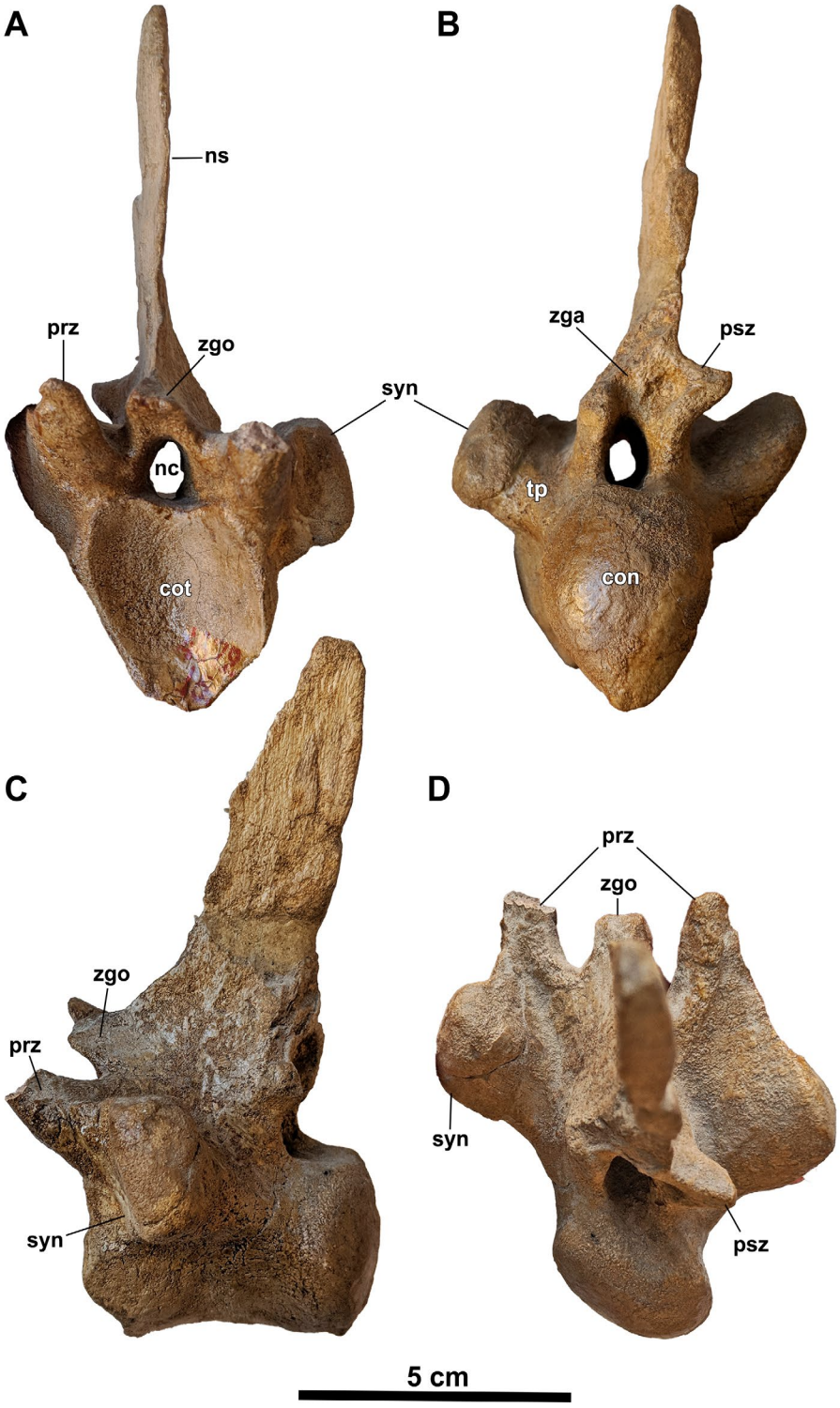

Figure 2.19. Anterior dorsal vertebrae of IRSNB R33 in (A) anterior, (B) posterior (C) lateral, and (D) dorsal views. Abbreviations: cot, cotyle; con, condyle; nc, neural canal; ns, neural spine; prz, prezygapophysis; psz, postzygapophysis; syn, synapophyseal process; tp, transverse process; zga; zygantra, zgo, zygosphene.

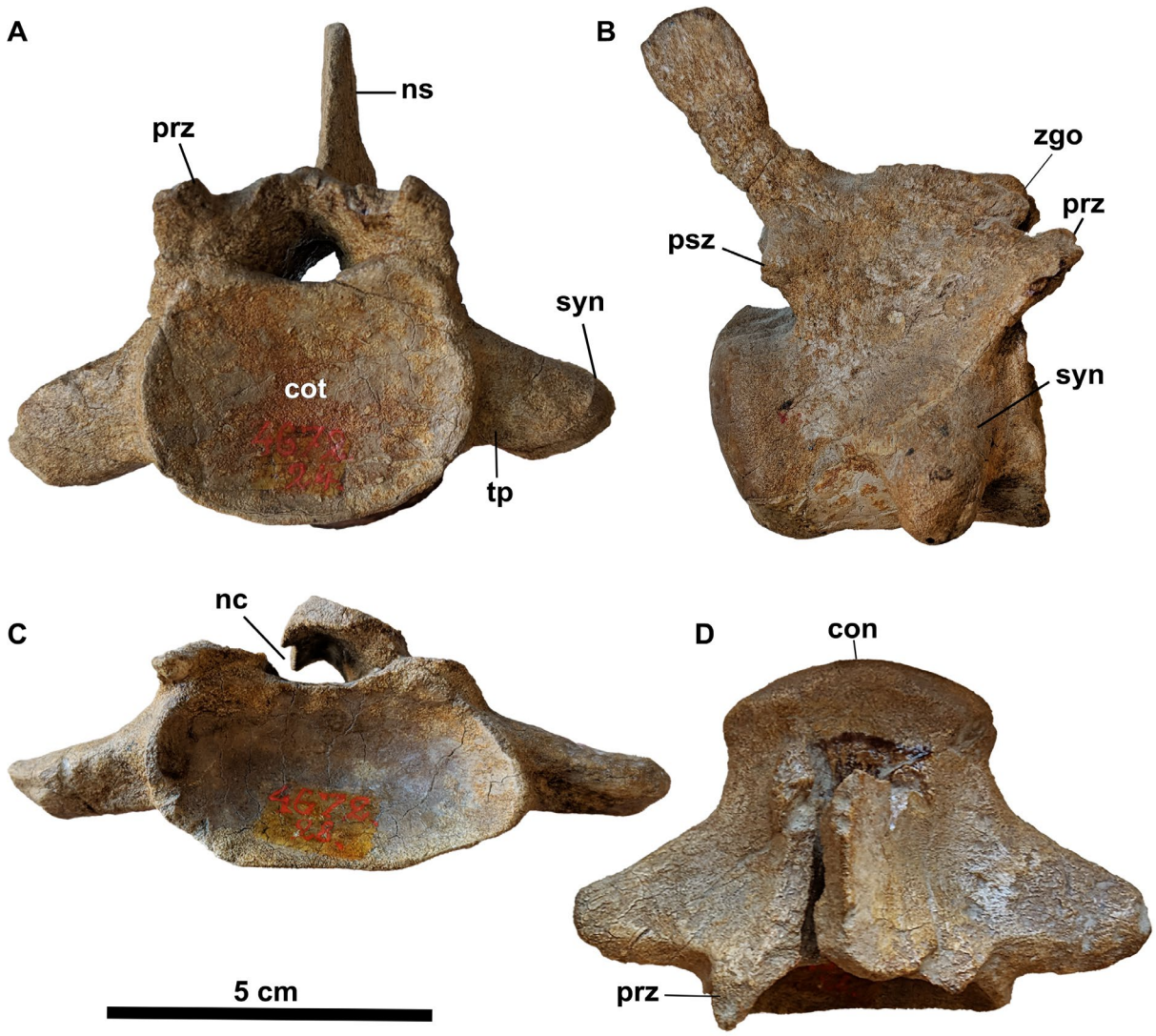

Figure 2.20. Select posterior dorsal vertebrae of IRSNB R33 in (A) anterior, (B) lateral, (c) anterior, and (D) dorsal views. Abbreviations: cot, cotyle; con, condyle; nc, neural canal; ns, neural spine; prz, prezygapophysis; psz, postzygapophysis; syn, synapophyseal process; tp, transverse process; zgo, zygosphene.

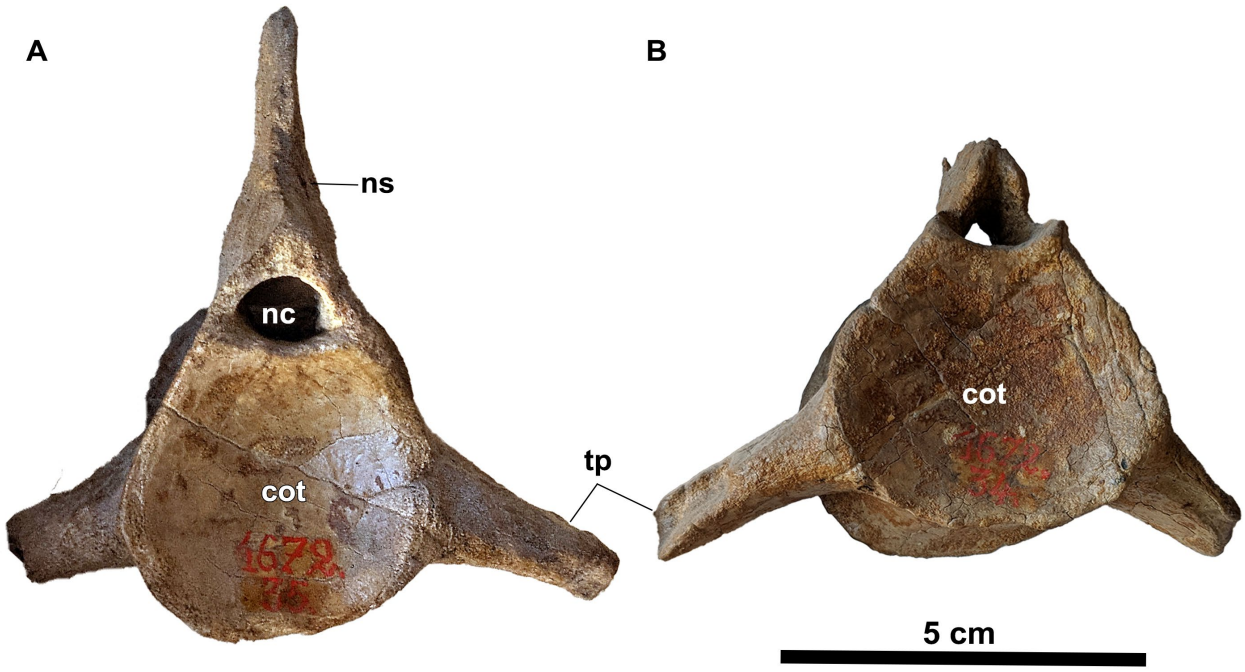

Figure 2.21. Select posterior pygal vertebrae of IRSNB R33 in anterior view. Abbreviations: cot, cotyle; nc, neural canal; ns, neural spine; tp, transverse process.

Figure 2.22. Ribs of IRSNB R33. (A) Series of cervical ribs; (B), (C), (D) series of dorsal ribs.

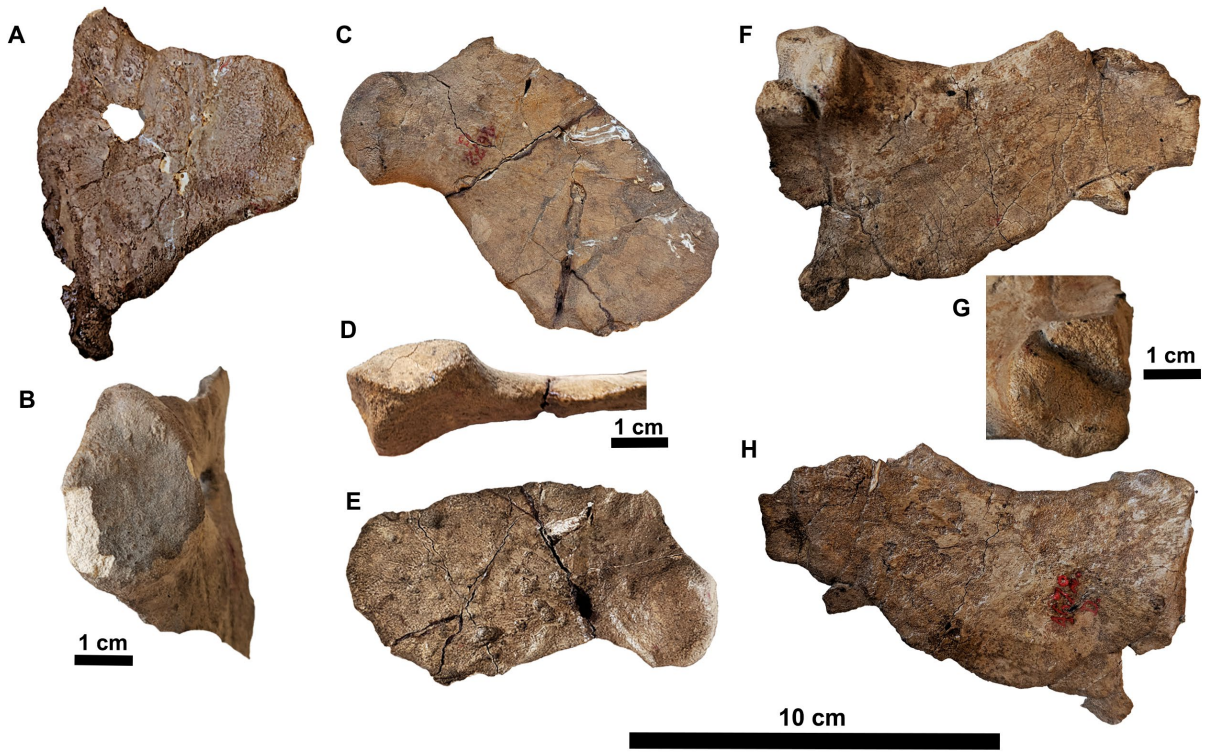

Figure 2.23. Scapulas and coracoid of IRSNB R33. Coracoid in (A) lateral and (B) internal views; left scapula in (C) lateral, (D) posterior, and (E) medial views; right scapula in (F) lateral, (G) internal, and (H) medial views.

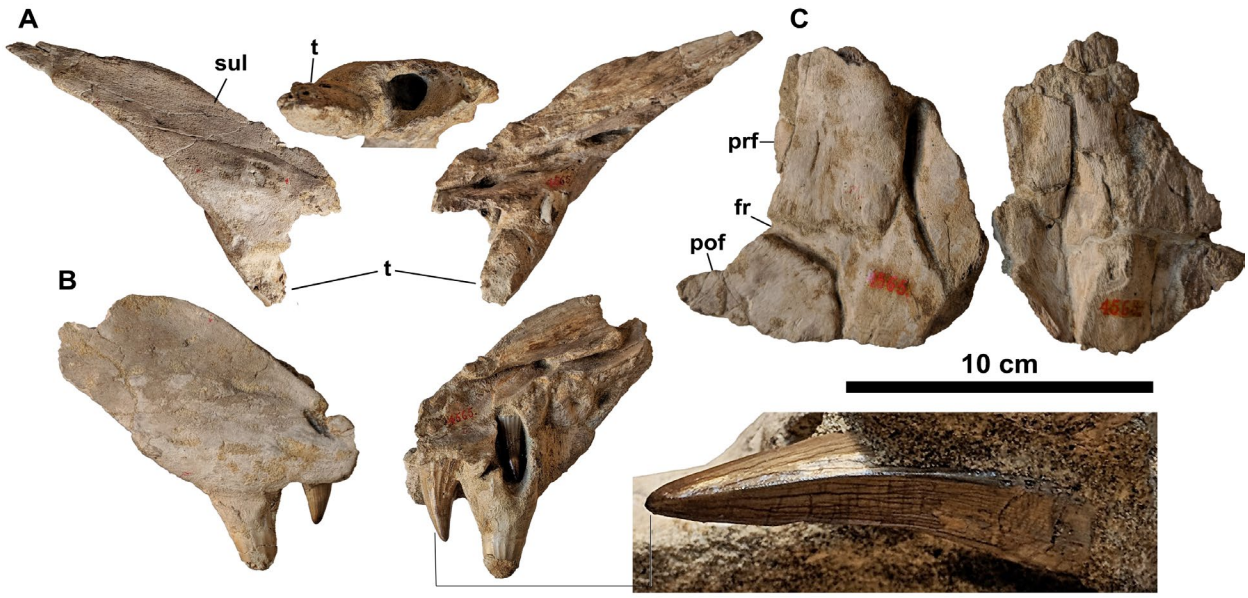

Figure 2.24. Upper jaw and skull roof fragments of IRSNB 0107. Premaxilla fragment in (A) dorsolateral, anterior, and ventrolateral views; anterior fragment of right maxilla in (B) lateral and medial views with magnified anterior view of first maxillary tooth; fragment of frontal in (C) ventral view. Abbreviations; fr, frontal; pof, postorbitofrontal; prf, prefrontal; sul, sulcus; t, tooth.

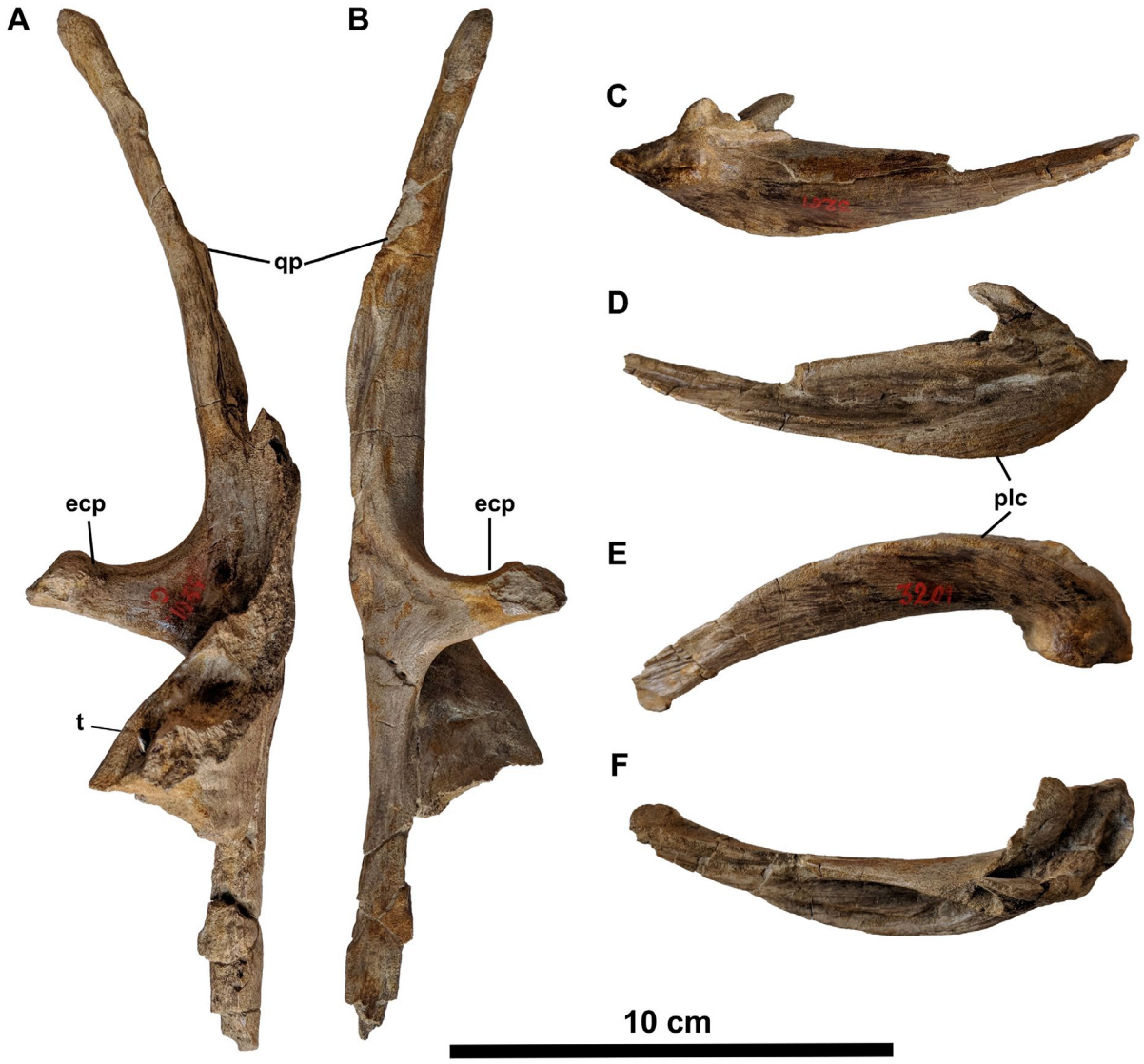

Figure 2.25. Palatal and skull roof fragments of IRSNB 0108. Left pterygoid in (A) medial and (B) lateral views; left squamosal in (C) ventral, (D) dorsolateral, (E) lateral, and (F) dorsal views. Abbreviations: ecp, ectopterygoid process; plc, posterolateral crest; qp, quadrate process; t, erupting tooth.

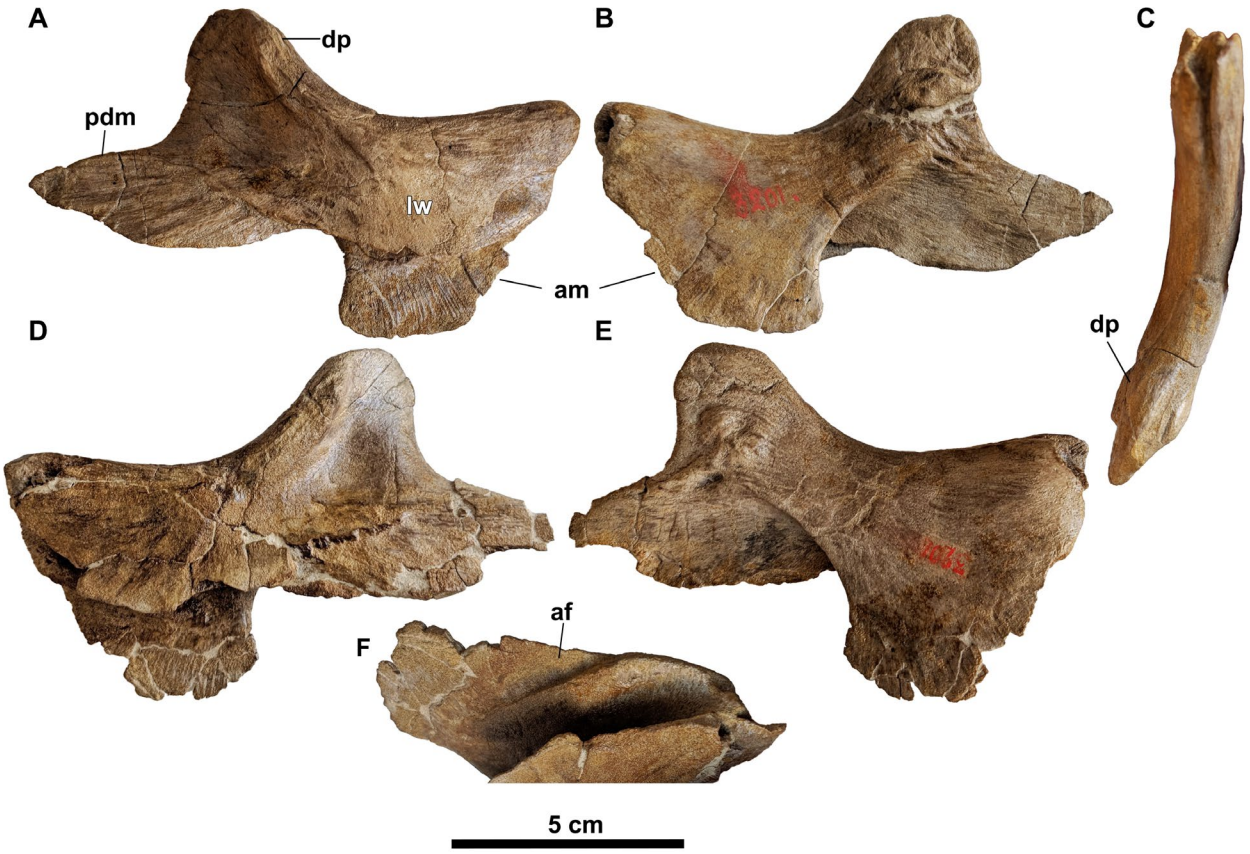

Figure 2.26. Lower jaw fragments of IRSNB 0107. Right dentary tip in (A) lateral and medial views; right dentary midsection in (B) lateral and medial views; left dentary midsection in (C) lateral, posterior, and medial views with magnified view of posterior crown and replacement teeth; right coracoid in (D) lateral and medial views; fragment of left coracoid in (E) internal view. Abbreviations: af, articular facet; am, anteromedial process; dp, dorsal (coronoid) process; lw, lateral wing; pdm, posterodorsomedial process.

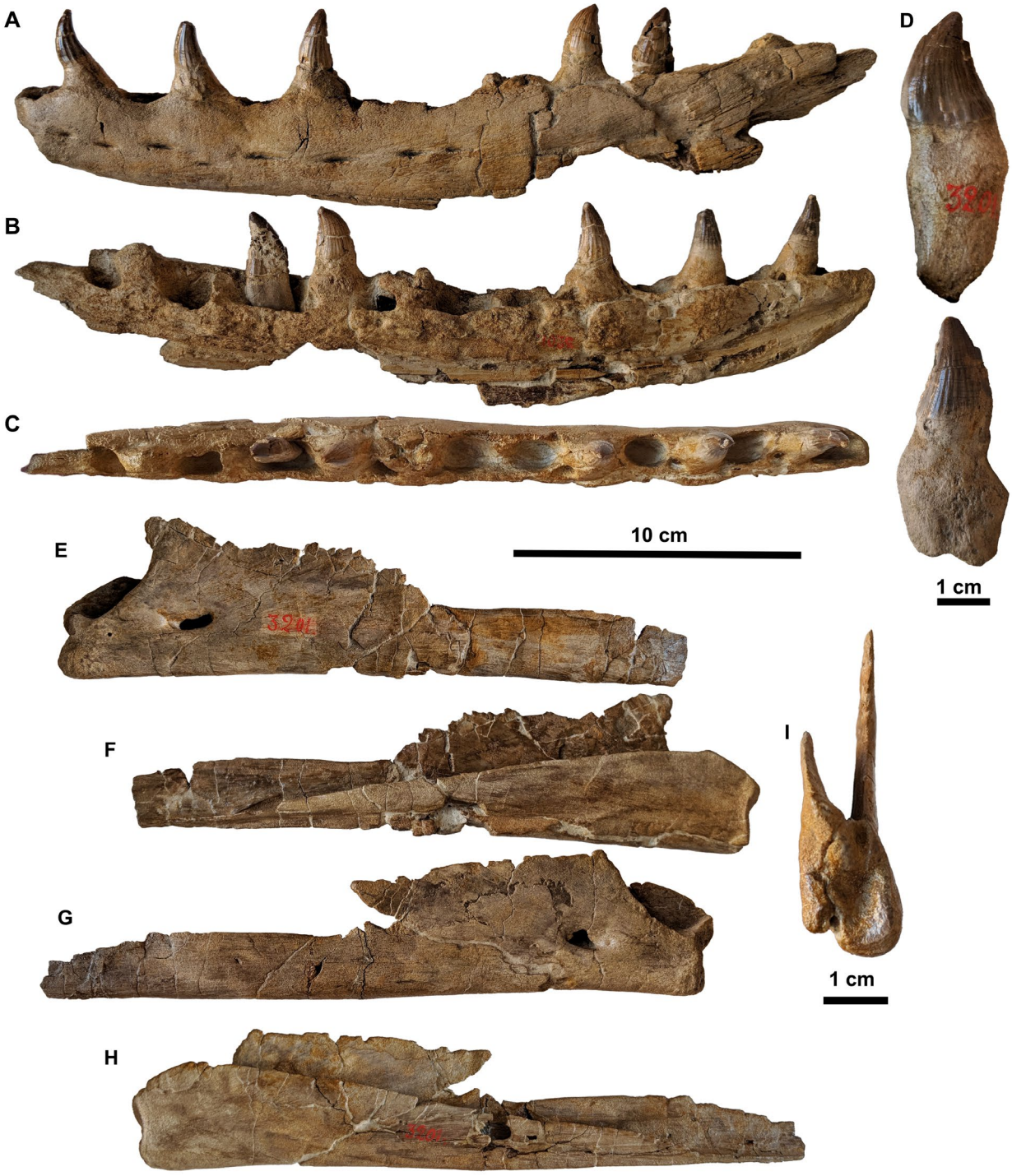

Figure 2.27. Anterior jaw fragments of IRSNB 0108. Left dentary in (A) lateral, (B) medial, and (C) dorsal views; (D) isolated teeth; right splenial in (E) medial and (F) lateral views; left splenial in (G) medial and (H) lateral views; right splenial in (I) anterior view.

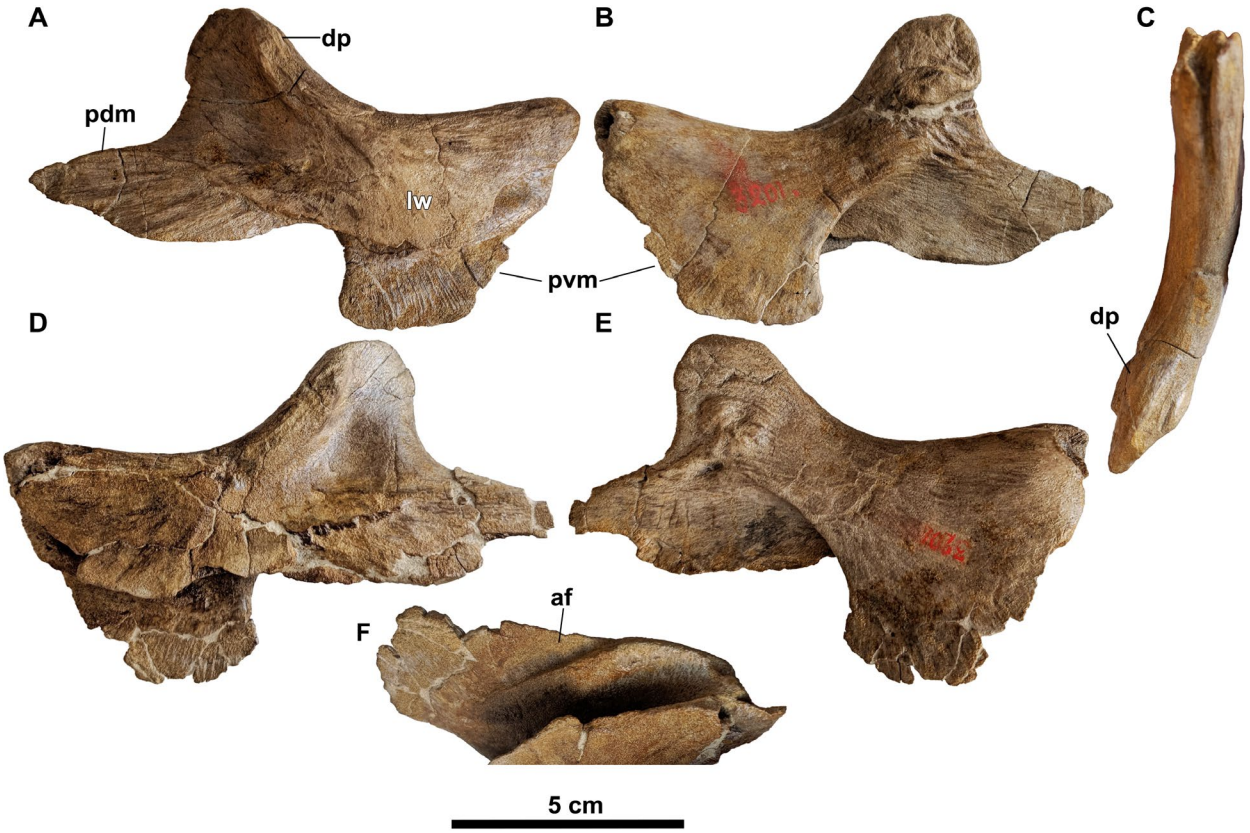

Figure 2.28. Left coronoid of IRSNB 0108 in (A) lateral, (B) medial, and (C) dorsal views. Right coronoid in (D) lateral, (E) medial, and (F) posterior internal views. Abbreviations: af, articular facet; dp, dorsal process; lw, lateral wing; pdm, posterodorsomedial process; pvm, posteroventromedial process.

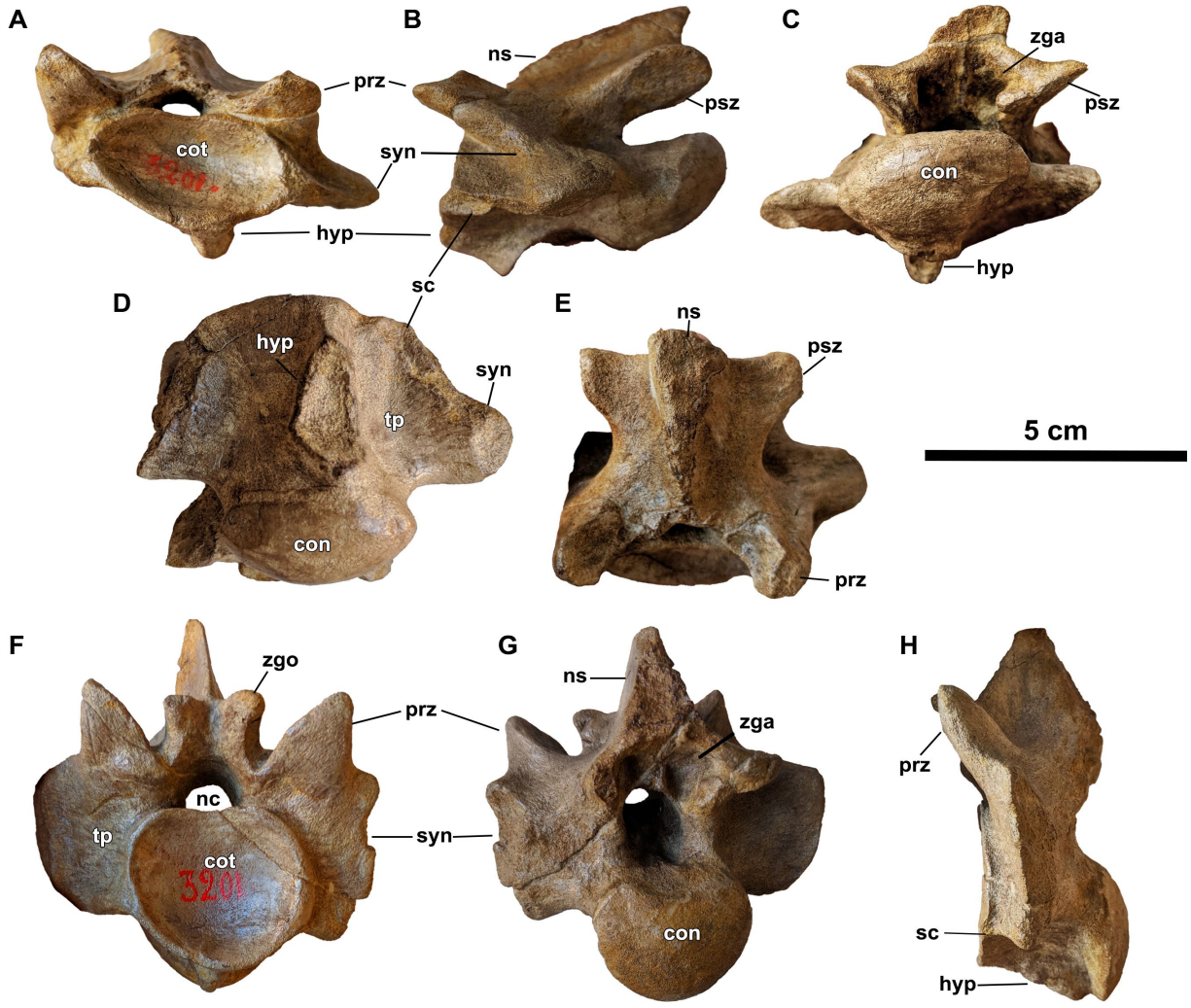

Figure 2.29. Cervical vertebrae of IRSNB 0108 in (A) anterior, (B) lateral, (C) posterior, (D) ventral, (E) dorsal, (F) anterior, (G) posterior, and (H) lateral views. Abbreviations: cot, cotyle; con, condyle; hyp, posterior fragment of hypapophysis; nc, neural canal; ns, neural spine; prz, prezygapophysis; psz, postzygapophysis; sc, synapophyseal crest; syn, synapophyseal process; tp, transverse process; zga; zygantra, zgo, zygosphene.

CHAPTER 3. REDESCRIPTION AND REDIAGNOSIS OF *PROGNATHODON GIGANTEUS*

INTRODUCTION

Represented by a single specimen (IRSNB 0106 (formerly 3103)), the holotype of *Prognathodon giganteus* Dollo, 1904 was collected from the Solvay quarry near Spiennes and accessioned by the Institut Royal des Sciences Naturelles de Belgique (IRSNB) in Bruxelles, Belgium some time around 1890 (Lingham-Soliar and Nolf, 1989). Like the Mesvin Solvay quarry where the type species was recovered, the Spiennes Solvay quarry is dominated by the Lower Maastrichtian Ciply Phosphatic Chalk. Aside from IRSNB 0106 deriving from a similar horizon to *P. solvayi*, there is no further information on where in the section the specimen was retrieved. *P. giganteus* received brief mention by Dollo (1904, 1909), who stated only that its teeth were smooth and it reached roughly 10 meters in length. Russell (1967) likewise provided only a short comment that, although no other characters were described, the smooth teeth of *P. giganteus* could indicate it is indistinguishable from *P. overtoni* or *P. rapax*. No in-depth study of the specimen was performed until Lingham-Soliar and Nolf (1989) described it alongside the type species, *P. solvayi*. Although both similarities with the type species and several unique features were observed, the authors concluded, in agreement with Russell (1967), that *P. giganteus* was most similar to *P. overtoni*, particularly the referred specimen SDSMT 3393. It is unclear how or why this decision was reached, as both the description and table comparing the key features between the three taxa list few examples of how *P. giganteus* resembles *P. overtoni* more so than *P. solvayi* (Lingham-Soliar and Nolf, 1989: fig. 48). The authors stated that the

subcircular teeth of *P. giganteus* resembled those of *P. overtoni*, although the cross-sectional shape of the marginal dentition of *P. solvayi* was also illustrated as elliptical to subcircular (Lingham-Soliar and Nolf, 1989: fig. 27). Likely due to its fragmentary nature, *P. giganteus* has also typically been excluded from phylogenetic analysis (Madzia and Cau, 2017; Simoes et al. 2017; Lively, 2020), and its inclusion in Longrich et al. (2022) did not show it closely allied with *P. overtoni*.

In light of the redescription of the type species and lack of clarity regarding the taxonomic relationships of *Prognathodon* as a whole, this study implements the revised diagnosis from Chapter 1 to provide an amended morphological description of *P. giganteus* and comparison with *P. solvayi* in order to determine if it represents a valid taxon within the genus.

MATERIALS AND METHODS

IRSNB 0106 was photographed using a Nikon D500 camera with a Nikkor AF-S 50 mm lens and a Google Pixel 2 smartphone. Photographs were processed and figures produced in Adobe Photoshop 25.1. As the material is highly fragmented, focus was placed on skeletal elements with discernable diagnostic features that could be readily compared to the holotype and referred specimens of *P. solvayi* (IRSNB, IRSNB 0107, and IRSNB 0108, respectively).

DESCRIPTION AND COMPARISON

Cranium

Skull—IRSNB 0106 is comprised mostly of a highly fragmented cranium, including partial components of the jaws and posterior mandibular unit (PMU). The skull roof is largely absent. When assembled, the skull is very large; Lingham-Soliar and Nolf (1989) estimated its length at

a little over one meter; nearly double the estimated size of the cranium of *P. solvayi*. Although mostly incomplete, the bone surfaces are not abraded.

Premaxilla—Like the holotype of *Prognathodon solvayi*, the premaxilla of *P. giganteus* is broad and short (Fig. 3.1A). The anterior-most edge is damaged, but the dorsal surface is flattened, and the alveoli closely abut the thin roof of bone much like in IRSNB R33 and the referred specimen IRSNB 0107 (Fig. 3.1B). This indicates a predental rostrum was likely absent, instead forming a blunt and slightly rounded tip. The lateral edges are preserved and like *P. solvayi* are sinusoidal in outline, expanding along the dentigerous section and forming a constriction posterior to the second tooth position before tapering towards the internarial bar (Fig. 3.1D). A shallow, broad sulcus extends along the midline on the dorsal surface of the premaxilla on *Prognathodon giganteus* (IRSNB 0106). The sulcus appears to taper and terminates just posterior to the tip. It is deepest midway along its length but flattens and becomes indistinct anterior to the internarial bar (Fig. 3.1B). A row of large foramina run laterally along both edges of the sulcus and appear restricted to the dentigerous portion of the premaxilla. Notably, neither of these features is visible in the holotype, which possesses a largely featureless dorsal surface of the premaxilla (Fig. 2.2A). However, the trace of a shallow sulcus and a possible foramen is preserved in IRSNB 0107 (Fig. 2.24A).

Lingham-Soliar and Nolf (1989) suggested the premaxillary teeth of *P. giganteus* were likely not as procumbent as those in *P. solvayi*, although there is no indication that this was the case. Instead, the alveoli of the second tooth positions are oriented at a similar inclination as the *P. solvayi*, as are both the bases of the teeth in the second position and the right replacement tooth visible on the ventral surface (Fig. 3.1B, C). The bases of the second set of premaxillary

teeth are elliptical in cross-section and oriented along the mediolateral axis, like in *P. solvayi*. The replacement tooth shows very fine serrations along the carinae, as well as faint striae or anastomosing texture near the crown apex. The most obvious difference between *P. solvayi* and *P. giganteus* is the apparent lack of flutes on the enamel surfaces of the teeth, in this instance on the premaxillary replacement tooth (although see dentary tooth description).

Maxilla—Only small fragments of maxillae are preserved in IRSNB 0106, with the most distinct being a piece of the anterior left maxilla. Lingham-Soliar and Nolf (1989) described the premaxillary-maxillary suture as odd, citing the sharp 45-degree angle of the suture that terminates at the second maxillary tooth position, which suggested the narial opening extended more anteriorly than usual. However, the dorsal margin and tip of the anterodorsal process are missing and therefore likely would have continued further, possibly to the third tooth position (Fig. 3.2A, B, C). This is attested by the suture in IRSNB 0107 ascending at a similar angle and terminating at the third maxillary tooth position. The same suture in the holotype of *P. solvayi* is slightly less inclined than in *P. giganteus*, but likewise ends at the third tooth position. Although the anterodorsal process is broken in *P. giganteus*, it was likely oriented dorsally and therefore visible in lateral view. The series of elongate foramina that forms an arch above the tooth row in *P. solvayi* is partially visible in *P. giganteus*, where two or three foramina ascend dorsally above the tooth row along the lateral maxillary surface. This row follows the slight concave curvature of the maxilla in *P. solvayi*, which may have also been the case in *P. giganteus*. A fragment of the posterior maxilla preserves a part of the lateral face dorsal to the tooth row (Fig. 3.3). The preserved wall is thinnest near its dorsal margin, which ascends posteriorly, suggesting that the posterodorsal process may also have been oriented dorsally and extended well above

anterodorsal process. A piece of the posterior termination of the maxilla is long, narrow, and pointed. An elongate groove near the posteroventral margin where the jugal would have articulated is present on the lateral surface (Fig. 3.3). These features are also present in *P. solvayi* and were also observed by Lingham-Soliar and Nolf (1989).

The second maxillary tooth in *P. giganteus* is slightly inclined, similarly to those in IRSNB and IRSNB 0107 (Fig. 3.2). The long, tapering shape also resembles the anterior crowns present in *P. solvayi*, with a convex labial surface and straight lingual surface, as well as a crown apex that points posterolingually. Unserrated carinae are present along the mesial and distal edges. As with the premaxillary dentition, flutes are conspicuously absent. Although most teeth are not preserved, the weak heterodonty along the tooth row in *P. solvayi* is also likely present in *P. giganteus*, with longer, tapering crowns present anteriorly and smaller, broader crowns located posteriorly (this feature is more evident in dentary where more teeth are preserved). Based on the tapering, thinner bone opposite the tooth row, a posterior fragment, possibly from the maxilla (although mounted with the dentary in Lingham-Soliar and Nolf, 1989: plate 7), preserves a shorter, laterally broad tooth with a more strongly curved anterior edge and apex pointing posteriorly (Fig. 3.2D). The carinae on the mature teeth lack serrations, but as with *P. solvayi*, replacement teeth show both small serrations as well as fine, subtle anastomosing texture concentrated near the apex of the crown (Fig. 3.2D). Also similar to *P. solvayi*, the maxillary teeth of *P. giganteus* are subcircular or asymmetrical ellipses in cross-section (Fig. 3.2C).

Prefrontal—An anterior portion of the left prefrontal is heavily fragmented and a supraorbital process is not preserved. The base of the concave posteromedial projection of the lateral wing is preserved dorsal to the base of the descending lamina. The anterior wing is elongate, tapered in

lateral view, and overall similar in shape to the same part of the prefrontal of *P. solvayi* (Fig. 3.4A, B). Although not as clear in *P. giganteus*, the prefrontals of both taxa show fine radiating striae extending across the lateral surface. A low ridge running along the anterior lamina demarcates the dorsal and lateral surfaces, and an elongate depression with a crescentic posterior end extends anteriorly on the medial surface of the anterior lamina in both *P. giganteus* and *P. solvayi*.

Jugal—A fragment of the horizontal ramus of the right jugal is preserved in *P. giganteus* (Fig. 3.4C). The similarities with the jugal of *P. solvayi* were noted by Lingham-Soliar and Nolf (1989), who observed the thinness and slight curvature of the horizontal ramus in both taxa. The posterior end of this fragment in *P. giganteus* is only partially preserved, but shows a similar degree of curvature and broadening of the ramus towards the vertical ramus to that seen in *P. solvayi*.

Pterygoid—The pterygoid of *P. giganteus* was not described by Lingham-Soliar and Nolf (1989); however, this study identifies a small fragment of the main tooth bearing platform of the left pterygoid (Fig. 3.5). A large circular foramen is slightly recessed into the dorsal surface, as in *P. solvayi* (Fig. 3.5A). In medial view, the pterygoid is slightly more robustly built, although some of its appearance may result from its poor preservation. Nevertheless, the pterygoid teeth descended directly from the thickened portion of the main pterygoid body as in *P. solvayi*, (Fig. 3.5B). What is interpreted as the lateral edge of the pterygoid has a strong convex curvature and greater distance between the bony margin and alveoli, coinciding most closely with the middle segment of the main pterygoid body in *P. solvayi* (Fig. 3.5C). Two empty alveoli and the base of

one pterygoid tooth at the hypothesized anterior end are preserved, likely representing the third to fifth tooth positions. An isolated pterygoid tooth was also identified, and is similar in size to the marginal teeth but more strongly curved, as well as lacks enamel features except for a posterior carina (Fig. 3.5B) (see also Lingham-Soliar and Nolf, 1989: fig. 3.40). Both the isolated tooth and preserved crown base are more circular in cross-section as opposed to elliptical. All these features are also present in the pterygoid teeth of *P. solvayi*.

Lower Jaw

Dentary—Several small fragments and a large anterior segment of the dentary are preserved in *P. giganteus* (Fig. 3.6). The anterior dentary fragment is more massive, although the outer dentary wall, for example, is not substantially thicker than those of the holotype and referred specimens of *P. solvayi* (Fig. 3.7B). The lateral and dorsal profiles also strongly resemble *P. solvayi*: an anterior extension of the dentary beyond the first tooth position is absent, and the ventral margin is curved (Figs. 3.6A, B, 3.7). Two rows of large, elongate nutrient foramina are also concentrated on the anterolateral surface and form a row posteriorly in both taxa. Lingham-Soliar and Nolf (1989) described the dorsal margins as largely straight and suggested the dentary was likely not bowed, although both the curvature of the ventral margin and the concave dorsal margin in lateral view contradicts this view. Furthermore, most of the curvature in the dentary of *P. solvayi* is visible midway near the 10th tooth position; this portion is largely missing in *P. giganteus,* and curvature may therefore appear less evident. In medial view, the anterior end of the Meckelian groove is open (Fig. 3.6C).

Like *P. solvayi*, the anterior dentary teeth of *P. giganteus* are procumbent. Although most of the tooth crowns are missing, the second tooth is inclined at a similar angular to *P. solvayi*

(Fig. 3.7). The alveolus of the first tooth position is steeply angled and abutting the anterior-most dentary wall, indicating the tooth was also strongly procumbent. Unique to *P. giganteus*, interdental pits, likely resulting from contact with the corresponding maxillary crown apices, are situated along the dorsal surface of the tooth row and on the anterolateral margins of the 4th to possibly the 6th tooth bases (Figs. 3.6A, D, 3.7B). These pits are not present further anteriorly because the premaxillary crowns are inclined and the apices cannot impinge on the dentary bone. Interdental pits also occur in other taxa including *Mosasaurus* (Street and Caldwell, 2017; Figs. 3.1A, Fig. 3.3), although these instead tend to occur on the anterolateral margin of the dentary. In dorsal view, the crowns are subcircular in cross-section (Figs. 3.6D, 3.7B) and possess smooth mesial and distal carinae. They are also offset from the midline and angled towards the lateral wall of the dentary, suggesting that like *P. solvayi*, the dentary teeth were slightly splayed (Figs. 3.6B, 3.7B). Lingham-Soliar and Nolf (1989) suggested *P. giganteus* was unique with tooth size appearing roughly constant throughout the tooth row. However, tooth size in *P. solvayi* also does not vary considerably beyond variation in crown width until the two posterior-most teeth (Figs. 3.3, 3.7A), which are not preserved in *P. giganteus*. The most glaring disparity between *P. giganteus* and *P. solvayi* is the lack of flutes; however, a replacement tooth in the 4th position shows faint fluting extending from the base of the crown and nearly to the apex (Fig. 3.6C).

Surangular, angular, articular—The posterior mandibular unit (PMU) is in good condition and preserved in articulation (Fig. 3.8). Lingham-Soliar and Nolf (1989: fig. 3.45, plate 7) described a very fragmented and unusually small coronoid, although it no longer appears to be included with the specimen. Based on the images provided by the authors, the element appears heavily worn and could alternatively represent only a small portion of the coronoid or derive from a

different element entirely. The remaining individual elements in the PMU of *P. giganteus* bear strong resemblance to *P. solvayi*: The posterior and anterior ends of the surangular are missing but is nevertheless a rhomboidal shape with a horizontal dorsal margin. A depression along the broken anterodorsal corner is in a similar position to the surangular fossa in *P. solvayi* (Fig. 3.8A). Although the posterolateral face is broken away, the posterior tip forms the anterolateral border of the glenoid fossa. The ventral border of the surangular is resting on the ventrolateral surface of the angular, which is partially exposed in lateral view. Medially, the adductor fossa forms a deep excavation with a curved ventral shelf in medial view (Fig. 3.8B). Anteriorly, the surangular inserts against the medial surface of the lateral wing of the angular, which with its medial wing forms a V-shape in anterior view (Fig. 3.8C). Posteriorly the dorsal margin of the articular follows the curve of the adductor fossa of the surangular, but the anterior arm curves dorsally midway along its length and is nested between the medial surface of the surangular and the medial wing of the angular. The angular foramen lacks a complete border and is situated along the dorsal margin of the medial wing near the intermandibular joint, similar to *P. solvayi* (Fig. 3.8B). The wing is also short and likely did not contact the descending medial wing of the coronoid. Instead, the coronoid likely only articulated with the anterior arm of the articular. The articular forms the posterolateral border of the glenoid fossa, which is a semicircular shape and tilted medially. A small eminence points dorsally from the posterior border of the fossa. As with *P. solvayi*, the retroarticular process is short and rounded, oriented parallel to the PMU, and lacking medial inflection.

Quadrate—The quadrate of *P. giganteus* is very poorly preserved (Fig. 3.9), but what is preserved bears some resemblance to the quadrate of *P. solvayi*. Neither the suprastapedial

process nor the suture between the suprastapedial and posterolateral processes are discernable (Fig. 3.9A). As in the quadrate of *P. solvayi*, the posterolateral process is narrow. The pillar-like process appears to have originated anteroventrally at the base of a weakly-developed tympanic crest and ascended at an acute angle to meet the suprastapedial process, like in *P. solvayi*. Although broken, the tympanic crest is largely straight and oriented near vertically. Lingham-Soliar and Nolf (1989) reconstructed the quadrate with an unusually large meatus, however; the edge of the ala appears broken instead, and likely does not represent the border of an opening. The left quadrate of *P. solvayi* shows breakage in a similar place, albeit to a lesser extent (Fig. 3.9B). What remains of the mandibular condyle also appears narrow and short.

Axial Skeleton

Cervical Vertebrae—Most cervical vertebrae in *P. giganteus* are heavily distorted and/or fragmentary. The best-preserved examples share several similarities with *P. solvayi* (Fig. 3.10), including large, broad-based prezygapophyses with tapered tips that angle anterolaterally, and transverse processes as tall as the centrum with equally synapophyseal processes. A thin ventral ridge extends from the synapophyseal process onto the margin of cotyle (Fig. 3.10A, C). Some examples also preserve a small notch along the dorsal margin of the centrum. The zygantra are not preserved, but the zygosphenes are large with narrow, rounded tips. Only a small portion of the base of the postzygapophyses remains. The neural spines are anteroposteriorly broad and angled posteriorly. Only a fragment of the posterior end of the axis of *P. giganteus* is preserved, and while similar in shape to the axis of *P. solvayi*, diagnostic features are either missing or difficult to discern and is therefore not discussed further here.

Dorsal Vertebrae—Most of the remaining dorsal vertebrae of *P. giganteus* compressed, with only a posterior example providing diagnostic features (Fig. 3.11). The overall shape of the posterior dorsal vertebrae in *P. giganteus* and *P. solvayi* are very similar; even compressed the centrum is longer than it is tall (Fig. 3.11A, B), and the transverse processes are situated anteriorly and on the midline of the centrum, tapering slightly towards the rounded synapophyseal process in dorsal view (Fig. 3.11C, D). The prezygapophyses are large with broad bases and rounded tips that point anterolaterally. While only the bases of the prezygapophyses are preserved in *P. solvayi*, they also appear to have been large and oriented in a similar direction (Fig. 3.11A, B). Likewise, only the bases of zygosphenes are preserved in *P. solvayi*, but in *P. giganteus* these are very well-developed with broad bases and tapered, rounded tips. Only the base of the neural spine is preserved but would have been thin and anteroposteriorly broad. Lingham-Soliar and Nolf (1989) described large zygantra were present (possibly on a different vertebra), but these are not visible on the figured example.

Pygal and Caudal Vertebrae—A single partial pygal vertebrae of *P. giganteus* is poorly preserved, but like *P. solvayi* the centrum is subcircular with a broader base and a shallow notch on the dorsal margin (Fig. 3.12A). Only a small fragment of the left transverse process is preserved, but it is positioned on the lower half of the centrum and angles ventrally as in *P. solvayi*.

Unlike in *P. solvayi*, *P. giganteus* preserves a small number of caudal vertebrae. The best example shows a thin, broad neural spine angled posteriorly and ornamented with elongate striae on the lateral face (Fig. 3.12B). The centrum is a similar subcircular shape to the pygal vertebra but is narrower, although this is likely due to compression. The bases of transverse processes are

preserved midway on the centrum and directly dorsal to the posteriorly angled haemal arches. The arches are fused to the centrum.

DISCUSSION AND TAXONOMIC CONCLUSIONS

Although Lingham-Soliar and Nolf (1989) concluded that *P. giganteus* is most similar to *P. overtoni*, our observations suggest that not only does *P. giganteus* strongly resemble *P. solvayi*, it is potentially similar to a degree to warrant synonymizing the two taxa. Size disparities notwithstanding, the overall shape of the skeletal elements and teeth are strongly similar if not identical in numerous instances. Key diagnostic characters shared between the IRSNB 0106 and *P. solvayi* include a flat, broad premaxilla with a dorsal median sulcus but lacking a predental rostrum, procumbent premaxillary and anterior dentary teeth, dorsally oriented anterodorsal and posterodorsal processes of the maxilla, proportionately large pterygoid teeth erupting from the main platform of the pterygoid, a bowed dentary, a rhomboidal or subrectangular surangular with horizontal dorsal and ventral edges lacking a coronoid buttress, a vertically oriented retroarticular process lacking medial inflection, a synapophyseal crest extending to the lateral margins of the centrum in the cervical vertebrae, and zygosphenes and zygantra on the cervical and dorsal vertebral series. Other notable similarities between the two taxa were also observed in the prefrontal, jugal, and angular fragments. Regarding the dentition, both *P. giganteus* and *P. solvayi* also have bicarinate, weakly heterodont and splayed marginal teeth (most evident in the dentary). The teeth are sub-circular in cross-section with replacement crowns showing faint anastomosing structure and serrated carinae. An apparent major disparity between the two taxa is the lack of flutes on the marginal dentition of *P. giganteus*. However, while the preserved erupted teeth are smooth, fluting is present on the enamel surface of a replacement tooth in the

dentary. Variability in enamel ornamentation in the same individual is not unusual, and there are multiple reports of facets occurring in larger examples but flutes in smaller individuals within the same taxon (Street et al., 2022). Although facets are not reported here, the extensive presence of flutes in the holotype and referred specimens of *P. solvayi*, but not in the considerably larger *P. giganteus,* is nevertheless consistent with previous observations of ontogenetic changes in enamel features. Ontogeny may also account for the differences in the topology of the dorsal surface of the premaxilla, wherein a shallow, broad median sulcus bordered by nutrient foramina is present in *P. giganteus* but not the holotype of *P. solvayi*. The sulcus and a possible foramen are however preserved in the partial premaxilla of the slightly larger referred specimen, IRSNB 0107. Variation in the robustness of the skeletal elements also appears to correspond to some degree to the relative sizes of the referred specimens. The smallest example of *P. solvayi* is IRSNB 0108 is also the most gracile, followed by the larger and slightly more heavily built (but by no means robust) holotype and IRSNB 0107. *P. giganteus* is the largest by a considerable degree, and also slightly more robust, particularly in the dentary and potentially the pterygoid, than its proposed counterparts.

The features that were initially suggested as unique to *P. giganteus*, including the short and steeply angled premaxillary-maxillary suture and the roughly similar marginal tooth size, instead also occur in *P. solvayi*. The dorsal and ventral margins of the dentary in *P. giganteus* appear curved rather than straight (particularly in lateral view), indicating the dentary was likely bowed as in *P. solvayi*. Although the small coronoid reported by Lingham-Soliar and Nolf (1989) is not currently included with the specimen, it would not necessarily be sufficient to differentiate *P. giganteus* from *P. solvayi* considering the other demonstrated morphological similarities. The unusually large quadrate meatus is interpreted here to instead be the broken surface of the

tympanic ala, and what little remains of the quadrate of *P. giganteus* is otherwise similar to that of *P. solvayi*, including the largely straight, vertically oriented tympanic crest. The presence of interdental pits on the anterodorsal surface of the tooth row is unique to IRSNB 0106, although with only a partial left dentary it is difficult to determine if this is diagnostic of a taxon, and like enamel ornamentation this feature may also occur primarily in larger individuals.

Despite the fragmentary nature of IRSNB 0106, diagnosable features are nevertheless discernable on several elements of the remaining material. The preponderance of diagnostic characters shared between *P. giganteus* and *P. solvayi* suggests that *P. giganteus* represents a large individual of *P. solvayi*, wherein *P. solvayi* would take priority (Dollo, 1889). While detailed locality data is not available, both IRSNB 0106 and the type specimen were retrieved from the Ciply Phosphatic Chalk, providing a temporal basis for synonymizing the two taxa.

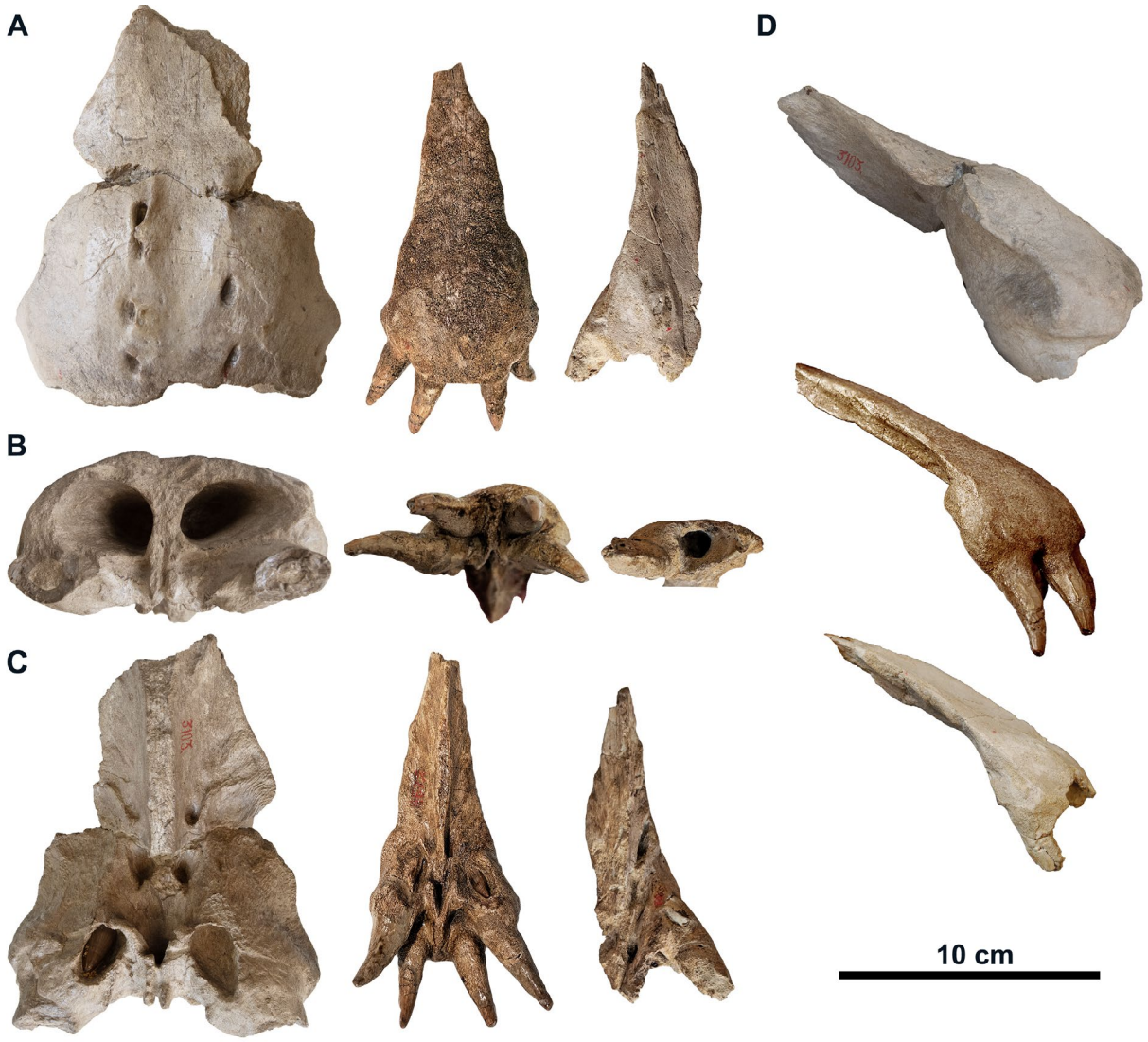

Figure 3.1. Premaxilla of *P. giganteus* (IRSNB 0106), *P. solvayi* holotype (IRSNB R33) and referred specimen of *P. solvayi* (IRSNB 0107) in A) dorsal, (B) anterior, (C) ventral, and (D) lateral views.

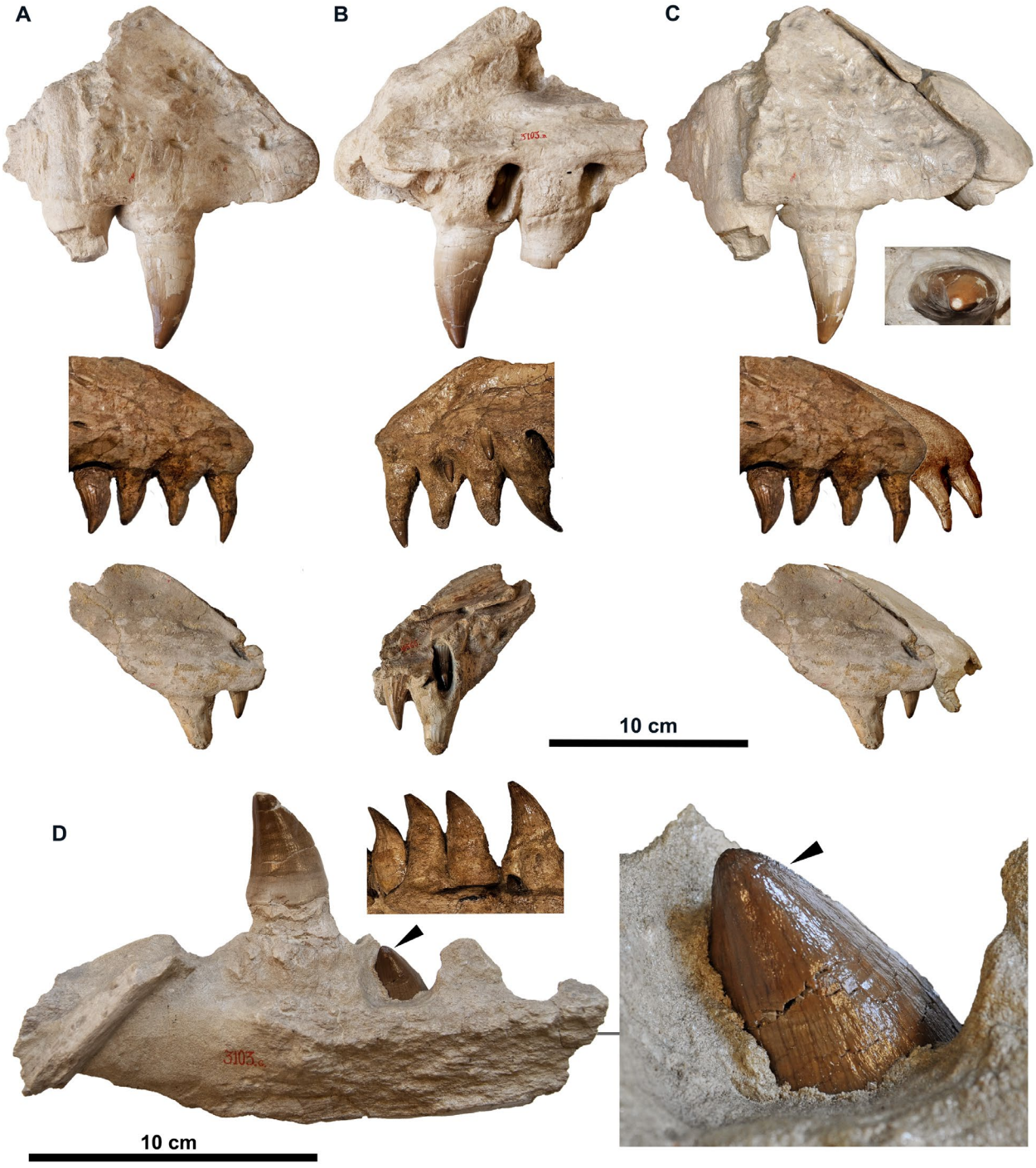

Figure 3.2. From top to bottom: anterior maxillae of *P. giganteus* (IRSNB 0106), *P. solvayi* holotype (IRSNB R33) and referred specimen of *P. solvayi* (IRSNB 0107) in (A) lateral and (B) medial views. Premaxillae and maxillae in articulation in (C) lateral views, with second maxillary tooth of *P. giganteus* in apical view. (D) Section of posterior maxilla or dentary with tooth compared to section of posterior maxillary tooth crowns from *P. solvayi*, and a closeup of a replacement tooth with serrations on the carina and anastomosing texture near crown apex, indicated by arrows.

Figure 3.3. Posterior maxillary fragments of *P. giganteus* (IRSNB 0106) (left) compared with maxilla of *P. solvayi* holotype (IRSNB R33) (right) in medial view. Posterior terminal maxillary fragment of *P. giganteus* is in lateral view.

Figure 3.4. Left prefrontal of *P. giganteus* (IRSNB 0106) (left) and *P. solvayi* (IRSNB R33) (right) in (A) lateral and (B) medial views. Jugal of *P. giganteus* (IRSNB 0106) (left) and *P. solvayi* (IRSNB R33) (right) in (C) lateral view.

Figure 3.5. Partial main body of left pterygoid of *P. giganteus* (IRSNB 0106) compared with complete right pterygoid of *P. solvayi* (IRSNB R33) in (A) dorsal, (B) medial, and (C) ventral views. (B) includes pterygoid tooth from *P. giganteus*. White arrows in (A) indicates foramen on dorsal surface of pterygoid. Black arrows in (C) indicates the hypothetical corresponding posterolateral edges of the pterygoid in *P. giganteus* and *P. solvayi*.

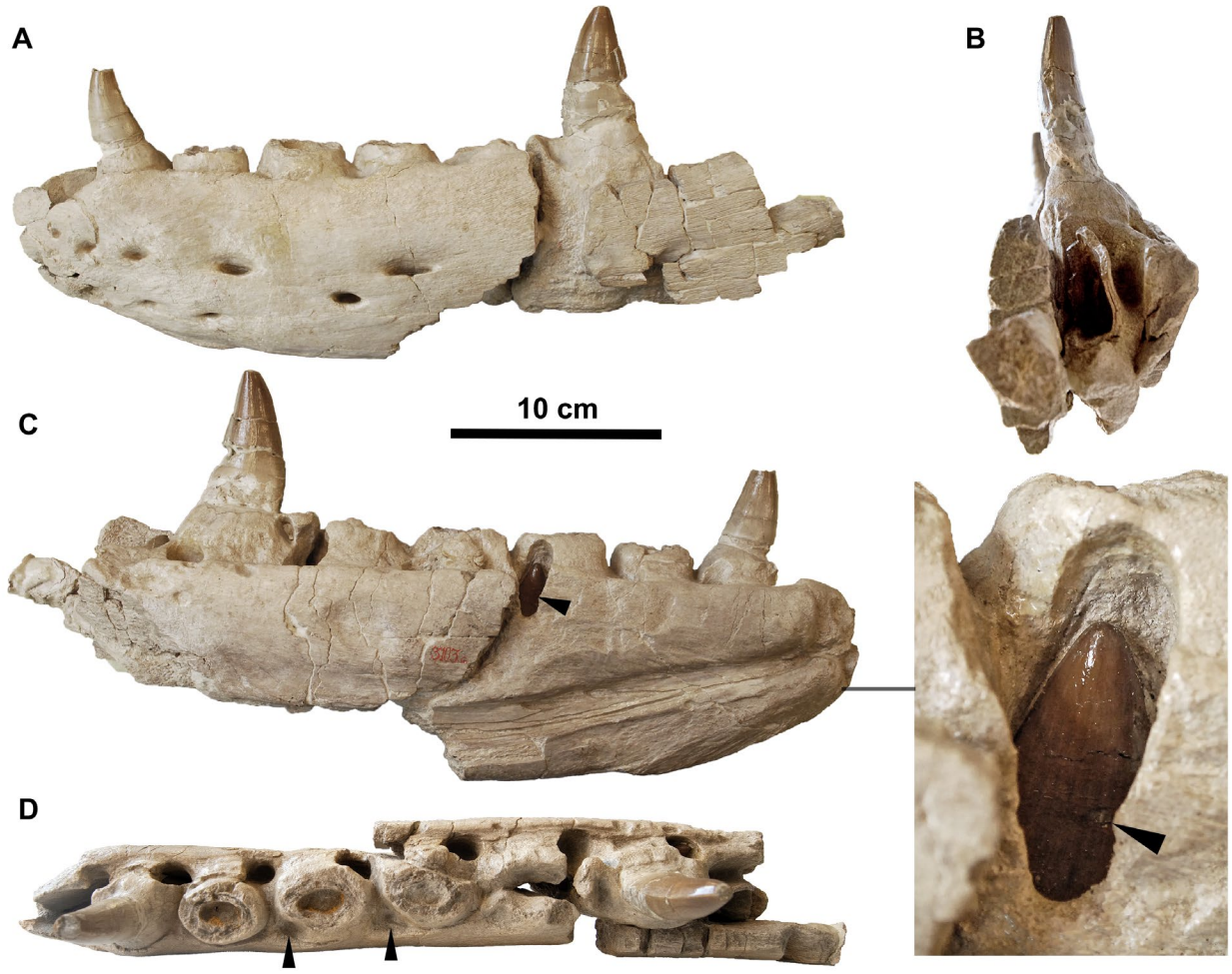

Figure 3.6. Section of anterior left dentary of *P. giganteus* (IRSNB 0106) in (A) lateral, (B) posterior, (C) medial, and (D) dorsal views. (C) shows a closeup of a replacement tooth with flutes extended from the base nearly to the apex (indicated by arrow). Arrows in (D) indicate interdental pits.

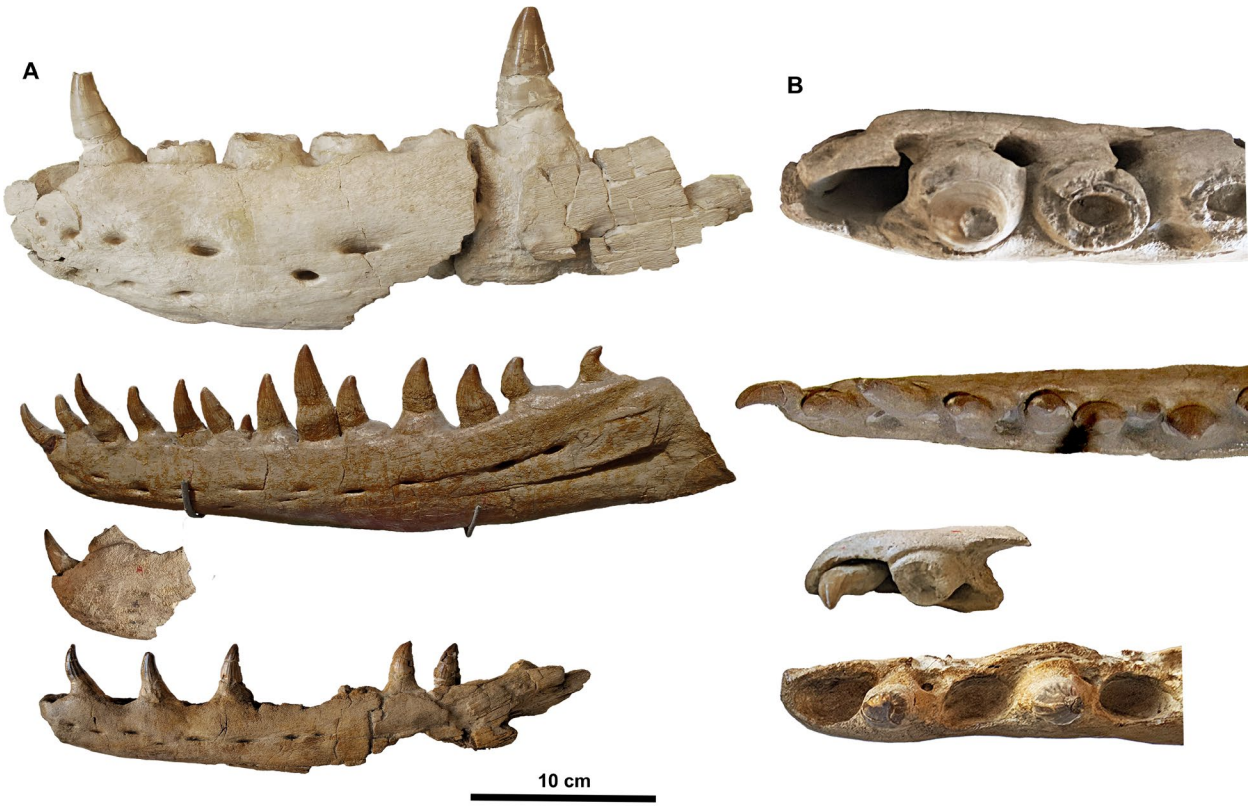

Figure 3.7. Comparison of dentaries from top to bottom of (A) *P. giganteus* (IRSNB 0106) and *P. solvayi* holotype (IRSNB R33); right dentary that has been mirror-imaged for comparative purposes), IRSNB 0107, and IRSNB 0108 in lateral view. (B) Compares the anterior sections of the same specimens in dorsal view. Note (B) is not to scale.

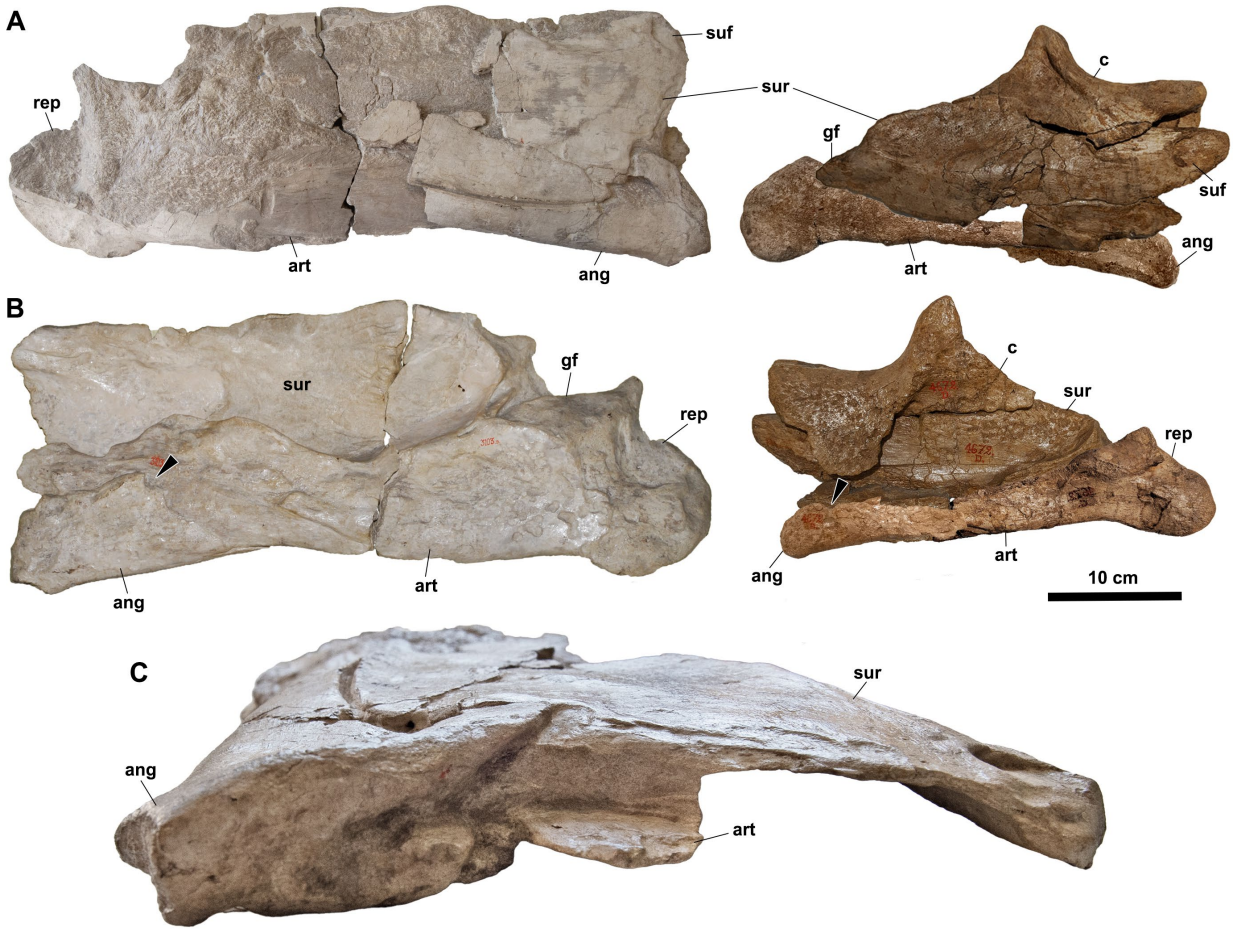

Figure 3.8. Posterior mandibular unit (excluding coronoid) of *P. giganteus* (IRSNB 0106) compared with the PMU of the holotype of *P. solvayi* (IRSNB R33) in (A) lateral, (B) medial and (C) anterior views. The left articular from *P. solvayi* is better preserved and have been mirror-imaged with the right angular transposed for better comparison. Abbreviations: ang, angular; art, articular; c, coronoid; gf, glenoid fossa; rep, retroarticular process; suf, surangular fossa; sur, surangular. Black arrows in (B) indicate the angular foramen.

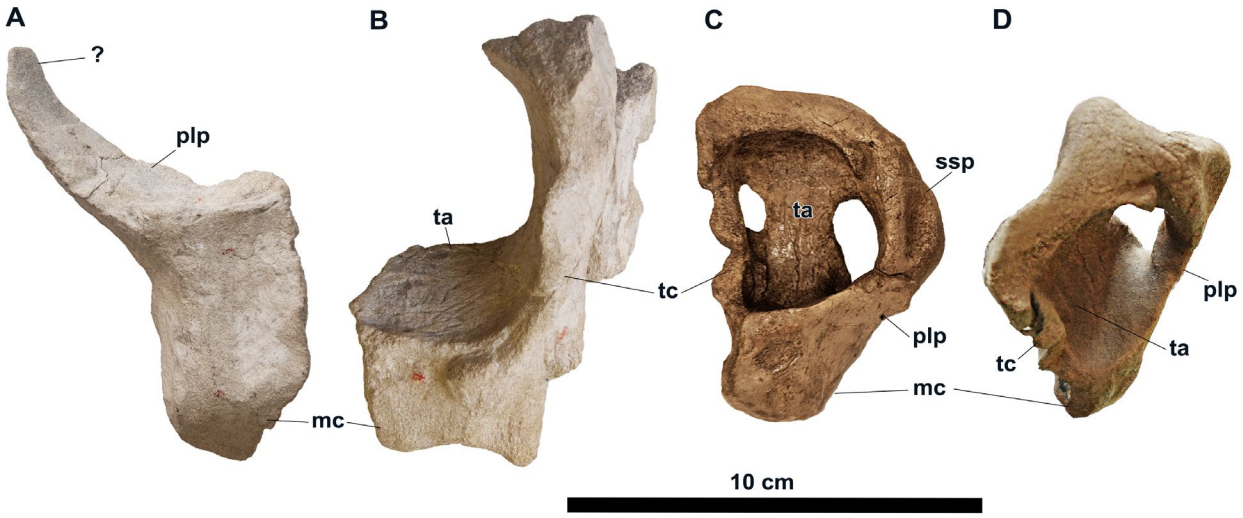

Figure 3.9. Partial quadrate of *P. giganteus* (IRSNB 0106). (A) anteroventral fragment in lateral view (B) posterior fragment in lateral view compared with the left quadrate of *P. solvayi* (IRSNB R33) in (C) lateral and (D) posterodorsal views. Abbreviations: mc, mandibular condyle; plp, posterolateral process; ssp, suprastapedial process; ta, tympanic ala; tc, tympanic crest. "?" in (A) indicates an indistinguishable section of either the suprastapedial or posterolateral process.

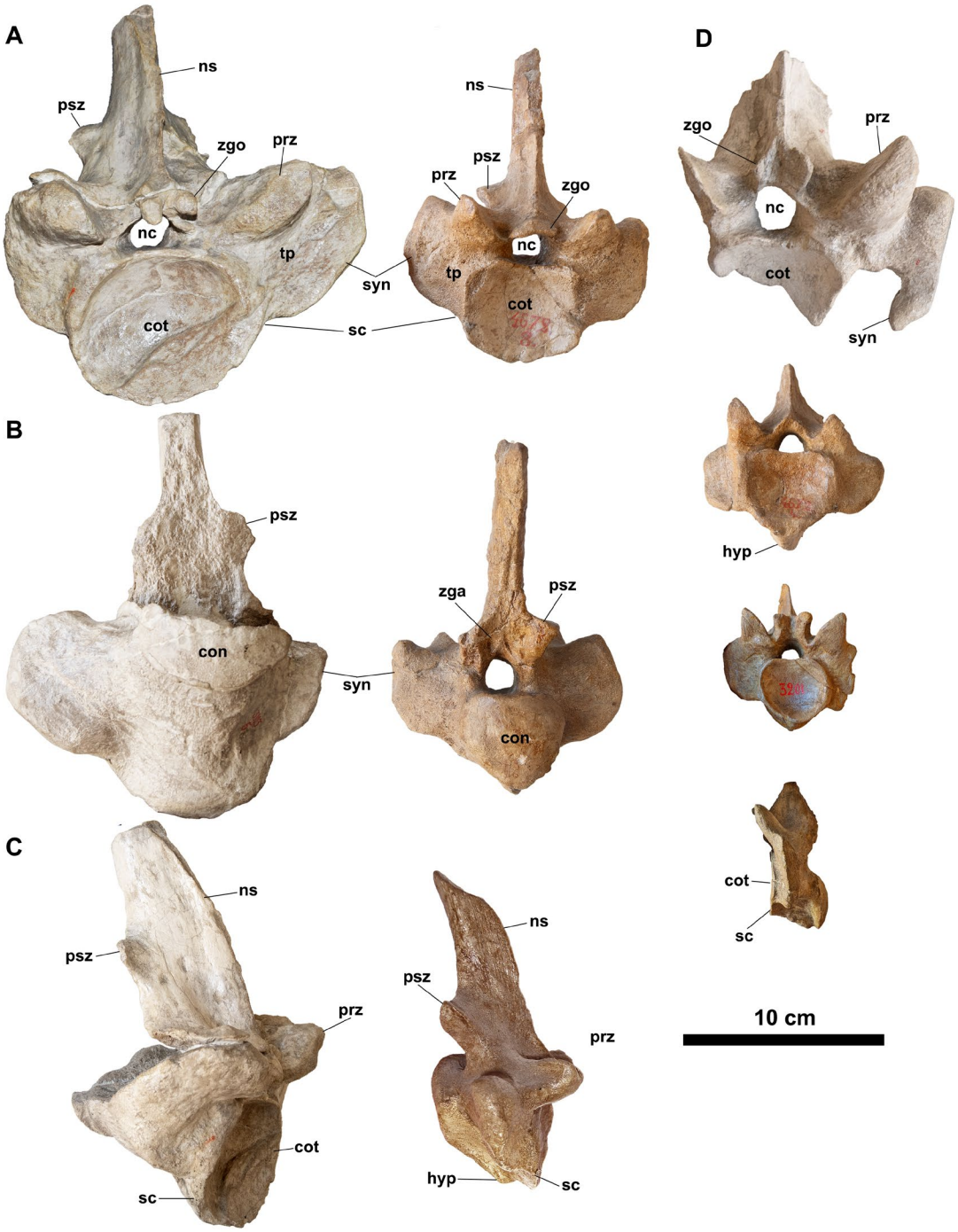

Figure 3.10. Select cervical vertebrae of *P. giganteus* IRSNB 0106 and *P. solvayi* IRSNB R33 in (A) anterior, (B) posterior and (C) lateral views. (D) Cervical vertebrae of *P. giganteus* IRSNB 0106, holotype of *P. solvayi* IRSNB R33, and referred specimen of P. solvayi (IRSNB 0108) in anterior view. Bottom image is IRSNB 0108 in lateral view. Abbreviations: cot, cotyle; con, condyle; hyp, posterior fragment of hypapophysis; nc, neural canal; ns, neural spine; prz, prezygapophysis; psz, postzygapophysis; sc; synapophyseal crest; syn, synapophyseal crest; tp, transverse process; zga; zygantra; zgo, zygosphene.

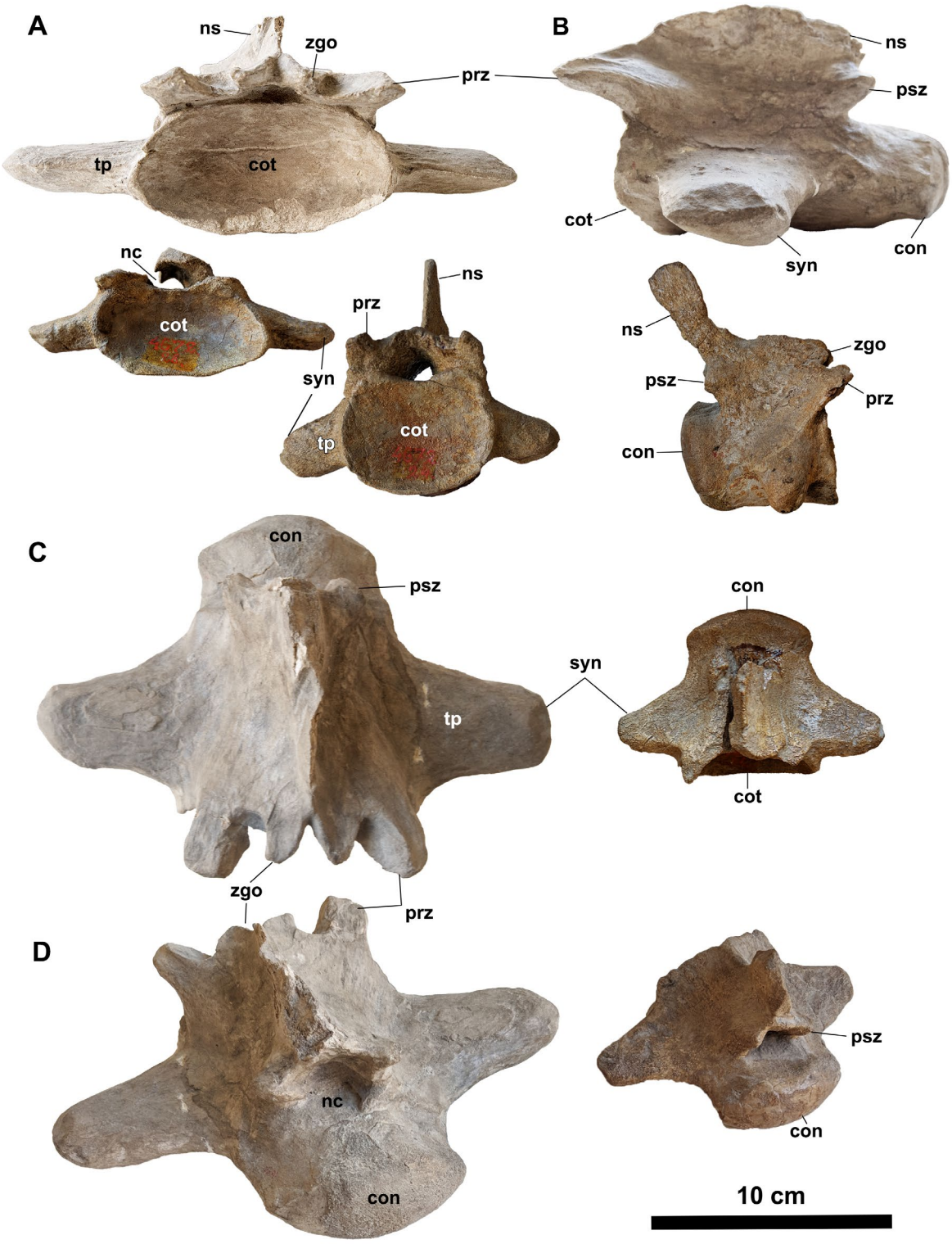

Figure 3.11. Select dorsal vertebra of *P. giganteus* IRSNB 0106 and *P. solvayi* IRSNB R33 in (A) anterior, (B) lateral, (C) dorsal, and (D) anterodorsal views. Abbreviations: cot, cotyle; con, condyle; nc, neural canal; ns, neural spine; prz, prezygapophysis; psz, postzygapophysis; syn, synapophyseal process; tp, transverse process; zgo, zygosphene.

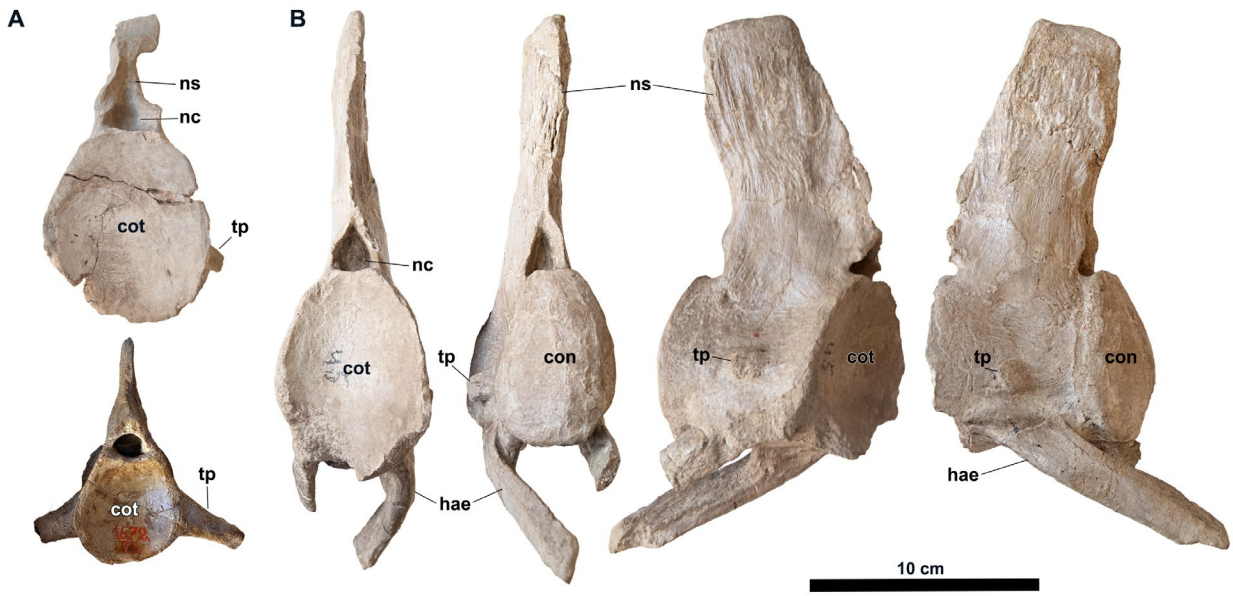

Figure 3.12. Partial pygal vertebra of *P. giganteus* (IRSNB 0106) and *P. solvayi* (IRSNB R33) in (A) anterior view. Select caudal vertebrae of *P. giganteus* IRSNB 0106in (B) anterior, posterior, and lateral views. Abbreviations: cot, cotyle; con, condyle; hae, haemal arch, nc, neural canal; ns, neural spine; tp, transverse process.

CHAPTER 4. REDESCRIPTION AND REASSESSMENT OF *PROGNATHODON SATURATOR*

INTRODUCTION

Prognathodon saturator (NHMM 1998141) is a very large, robustly built mosasaur represented by a single partial skeleton, estimated at a total length of between 10 and 14 meters. (Dortangs et al. 2002; Schulp 2006). NHMM 1998141 was recovered from the Lanayne Member calcarenites of the Gulpen Formation near the city of Maastricht, the Netherlands. Both Dortangs et al. (2002) and Schulp (2006) relate that the deposits in question were laid down during the late Maastrichtian (approx. 66.1 MYA). Consisting mainly of an incomplete skull and vertebral column, NHMM 1998141 was referred to *Prognathodon* on the basis of its angled anterior tooth roots, a tall, bowed dentary, low marginal tooth count, large pterygoid teeth similar in size to the marginal dentition, and the fusion of the suprastapedial and posterior pillar-like processes (after Palci et al. 2021) of the quadrate (Dortangs et al. 2002). The species diagnosis also included a gently convex ventral margin of the maxilla, the dorsolateral alar ridge on the quadrate is absent, a thin crest on the dorsal medial ridge is absent, and the presence of zygosphenes and zygantra on the cervical and dorsal vertebrae. NHMM 1998141 was distinguished from other *Prognathodon* species in general by its massive size and overall heavier construction, but Dortangs et al. (2002) further differentiated *P. saturator* from *P. waiparensis* by the latter's straighter, narrower dentary and longer posterior mandibular unit (PMU). *Prognathodon saturator* also lacked the reported straight dentary, rectangular PMU with a short retroarticular process, less robust quadrate, and small coronoid of *P. giganteus*. No direct comparison to the type species *P. solvayi* was included beyond the account of the procumbent anterior tooth roots.

Schulp (2006) used the character matrices by Bell (1997) and Bell and Polcyn (2005) for phylogenetic analyses, and as a basis for a redescription of NHMM 1998141 and a more detailed comparison with *P. currii*, *P. overtoni* and *P. solvayi*, but did not supply an updated diagnosis. Phylogenetic analysis by Dortangs et al. (2002) and Schulp (2006) both supported the inclusion of NHMM 1998141 within *Prognathodon*. Subsequent analyses typically recovered *P. saturator* in either an unresolved polytomy amongst other members of *Prognathodon*, or as a single taxon within a Hennigian comb (Madzia and Cau, 2017; Simoes et al. 2017, Lively 2020), and most recently within the clade Prognathodontini (Longrich et al. 2022).

Prognathodon saturator exemplifies the concept of *Prognathodon* as a group of large-bodied and robust mosasaurs; however, the redescription of *P. solvayi* (Chapter 2) discards this notion and necessitates the re-examination of other referred taxa as a result. Using a similar schematic by which *P. giganteus* was synonymized with the type species, the following study applies the updated generic diagnosis alongside a comparative redescription of *P. saturator* to assess its validity as a member of the group, as well as formulates an amended diagnosis to further distinguish the taxon.

MATERIALS AND METHODS

NHMM 1998141, IRScNB R 33 (4672), IRScNB 0107, IRScNB 0108, and IRScNB 0106 (3103) were photographed using a Nikon D500 camera with a Nikkor AF-S 50 mm lens and a Google Pixel 2 smartphone. Line drawings were traced from photographs and stippled using a Wacom Intuos pro pen tablet. Photographs were processed and figures produced in Adobe Photoshop CS6 and Adobe Photoshop 25.1. Direct measurements on NHMM 1998141 were not possible and photographs were difficult to take as the specimen is permanently enclosed in a

glass display case. As a result, most figures cannot show the individual elements with clarity or in an optimal arrangement. Line drawings are included in instances where sutures or structures are obscured due to the specimen itself or the image quality. Elements that are poorly or not preserved in either NHMM 1998141 or *P. solvayi* but have existing descriptions and/or lack diagnostic features are excluded from comparison, including the sclerotic ossicles and radius. The vomer and palatines are in articulation in NHMM 1998141 and are only partially exposed in ventral view, but diagnostic features are mostly obscured by the dentary, surrounding maxillae, and teeth, as well as by possible minor compression of the skull. Some elements in NHMM 1998141 have not previously been described in detail and are added here, including the supraoccipital, vertebral series, scapula, and coracoid.

DESCRIPTION AND COMPARISON

Cranium

Skull—The skull of NHMM 1998141 is massive and robust and possibly taphonomically compressed, as well as missing a large portion of the anterior end of its upper and lower jaws (Fig. 4.1A, B). The premaxilla is not preserved, therefore key diagnostic features of *Prognathodon,* including the lack of a predental rostrum and procumbent premaxillary teeth, are not discernable. The internarial bar is the only surviving portion of the premaxilla, but it is poorly preserved and diagnostic features are likewise not apparent. In dorsal view, the skull table is narrower and proportionately longer compared to the broad, short posterior cranium of *P. solvayi* (Fig. 4.1C, D). The orbits are large but proportionately smaller than those of *P. solvayi*. NHMM 1998141 is overall substantially larger than most specimens of *P. solvayi* except for IRSNB 0106 (formerly *P. giganteus*).

Maxilla—The anterior portion of the maxillae of NHMM 1998141 is missing and does not preserve the anterodorsal process or expanded section of the narial opening, and only the left maxilla is easily observed. Much of the bone surface is broken away and poorly preserved, but a series of shallow rounded pits represents a row of foramina dorsal to the tooth row (Fig. 4.2A, B). Although only a few are visible, they occur in a line above the reportedly gently convex ventral margin of the maxilla (Dortangs et al., 2002; Schulp, 2006), although it is not well enough preserved to determine the shape of its outline. If present, this would contrast with the slightly concave margin of the maxillae in *P. solvayi*. Posteriorly, the maxilla of NHMM 1998141 is not as deep as in *P. solvayi*; the posterodorsal process extends only slightly above the anterior dorsal margin, as it is oriented more medially than the dorsally oriented posterodorsal process of *P. solvayi* (Fig. 4.2). The triangular posterior tip of the right maxilla is possibly exposed at the anteroventral margin of the right orbit (Fig. 4.4).

The maxillary teeth in NHMM 1998141 differ considerably from those of *P. solvayi*: the crowns are more robust with broader, circular bases as opposed to subcircular or lenticular (Fig. 4.2). NHMM 1998141 also appears to lack the faint lingual curvature of the apex and slight laterocumbent orientation apparent in *P. solvayi*. In labial and lingual views, the anterior and posterior edges are both curved, contrasting with the more strongly curved anterior and straighter posterior margins of the teeth in *P. solvayi*. Only the unerupted teeth of *P. solvayi* show serrations on the carinae and fine anastomosing texture near the apex, but the mature crowns in NHMM 1998141 show both minute serrations along the anterior and posterior carinae and anastomosing ridges at the crown apex (Fig. 4.2; Schulp, 2006). Flutes are absent in NHMM

1998141, including on the unerupted teeth, although only the tips are visible in the few examples that are exposed.

Frontal—The frontal of NHMM 1998141 is longer and narrower than the frontal of *P. solvayi* (Fig. 4.3). The lateral borders in *P. solvayi* are sinusoidal in outline and convex for most of the element's extent, whereas the convex posterolateral borders NHMM 1998141 curve inwards above the prefrontals and narrow gradually anteriorly. The lateral edge of the frontal in NHMM 1998141 is not excluded from the orbital margin by the prefrontal and postorbitofrontal but forms a larger portion of the dorsal edge of the orbit than does *P. solvayi*. Although damaged, NHMM 1998141 preserves a median ridge along the anterior portion of the frontal, a feature that is absent in *P. solvayi*. The anteromedian process is also heavily damaged, and the precise shape is difficult to discern, but the laterally-positioned, shoulder-like protrusions in *P. solvayi* appear to be absent in NHMM 1998141; the anterior borders of the narial opening are instead weakly concave. An anterolateral extension of the frontal forms the posterior borders of the narial opening to contact the maxilla (Figs. 4.3A, B). The posterolateral alae in NHMM 1998141 are poorly preserved, but a depression on the right postorbitofrontal suggests they would have been rounded and projected posterolaterally. Like *P. solvayi*, the suture with the overlapping postorbital processes of the parietal curves anteriorly. Although not recognisable in *P. solvayi*, the long, tapering posteromedial processes are well-preserved in NHMM 1998141 and extend past the posterior border of the parietal foramen, enclosing it and a square-shaped portion of the parietal.

A small ventral portion of the frontal is visible NHMM 1998141 (Fig. 4.4), although some borders are obscured or damaged. Unlike in *P. solvayi*, the edges of the subolfactory processes curve medially and form an extensive contact along the midline.

Prefrontal—The left prefrontal of NHMM 1998141 is well-exposed, although the dorsal and ventral sides of the right prefrontal are also partially visible. Laterally the bone surface is heavily damaged, but both elements preserve the prominent supraorbital process, as is the case in *P. solvayi* (Fig. 4.5). The anterior laminae are narrow and elongate in dorsal view, but due to poor preservation the outline of contact with the maxillae and the extent to which they form the border of the narial opening is obscured; however, an anterolateral projection from the frontal appears to underlap the anterior wing of the prefrontal, excluding it entirely from the narial border (Fig. 4.5A, B) (contra Schulp (2002) scoring this character as unknown). This condition is present in the mosasaurine mosasaur *Plotosaurus* (LeBlanc et al. 2013: fig. 2), but not in *P. solvayi*, where the prefrontal instead forms a large portion of the posterolateral border of the narial opening (Fig. 4.5C). Also, like *Plotosaurus*, a small tongue of the anterior prefrontal invades the posterodorsal edge of the maxilla. The anterodorsal margin of the prefrontal appears to have slightly disarticulated from the contact with the frontal. The thin, planar sheet of bone of the descending lamina in *P. solvayi* is conversely represented by a thick, rounded column in NHMM 1998141 (Fig. 4.5D). Ventrally, some suture lines are difficult to observe due partially to damage, but the posterior wing of the prefrontal is broad and fan-shaped, and slightly overlaps the anterior wing of the postorbitofrontal. This contrasts sharply with the condition in *P. solvayi* where the two elements do not directly contact one another.

Postorbitofrontal—Only the dorsal and anteroventral surfaces of the right postorbitofrontal are visible in NHMM 1998141, and only the ventral surface of the left postorbitofrontal is preserved (Figs. 4.3, 4.4, 4.6A). The anterior wing in the left element inserts between the frontal and

prefrontal in ventrolateral view. Medially, the outline of the suture with the parietal is obscured but appears to have curved posteriorly. Dorsally, an overhanging process is preserved on the lateral margin of the right element, although this is less extensive and more rounded in shape than in *P. solvayi* (Fig. 4.3; note the slightly more triangular shape of the better-preserved right element). This process is also thicker and ornamented with shallow elongate grooves near its lateral margin. Its lateral border with the squamosal is difficult to identify due to these grooves and nearby cracks in the bone. The robust posterior ramus projects off the lateral margin and inserts into a deep facet of the squamosal, its tip narrowing posteriorly and terminating anterior to the limit of the parietal process. In *P. solvayi*, the process extends further posteriorly (Fig. 4.6B). Like the overhanging process, elongate grooves that appear continuous with the corresponding squamosal are present on the posterolateral surface of the ramus (Fig. 4.6A).

Parietal—The parietal in NHMM 1998141 is well preserved and visible in multiple aspects. The postorbital processes resemble those of *P. solvayi* but are even more broadly exposed in dorsal view, invading the frontals anteriorly (Fig. 4.6A). The lateral borders of the processes in *P. solvayi* are lobed and emarginate, but the bone surface is worn in NHMM 1998141 and this detail is not readily discernable. The pineal foramen is enclosed entirely in the parietal, although this is also not easily comparable with the obscured frontoparietal suture in *P. solvayi*. The faint triangular platform in between which the pineal foramen is situated in *P. solvayi* is absent in in NHMM 1998141 (Fig. 4.6B). The parietal table is considerably narrower and longer than in *P. solvayi* and the anterior platform is less triangular as a result. The posterior point of this platform also does not extend as far posteriorly along the temporal arcade, and the anterolateral edges do not overhang the temporal fenestrae. The posterior end of the table is heavily damaged, but its

anterior extent preserves a large central ridge originating at the parietal table and dividing two narrower lateral sulci, all of which likely stretched to the posterior limit of the bone. Although mostly incomplete, the base of the suspensorial rami of the parietal in NHMM 1998141 differ from *P. solvayi* in their orientation, originating further posteriorly and attaching vertically at their bases as opposed to horizontally. They likely would have twisted posteriorly and aligned horizontally with the parietal process of the supratemporal.

The ventral surface of the parietal in NHMM 1998141 is mostly obscured from view, but the pineal foramen appears to be recessed and bounded by a raised mass of thickened bone rather than a thin ridge in *P. solvayi* (Fig. 4.4). Posteriorly, the left ventrolateral surface of the parietal is relatively well-preserved. Laterally, the descending processes of the parietal (and much of the braincase as a whole) are broader and considerably shorter in *P. solvayi* (Fig. 4.9).

Jugal—Schulp (2006) noted that the jugal of NHMM 1998141 is more robust than that of *P. solvayi* and features a more angular shape overall (Fig. 4.7A). Although missing the anterior-most tip, the horizontal ramus of the jugal in *P. solvayi* is strongly bowed and narrow across its entire length, whereas the ramus is straighter and the anterior end is noticeably expanded in NHMM 1998141. The vertical ramus also extends dorsally at a slightly obtuse angle as opposed to the gentle curvature in *P. solvayi*. A small, pointed posteroventral tuberosity projects from the posterior margin of the vertical ramus and above the horizontal ramus (Schulp, 2006), a feature which is likewise absent in *P. solvayi.*

Pterygoid, Ectopterygoid—The pterygoid of NHMM 1998141 is overall considerably more robust than that of *P. solvayi* (Fig. 4.8A-C). Ventrally, the tooth row erupts from a thick, rounded

eminence extending ventrally from the main pterygoid body (Schulp, 2006: fig. 11C, D), contrasting primarily in the thickness of the element in *P. solvayi*, which lacks a large ventral extension of the main body. The main body in NHMM 1998141 is also a similar width across its length and less curved overall than in *P. solvayi*, instead having nearly straight lateral and medial edges (Fig. 4.8D, E) (Schulp, 2006: fig. 11D, E). A possible pterygoid foramen is present on the dorsal surface, although this may simply be damaged bone. The thin, narrow quadrate process of *P. solvayi* is likewise contrasted by the much thicker and broader process in NHMM 1998141 which is nearly circular in cross-section. The ectopterygoid process is large, robust, and columnar in shape, expanding at its distal contact with the ectopterygoid. This process in *P. solvayi* is considerably smaller in proportion and lacks an enlarged distal end, its articular surface instead slanting posteriorly. Posteromedially, the space between the basisphenoid process and the quadrate process is reduced compared to *P. solvayi*, and the process is more elongate and rectangular in shape as opposed to short and triangular.

NHMM 1998141 likely had 6 pterygoid tooth positions (Schulp, 2006). Like *P. solvayi*, the pterygoid teeth of NHMM 1998141 are only slightly smaller than the marginal dentition, and the teeth are circular in cross-section. The crowns also appear to decrease slightly in size posteriorly. They otherwise differ in shape, being less strongly curved than those of *P. solvayi*. Schulp (2006) also noted anterior and posterior carinae and anastomosing texture near the apex in the larger teeth, whereas only posterior carinae are apparent in some examples in *P. solvayi*. Most notably, the enamel surface of a few of the crowns in NHMM 1998141 are gently fluted; this is visible on the replacement tooth on the lateral surface of the left pterygoid, and the mature teeth in the right pterygoid (Fig. 4.8F). This feature is absent in *P. solvayi*, in which the pterygoid tooth crowns are smooth and otherwise featureless.

In NHMM 1998141, the posterior edge of the ectopterygoid is straight, and a small eminence protrudes from the posterolateral corner directly opposite the lateral prong, resting against a shallow fossa on the posteromedial surface of the horizontal ramus of the jugal (Fig. 4.7B). The proposed ectopterygoid in *P. solvayi* is incomplete and poorly-preserved, but notably lacks a posterolateral process extending beyond its angled posterolateral edge (Fig. 4.7D). Although Schulp (2006) was uncertain whether the ectopterygoid contacted the maxilla, the anterior horizontal ramus appears to abut against the posteroventral margin of the maxilla dorsal to the exposed triangular posterior tip (Fig. 4.2).

Squamosal—Only the right squamosal is preserved in NHMM 1998141, but much of it is concealed by other elements of the skull. It is overall broader and more robust than in *P. solvayi*. In dorsal view, a posterolateral crest is present but appears to be thickened and rounded as opposed to a narrow shelf (Fig. 4.6). Long, deep grooves extend from the posterior edge across the dorsal surface of the crest, terminating near the contact with the postorbitofrontal. The parietal process is poorly preserved and not readily comparable. The posteromedial portion overlaps a small, damaged remnant of the supratemporal.

Prootic, Opisthotic-Exoccipitals, Supraoccipital—Although present in articulation with the parietal, basisphenoid, and basioccipital, the surface of the prootic of NHMM 1998141 is weathered and cranial nerve foramina are not apparent. The descending processes extend anteroventrally to contact the alar processes of the basisphenoid horizontally as opposed to at an angle as in *P. solvayi* (Figs. 4.9, 4.10A, 4.11A).

The opisthotic in NHMM 1998141 preserves the right paroccipital process or bar and the base of the left (Figs. 4.6, 4.10A, 4.11A). Comprised mainly of the opisthotic, the base of the bars is robust and rounded in cross-section, gradually flattening and broadening posteriorly at the contact with the supratemporals. The base of the exoccipitals are broadly fused to the opisthotic. Although these are broken or missing in *P. solvayi* and the skull of the holotype is distorted, it appears the exoccipitals in NHMM 1998141 are considerably taller.

The supraoccipital is damaged and distorted in *P. solvayi*, but this element has not been described for NHMM 1998141. The supraoccipital is tall and narrow (Figs. 4.10A, 4.11A). Dorsally, the processus ascendens tectum synoticum abuts the parietal at the base of the supratemporal processes, the lateral edges contacting the anterior margin of the descending processes. A thin median crest situated between two shallow sulci extends across the posterior surface from the tectum synoticum to the posteroventral base of the supraoccipital.

Basisphenoid—The basisphenoid is one of the few well-preserved elements of the braincase in NHMM 1998141, and remains in articulation with the damaged prootic, basioccipital, and parasphenoid (Fig. 4.10B, C). Dorsally, the alar process ascends to meet the descending process of the prootic, forming a broad pedestal. NHMM 1998141 however lacks the anterior extension of the alar processes apparent in *P. solvayi* (Fig. 4.10D). Anteriorly, the parasphenoid process extends anteriorly, inserting anterodorsally against the parasphenoid. The thin walls of bone that are situated between the parasphenoid and alar processes and buttress the sella turcica are reduced in both length and height compared to those of *P. solvayi*. The vidian canal that is incised along the lateral side of the basisphenoid in *P. solvayi* is absent in NHMM 1998141. Overall, the basisphenoid of NHMM 1998141 is more elongate with a less pronounced

constriction between the basipterygoid and posterior processes. Unlike *P. solvayi*, the basipterygoid processes themselves lack constricted bases and are long with narrow, medially curved tips. The posterior processes in NHMM 1998141 are laterally broad, similar to *P. solvayi*, but the articular facets for the basioccipital tubera are angled more posteriorly and V-shaped in cross-section rather than weakly concave. Ventrally, the deep groove that extends along the midline of the basisphenoid in *P. solvayi* is less apparent in NHMM 1998141, occurring primarily between the posterior processes.

Basioccipital—The left basioccipital tuber of NHMM 1998141 is exposed and is long and narrow across its whole length, contrasting with the short, wide tubera in *P. solvayi* (Fig. 4.11). The slender shape in NHMM 1998141 forms a more strongly concave ventral border and therefore a larger degree of separation between the two tubera. The occipital condyle is large, robust, and U-shaped, with a deep depression incised on the dorsal surface. An opening for the basioccipital canal within the central depression, diagnostic of *Prognathodon*, is absent.

Lower Jaw

Dentary—Like much of the rest of the skull, the dentaries of NHMM 1998141 are robustly built (Fig. 4.12A). Similarities shared with *P. solvayi* include a bowed dentary with concave dorsal margins and a row of large, elongate foramina extending across the midline on the lateral surface of the left dentary (Fig. 4.12B). Unique to NHMM 1998141, a broad shallow groove continuous with the adjacent surangular fossa is situated along the dorsolateral surface (Fig. 12A).

Dortangs et al. (2002) and Schulp (2006) described the anterior dentary tooth roots of NHMM 1998141 as inclined and therefore likely procumbent, a key characteristic present in *P.*

solvayi. Although this feature is visible in NHMM 1998141, the anterior region is crushed and there is a possibility that the slanting of the roots is exaggerated by damage to the bone. The dentary teeth otherwise differ between NHMM 1998141 and *P. solvayi* in the same way as the maxillary dentition: in NHMM 1998141 the crowns are robust and more circular in cross-section, with curved anterior and posterior edges (Fig. 4.12C, D). Fluting is absent. Mesial and distal carinae with minute serrations are present, as well as anastomosing texture near the crown apices. The latter two features are largely only present in the replacement teeth of *P. solvayi*. Crown shape does not vary as strongly across the jaw in NHMM 1998141; the posterior teeth are smaller and slightly narrower but more closely resemble the shape of the anterior teeth (Fig. 4.12). This contrasts with the short, blunt, and strongly hooked posterior teeth in *P. solvayi*.

Splenial—The lateral face of the splenial in both NHMM 1998141 and *P. solvayi* is largely only visible as a thin splint along the ventral edge of the dentary, with a wedge-shaped portion of the cotyle extending posteriorly from the posteroventral margin (Figs. 4.12A, B, 4.13A, B). The medial wing of the splenial in *P. solvayi* is similar in height but extends to more than halfway along the length of element, its dorsal margin descending evenly at a shallow angle (Fig. 4.12B). In NHMM 1998141, the medial wing is tall and extends to just below the tooth row, the dorsal margin flattening out and descending ventrally to follow the concave curvature of the dorsal edge of the dentary. The dorsal margin is interrupted by a large incomplete foramen which is absent in *P. solvayi*. A large foramen is present at the base of medial wing and is positioned more dorsally than in *P. solvayi* (Lingham-Soliar and Nolf, 1989: fig. 21). The lateral wings are concealed by the dentaries in NHMM 1998141 as is most of the posterior cotyle, but the articular surface is deeply concave to receive the angular.

Angular—Both angulars in NHMM 1998141 are in articulation with the surangular and articular, and the anterior ends are largely concealed as a result, although the articular surface is convex and inserts into the concave splenial cotyle (Fig. 4.13A,B). The lateral surface of the left angular in NHMM 1998141 is more broadly exposed than in *P. solvayi*, where only a thin anteroventral wedge would likely have been visible (Fig. 4.13C). The lateral wing is considerably taller, forming a rounded margin anterodorsally which descends posteriorly and is overlapped by the surangular. A small wedge of the angular reappears posteriorly along the posteroventral margin of the surangular and overlies the articular (Fig. 4.13A, B). The medial surface of the right angular is visible but its center is partially damaged. NHMM 1998141 and *P. solvayi* differ considerably in the height of the medial wing; in the former it is considerably taller and broadly contacts the ventral margin of the anteromedial wing of the coronoid (Fig. 4.13A, B, Fig. 14A, B). Schulp (2006) reported that the coronoid and angular contacted in *P. solvayi* as well, but neither the coronoid anteromedial wing nor the medial wing of the angular are long enough to do so (Fig. 4.13C). Unlike *P. solvayi*, an angular foramen also appears to be absent.

Surangular—The individual elements of the PMU in NHMM 1998141 are massively constructed, including the surangulars (Fig. 4.13A, B; note that the surangular is slightly deeper than what the ventrolateral angle in the image shows, but features would otherwise be obscured by the overhead lights and glare. See Fig.1B.). Laterally, the element is deep and triangular in shape, the dorsal margin of the expanding anteriorly to form a buttress against the coronoid. This contrasts sharply with the flat, parallel margins of the rectangular surangular in *P. solvayi*. A crescentic surangular fossa is present on the anterodorsal edge of the surangular in both NHMM

1998141 and *P. solvayi*, although in the latter this feature is narrower and more elongate posteriorly. The deep excavation or fossa on the posterolateral surface of the surangular in *P. solvayi* is present but slightly shallower in NHMM 1998141 (Fig. 4.14A, C). The ventral margin of the depression is sharply delimited by a narrow shelf in NHMM 1998141 (similar to *Gnathomortis stadtmani*, Lively (2020): fig. 8), which is less distinct and smoother in *P. solvayi*. Apart from the adductor fossa that follows the shape and curvature of the articular, the medial face of the right surangular in NHMM 1998141 is largely obscured by other cranial elements and a large chert nodule (Fig. 4.14A, B).

Coronoid—The coronoid morphology in NHMM 1998141 and *P. solvayi* do not differ strongly; the shape and extent of the lateral wing is similar, and both taxa show a rounded, overhanging shelf ornamented with fine, elongate striae, extending across the lateral surface of the coronoid process (Fig. 4.13). However, the medial deflection of the coronoid process in *P. solvayi* is absent in NHMM 1998141, where the process is instead aligned parallel to the coronoid. The coronoid process itself is also shorter and broader anteroposteriorly in NHMM 1998141 than in *P. solvayi*. Anteriorly, the transition between the lateral wing and coronoid ramus is more smoothly continuous in *P. solvayi*, whereas the anterior margin ventral to the coronoid ramus is notched in NHMM 1998141 and conforms to the shape of the large surangular fossa. Medially, the anteromedial wing of the coronoid in NHMM 1998141 is considerably larger than in *P. solvayi*, extending further ventrally to contact the dorsal edge of the medial wing of the angular (Figs. 4.13A, B, 4.14A, B). The presence or absence of the posterodorsomedial process reportedly could not be ascertained in NHMM 1998141 (Schulp, 2006), but a posterior extension

of the coronoid overlapped by the surangular buttress is visible on the left coronoid (Fig. 4.14A, B).

Articular—Both articulars in NHMM 1998141 are in articulation with the other elements of the PMU and partially concealed as a result (Figs. 4.13A, B, 4.14A, B). The lateral surface of both elements shows the articular primarily forms the posterior edge of the glenoid, whereas the articular also partially contributes to the lateral margin of the glenoid fossa in *P. solvayi* (Fig. 4. 13C). Posteriorly, the retroarticular process is rotated obliquely relative to the PMU in NHMM 1998141, differing notably from the parallel orientation of the process in *P. solvayi* (Figs. 4.13, 4.14). A large, oval articular foramen is also present on the dorsal surface of the retroarticular process in NHMM 1998141; no foramina are visible on the articulars of *P. solvayi*.

Quadrate—Despite the similarities in overall shape of the element particularly in medial view, there are a few features of the quadrate in NHMM 1998141 that are otherwise distinct from that of *P. solvayi*. The quadrate bone of NHMM 1998141 is thickened and considerably more robust as a result, but narrower and more elongate in lateral view (Fig. 4.15A, B, D). The large, broad, and bulbous mandibular condyle of NHMM 199814 expands medially in posterior view, contrasting with the small, short, tapering condyle in *P. solvayi*. A slight central bulge is present on the ventral surface of the condyle and is only slightly shorter than the medial expansion. Due to distortion, this feature is not clearly visible in *P. solvayi*. Dortangs et al. (2002: fig. 3A, C) and Schulp (2002: fig. 14C) illustrate the anterior surface of the mandibular condyle extending dorsally onto the anteroventral surface of the quadrate (Fig. 4.15A, C), which is also somewhat

visible laterally as slight anteriorly shifted shelf. This feature is either not preserved or not present in *P. solvayi*.

Laterally, the tympanic crest of NHMM 1998141 is distinct: it expands and curves from the ala posteriorly to conceal much of the quadrate conch, such that the flattened surface of the tympanic crest is deflected to face posteriorly (Fig. 4.15A, D). The ala in *P. solvayi* entirely lacks this posterior extension and the tympanic crest is instead aligned nearly vertically with the ala in lateral view and angled posterolaterally (Fig. 4.15D).

Posteriorly, the suprastapedial process descends abruptly just posterior to the cephalic condyle in NHMM 1998141. In contrast, the base of the suprastapedial process in *P. solvayi* extends horizontally from the cephalic condyle before curving ventrally to meet the pillar-like process (Fig. 4.15A). The suprastapedial process is slightly longer in *P. solvayi*, terminating a little over halfway on the quadrate shaft. In posterior view, the process in NHMM 1998141 is mediolaterally expanded. The dorsomedial surface of the process is excavated by a groove, although this is somewhat less pronounced than in *P. solvayi*. A tight fusion is present between the suprastapedial and pillar-like/posterolateral processes in both taxa but is broad and oriented mediolaterally in NHMM 1998141 in posterior view, as opposed to narrower and directed anteroposteriorly in *P. solvayi* (see dorsal view of *P. solvayi* quadrate in Fig. 4.15C and posterior view of NHMM 1998141 in Fig. 4.15D). Medially, the distal tip of the suprastapedial process tilts ventrally in NHMM 1998141 and overlaps the pillar-like process, although the suture appears horizontal in posterior view. The contact in *P. solvayi* has a minimal anteroventral slant but is largely horizontally oriented in all aspects.

Palci et al. (2021) hypothesized that a combination of the posteromedial and posterolateral processes forms the broad posterior pillar-like process in *Prognathodon*. In

NHMM 1998141, the process is short, pedestal-shaped, and extends further onto the medial surface than in *P. solvayi*. It is expanded in posterior view and a similar width to the suprastapedial process, broadly spanning across much of the quadrate shaft (Fig. 4.15B, D), suggesting it is more accurately termed as the posterior pillar-like process, as per the observations of Palci et al. (2021). In contrast, this process in *P. solvayi* is considerably narrower, particularly at its base, and is confined to the lateral surface of the quadrate (Fig. 4.15B, C), more closely resembling the posterolateral process of *Selmasaurus* (Palci et al. 2021: fig. 3A) (Chapter 2). The right quadrate of *P. solvayi* is distorted and the processes may appear superficially similar to the condition in NHMM 1998141 (Fig. 4.15D).

In medial view, the median ridge in *P. solvayi* is positioned slightly anteriorly and is roughly continuous with the dorsomedial eminence or crest, such that its dorsal extent forms a raised anterior margin of the stapedial pit (Fig. 4.15B). In contrast, the median ridge in NHMM 1998141 is positioned slightly further anteriorly and terminates ventral to the stapedial pit. A dorsomedial eminence extending above the stapedial pit and the dorsal margin of the quadrate ala is absent in NHMM 1998141, although a small section of bone dorsal to the stapedial pit appears to curve ventrally against the medial surface of the quadrate conch, and may represent the same structure in a different orientation.

Axial Skeleton

The axial skeleton of NHMM 1998141 is better preserved than in *P. solvayi*, with anterior segments of the vertebral column in loose articulation. Like the cranium, the vertebral elements are massively constructed.

Axis—The anterior cervical vertebrae of NHMM 1998141 were not described in detail by Dortangs et al. (2002) or Schulp (2006) and are largely only exposed in lateral view. Although the atlantal elements are not discernable, the axis remains and is well-preserved (Fig. 4.16A-C). The axis of *P. solvayi* is heavily fragmented, but the neural arches in NHMM 1998141 are thicker and robust, expanding laterally towards the base of the bulbous transverse processes (Fig. 4.16C, D). The neural canal is more oblong and dorsoventrally tall. The neural spine is stout and very broad anterodorsally. Its dorsal margin is damaged but appears to descend anteroventrally at a shallower angle and terminate farther dorsally above the anterior articulations than in *P. solvayi*. Although the distal ends of the postzygapophyses are missing in *P. solvayi*, in NHMM 1998141 they are spaced more widely apart and angled posterolaterally.

The anterior articulations for the atlas synapophyseal processes in *P. solvayi* are small, but with a less tapered profile and rounded articular surfaces (Fig. 4.16). In NHMM 1998141, these structures taper anteriorly to a proportionately smaller and flat surface in lateral view. An anterior median concavity for the axis intercentrum is not visible. Posteriorly, the neck of the centrum is constricted just anterior to the condyle edge. The condyle itself is subcircular in shape with a flat dorsal margin, and its posterior limit extends beyond the dorsal edge of the strongly posteroventrally angled hypapophysis. The axis centrum is not preserved in *P. solvayi* and therefore cannot be compared.

Cervical Vertebrae—The cervical vertebrae of NHMM 1998141 are preserved in articulation and only their lateral surfaces are easily observable (Fig. 4.17A-D). The neural spines are tall, anteroposteriorly broad, and angled posteriorly. The neural canal, cotyle and condyles are not visible, although a precondylar restriction is present as well as more pronounced than in *P.*

solvayi (Fig. 4.17E). The transverse processes project horizontally and their dorsal edge is roughly level to the dorsal margin of the centra. Like *P. solvayi* they appear to be roughly the same height as the centrum, although they are narrower, positioned further posteriorly, taper slightly to a broad, rounded synapophyseal process (e.g., third cervical vertebrae, Fig. 4.17), and project posterolaterally as opposed to laterally. The dorsal edge is continuous with the base of the prezygapophyses. A sinuous, thin synapophyseal crest that extends to midway on the cotyle margin is absent in NHMM 1998141; the thick, ventral edge of the crest instead terminates midway on the anterolateral surface of the centrum (Fig. 4.17A, C, D). The prezygapophyses are broad, robust, with minimal tapering towards the flat, rounded tips, and they curve medially rather dorsomedially. The postzygapophyses are very short with posteroventrolaterally directed facets, and are situated dorsal to the tall, embayed posterior margin of the neural arches that accommodate the large prezygapophyses. The hypapophyses are more strongly oriented posteroventrally that in *P. solvayi*. As observed by Dortangs et al. (2002) and Schulp (2006), zygosphenes and zygantra are present but largely obscured from view (Fig. 4.17D).

Dorsal Vertebrae—NHMM 1998141 preserves multiple isolated examples of the dorsal vertebrae in addition to articulated series (Figs. 4.18, 4.19). They are massively built, and the bone surface is heavily textured with horizontally-oriented striae covering the centra and zygapophyses. These striae angle more vertically near the base of the neural arch. In all instances the neural spines are damaged and missing their distal extremities but were otherwise robust and anteroposteriorly broader than the cervical neural spines. In the anterior vertebrae, the neural canals are oval and bounded by robust neural arches. Despite distortion in the vertebrae of *P. solvayi*, the centra in NHMM 1998141 are circular and appear wider mediolaterally (Fig. 4.18A-

D; Schulp 2006: fig. 21A). The dorsal margin of the centra is notched in both taxa. Laterally the centra are more elongate that in *P. solvayi*, particularly the posterior condylar region (Fig. 4.18A). A prominent constriction is present anterior to the sharp border of the condyles. Unlike *P. solvayi*, the transverse processes of the anterior dorsal vertebrae NHMM 1998141 are broader dorsoventrally and originate further ventrally on the centrum, although they project slightly dorsally in both taxa. In more complete examples in NHMM 1998141, the synapophyseal processes are massively expanded distally and bulbous in shape (Fig. 4.18C). The prezygapophyses in the anterior dorsals in particular are remarkably large and robust with medially oriented facets. Like *P. solvayi*, the postzygapophyses are short, tapered, and project posterolaterally in all dorsal vertebrae. Zygosphenes on the anterior dorsals are either not well-preserved or concealed, but the corresponding zygantra are large and deep (Fig. 4.18B, C), suggesting that the zygosphenes were likewise well-developed.

Most of the posterior vertebrae in NHMM 1998141 are preserved in articulation (Fig. 4.19A-D). The remaining portions of the neural spines are distinctly broad anteroposteriorly, such that the posterior margin abuts against the neural spine of the succeeding vertebra (Fig. 4.19A). Most of the centra are distorted, but a notch in the dorsal margin is visible in multiple examples (Fig. 4.19B). A prominent precondylar restriction is visible in one example exposed in ventral view (Fig. 4.19B), and the centrum is taller than broad in shape, contrasting both with the anterior vertebrae and the posterior vertebrae of *P. solvayi*. Differing substantially from the anterior dorsals, the transverse processess orient horizontally and taper towards a narrower synapophyseal process, which also occurs in *P. solvayi* (Fig. 4.19C, D). However, they are positioned further anteriorly on the centrum in *P. solvayi*. Like in the anterior dorsals, the transverse processes in the posterior dorsals are positioned more dorsally on the centrum in

NHMM 1998141 and lack the ventrolateral orientation present in *P. solvayi*. The bases of zygosphenes are visible in the articulated series of dorsals and appear large and oriented anteriorly.

Pygal and Caudal Vertebrae—The pygals and caudals of NHMM 1998141 are more robust but largely similar to those of *P. solvayi*: the neural canals are circular, the centra are taller than they are wide with a notch on the dorsal margin, and the haemal arches are fused to the centra (Fig. 4.20). The lateral surfaces of the neural spines are also heavily striated. The neural spines in the caudal vertebrae of NHMM 1998141 are more strongly angled posteriorly, and the transverse processes are broader and angled more ventrally (Fig. 4.20C-E). The transverse processes in the pygal vertebrae of NHMM 1998141 are robust and taper more gradually compared to those of *P. solvayi* (Fig. 420A, B). The pygals of NHMM 1998141 have narrow transverse processes, although these are not comparable to the broken examples in *P. solvayi* (IRScNB 0106) (Fig. 4.20C-E).

Ribs—The ribs in NHMM 1998141 are overall more massively constructed than in *P. solvayi* (Fig. 4.21). The cervical and dorsal ribs in the two taxa are similar in shape, possessing a simple, fan-shaped rid head with a straight to slightly rounded proximal margin. The larger dorsal ribs of NHMM 1998141 possess a deep groove on the posterior surface that extends midway along the rib shaft, whereas this manifests as a less extensive, shallow concavity in *P. solvayi*.

Appendicular Skeleton

Scapula and coracoid—These elements are poorly preserved in *P. solvayi* and only a few features are comparable. The scapula expands abruptly from the neck to form an oblong fan-shaped blade with an elongated posterior corner, shorter anterior corner, and a convex outer margin (Fig. 4.22). Both the scapular and coracoid necks are broader in NHMM 1998141, but as in *P. solvayi* the facets are a similar width. Dortangs et al. (2002) described the two bones as fused, and although partially obscured, it is more likely that the two elements are joined by tight interdigitating suture, similar to that of *P. overtoni* (Konishi et al. 2012). A glenoid facet is not visible.

The broad neck of the coracoid of NHMM 1998141 is positioned midway between the symmetrical, fan-shaped blade. A large foramen is situated slightly anteriorly on the coracoid neck and near the facet with the scapula, which resembles the condition in *P. solvayi* (Fig. 4.22B).

DISCUSSION

This comparative description of NHMM 1998141 with *P. solvayi* demonstrates a multitude of characters that differentiate the two taxa. Both the initial species diagnosis and referral of NHMM 1998141 to *Prognathodon* were based on a comparatively few number of features (Dortangs et al. 2002), hearkening back to the earliest brief descriptions of *P. solvayi* and likely in accordance with the characterization of the genus based in large part on the robust North American representatives (Russell, 1967; Lingham-Soliar and Nolf, 1989). The application of the character matrices of Bell (1997) and Bell and Polcyn (2005) provided a more detailed description and comparison of *P. saturator* (Schulp, 2006); however, there is disagreement

between the character scorings and our redescription of *P. solvayi* that likely affected the resulting tree topology. Several characters from Schulp (2006) should be rescored, including: contact between the coronoid and angular (absent), coronoid buttress of surangular (absent), rotated retroarticular process (absent), flutes on marginal teeth (present), absence of a posteromedial process of the coronoid (present), and posterior invasion of the frontal onto the parietal (?). Additionally, several of the morphological disparities identified between the taxa examined here are not necessarily captured by this list. For example, character (42) describes the pterygoid tooth row as originating from either the main body directly (0) or elevated on a thin descending ridge (1). Both NHMM 1998141 and *P. solvayi* were scored as (1) following Dortangs et al. (2002); however, in agreement with Christiansen and Bonde (2002), this ridge is absent in *P. solvayi* and manifests in NHMM 1998141 as a rounded, thickened expansion, demonstrating that the character states did not necessarily adequately separate between the different conditions. Similarly, character (31) codes for the type of overlap between the prefrontal and postorbitofrontal, which accounts for the condition in NHMM 1998141, but not for the lack of contact of these elements in *P. solvayi*. Finally, multiple elements were not included in the phylogenetic analysis, particularly the vertebrae and the braincase (prootic, exoccipitals, opisthotic, parts of the basisphenoid), although distinct characteristics were identified for nearly all cranial elements.

In addition to the overall larger size, narrower and longer skull, and decidedly more massive construction of NHMM 1998141, features that differ from the diagnostic characters of *P. solvayi* include: the prefrontal overlapping the postorbitofrontal in ventral view, the prefrontal excluded from the narial border by anterolateral extensions of the frontal, a dorsal median ridge on the frontal, a jugal with a straighter horizontal ramus and small posteroventral tuberosity, the

pterygoid tooth row descending from thickened expansion of the main body, the supratemporal rami originating further posteriorly and oriented vertically at the base of parietal, a rotated retroarticular process oriented horizontally relative to the PMU, no medial deflection of coronoid process, an expanded tympanic ala with tympanic crest oriented posteriorly, lack of a basal canal on the dorsal surface of the basioccipital, large, robust marginal dentition that is circular in cross-section, a smooth enamel surface on the marginal teeth with the exception of anastomosing ridges near crown apex, serrated carinae on the mature teeth, and cervical vertebrae lacking a ventral synapophyseal crest contacting the cotyle anteriorly. Other notable distinguishing characteristics include the broad mediolateral orientation of the suprastapedial-pillar like process contact in the quadrate, midline contact of the subolfactory processes on the frontal, broad contact between the medial wings of the coronoid and angular, massive medially-oriented prezygapophyses on the cervical and anterior dorsal vertebrae, and centrally-positioned synapophyses on the posterior dorsal vertebrae.

Diagnostic features shared by NHMM 1998141 and *P. solvayi* include a bowed dentary, enlarged pterygoid teeth, six pterygoid teeth, a fossa on the posterolateral surface of the surangular, fused suprastapedial and posterior pillar-like processes of the quadrate, zygosphenes and zygantra on the cervical and dorsal vertebrae, fused haemal arches of the caudal vertebrae, and procumbent anterior dentary teeth. With regards to the latter key feature, Dortangs et al. (2002) and Schulp (2006) suggested that the anterior dentary teeth of NHMM 1998141 (and therefore the premaxillary teeth) were procumbent like *P. solvayi* based on the incline of the preserved roots. Potential taphonomic influence notwithstanding, procumbent dentary teeth alone are not necessarily diagnostic of *Prognathodon*, as this feature is also present in other taxa such as *Mosasaurus glycys* (Street, 2016: formerly *M. hoffmannii* (Mulder, 1999: fig. 5)) and

Mosasaurus hoffmannii (Lingham-Soliar and Nolf, 1995; Mulder, 1999: fig. 4). The extension of the anterior teeth beyond the bony rostrum and/or dentary tips is specifically characteristic of *Prognathodon*. Since NHMM 1998141 lacks the anterior ends of its jaws, its procumbent teeth cannot therefore be used as evidence of an affinity with the genus.

CONCLUDING STATEMENTS

This study further provides a benchmark for comparing the type species of *Prognathodon* with other conspecifics to more accurately address the inclusion of robust members within the genus. The lack of evidence of procumbent anterior dentition extending anteriorly beyond the snout and the dominance of a large array of differing features demonstrates that NHMM 1998141 is largely distinct from *Prognathodon*, and although potentially closely related, should not be considered a valid member of the genus. An updated phylogenetic analysis using a character matrix with modified characters and character states, as well as corrected character scorings, will better incorporate important distinct features and ultimately function to clarify the complex evolutionary relationships of the genus *Prognathodon*.

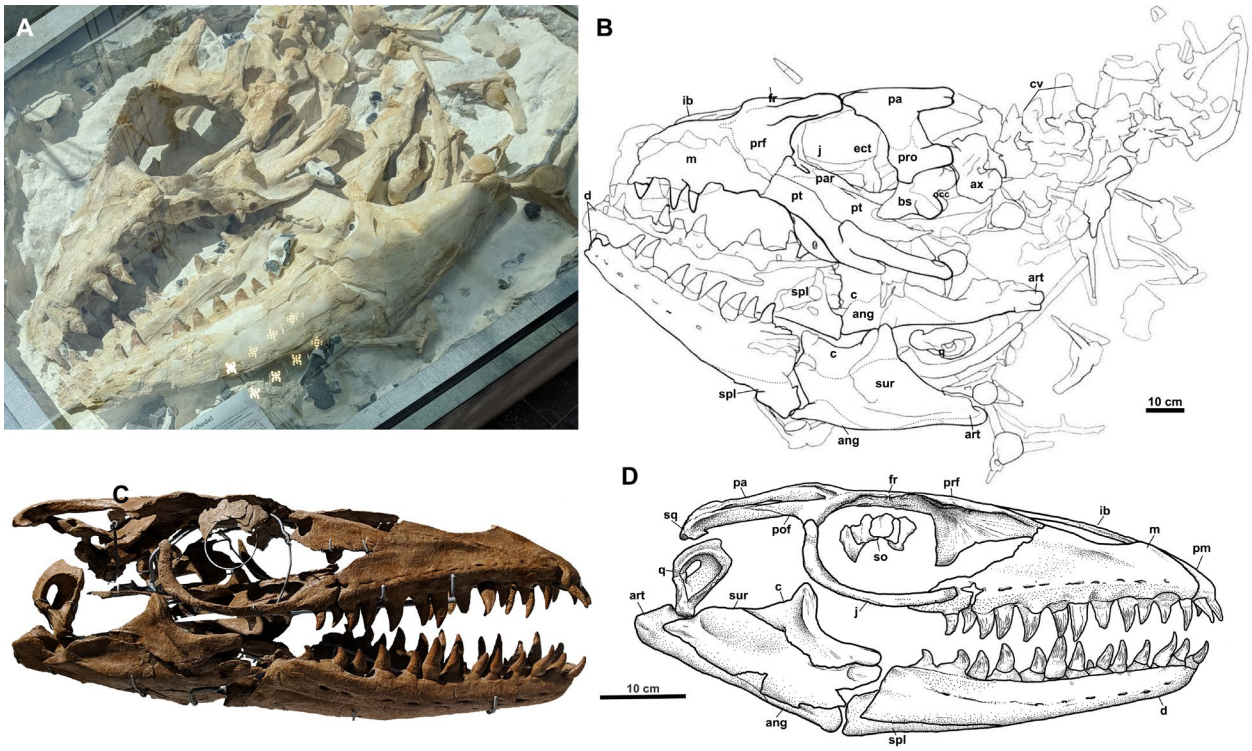

Figure 4.1. Cranium and associated vertebral elements of NHMM 1998141 in (A) lateral view and (B) labelled lateral view. Cranium of *P. solvayi* (IRScNB R33) in (C) lateral view and (D) reconstructed and labelled cranium in lateral view. Figure (B) is modified from Dortangs et al. (2002: fig. 2, by Rogier Trompert Medical Art). Dotted lines were added to indicate or correct suture lines. Abbreviations: ax, axis; ang, angular; art, articular; c, coronoid; cv, cervical vertebrae; d, dentary; j, jugal; fr, frontal; ib; internarial bar; pa, parietal; pf, parietal foramen; pm, premaxilla; pof, postorbitofrontal; prf, prefrontal; pro, prootic; pf; parietal foramen; q, quadrate; spl, splenial; so, sclerotic ossicles; sq, squamosal; sur, surangular.

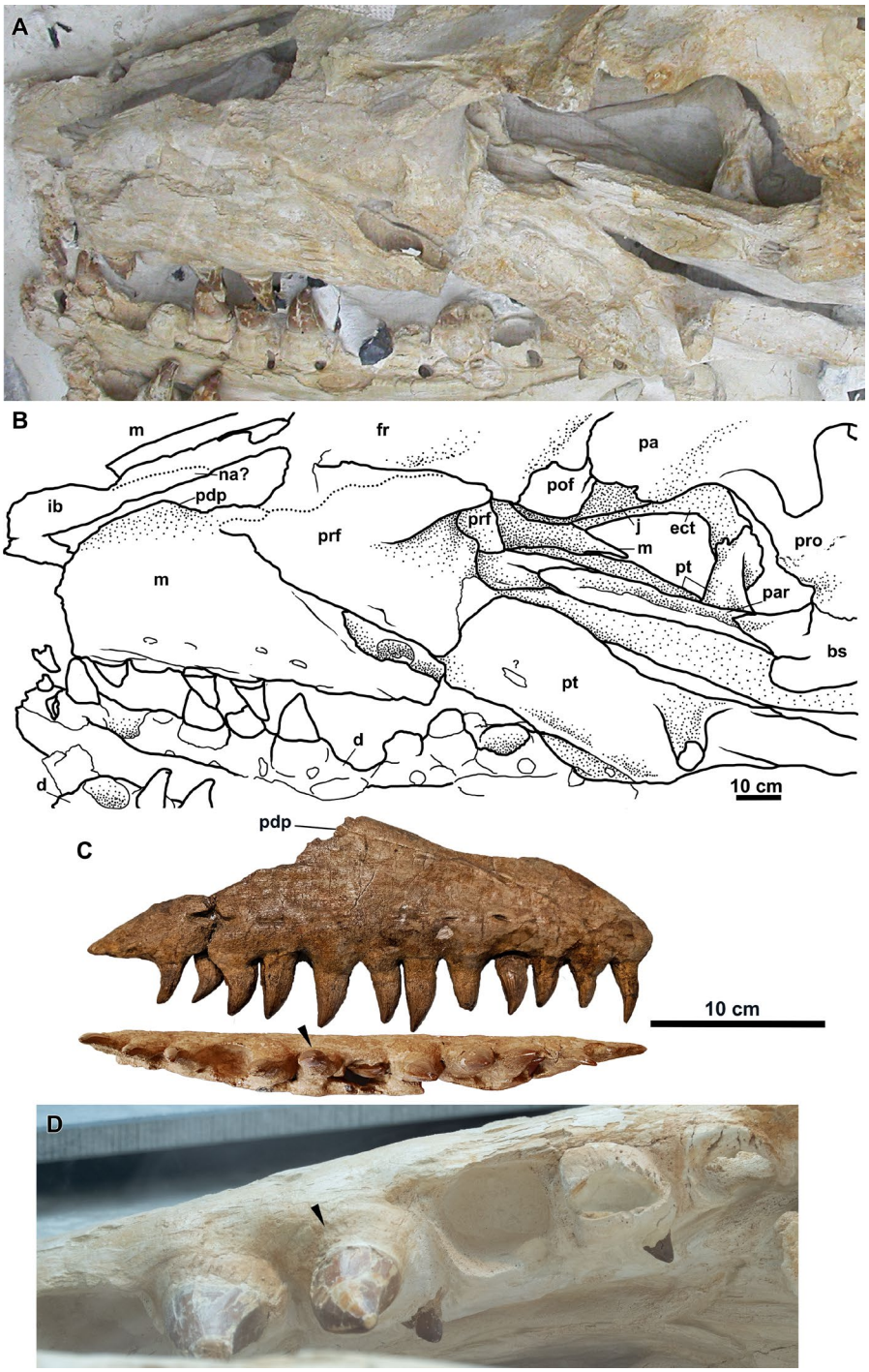

Figure 4.2. Anterior skull elements of NHMM 1998141 in (A) dorsolateral view and (B) labelled dorsolateral view. Right and left maxillae of *P. solvayi* (IRScNB R33) in (C) lateral and dorsal views, respectively, compared with the left maxillary tooth row in NHMM 1998141 in (D) view. Black arrows indicating teeth for comparison. Abbreviations: bs, basisphenoid; ect, ectopterygoid; d, dentary; j, jugal; fr, frontal; ib; internarial bar; pa, parietal; pf, parietal foramen; pa, parietal; par, parasphenoid; pdp, posterodorsal process; pm, premaxilla; pof, postorbitofrontal; prf, prefrontal; pro, prootic; pt, pterygoid.

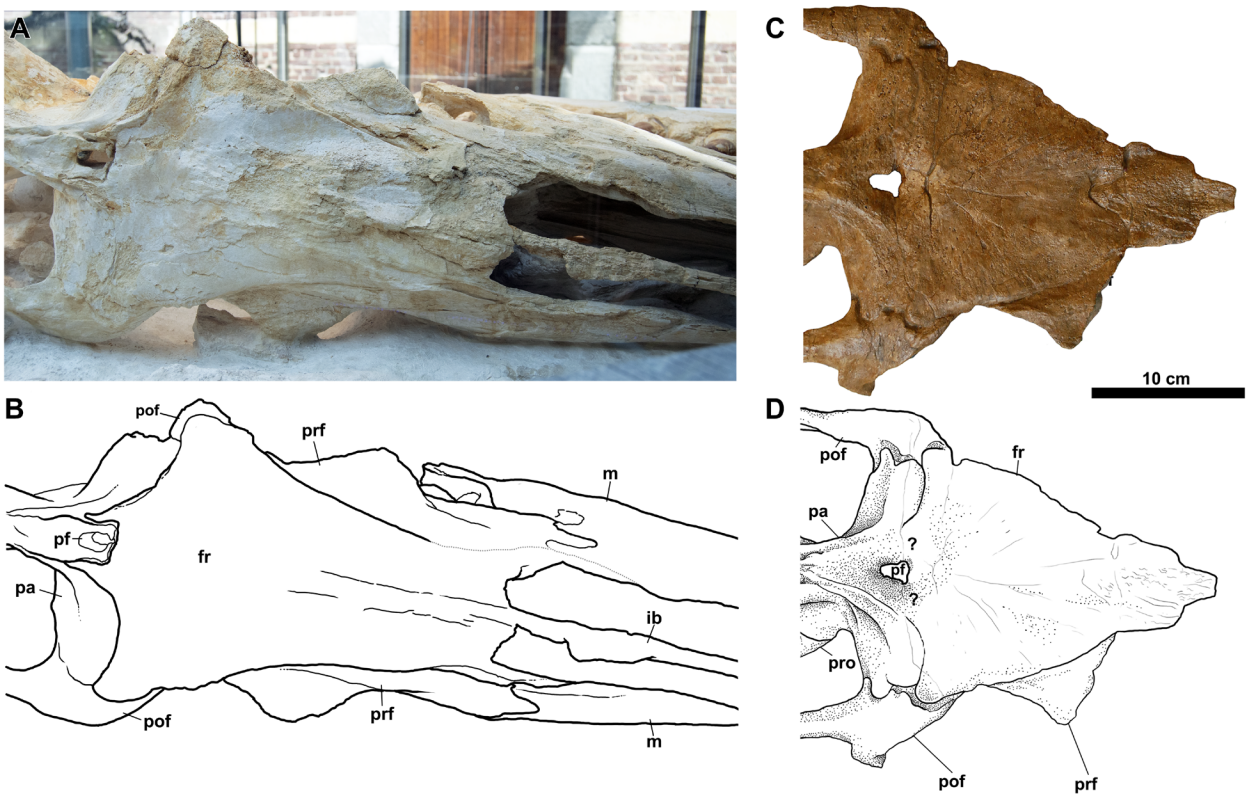

Figure 4.3. Frontal and surrounding elements in dorsal view in (A), (B) NHMM 1998141 and (C), (D) *P. solvayi* (IRScNB R33). Abbreviations: fr, frontal; ib; internarial bar; pf, parietal foramen; pof, postorbitofrontal; prf, prefrontal; pro, prootic; pf; parietal foramen. Dotted line in (B) represents suture reconstruction. Specimens not to scale.

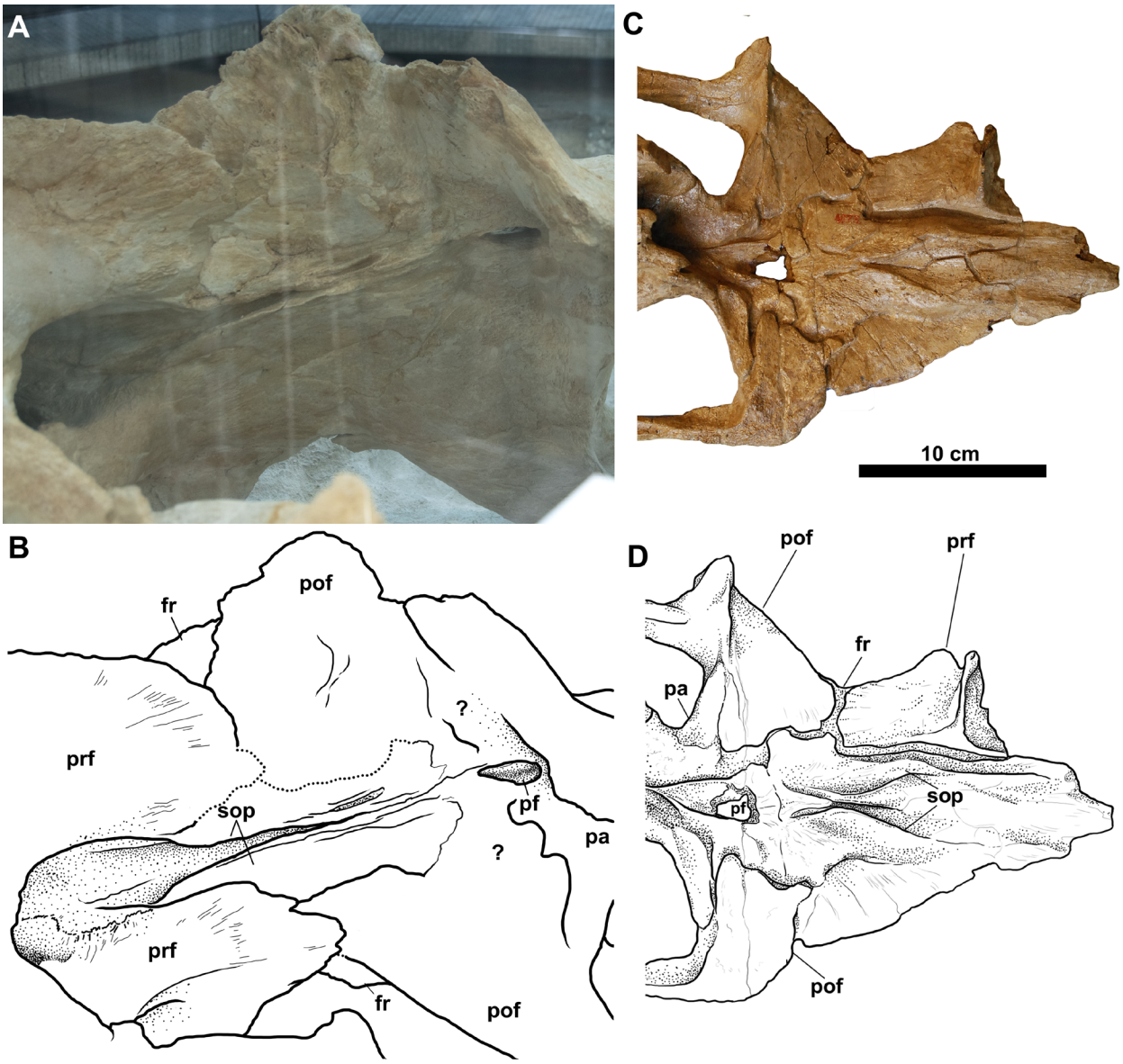

Figure 4.4. Ventral view of frontal and surrounding elements in A), B) NHMM 1998141 and C), D) *P. solvayi* (IRScNB R33). Due to its placement in the glass enclosure, NHMM 1998141 cannot be measured and is therefore not to scale. Abbreviations: fr, frontal; pf, parietal foramen; pof, postorbitofrontal; prf, prefrontal; pf; parietal foramen; sop, subolfactory processes. Dotted lines in (B) indicate reconstructions and hypothetical suture lines. "?" denotes uncertain suture lines. Specimens not to scale.

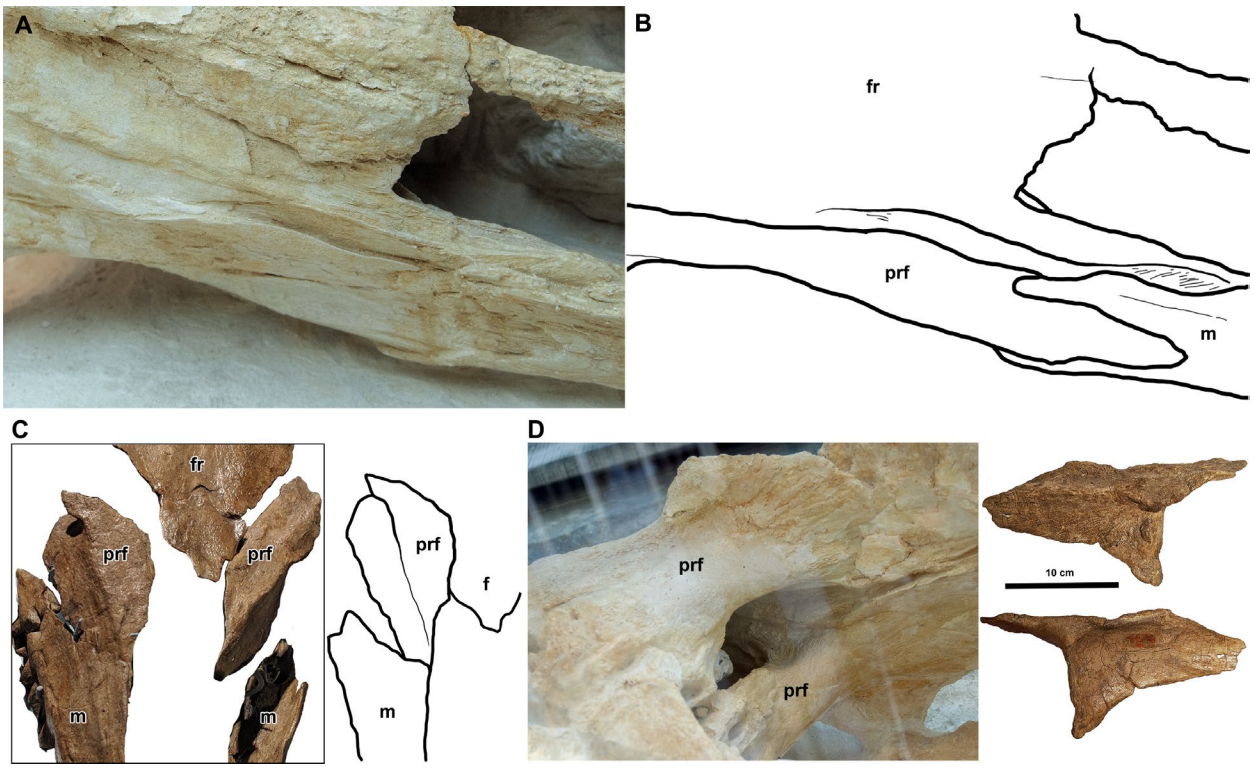

Figure 4.5. Closeup of prefrontal of NHMM 1998141 and surrounding elements in (A) dorsal and (B) labelled dorsal view; mounted skull elements of *P. solvayi* (IRScNB R33) and a reconstruction of the prefrontal and frontal in hypothetical natural position in (C) dorsal view; prefrontals of NHMM 1998141 in (D) posteroventral view and compared with prefrontals of *P. solvayi* ((IRScNB R33 (4672)) in lateral and medial views. Abbreviations: f, frontal; m, maxilla; prf, prefrontal. Specimens not to scale.

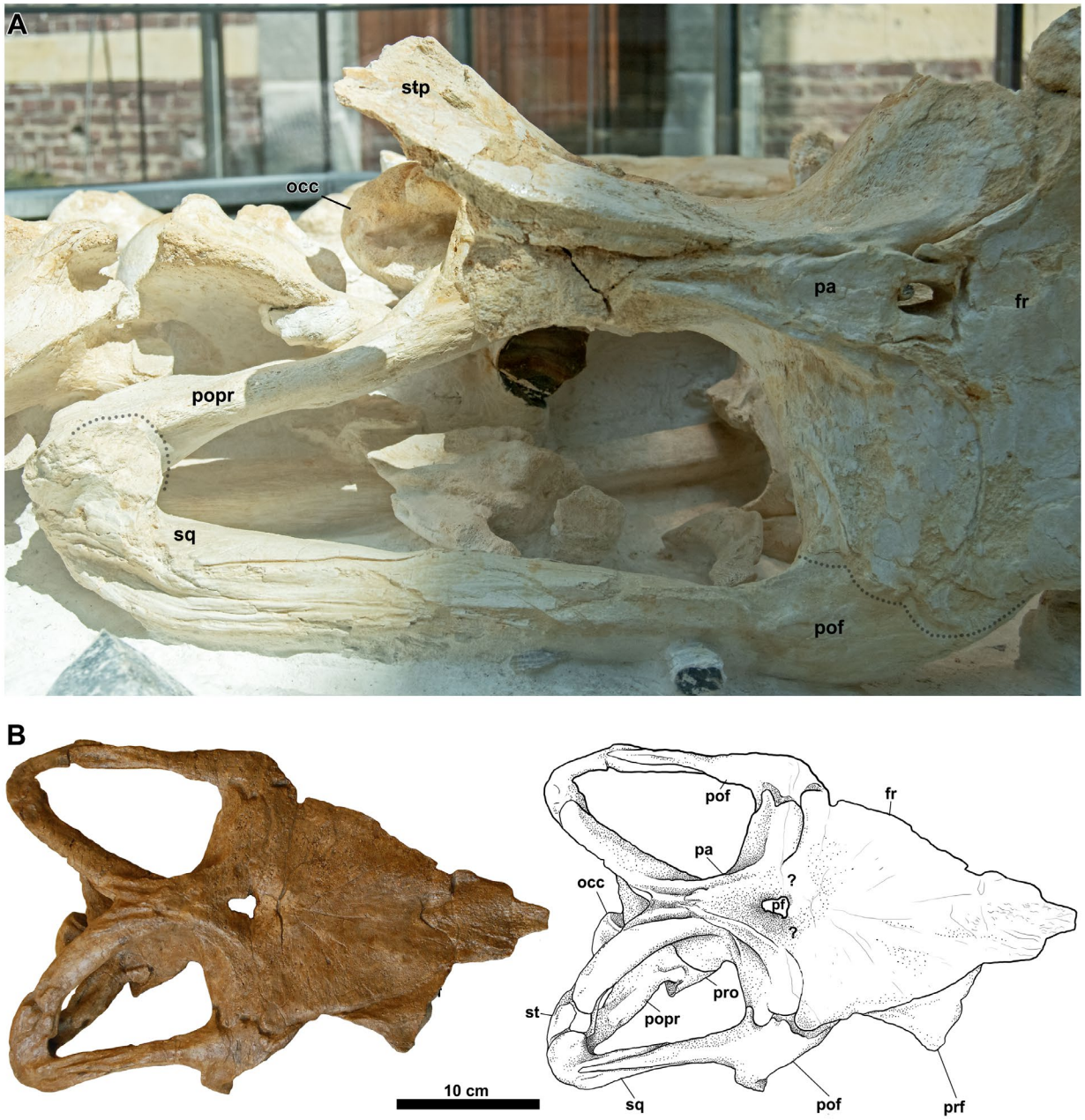

Figure 4.6. Dorsal view of postorbitofrontal and associated elements in (A) NHMM 1998141 and (B) *P. solvayi* (IRScNB R33). Abbreviations: Abbreviations: fr, frontal; occ, occipital condyle; pa, parietal; pof, postorbitofrontal; popr, paroccipital process of the opisthotic; prf, prefrontal; pro, prootic; sq, squamosal; stp, supratemporal process of the parietal. Dotted line in (A) outlines the hypothetical border of the parietal process of squamosal and suture outline of the postorbitofrontal, parietal, and frontal. Specimens not to scale.

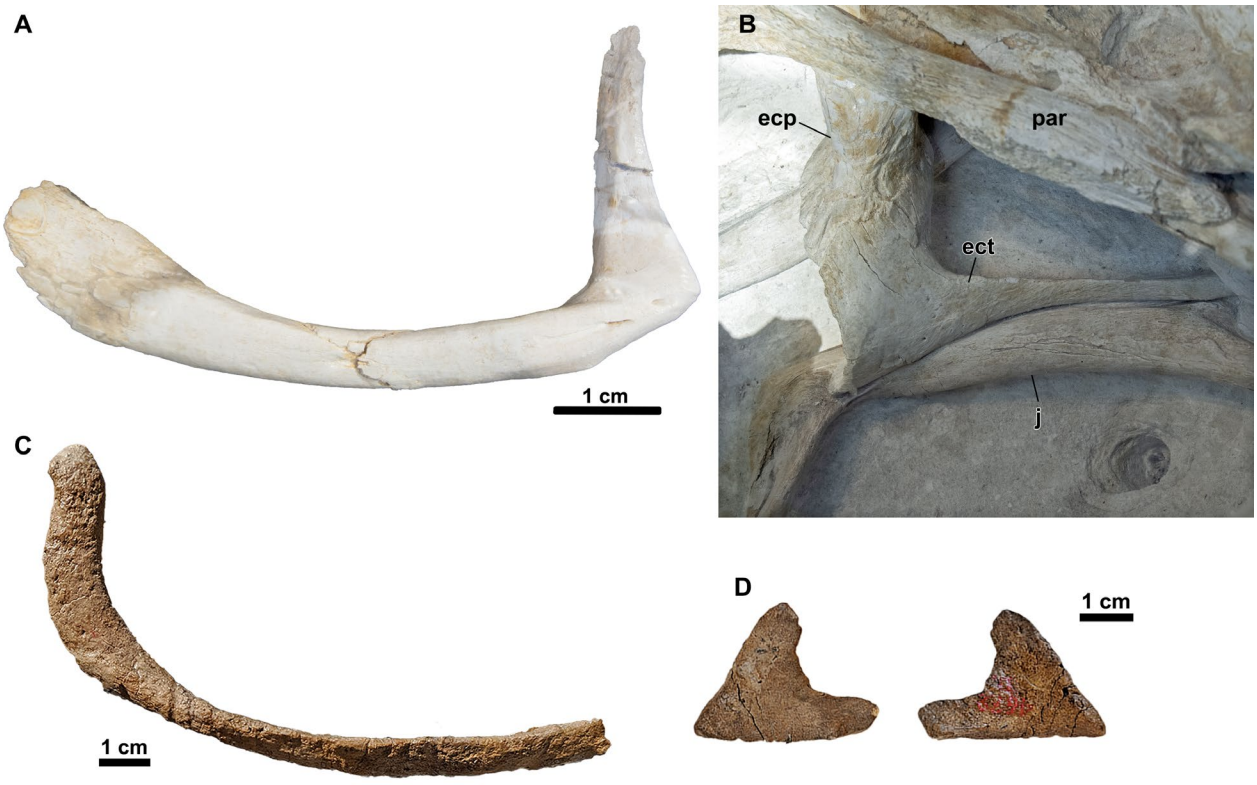

Figure 4.7. Left jugal of NHMM 1998141 in (A) lateral view; right jugal and ectopterygoid of NHMM 1998141 in (B) Internal view; right jugal of *P. solvayi* (IRScNB R33) in (C) lateral view, and (D) presumed ectopterygoid. Abbreviations: ecp, ectopterygoid process of pterygoid; ect, ectopterygoid; j, jugal; par, parasphenoid.

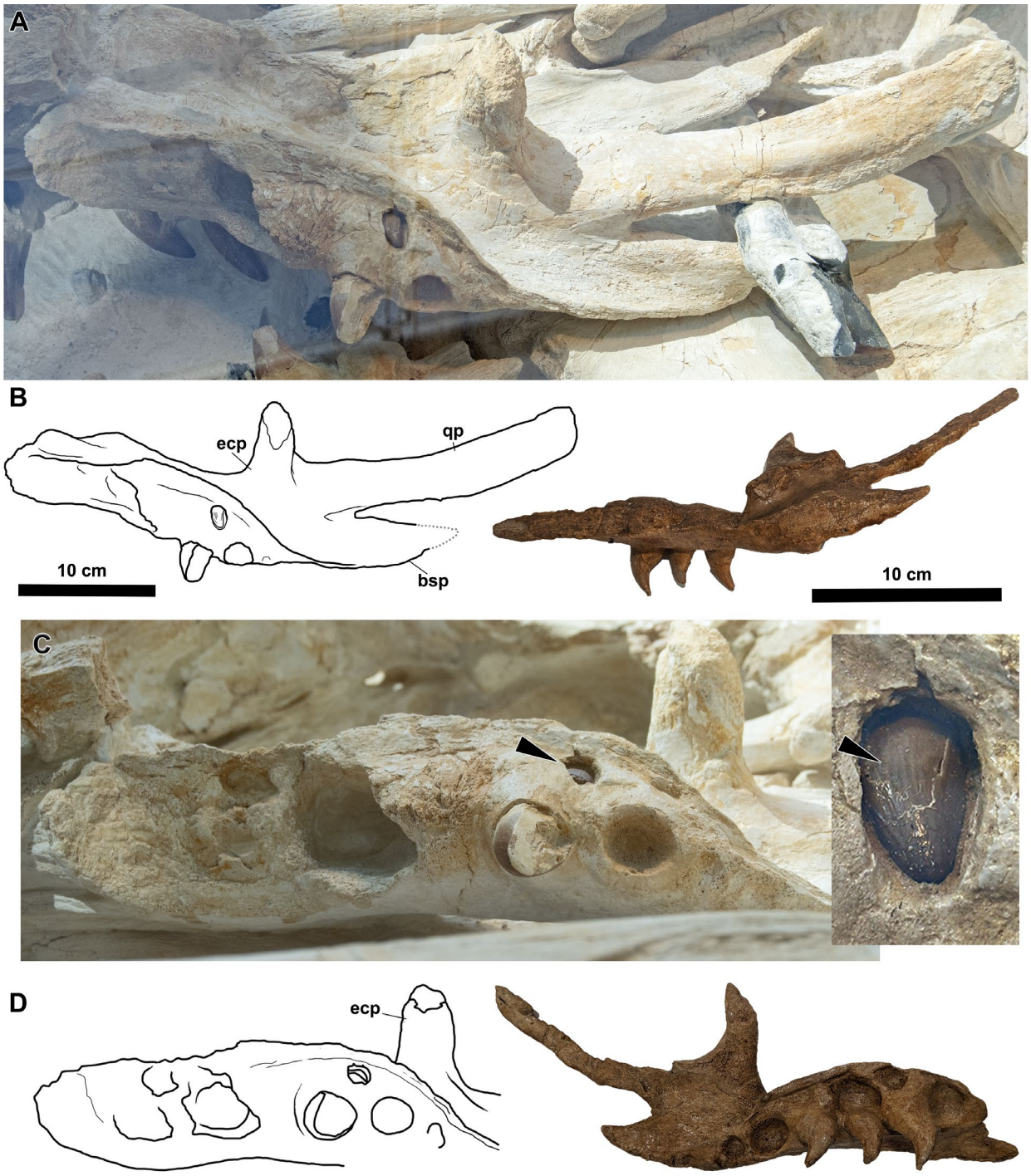

Figure 4.8. Left pterygoid of NHMM 1998141 in (A) lateral view; comparison of labelled line drawing of NHMM 1998141 pterygoid with the pterygoid of *P. solvayi* (IRScNB R33); ventral view of pterygoid of NHMM 1998141 in (C) ventral view, with closeup of replacement pterygoid tooth with faint flutes on enamel surface; comparison of pterygoids of NHMM 1998141 and *P. solvayi* in (D) ventral view. Dotted line in (B) indicates reconstruction. Abbreviations: bsp, basisphenoid process; ecp, ectopterygoid process; q, quadrate process.

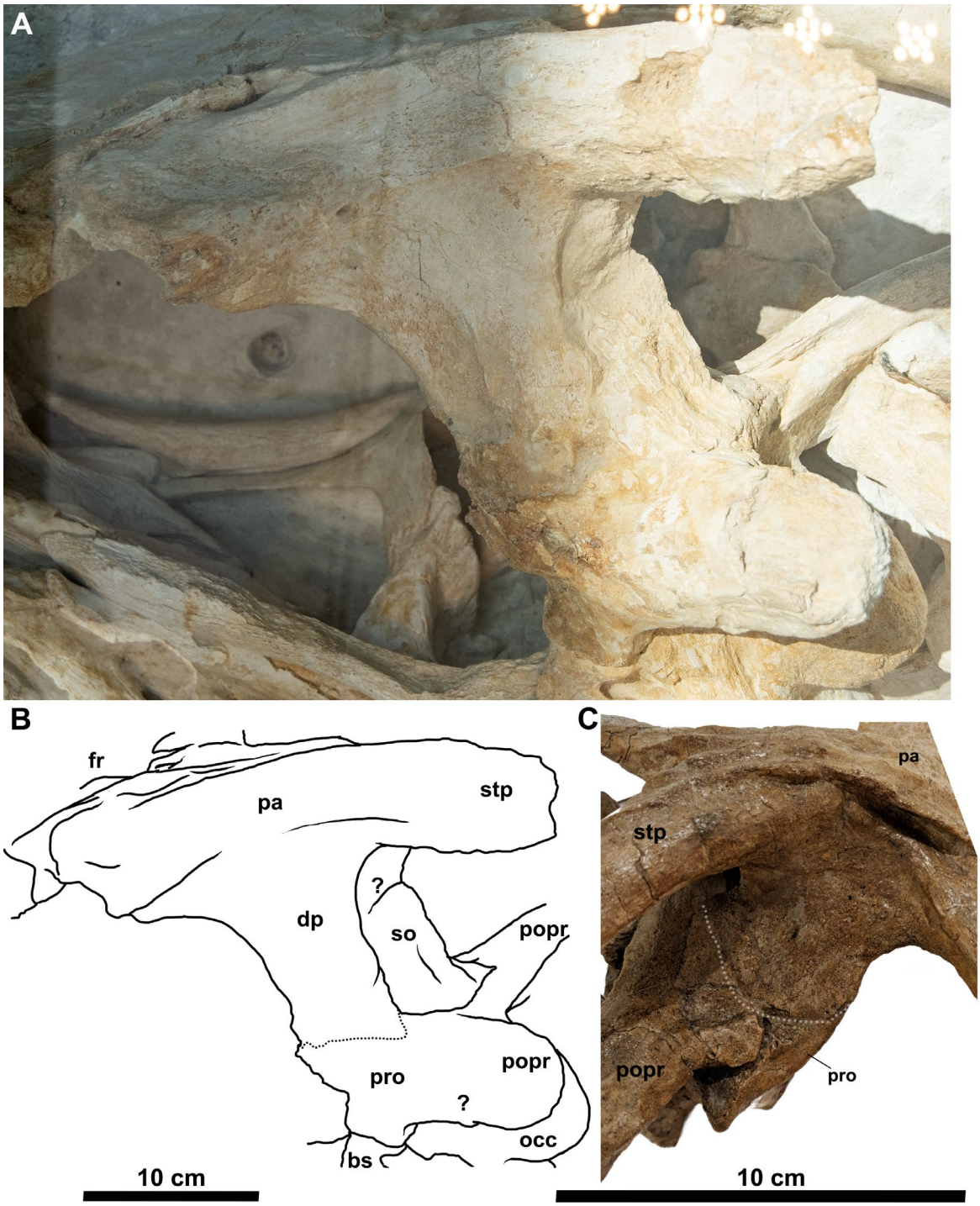

Figure 4.9. Skull roof and braincase elements of NHMM 1998141 in (A) lateral view and (B) labelled lateral view; braincase of *P. solvayi* (IRScNB R33) in (C) lateral view. Dotted lines in indicates hypothetical suture line reconstruction. Abbreviations: bs, basisphenoid; dp, descending process of parietal; fr, frontal; pa, parietal; popr, paroccipital process of the opisthotic; pro, prootic; occ, occipital condyle; so, supraoccipital; stp, supratemporal process of the parietal. (?) denotes an uncertain suture.

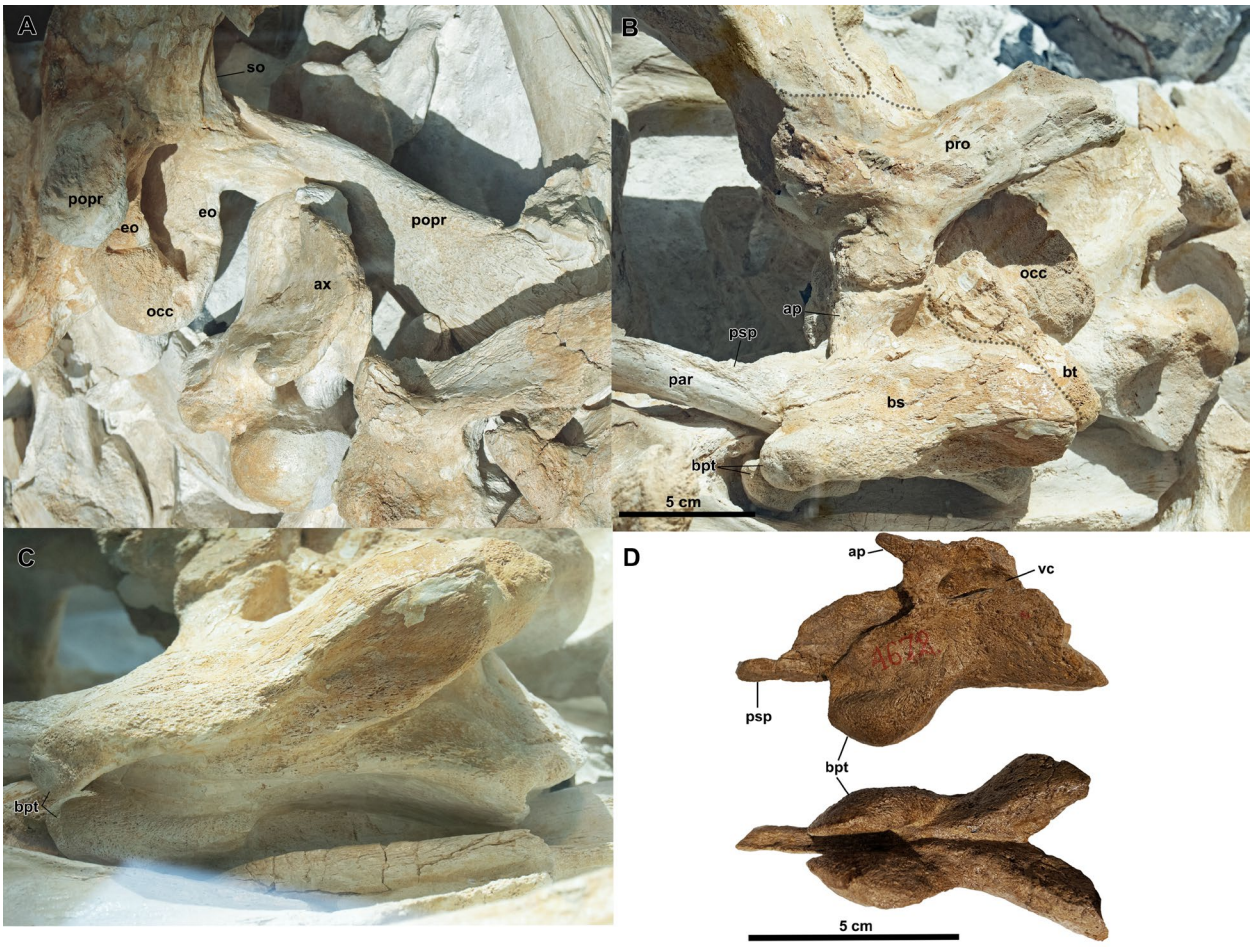

Figure 4.10. Braincase elements of NHMM 1998141 in (A) posterodorsal, (B) lateral, and (C) ventral views; basisphenoid of *P. solvayi* (IRScNB R33) in (D) lateral and ventral views. Dotted lines indicate suture lines. Abbreviations: ap, alar process; ax, axis; bpt, basipterygoid process; bs, basisphenoid; bt, basioccipital tubera; eo, exoccipital; par, parasphenoid; popr, paroccipital process of the opisthotic; pro, prootic; psp, parasphenoid process; occ, occipital condyle, so, supraoccipital condyle; vc, vidian canal.

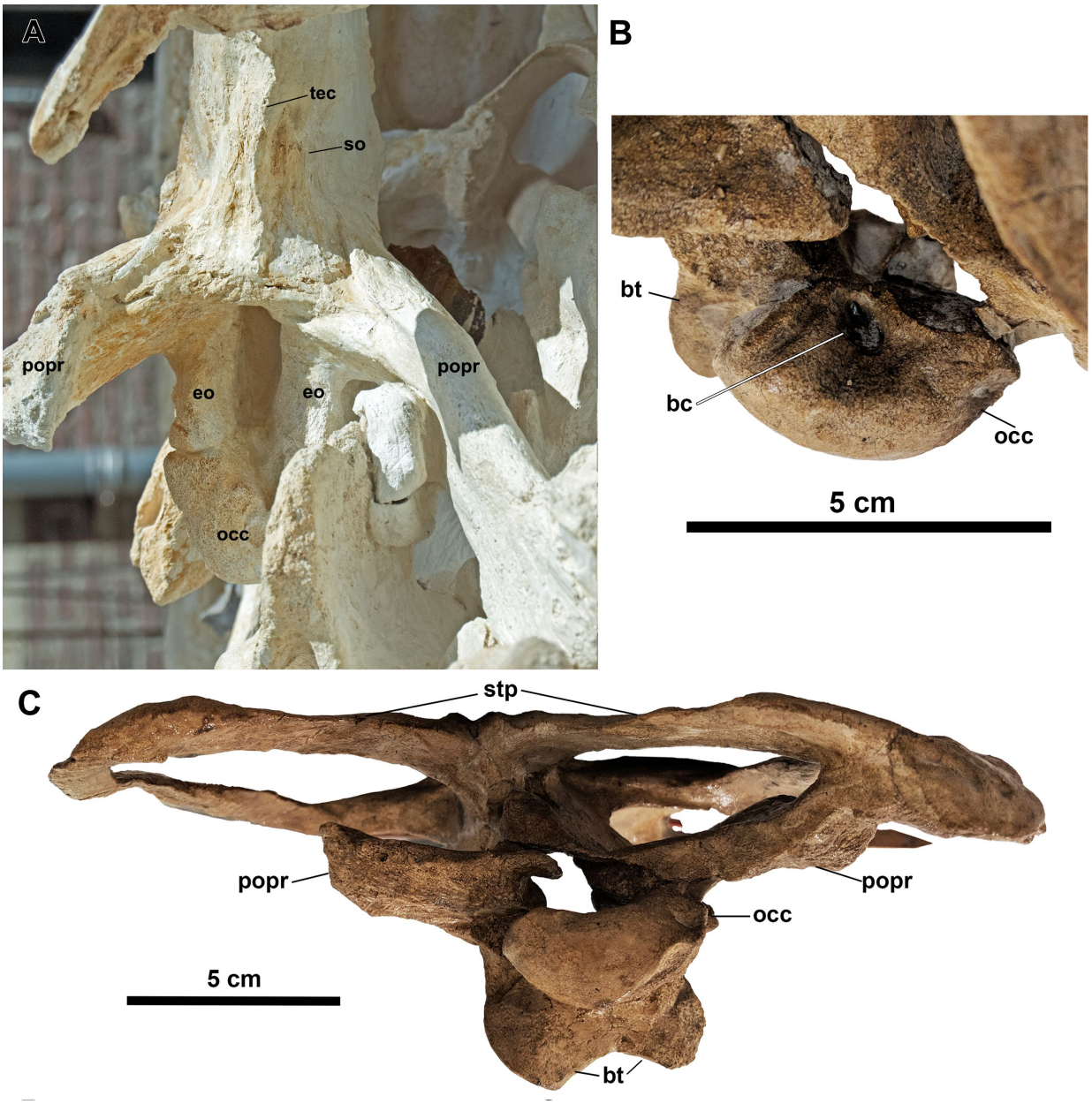

Figure 4.11. Braincase elements of NHMM 1998141 in (A) posterodorsal view; basioccipital of *P. solvayi* (IRScNB R33) in (B) dorsal view; skull roof and braincase elements of *P. solvayi* (IRScNB R33) in (C) posterior view. Abbreviations: bc, basal canal; bt, basioccipital tubera; eo, exoccipital; popr, paroccipital process of the opisthotic; occ, occipital condyle; so, supraoccipital; tec, processus ascendens tectum synoticum of the supraoccipital.

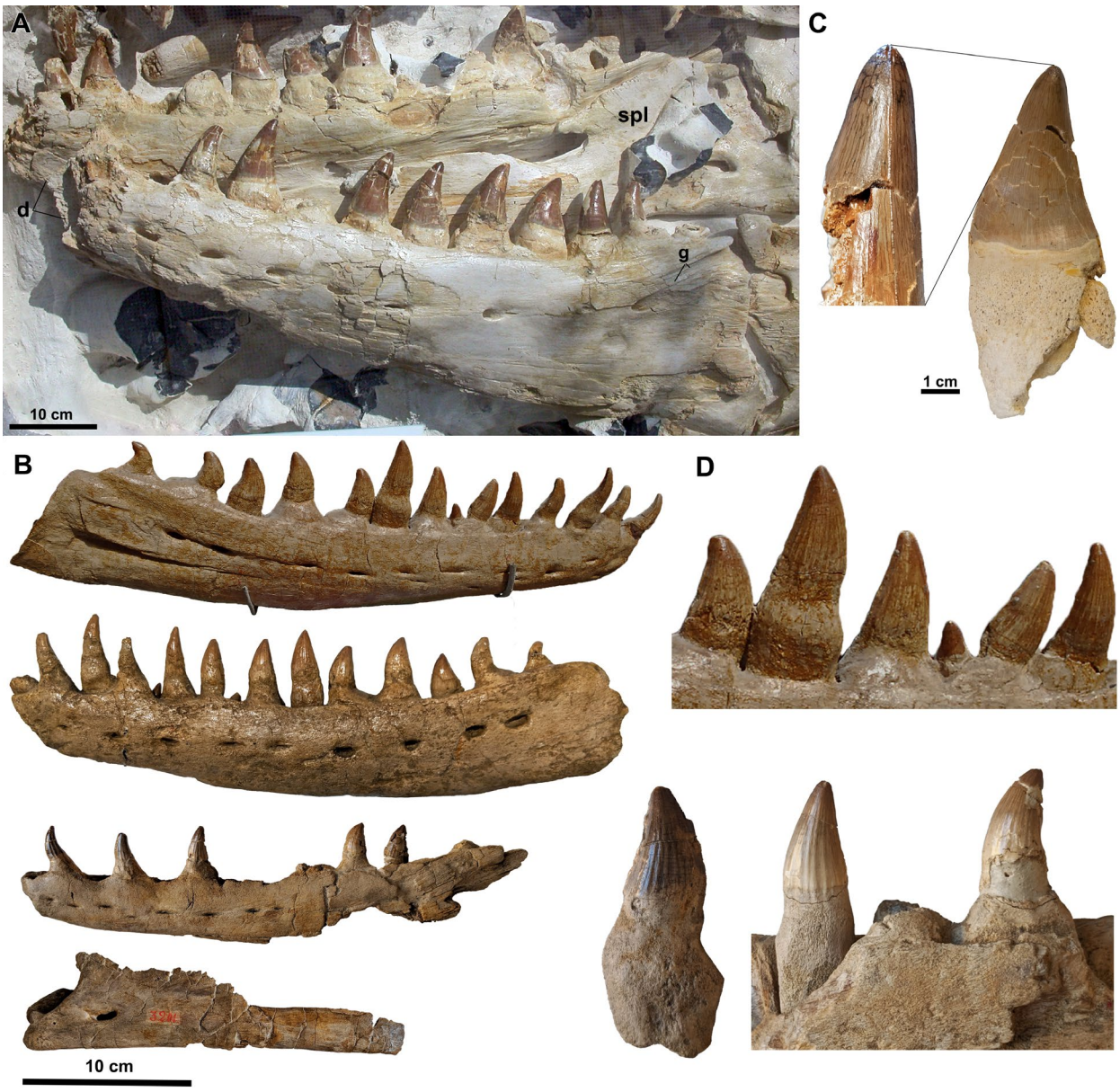

Figure 4.12. Left and right dentaries of NHMM 1998141 in (A) lateral and medial view; right and left dentaries of *P. solvayi* (IRScNB R33, IRScNB 0108) in (B) lateral view; example of marginal tooth of NHMM 1998141 in (C) anterior and labial/lingual view; (D) examples of marginal teeth of *P. solvayi* (IRScNB R33, IRScNB 0108, IRScNB 0107) (not to scale). Abbreviations: d, dentary; g, groove continuous with surangular fossa; spl, splenial.

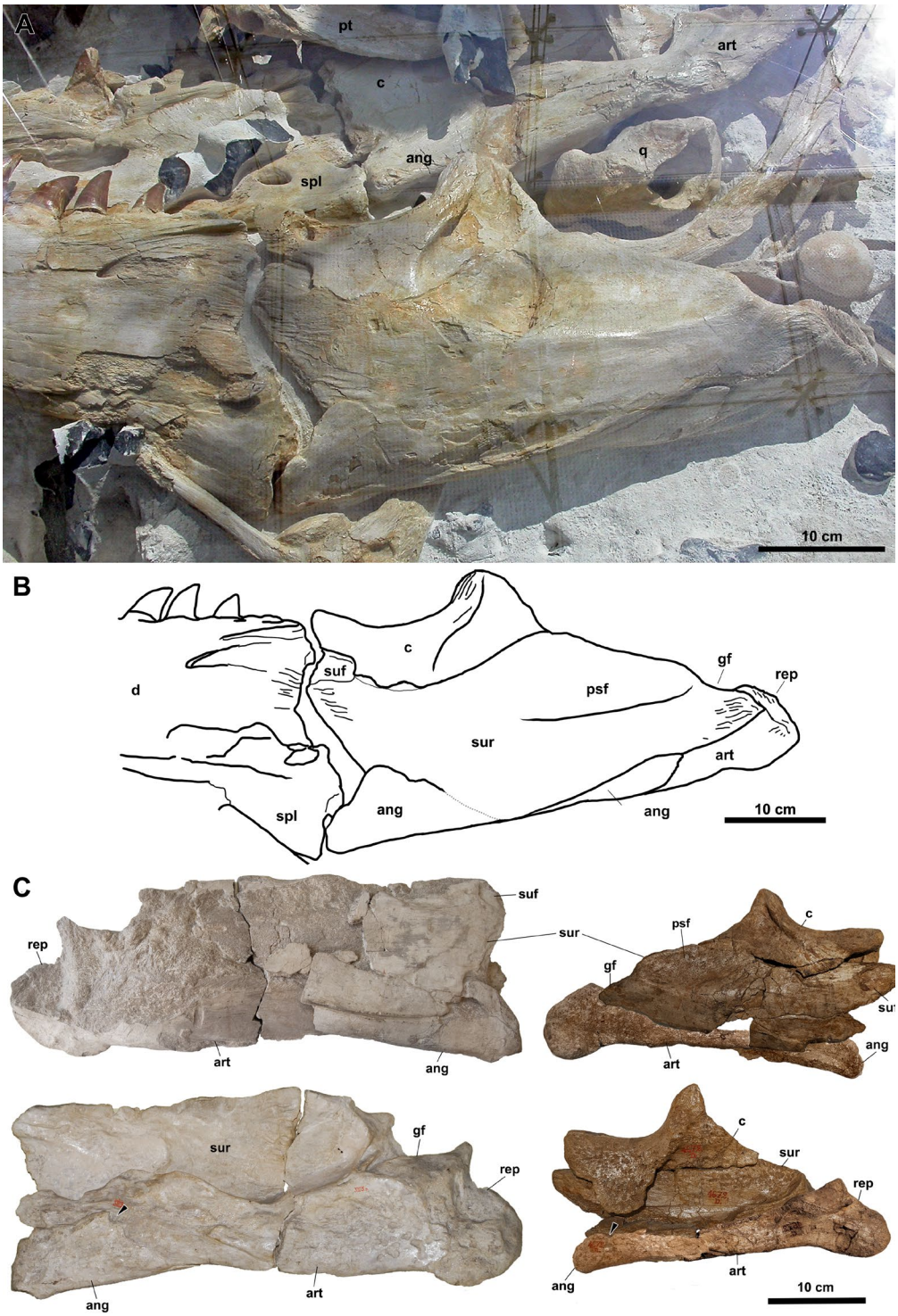

Figure 4.13. Posterior mandibular unit (PMU) of NHMM 1998141 in (A) ventrolateral view; (B) labelled ventrolateral view; PMUs of *P. solvayi* (IRScNB 0106, IRScNB R33) in (C) lateral and medial views. Abbreviations: Abbreviations: ang, angular; art, articular; c, coronoid; d, dentary; gf, glenoid fossa; psf, posterolateral surangular fossa; rep, retroarticular process; spl, splenial, suf, surangular fossa. Dotted line in (B) represents hypothetical reconstruction of angular suture. Black arrows in (C) indicates the angular foramen.

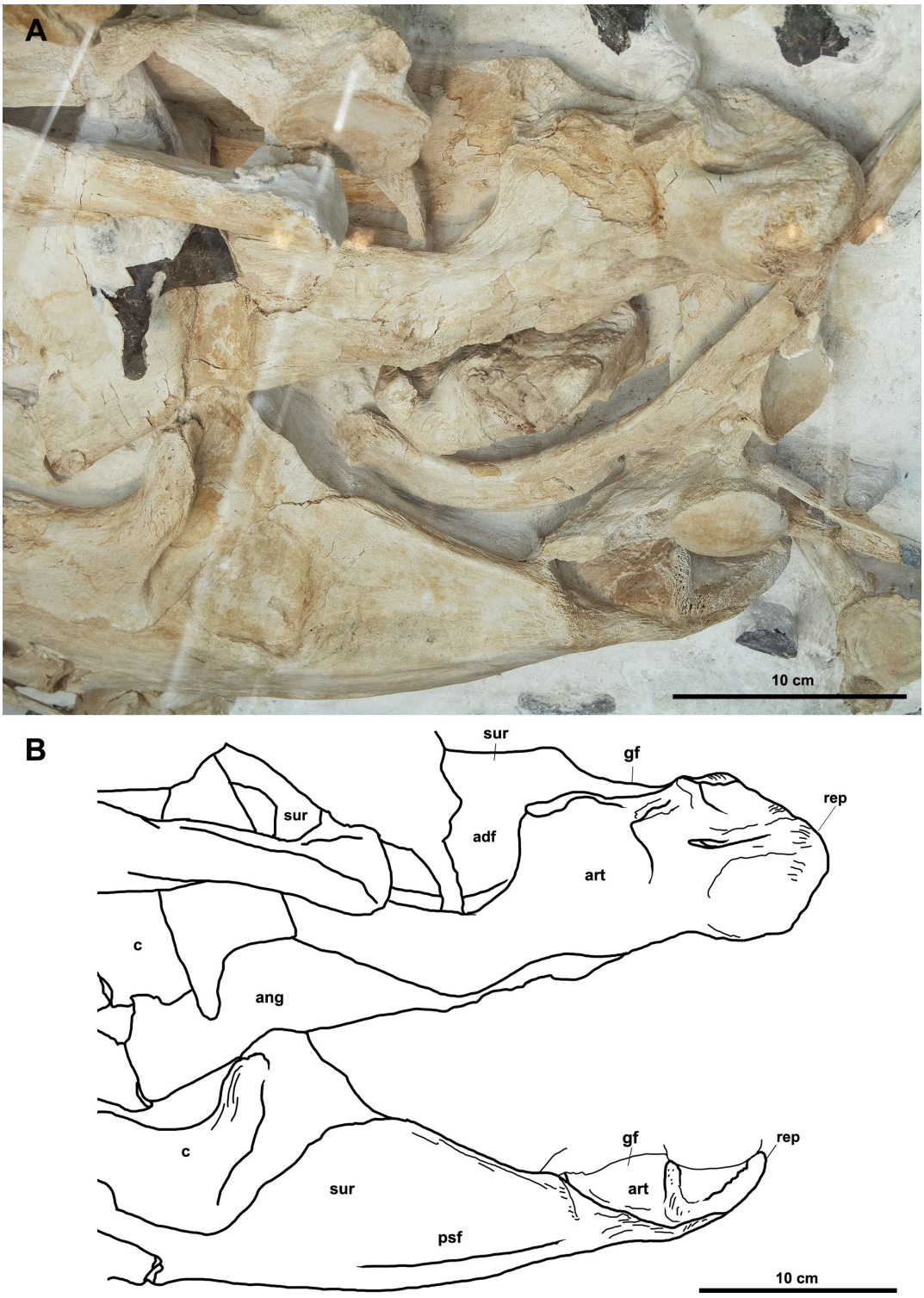

Figure 4.14. Posterior region of posterior mandibular unit (PMU) of NHMM 1998141 in (A) dorsal/internal view; (B) labelled dorsal/internal view. Abbreviations: adf, adductor fossa; ang, angular; art, articular; c, coronoid; gf, glenoid fossa; psf, posterolateral surangular fossa; sur, surangular; rep, retroarticular process.

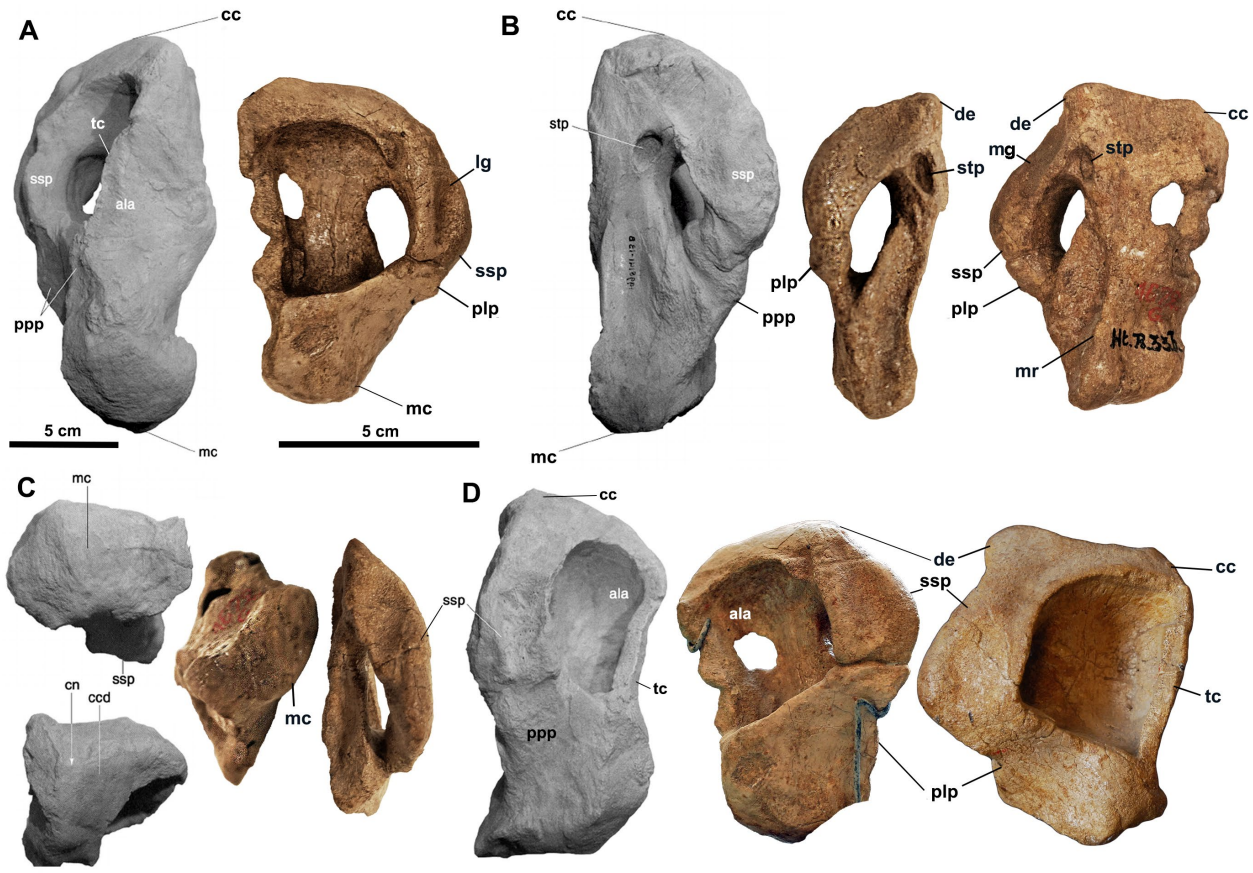

Figure 4.15. Left quadrate of NHMM 1998141 (left) and right quadrate of *P. solvayi* (IRScNB R33) (right) in (A) lateral and (B) medial views. Left quadrate of NHMM 1998141 in (C) ventral (top) and dorsal (bottom) views; left quadrate of *P. solvayi* (IRScNB R33) in ventral (left) and dorsal (right) views. Left quadrate of NHMM 1998141 in (D) posterior view, and right and left quadrate of *P. solvayi* (IRScNB R33) are in posteroventral (left) and posterolateral (right) views. Images of NHMM 1998141 are modified from Konishi (2008) and Schulp (2006). Abbreviations: ala, tympanic ala; cc, cephalic condyle; de, dorsomedial eminence; lg, lateral groove; mc, mandibular condyle; mg, medial groove; mr, median ridge; plp, posterolateral process; ppp, posterior pillar-like process; ssp, suprastapedial process; stp, stapedial pit; tc, tympanic crest.

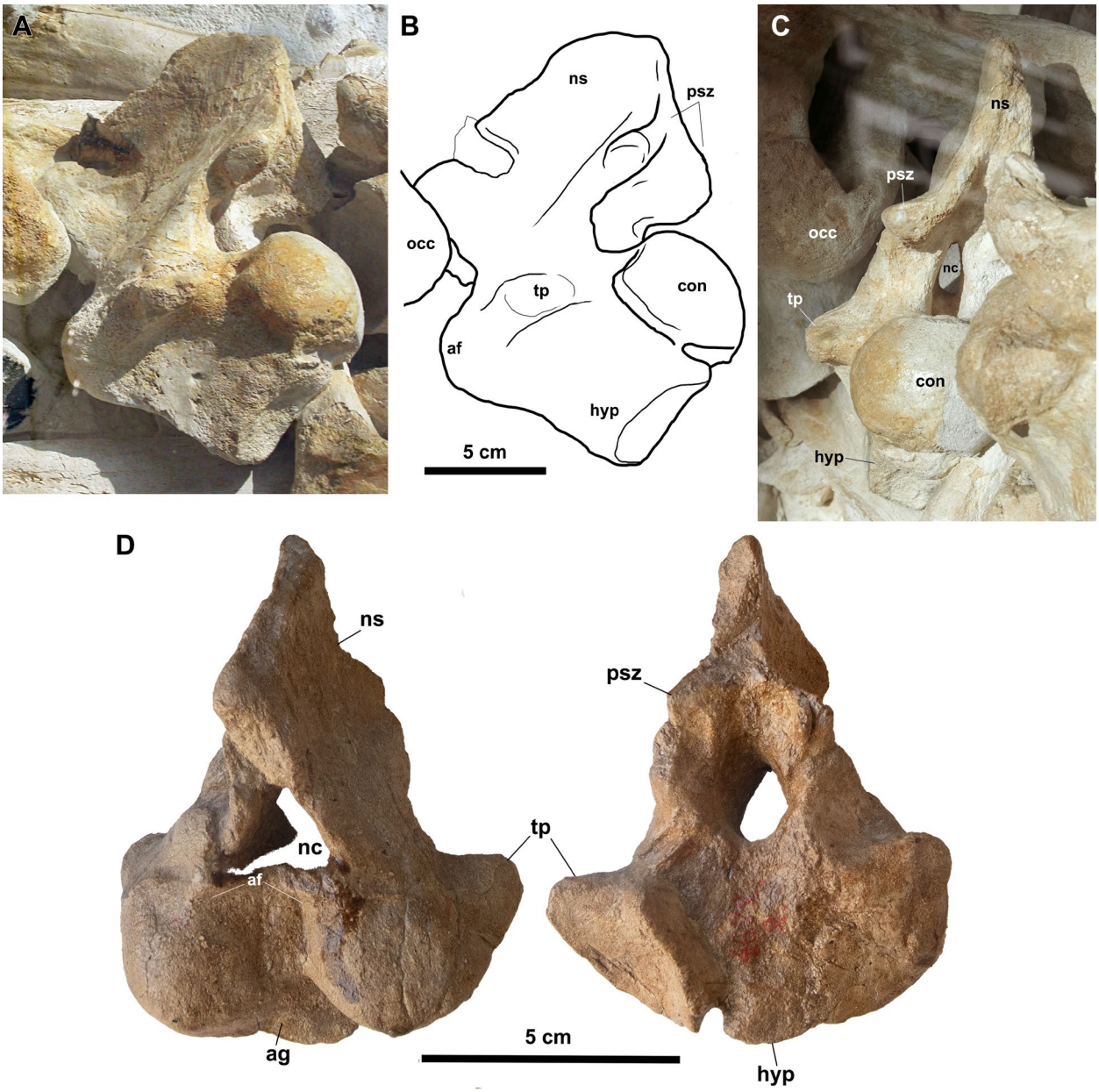

Figure 4.16. Axis vertebrae of NHMM 1998141 in (A) lateral, (B) labelled lateral, and (C) posterior views; axis vertebrae of *P. solvayi* (IRScNB R33) in (D) anterior and posterior views. Abbreviations: af, articular facets for atlas synapophyses; ag, anterior groove; con, condyle; hyp, hypapophysis; nc, neural canal; ns, neural spine; occ, occipital condyle; psz, postzygapophyses; tp, transverse process.

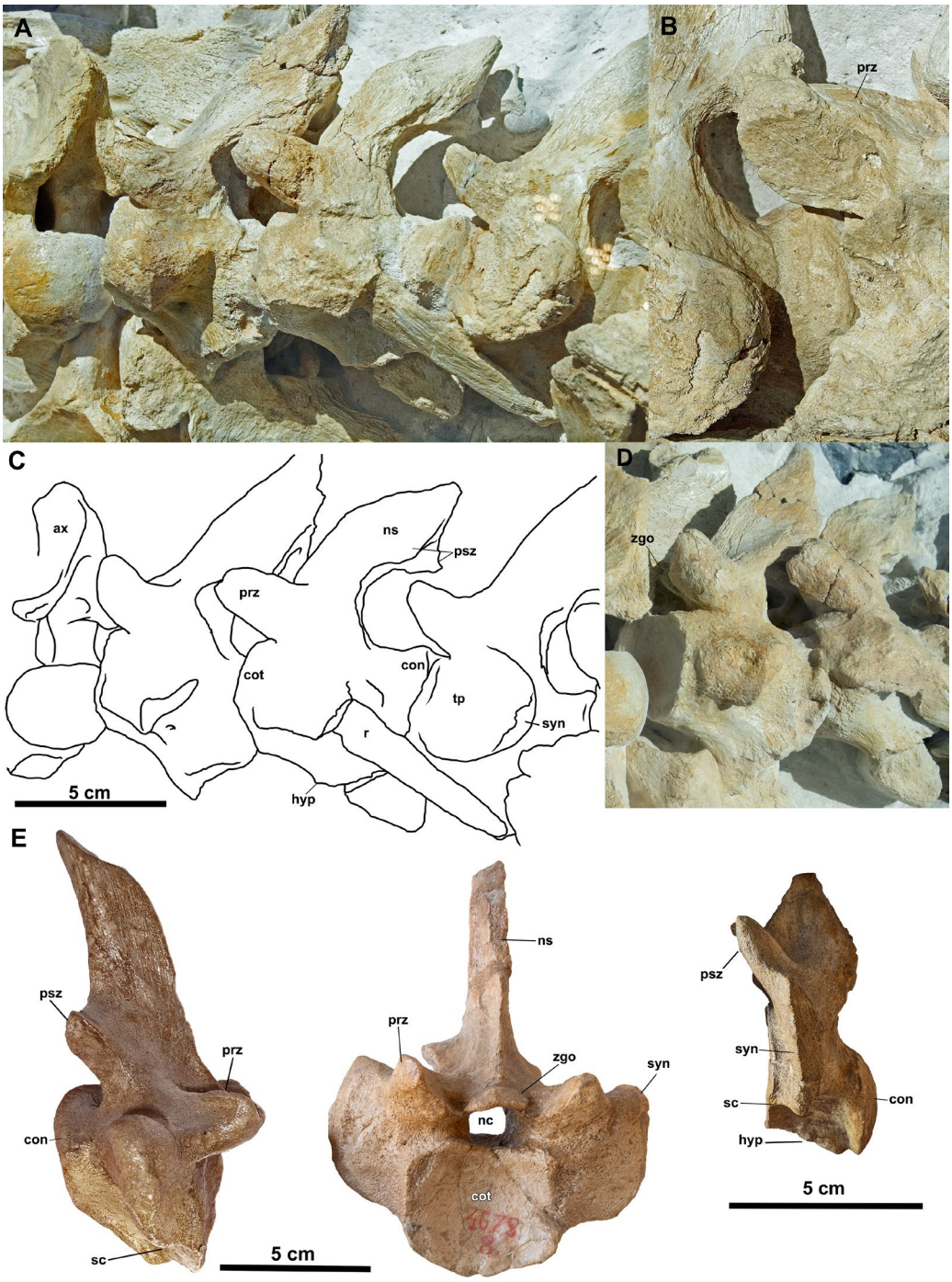

Figure 4.17. Articulated cervical vertebrae of NHMM 1998141 in (A) lateral view; prezygapophysis of fourth cervical vertebra in (B) medial view; (C) labeled articulated cervical vertebrae; first and second cervical vertebrae in (D) anterolateral view; select cervical vertebrae of *P. solvayi* (IRScNB R33) in (D) labeled lateral and anterior views, IRScNB 0108 in lateral view. Abbreviations: ax, axis; con, condyle; cot, cotyle; hyp, hypapophysis; ns, neural spine; prz, prezygapophysis; psz, postzygapophysis; r, rib; sc, synapophysal crest; syn, synapohyseal process; tp, transverse process.

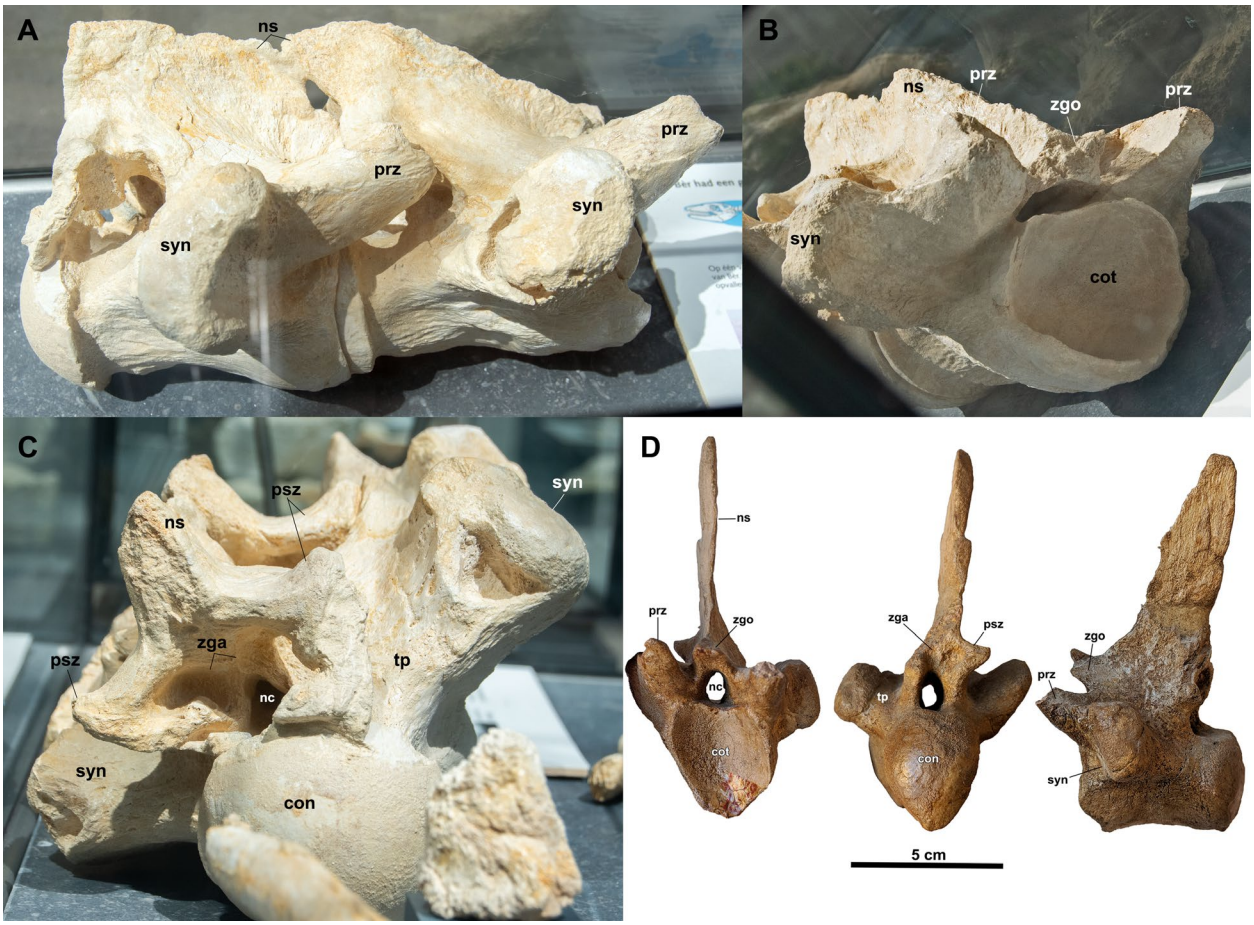

Figure 4.18. Selected anterior dorsal vertebrae of NHMM 1998141 in (A) lateral, (B) posterolateral, and (C) anterior views; select anterior dorsal vertebra of *P. solvayi* (IRScNB R33) in (D) anterior, posterior, and lateral views, respectively. Abbreviations: con, condyle; cot, cotyle; hyp, hypapophysis; nc, neural canal; ns, neural spine; prz, prezygapophysis; psz, postzygapophysis; syn, synapohyseal process; tp, transverse process; zga, zygantra; zgo, zygosphenes. Vertebrae of NHMM 1998141 not to scale.

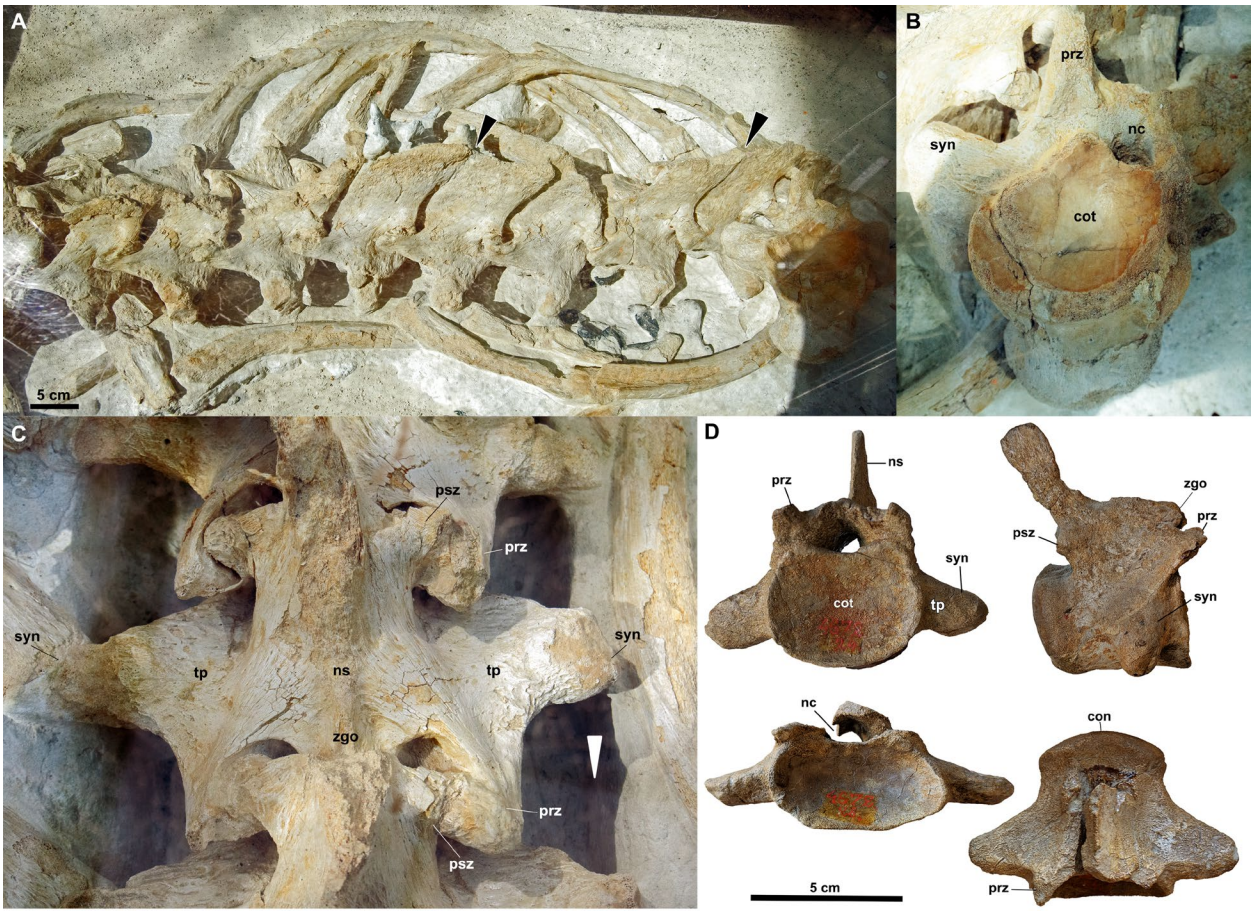

Figure 4.19. Articulated dorsal vertebral section and ribs of NHMM 1998141 in (A) dorsolateral view; disarticulated dorsal vertebra in (B) posteroventral view; posterior dorsal vertebra in (C) dorsal view; select posterior dorsal vertebrae of *P. solvayi* (IRScNB R33) in (D) (clockwise from top left) anterior, lateral, anterior, and dorsal views. Abbreviations: con, condyle; cot, cotyle; nc, neural canal; ns, neural spine; prz, prezygapophysis; psz, postzygapophysis; syn, synapohyseal process; tp, transverse process; zgo, zygosphenes. Black arrows in (A) indicate tightly contacting neural spines. White arrow in (C) indicates anterior direction.

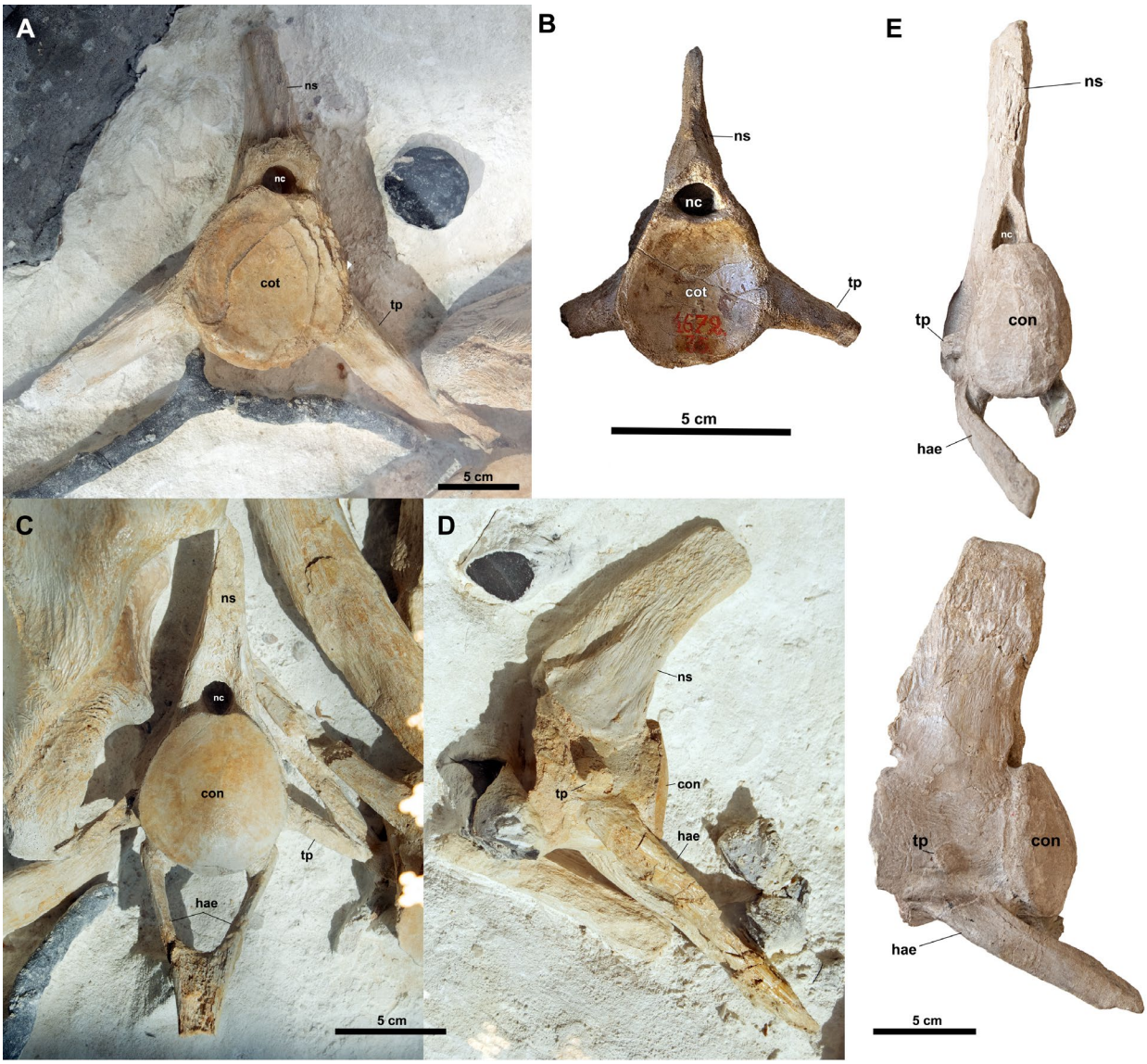

Figure 4.20. Pygal vertebra of NHMM 1998141 in (A) anterior view; pygal vertebrae of *P. solvayi* (IRScNB R33) in (B) anterior view; caudal vertebrae of NHMM 1998141 in (C) posterior and (D) lateral views; caudal vertebrae of *P. solvayi* (IRScNB 0108). Abbreviations: con, condyle; cot, cotyle; nc, neural canal; hae, haemal arch; ns, neural spine; tp, transverse process.

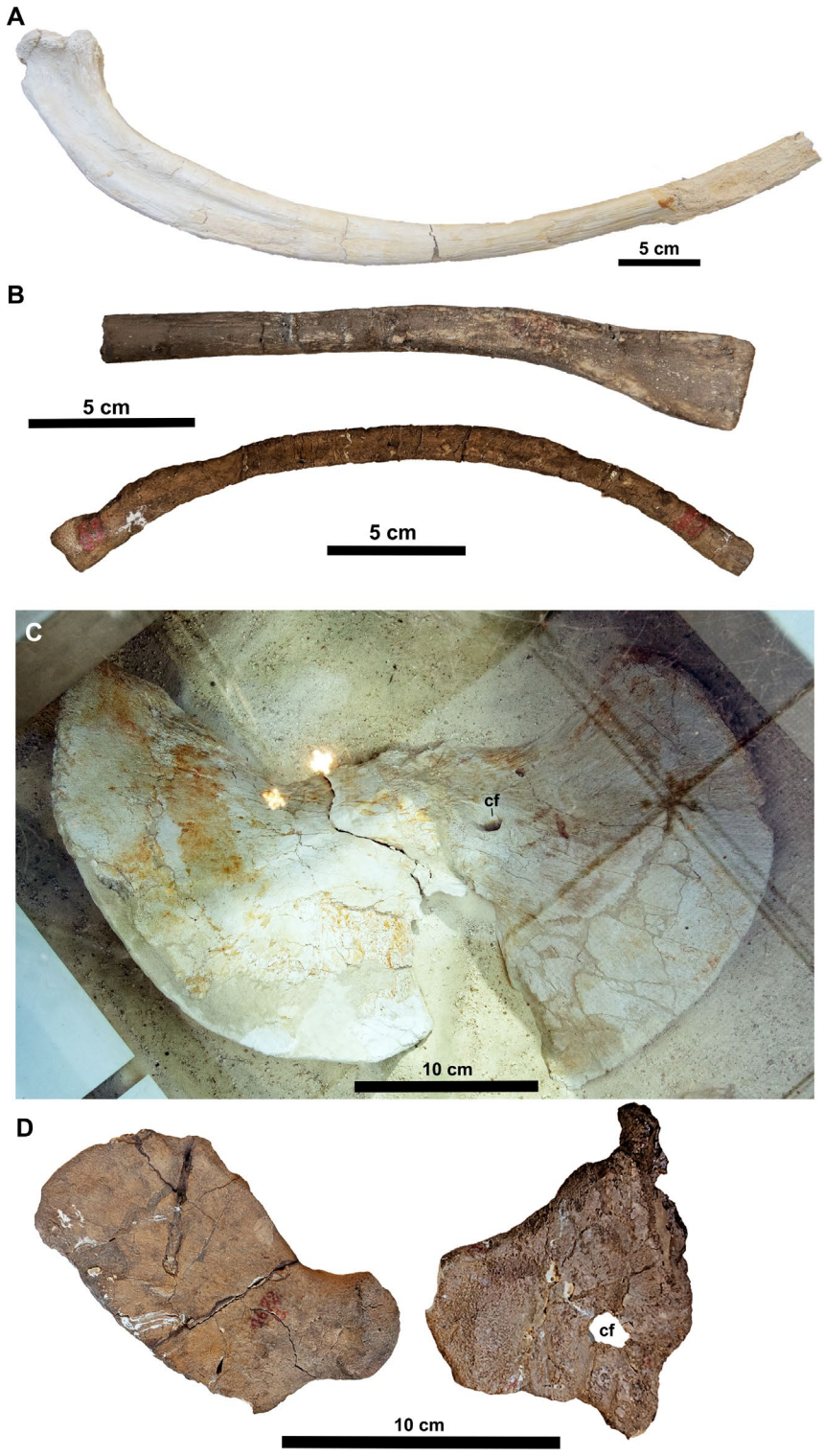

Figure 4.21. Rib of NHMM 1998141 in (A) posterior view; ribs of *P. solvayi* (IRScNB R33 (4672)) in (B) posterior view; scapula (left) and coracoid (right) of NHMM 1998141 in (C) lateral view; scapula (left) and coracoid (right) of *P. solvayi* (IRScNB R33) in (D) lateral view. Abbreviations: cf, coracoid foramen.

CHAPTER 5. A NEW, NEARLY COMPLETE SPECIMEN OF *PROGNATHODON OVERTONI* (SQUAMATA: MOSASAURIDAE) FROM THE CAMPANIAN BEARPAW FORMATION OF ALBERTA, CANADA, AND A COMPARATIVE STUDY OF *PROGNATHODON*

INTRODUCTION

Prognathodon overtoni is a medium to large-sized mosasaur from North America with a proportionately large, robust skull and currently one of the only Campanian representatives of the genus. Recovered from the Pierre Shale in South Dakota, the holotype KU 950 was at the time referred to the genus *Brachysaurus* and consisted of a small number of very fragmented pieces of the skull, vertebrae, and appendicular skeleton (Williston, 1897). Making particular note of the robustness of the individual elements and dentition, Williston's (1897) description of *Brachysaurus* was more detailed than Dollo's (1889) account of *P. solvayi* and also provided brief comparisons to other mosasaur taxa such as *Clidastes*, *Mosasaurus*, *Platecarpus*, and *Tylosaurus*. Reassigned to *Ancylocentrum* by Schmidt (1927) for a time, Russell (1967) later reinstated the genus *Prognathodon* following a description of *P. crassartus* (later assigned to *Plioplatecarpus* by Lingham-Soliar and Nolf, 1989), *P. overtoni*, and *P. rapax*. The holotype of *P. overtoni*, KU 950, and a partially preserved skull of a new specimen from the Upper Pierre Formation of South Dakota (SDSMT 3393) formed the basis of much of the resulting generic diagnosis of *Prognathodon*, which was then included within the Plioplatecarpinae. The referral was based on several key diagnostic features, including a groove located basally on the basioccipital and basisphenoid, as well as fused processes of the quadrate. The species diagnosis of *P. overtoni* was comparatively short, including only a non-constricted suprastapedial process

of the quadrate, lack of a tuberosity on the anterior edge of the quadrate shaft, fused chevrons on the caudal vertebrae, and a small, anteriorly located pectoral crest of the humerus. Russell (1967) differentiated *P. overtoni* from the European type species *P. solvayi* by the absence of both procumbent anterior teeth and fluting on the enamel surface. Lingham-Soliar and Nolf (1989) would later expand upon these early comparisons in their redescription of *P. solvayi*, finding other means by which to differentiate the two taxa but ultimately retaining them as plioplatecarpines.

Since the initial description of *P. overtoni*, numerous other fragmentary remains from various localities throughout North America have been attributed to the taxon (Lucas et al. 2005; Konishi et al. 2011). Alongside the skull of SDSMT 3393, it is now known from two very well-preserved specimens (TMP 2002.400.0001, TMP 2007.034.0001) from Alberta that included the skull, large portions of the axial skeleton, partial pectoral and pelvic girdles, and hind paddles (Konishi et al. 2011). A new specimen, TMP 2018.042.0005, recovered by Korite International during mining operations in Alberta and accessioned by the Royal Tyrrell Museum of Palaeontology, represents one of the largest and most complete examples of *P. overtoni* to date. Consisting of a mostly articulated skeleton set apart on four separate blocks, TMP 2018.042.0005 includes a skull, large portions of the vertebral column, pectoral and pelvic girdles, most of the hindlimbs, and the first example of an articulated front paddle within the genus.

A description and comparison of TMP 2018.042.0005 with other conspecifics further expands our osteological knowledge of *P. overtoni*, as well as provides the potential opportunity to assess intraspecific variation within the taxon. In addition, the morphological reassessment and comparisons of *P. overtoni* to other taxa by Konishi et al. (2011) corroborated the recovery

of *Prognathodon* as a member of the Globidensini alongside *Globidens* (Bell, 1997). Despite this, the precise systematic relationships within *Prognathodon* remains poorly resolved (Simoes et al. 2017; Lively 2022). The referral of *P. overtoni* to *Prognathodon* is in large part responsible for the current interpretation of the genus as including mosasaurs with large, robust crania and dentition (Russell, 1967; Lingham-Soliar and Nolf, 1967; Bell, 1997), and this species therefore central to our historic and current understanding of the group. As the updated description of the type species *P. solvayi* fundamentally revises this paradigm, the inclusion of *P. overtoni* within *Prognathodon* is readdressed by applying the revised generic diagnosis to a morphological comparison between the two taxa.

MATERIALS AND METHODS

Prognathodon overtoni (SDSMT 3393, TMP 2002.400.0001, TMP 2007.034.0001, and TMP 2018.042.0005) and *Prognathodon solvayi* (IRScNB R33 (4672), IRScNB 0106, IRScNB 0107, IRScNB 0108) were photographed using a Nikon D500 camera. KU 590 was referenced using photographs taken by T. Konishi. Line drawings and reconstructions were drawn in Photoshop CS6 Version 13.0.1. were measured and photographed using a Nikon D500 camera with a Nikkor AF-S 50 mm lens and a Google Pixel 2 smartphone. Photographs were processed and figures produced in Adobe Photoshop CS6 and Adobe Photoshop 24.6.0. Line drawings were traced from photographs and stippled using a Wacom Intuos pro pen tablet.

DESCRIPTION

The skull and skeleton of TMP 2018.042.0005 are separated into four large blocks: block one contains the skull, the second block houses part of the anterior dorsal vertebral series, the rib

cage, and forelimb(s), the third block consists of the pelvic girdle, hindlimbs, and posterior dorsal, pygal, and intermediate caudal vertebral series, and the caudal region is contained within block four.

Cranium

Skull—The skull of TMP 2018.042.0005 is exposed only in left lateral view but the visible portions are very well-preserved (Fig. 5.2). Taking the greatest distance from tip of the rostrum to the retroarticular process, TMP 2018.042.0005 measures approximately 110 cm in length; it is larger than SDSMT 3393 (approx. 84 cm), TMP 2002.400.0001 (estimated 85-90 cm, although the retroarticular process is damaged), and TMP 2007.034.0001 (approx. 86 cm) (Fig. 5.3). The lower mandibles are in articulation with the upper jaws. The skull is overall massively built, and the snout is proportionately short compared to other mosasaur taxa such as *Mosasaurus* (Street and Caldwell, 2017). The ventral margins of the right dentary, splenial, and angular are exposed beneath the left counterparts. Internal bones of the palate and pterygoid are not visible. The braincase and much of the skull roof elements, including the parietal and most of the frontal, are either crushed or concealed by matrix.

Premaxilla—The dorsal and left lateral surfaces on the premaxilla of TMP 2018.042.0005 are partially crushed, although like SDSMT 3393, TMP 2002.400.0001 and TMP 2007.034.0001, a short, blunt rostrum protrudes anterior to the first premaxillary tooth position (Fig. 5.2). The pair of dorsal parallel ridges described by Konishi et al. (2011) are not preserved. The main body of the element is short, and the premaxillary-maxillary suture extends posteriorly to roughly the third maxillary tooth position, as in other referred specimens. Although the anterior edge of the

suture on the premaxilla is distorted, the corresponding edge of the anterior maxilla is slightly sinusoidal in outline (Konishi et al. 2011). The dorsal surface is also crushed and obscured by matrix, and a pair of ridges and central concavity described by Konishi et al. (2011) in other specimens is not discernable as a result. The internarial bar is not visible.

The fragmented base of the right first premaxillary tooth is preserved within its alveolus, although no diagnostic features are preserved. A small, conical, straight crown and partial root situated between the first and second dentary teeth is interpreted here as the second left premaxillary tooth that was broken off at its base and shifted slightly posteriorly. Only an anterior carina is present. Konishi et al. (2011) described the first premaxillary teeth as weakly procumbent, although this largely only apparent in TMP 2002.400.0001, and SDSMT 3393 and TMP 2007.034.0001 lack this feature. Only the base of the right first premaxillary tooth is preserved in TMP 2018.042.0005, but it does not appear to have been procumbent. The incline to the tooth in TMP 2002.400.0001 is therefore interpreted here to most likely result from taphonomy.

Maxilla—The left maxilla of TMP 2018.042.0005 is well preserved (Fig. 5.2). Similar to other specimens (Konishi et al. 2011), the premaxillary-maxillary suture extends to the posterior edge of the third tooth position, and the suture itself has a pinched appearance across its length. The expanded region of the external nares reaches from the third to sixth tooth positions. As in SDSMT 3393, TMP 2002.400.0001 and TMP 2007.034.0001, both the anterodorsal and posterodorsal processes are oriented dorsally and therefore visible in lateral view, the latter being slightly greater in height than the former (Figs. 5.2, 5.3). The posterodorsal edge of the maxilla is also sinusoidal in outline and interfingers with the prefrontal, whereas the posteroventral margin

is overlapped by the horizontal ramus of the jugal. Ventrally, the dental margin is straight. A row of prominent foramina (described as exits of the fifth cranial nerve by Konishi et al. 2011) runs parallel to the margin along the entire length of lateral surface. Unlike TMP 2007.034.0001, the foramina arch slightly on the anterior half of the maxilla (Fig. 5.1; Konishi et al. 2012; figs. 2, 3). A network of irregular shallow grooves extends across the anterolateral face until the sixth or seventh tooth position, a feature also most clearly visible in TMP 2002.400.0001 (Konish et al. 2011: fig. 3).

There are twelve tooth positions in the maxilla, as in SDSMT 3393 and TMP 2007.034.0001, although most of the teeth are damaged or missing (Figs. 5.2, 5.3). TMP 2002.400.0001 retained thirteen tooth positions in both maxillae (Konishi et al. 2011). The remaining crowns in TMP 2018.042.0005 are weakly heterodont, wherein the narrower anterior crowns broaden posteriorly, and the posterior-most tooth crowns gradually reduce in size. In contrast, the teeth of TMP 2002.400.0001 are narrower throughout the jaw and heterodonty is less pronounced as a result. This feature is more difficult to assess in SDSMT 3393, as several teeth are reconstructed or have been glued in incorrect positions. The crown apices in TMP 2018.042.0005 point slightly posteriorly as well as lingually, and the degree of crown curvature does not appear to vary considerably across the tooth row. The enamel surfaces are generally not as well preserved as in other specimens of *P. overtoni*; however, mesial and distal carinae with minute serrations are visible on some examples positioned anteriorly and midway along the maxilla. Well-developed crenulations or anastomosing texture is present on the crown apices, occasionally extending slightly further down along the anterior and posterior edges of the crown (Fig. 5.4). Flutes or facets are absent and the enamel surfaces are otherwise smooth, a feature shared with SDSMT 3393 and TMP 2007.034.0001. In contrast, weakly-developed facets are

present on the anterior teeth of TMP 2002.400.0001 (Fig. 5.4B), and two or three anterior teeth of TMP 2007.034.0001.

Frontal—Most of the frontal in TMP 2018.042.0005 is unexposed and only the left lateral contact with the prefrontal and postorbitofrontal is visible. The suture is irregular in outline and roughly textured, a feature visible in other specimens as well (Fig. 5.2). As in other specimens of *P. overtoni*, the frontal is excluded from the border of the orbit by the prefrontal and postorbitofrontal.

Prefrontal—The close, sinusoidal contact between the prefrontal and maxilla described by Konishi et al. (2012) is likewise evident in TMP 2018.042.0005 (Fig. 5.2). Although most of the left external naris is mostly hidden by matrix, the prefrontal comprises a large portion of its posterolateral border. Laterally, the triangular supraorbital process is well-preserved but bent ventrally. Like the frontal, the bone surface of the lateral edges of the process are heavily textured and striated. A smooth, flat-bottomed triangular depression with well-defined margins forms the anteroventral surface of the prefrontal (Figs. 5.2, 5.3). Bordered by the maxillary suture anterior horizontal ramus of the jugal, this structure is also discernable in TMP 2007.034.0001 and to a lesser extent in TMP 2002.400.0001 and SDSMT 3393, although in these specimens this region is either crushed or reconstructed with plaster (Fig. 5.2). Although somewhat damaged, the posterodorsal edge of the prefrontal closely contacts and overlaps the postorbitofrontal near the edge of the orbit.

Postorbitofrontal—Most of the postorbitofrontal is not visible in TMP 2018.042.0005. A broad shelf of thick, textured bone aligned with the supraorbital process of the prefrontal overhangs the posterior edge of the orbit (Fig. 5.2). Posteroventrally, a flange of bone presumably representing the jugal process descends ventrally and overlaps the vertical ramus of the jugal, although Konishi et al. (2011) did not find a clearly identifiable jugal process in any other specimens. Only the proximal end of the squamosal process is visible along the temporal bar.

Jugal—As in other specimens, the horizontal ramus of the jugal in TMP 2018.042.0005 is roughly twice as long as the vertical ramus, slightly bowed across its length, and extends to the anterior limit of the supraorbital process of the prefrontal (Figs. 5.2, 5.3). The bone expands slightly where it meets the posterior extend of the maxilla before tapering towards its anterior extent. The vertical ramus rises dorsally somewhat abruptly at a 90 degree angle from the posterior extent of the horizontal ramus (Lingham-Soliar and Nolf, 1989). A posteroventral process is absent.

Sclerotic Ossicles—Roughly ten sub-rectangular to dumbbell-shaped ossicles are preserved, although most are out of place, damaged, or obscured by other ossicles (Fig. 5.2). Yamashita et al. 2015 describes three types of ossicles: plus type, wherein both sides of the ossicle overlap its neighbours, minus type, which is overlapped by an adjacent ossicle on both sides, and imbricating type, where only one side is overlapped the neighbouring ossicle. In TMP 2018.042.0005, there are two plus types, at least one minus type, and at least two examples of the imbricating type.

Squamosal—The squamosal ramus extends to the anterior edge of the temporal fenestra (Fig. 5.2). Striae run longitudinally across its length and continue onto the squamosal process of the postorbitofrontal. Present in all other specimens, the squamosal expands midway along the bone and forms a long, narrow-edged posterolateral crest that overhangs the lower temporal fenestra (Figs. 5.2, 5.3). This portion of the bone likewise curves ventrally towards the broad quadrate articulation, which is angled posteriorly and embraces the posteroventral surface of the suprastapedial process of the quadrate. Dorsally, the parietal process that would extend medially onto the suspensorial ramus is not visible.

Supratemporal—Most of the supratemporal is concealed by the overlapping quadrate articulation of the squamosal (Figs. 5.2, 5.5A). A small ventral portion extends out from the medial surface of the squamosal to clasp the posteroventral surfaces of the suprastapedial and posterior pillar-like processes.

Lower Jaw

Dentary—The dentaries of TMP 2018.042.0005 are robustly built with bowed dorsal and ventral margins (Fig. 5.2). Like the premaxilla, the anterior edge extends slightly beyond the first tooth position. The row of foramina extending across the lateral surface present in other specimens is likewise present in TMP 2018.042.0005, although they increase in number and intersperse across the anterior tip of the bone. The outer margins of the right dentary are exposed beneath the left element. The right dentary is shifted slightly anterior relative to its counterpart, and a small portion of what likely represents the anterior limit of the Meckellian groove is visible on the exposed medial surface. The groove is closed at its tip, a feature also present in SDSMT 3393.

The dentary teeth are in slightly better condition than those in the maxilla and more examples are preserved (Fig. 5.2). As with TMP 2002.400.0001 and TMP 2007.034.0001, there are fifteen tooth positions (Fig. 5.3). The anterior dentary crowns are not procumbent. Although also exhibiting weakly heterodont, robust and bicarinate crowns with heavily crenulated apices, the teeth of TMP 2018.042.0005 are proportionately larger in size relative to the jaw than in other specimens (Figs. 5.3, 5.4). The teeth are less bulbous in shape than those of TMP 2007.034.0001, but the crowns midway and posteriorly in the jaw are broader than those in TMP 2002.400.0001. The posterior-most tooth in the dentary is not preserved or fully visible in other examples (note that in SDSMT 3393, the posterior tooth is plastered in place and may not belong in that position); however, in TMP 2018.042.0005, this crown is considerably smaller and has a more strongly curved apex. The anterior dentary teeth are not procumbent.

Splenial—Only the ventral margin of the right splenial and posterolateral wedge-shaped surface of the left are visible in TMP 2018.042.0005 (Fig. 5.2). The bones are thick like most of the skull, but few diagnostic features are evident beyond the concave articular face with the angular. The condition described by Konishi et al. (2011) wherein the intramandibular joint is partially visible on the lateral surface of the bone is not especially clear, and instead appears to be a small lip bounding the lateral edge.

Angular—Like the splenial, the anteroventral edge of the right angular and the base of the medial wing are exposed beneath the left element, with the articular overlapping the posteroventral portion (Fig. 5.2). The ventrolateral surface of the left angular is broadly exposed across its entire length. Its anterolateral surface is wedge-shaped and extends dorsally on the

surangular to the same height as the splenial. The articular surfaces are convex and fit inside the corresponding concave facet of the splenial.

Surangular—The left lateral surface of the surangular in TMP 2018.042.0005 is very well preserved and in tight articulation with the other elements constituting the PMU (posterior mandibular unit) (Fig. 5.2). Like other examples of *P. overtoni*, the surangular is relatively deep and triangular in shape, the dorsal margin expanding slightly anteriorly to buttress the posterior edge of the coronoid (Fig. 5.3). The surangular of SDSMT 3393 initially appears narrower overall, although the margin near the coracoid has been partially reconstructed with plaster (Fig. 5.3D). The anterior surangular foramen is represented by a short, semi-circular fossa that forms the anterodorsal margin of the surangular, a series of elongate, horizontal ridges extending across its surface. A broad excavation extends across the upper half of the posterolateral surface and is bordered posteriorly by a low shelf. Posterior to this shelf, the dorsal edge forms the lateral margin of the glenoid facet, then narrows to a point that laterally overlaps most of the retroarticular process. This large degree of overlap is also present in SDSMT 3393 but is considerably reduced in TMP 2007.034.0001, wherein the posterior extremity of the surangular terminates at the posterior border of the glenoid fossa (Konishi et al. 2011: fig. 2A). The contact between the surangular and articular is not readily discernable in lateral view; however, in dorsal view the dorsal margin of the surangular appears to continue posteriorly, overlapping the articular laterally as seen in SDSMT 3393 and TMP 2018.042.0005.

Coronoid—The coronoid process is not fully exposed in either TMP 2002.400.0001 or TMP 2007.034.0001 (Konishi et al. 2011), and although the dorsal tip is also partially hidden in TMP

2018.042.0005, its margin is likely rounded (Figs. 5.2, 5.3). A broad, robust shelf originating on the coronoid process projects laterally and slopes ventrally onto the lateral wing. The ventral margin of the lateral wing is convex and extends roughly halfway on the surangular. Its anterior edge is indented where it accommodates the anterior surangular fossa. The solid dorsal margin of the anterior wing described in the Alberta specimens by Konishi et al. (2011) is not observable in TMP 2018.042.0005.

Articular—A ventral portion of the right articular/prearticular covers much of the angular medially in TMP 2018.042.000 and angles dorsally against the angular midway along the mandible (Fig. 5.2). Much of the posterior end of the left element is obscured laterally by the surangular, but dorsally the articular forms the medial and posterior edges of the glenoid fossa. Posterior to this point (and despite some compression), the retroarticular process is rotated nearly horizontally with respect to the orientation of the PMU. A strongly inflected retroarticular process is shared with SDSMT 3393, TMP 2002.400.0001, and TMP 2007.034.0001 (Konishi et al. 2011) (Fig. 5.3).

Quadrate—The quadrate morphology of TMP 2018.042.0005 strongly resembles that in other described specimens, although only the lateral face of the left quadrate is visible (Figs. 5.2, 5.4A-C). The quadrate is articulating with the glenoid fossa and the suspensorium, its posterior surface embraced firmly by the squamosal and supratemporal. As a result, the quadrate is posteroventrally tilted, a condition apparent in TMP 2007.034.0001 and present in other mosasaur taxa, such as plioplatecarpines and *Tylosaurus* (Palci et al. 2021). The left lower jaw unit appears slightly offset posteriorly and may exaggerate the degree of tilting.

The lateral edges of the tympanic ala and suprastapedial process appear to be slightly crushed or broken away (Fig. 5.4A). As described by Konishi et al. (2011), the outer margin of the quadrate conch is deeply concave and circular, but other features on the anterolateral surface are poorly preserved. The suprastapedial process is fused to the posterior pillar-like process (Palci et al. 2021), which broadly spans much of the posteroventral surface of the quadrate. The expanded tympanic rim that angles posteriorly over the ala present in some other members of *Prognathodon* (Figs. 5.4A-C, 7.2) appears to be absent in *P. overtoni*. Ventrally, the mandibular condyle is large and bulbous with a strongly convex ventral margin. The anteroventral surface is upturned dorsally and forms a small lip on its anterior face. From the cephalic condyle to the mandibular condyle, the quadrate of TMP 2018.042.0005 is 15 cm in length, slightly larger than the roughly 14 cm long quadrate of KU 590.

Axial Skeleton

The postcranial skeleton of TMP 2018.042.0005 represents one of the most complete examples for the genus and includes the first preserved partially articulated forelimb (Fig. 5.1). The pelvis, hindlimbs, and the posterior axial skeleton are nearly complete, the latter apparently lacking a small section of dorsals, intermediate caudals, and the tip of the tail. The cervical vertebrae are either not preserved or are hidden within the matrix.

Dorsal Vertebrae—The anterior dorsal vertebrae are only represented by three or four tall and narrow but largely poorly preserved synapophyseal processes articulating with a series of broken ribs (Fig. 5.6). Situated just posterior to the rib cage, there are six laterally exposed articulating posterior dorsal vertebrae (and the neural spine of a seventh) on the second block, and a further

twelve within the vertebral column in the third block. The prezygapophyses of the first set of dorsals are elongate with narrower bases and broad articulating facets. A thin ridge connects the dorsal margins of the prezygapophyses with the transverse processes. The transverse processes are situated anteriorly and a little higher than midway on the centrum. In ventral view (visible on the third block; Fig. 5.7), they have a flat, broad base and gently tapering, rounded distal synapophyseal processes. The synapophyseal facets are subrectangular in shape and oriented dorsoventrally and (Fig. 5.6, 5.7). A pair of large zygosphenes are visible on a single disarticulated and damaged vertebra (Fig. 5.6C). The cotyle is subcircular and has a notched dorsal margin. Directly posterior to the cotyle, the centrum is only slightly constricted. The postzygapophyses are short and stout with flat, oval articular surfaces. A peculiarity of *P. overtoni* is the anteroposteriorly wide neural spines with edges that appear broadly fused to their neighbouring counterparts (Konishi et al. 2011). However, the neural spines are likely only tightly abutting as opposed to fused, as the anterior and posterior margins on each spine are still discernible. Additionally, breakage along the dorsal series in the second block would not likely have left the posterior border of the neural spine of the second vertebra and the anterior border of the neural spine on the last vertebra intact if they had been fully fused to the adjacent vertebra (Fig. 5.6A, B). Regardless, this condition was only described in the fourth to seventh dorsals of TMP 2007.034.0001 but is also present from the set of seven anterior dorsals until the second or possibly third pygal vertebra in TMP 2018.042.0005 (Figs. 5.7, 5.8). Although the neural spines are not visible on the first four dorsals on the third block and the section is offset from the column, it is likely that the entire dorsal series exhibited the same condition, as the elements remain in approximate alignment with one another. The neural spines re-emerge at the sixth

vertebra in the section where the remaining dorsals are articulating with the column and are exposed in lateral view.

Roughly seven dorsal ribs are preserved on the second block. Anteriorly, the proximal heads are in articulation with the synapophyses of the corresponding dorsal vertebrae, but little of their morphology is readily observable as a result of poor preservation. The rib heads appear slightly expanded and taper only slightly along the shaft. The shafts are long and curved but decrease in length posteriorly.

Caudal Vertebrae—There are thirteen pygal vertebrae in TMP 2018.042.0005, as opposed to eleven in TMP 2007.034.0001 and twelve in TMP 2002.400.0001. The anterior pygal centra are slightly shorter than those of the dorsals and continue to gradually decrease in length posteriorly along the series (Figs. 5.7, 5.8). The neural spines of the pygal vertebrae are roughly the same width as in the dorsal series, but beyond this point the margins are less tightly contacting and instead overlap, likely due to the dorsal bending of the vertebral column (Fig. 5.8). On the posterior pygals, the anterior margin of the neural spine forms a large expanded region that in its original position may have contacted the posterior margin of the preceding vertebra. The prezygapophyses are very short and decrease in size posteriorly. The horizontally oriented base of the transverse processes is broad, situated midway along the centrum, and extends across most of the lateral surface of the centrum.

There are five intermediate caudal vertebrae articulating with the pygals on the third block, and ten on the fourth (Figs. 5.7, 5.8). The transverse processes reduce in length and size posteriorly, although the migration of the base dorsally on the centrum described by Konishi et

al. (2011) is not evident in TMP 2018.042.0005. The haemal arches are partially contained within the matrix but are fused to the caudal centra.

There are fifty-five terminal caudals preserved, all of which are in articulation (Fig. 5.7). Unlike the dorsal, pygal, and intermediate caudals in which the neural spines are angled posteriorly, the first one or two terminal caudal spines are oriented vertically (Fig. 5.7B). Konishi et al. (2011) observed that the successive neural spines in TMP 2002.400.0001 and TMP 2007.034.0001 begin to angle anteriorly, a condition also present in TMP 2018.042.0005. By the twelfth terminal caudal, the neural spines straighten once again and begin to incline posteriorly at the fifteenth. A broad ridge of thickened bone extends a little over midway up the center of the lateral surface on nearly all the neural spines and is visible until roughly the forty-first caudal (Fig. 5.7). In TMP 2002.400.0001 and TMP 2007.034.0001, the appearance of these features coincides with a ventral downturn of the vertebral column and is associated with the expanded, fluke-like section of the tail. In TMP 2018.042.0005, the column is instead bent slightly upwards likely as a result of deformation or other taphonomic processes, although the inflection point is at the same position along the column as in the other Alberta specimens. Both the neural and haemal spines increase in length until roughly the sixteenth vertebra, after which they decrease in size towards the tip of the tail. A posterior portion of the haemal spines is covered by an undescribed fish skull, and a smooth-bordered semicircular section of damaged and missing neural spines provides evidence TMP 2018.042.0005 was scavenged on shortly before or soon after its death.

Scapula and Coracoid—Both elements are preserved largely in their life position along the rib cage and in articulation with the humerus of the left forelimb (Fig. 5.9). The tight interdigitating

suture between the two elements described by Konishi et al. (2011) is not visible. The scapula is well-preserved and crescentic in shape with an elongate posterior wing. A distinct scapular neck is virtually absent, as the edges expand abruptly dorsal to the suture. Apart from a slightly crushed distal margin, the coracoid is likewise well-preserved. Its lateral surface is expanded relative to the scapula and more fan shaped as a result. The articulating surface with the scapula is broad, as is the short coracoid neck. A flat, damaged plate of bone underlying the anteroventral border of the coracoid may be the partially exposed interclavicle and/or the internal surface of the right coracoid.

Appendicular Skeleton

Forelimb—Excluding distal portions of the digits, the left front paddle of TMP 2018.042.000 is in articulation and preserves nearly all of its major elements (Fig. 5.9). The unique convex glenoid condyle of the humerus that extends above the postglenoid process described by Konishi et al. (2011) is present in TMP 2018.042.0005. Opposite to the broad and robust postglenoid process, the smaller deltoid process overlays the pectoral crest. As in TMP 2002.400.0001, The midsection of the humerus is strongly constricted (Konishi et al. 2011: fig. 9). Distally, the ectepicondyle is narrow and peg shaped, whereas the distal extremity of the larger entepicondyle appears embedded in the matrix. The broad radial and ulnar facet converge at an obtuse angle roughly 135 degrees, as reported by Konishi et al. (2011).

The radius is largely complete with only minor damage (Fig. 5.9). The forelimb elements preserved in TMP 2002.400.0001 reportedly closely resembled those of *Clidastes* (Konishi et al. 2011); aside from the broader proximal facet, this holds true for the general shape of the radius in TMP 2018.042.0005 (Russell, 1967: figs. 51). Its postaxial margin distal to the humeral facet is

broadly constricted, but a preaxial concavity is abbreviated by a flange that extends along most of the central shaft. The flange border is straight and forms a continuous border with the distal surface of the radius. Notably, the postaxial edge of the distal facet differs from the condition seen in *Clidastes* in that it contacts the intermedium, excluding the radiale from the border of the antebrachial foramen.

As in TMP 2018.042.0005 (Konishi et al. 2011: fig. 9), the humeral facet of the ulna is markedly broader than its distal end in TMP 2018.042.000 (Fig. 5.8). The main shaft is broadly constricted on both sides, although the proximal postaxial region is marked by a prominent and rounded olecranon process. A small, posteriorly facing facet on the distal postaxial border indicates a pisiform would have been present. A small nearby fragment of bone partially exposed from under metacarpal V and a proximal phalanx may represent the pisiform. A short, upturned portion of distal facet bordering the antebrachial foramen contacts the intermedium. The intermedium itself is cracked down its center but has maintained its crescentic shape with a notched proximal border. The concave inner margins of the intermedium, radius, and ulna form the circular border of the large antebrachial foramen.

The radiale is roughly ovate to subrectangular in shape with distinct facets that articulate tightly with the radius, intermedium, and distal carpal II (Fig. 5.9). The distal carpals are more circular in shape and smaller than the radiale, and have flattened edges where they contact the surrounding elements. Distal carpal 2 is the largest of the three. The ulnare is similar in both size and shape to the distal carpals but is longer than it is wide. Its margins are straight where it articulates with the intermedium, ulna, and metacarpal IV, whereas its postaxial edge is rounded and convex. These elements also resemble those of *Clidastes* in terms of overall shape and

relative size, although the more rectangular radiale is more similar to that of *Mosasaurus* (Russell 1967: fig. 50, 51).

The proximal end of the digits remains in articulation with the forelimb, but the distal-most phalanges are either disarticulated, buried in matrix, or missing altogether (Fig. 5.9). Digit 1 consists of only metacarpal I and a proximal phalanx. The proximal facet of metacarpal I is wider than the distal end and bears a rounded, expanded preaxial border. The proximal phalanx is smaller and narrower, but its proximal surface is likewise expanded relative to the distal end. Both elements have only shallowly constricted central margins. The metacarpals of digits 2, 3, and 4 are longer, narrower, have only slightly large proximal facets, and more constricted shafts. Two phalanges are preserved in both digits 2 and 3 and strongly resemble the metacarpals in shape. The distal elements in digit 4 are dispersed and appear to be intermingled with the phalanges and other proximal elements from the underlying right front paddle. Metacarpal 5 is short with a broad distal end that bears two distinct facets, one of which would have articulated with the proximal phalanx. Due to its enlarged proximal end, what is likely the proximal phalanx has been displaced to overlie the postaxial margin of metacarpal 5.

Pelvic Girdle—The pelvic girdle of TMP 2018.042.0005 is preserved in a rather unique orientation (with the partial exception of TMP 2007.034.0001), wherein both ischia, pubes, and hindlimbs remain in articulation and lie parallel to the vertebral column (Fig. 5.8). The entirety of the complex is exposed ventrally. The right ilium underlies the vertebral column and only the concave facet for the acetabulum is partially exposed beneath the right pubis. The proximal region of the left pubis is damaged, whereas the right is essentially complete. The anterior border of the pubes faces dorsally with the distal tip of the pubic tubercle overlapped both by the

synapophysis of a pygal vertebra and a single displaced distal phalanx (Fig. 5.8). As described by Konishi et al. (2011), the tubercle is rectangular in shape, as well as heavily striated. The oval obturator foramen perforates the pubic head at the base of the tubercle. Posteriorly, only the broad, slightly concave facet with the acetabulum is visible. A thickened ridge of bone forms the ventral surface of the elongate pubic shaft. The shaft itself is flattened in cross-section with a narrower base that expands distally towards the pubic symphysis, which is maintained as a tight contact between the two pubes. The bone surface directly adjacent to the symphysis is highly rugose in appearance.

Directly below the pubes, the ischiadic symphysis is likewise intact (Fig. 5.8). The distal termination of the left and right ischia is broadly expanded and slightly compressed relative to the main shaft. The two elements are positioned with their posterior surfaces oriented ventrally, such that the ischiadic tubercles adorning the posterior margin are directed downwards into the matrix. The base of the tubercles is broad and would have formed a large, triangular-shaped process like that observed by Konishi et al. (2011) in TMP 2002.400.0001. The main shafts are straight and constricted near the center. The proximal heads are expanded relative to the shaft and have a slightly convex facet for the acetabulum.

Hindlimb—The left and right hindlimbs are aligned parallel to the vertebral column and positioned opposite to each other, both exposed in extensor aspect (Fig. 5.8). The proximal sections of the right femora are in articulation up until the metatarsals, after which the phalanges are dispersed or missing. Both the left and right femora of TMP 2018.042.0005 are associated with, but still slightly dislocated from the acetabula. Similar to TMP 2002.400.0001, the femora of TMP 2018.042.0005 are elongate with a central constriction and expanded, convex proximal

and distal ends. The internal trochanters are not readily observable as it appears largely broken away on the left femur appears and mostly concealed by matrix on the right. The tibial and fibular facets are clearly separated and offset from each other at an obtuse angle.

The tibia, fibula, and tarsals of TMP 2018.042.0005 are well-preserved on the right paddle, and are virtually identical in terms of shape and relative size to the other Alberta specimens (Konishi et al. 2011) (Fig. 5.8). The bone surface of the tibia is more rugose and striated near the facets in comparison to TMP 2002.400.0001, and the three distal facets on the fibula are even more strongly demarcated. The left paddle is lacking its tibia.

The asymmetrical astragalus is nestled firmly between the fibula, calcaneum, and fourth distal tarsal. The proximal articulation with the tibia is short, resulting in the effective exclusion of the astragalus from the border of the crural foramen (Fig. 5.8). However, the left astragalus has the typical proximally extended facet like that seen in TMP 2002.400.0001, suggesting the right element was damaged. The circular distal tarsal and slightly compressed calcaneum described in TMP 2002.400.0001 are likewise present in TMP 2018.042.0005, although they are only preserved on the right limb. The broadly semicircular metatarsal 5 (also only remaining on the right limb) remains in articulation with the calcaneum and fourth distal tarsal but is partially obscured by the overlying vertebral column.

The pedal digits are not as well-preserved as in TMP 2002.400.0001 (Konishi et al. 2011), as most of the distal phalanges are either in the matrix or have been disarticulated and scattered throughout the block (Fig. 5.8). Digits II and III of the left paddle are partially overlain by digit I and the vertebral column. On the right paddle, the central three metatarsals are narrow and elongate with slightly broader proximal heads. Only the inner two remain on the left limb. Metatarsal 1 is preserved on both paddles and is shorter and markedly broad, particularly at the

proximal facet. Its central margins are more noticeably constricted than the central metatarsals. The first phalanx remains in articulation on both sides and is slightly longer but considerably narrower than metatarsal 1. The remaining phalanges more closely resemble the inner metacarpals in shape, although are slightly more elongate and strongly constricted at the center of the shaft.

DISCUSSION

Variation within *P. overtoni*

Konishi et al. (2011) estimated *P. overtoni* could reach lengths of approximately ten meters. With the separate sections combined, the estimated total length of the skeleton of TMP 2018.042.0005 is between seven and eight meters, and possibly longer. TMP 2018.042.0005 is the largest of the TMP and SDSMT specimens, and may have been most similar in size to the KU 950, although this is an assumption based only on similar heights of the quadrate and it is currently not known if this measurement is a reliable or accurate predictor of relative skull or total body length. Despite the existence of other well-preserved specimens within which to assess variation with the species, drawing comparisons is difficult due to differing degrees of preservation within the specimens themselves. The poor preservation of large portions of the skull in TMP 2002.400.0001 and the considerable amount of reconstruction of SDSMT 3393 allows for only tentative estimates. Ratios of skull length to large components of the jaw, such as the dentary and surangular, is a simple means to evaluate whether there are any noticeable size differences between specimens. From the tip of the snout to the retroarticular process, the skull of TMP 2018.042.0005 is measured at 110 cm (Table 1). With a dentary (from its anterior tip to posteroventral corner where it meets the splenial) of 71 cm, the maximum skull length to dentary

ratio is 1.54. This ratio is 1.55 for TMP 2007.034.0001, 1.59 in SDSMT 3349, and an estimated 1.68 for TMP 2002.400.0001. The maximum skull length to surangular ratio is 2.50 for TMP 2018.042.0005, 2.36 for TMP 2007.034.0001, 2.47 for SDSMT 3349, and an estimated 2.34 for TMP 2002.400.0001. The skulls of TMP 2002.400.0001, TMP 2007.034.0001, and SDSMT 3349 are all roughly similar in size and vary only slightly in terms of relative lengths of the lower jaw components. The surangular ratio is more variable, although accurate measurements were only available from TMP 2018.042.0005, TMP 2007.034.0001, and possibly SDSMT 3393. The snout of TMP 2007.034.0001, although likely somewhat distorted, appears to be relatively shorter compared to the other three skulls (Fig. 5.3).

The highest degree of variation between the specimens is visible in the dentition. The maxillary and dentary teeth in TMP 2018.042.0005 are proportionately larger, especially compared to the teeth midway on the jaw in TMP 2007.034.0001. Relative to TMP 2002.400.0001, the tooth crowns of TMP 2007.034.0001 are considerably shorter in height. In all the Alberta specimens, the crown bases begin to widen at roughly the fifth maxillary tooth position, but in TMP 2002.400.0001 the teeth are narrower overall as well as taller than those of TMP 2007.034.0001, instead more closely resembling the crown shape in SDSMT 3393.

Regarding enamel ornamentation, many of the teeth of SDSMT 3393 are largely featureless and smooth, although like the skull itself, several crowns are partially if not mostly reconstructed in plaster. Anastomosing texture on the tooth enamel is present in all the Alberta specimens (and possibly SDSMT 3393). TMP 2018.042.00 appears to lack facets, which are present in TMP 2002.400.0001 and TMP 2007.034.0001 (albeit to a much lesser extent). The variable occurrence of enamel ornamentation within the same taxon is not unusual for mosasaurs, as both flutes and facets can occur in the same individual, and enamel structures can

also change throughout ontogeny (Street et al. 2020). Despite its larger size and outside of variation in the dentition and greater number of pygal vertebrae, the comparisons drawn between TMP 2018.042.0005, and its smaller, well-preserved conspecifics demonstrated few osteological differences that could indicate major ontogenetic shifts in the gross morphology of the cranium and postcranium in *P. overtoni*.

Comparison with *P. solvayi* and taxonomic conclusions

Features described by Konishi et al. (2011) which *P. overtoni* and *P. solvayi* have in common include a short, anteriorly constricted frontal with sinusoidal margins, distal carinae on the pterygoid teeth, proportionately large pterygoid teeth, presence of a medial excavation along the suprastapedial process of the quadrate, and a rounded retroarticular process (Fig. 5.3A-D). Based on the revised generic diagnosis of *P. solvayi* (Chap. 2), other key features present in both taxa include a premaxillary-maxillary suture extending the distance of roughly three tooth positions, a dorsally oriented anterodorsal process of the maxilla, a dorsally oriented posterodorsal process of the maxilla greater in height than the anterodorsal process, the prefrontal forms a large portion of the posterior border of the nares, a bowed dentary, fused suprastapedial and posterior pillar-like processes of the quadrate, a single blind-ended basioccipital canal, zygosphenes and zygantra on the vertebrae, and fused haemal arches of the caudal vertebrae. A faint triangular platform situated anterior to the parietal table (SDSMT 3393, TMP 2007.034.0001 is also present in both taxa (Konishi et al. 2011: fig. 2), as is a posterolateral crest on the squamosal, and a posterolateral excavation on the surangular.

Other characteristics of note include the presence of a dorsal median sulcus on the premaxilla (SDSMT 3393, TMP 2002.400.0001). In *Prognathodon overtoni* and *Globidens*

dakotensis, the sulcus is situated between two ridges that meet posteriorly to form a single ridge that extends onto the internarial bar (Konishi et al. 2011). The sulcus itself appears shallowly V-shaped, and a third low ridge can be seen extending along its center in SDSMT 3393, TMP 2002.400.0001, and *G. dakotensis* (pers. obs.) (Fig. 5.10A, B). In contrast, the dorsal median sulcus in *P. solvayi* (IRSNB 0106, 0107, Fig. 3.1A) is a shallow U-shape that lacks both the outer posteriorly converging and the central ridges (Fig. 5.10C). It is also largely restricted to the center of the premaxilla, becoming shallower and largely disappearing anterior to the internarial bar. Konishi et al. (2011) surmised the sulcus is a homologous feature of *P. solvayi*, *P. overtoni*, and *G. dakotensis*, although the differing morphology of *P. solvayi* casts doubt on this notion.

Additional differences between *P. overtoni* and *P. solvayi* mentioned by Konishi et al. (2011) include a more robust jugal and ectopterygoid (TMP 2002.400.0001), and a rounded coronoid process. The skull and dentition of *P. overtoni* is also more robust overall. The tooth crowns are broader, circular in cross-section, shorter in height, occasionally faceted, and are more heavily adorned with anastomosing texture. Heterodonty is more pronounced in *P. overtoni*, but the well-developed fluting on the teeth that is present in smaller specimens of *P. solvayi* is absent, as are elongate, sinusoidal anterior crowns. The procumbent anterior dentition is also unique to *P. solvayi*: although Konishi et al. (2011) stated that the first set of premaxillary teeth are weakly procumbent in *P. overtoni*, the variability of this condition across different specimens would suggest it is instead a result of deformation. A small predental rostrum is also present in *P. overtoni* but lacking in *P. solvayi*, and although Lingham-Soliar and Nolf (1989) described the two as very similar in shape dorsally, in the former it tapers anteriorly to a rounded point rather than a broad and blunted margin.

A median ridge on the frontal is also present in *P. overtoni* but absent in *P. solvayi*. The frontal is excluded from the orbital margin by the overlap of the prefrontal and postorbitofrontal in *P. overtoni*, but in *P. solvayi* the frontal forms a small portion of the border due to the lack of contact between the prefontal and postorbitofrontal. The vertical ramus of the jugal is oriented at 90 degrees, the parietal foramen is small, circular, and located further posteriorly on the parietal, the pterygoid teeth are situated on a ventral ridge descending from the main body of the pterygoid, a medially deflected coronoid process is absent, the medial wings of the coronoid and angular are contacting one another, and the retroarticular process is oriented horizontally as opposed to parallel to the PMU. The dorsal margin of the surangular is slightly more expanded dorsally than in *P. solvayi* and oriented less horizontally than initially reconstructed (Russell, 1967: fig 90; Konishi et al. 2011), as this region near the posterior base of the coronoid is rebuilt with plaster in SDSMT 3393 (pers. obs). The distance between the glenoid fossa and posterior margin of the coronoid is considerably shorter in *P. solvayi* (Lingham-Soliar and Nolf, 1989), as is the temporal arcade overall.

The quadrate of *P. overtoni* as a whole is narrower and taller than that of *P. solvayi*, and like the rest of the skull is more robustly built (Fig 5.5). The mandibular condyle is considerably larger and features a distinctly upturned anterior surface, whereas this feature is either not present or not preserved in *P. solvayi* beyond a slightly anterior tilting to the entire condyle. *P. overtoni* also lacks the dorsal eminence that extends dorsally above the stapedial pit. The posterior surface of the quadrate in *P. overtoni* is characterized by a mediolaterally broad fusion between the suprastapedial and posterior pillar-like processes. Although Palci et al. (2021) attribute this morphology to *Prognathodon* in general (Fig. 5.3B, C), the ventral process in *P. solvayi* originates and occupies the lateral surface of the quadrate, forming a comparatively

smaller and anteroposteriorly oriented contact with the suprastapedial process (Fig. 5.3D). This structure is instead more accurately referred to as the posterolateral process.

In addition to zygosphenes and zygantra, *P. overtoni* and *P. solvayi* share a notched dorsal margin of the centrum (Fig. 5.5C). However, the vertebrae of *P. overtoni*, like much of the skeleton, are more robustly built than in *P. solvayi*. The synapophyseal processes in the posterior dorsal vertebrae are more tapered, thinner and narrower in profile in more well-preserved examples than those of *P. overtoni* (Figs. 3.11, 5.6, 5.8), and the tips of the prezygapophyses in the anterior and posterior dorsals of *P. solvayi* are shorter and tapered rather than distally expanded (Figs. 3.10, 3.11., 5.6, 5.8). The transverse processes of the pygal vertebrae in *P. solvayi* are also considerably longer than in *P. overtoni* (Fig. 5.8; Lingham-Soliar and Nolf, 1989: fig. 34;). In ventral view, the centra in *P. solvayi* are slightly more constricted at the condyle. The neural spines are mostly broken and whether they tightly contacted the adjacent vertebrae like in TMP 2007.034.0001 and TMP 2018.042.0005 is difficult to determine, although the dorsal vertebrae of IRSNB 0106 have longer centra that extend well beyond the posterior border of the neural spine, which may have prevented contact as a result (Figs. 3.11B, 5.5, 5.6). Notably, *P. saturator* preserves a short series of dorsals that also exhibit broad neural spines closely abutting the adjoining vertebrae (Fig. 5.19). Konishi et al. (2011) surmised that this functioned to stiffen the vertebral column. A rigid vertebral column that restricts motion is not an uncommon feature in marine vertebrates and is achieved in part through various modifications of the vertebrae. Steeply inclined intravertebral joints, short and broad vertebral centra, and the presence of zygosphenes and zygantra can limit and/or stabilize lateral movements of the axial skeleton (Lingham-Soliar 1991; Lindgren et al. 2007). Additionally, the epaxial musculature in modern lizards was demonstrated to act as stabilizers for the column as it bends laterally during

locomotion (Ritter, 1996). Rather than the broad, contacting neural spines in *P. overtoni* and *P. saturator* increasing stiffness between the individual dorsal vertebrae per se, they may have instead served as larger attachment sites for the axial muscles to enhance rigidity along the column during lateral undulation.

CONCLUDING STATEMENTS

As the largest articulated specimen of *P. overtoni* to date, TMP 2018.042.0005 is a key specimen that provides new important osteological information for the taxon. With the exception of the elements that border the antebrachial chamber, this study also supports earlier assessments that find numerous similarities in the postcranium with the basal mosasaurine *Clidastes* (Konishi et al. 2011). Several similarities were also observed between *P. overtoni* and the type species of *Prognathodon*, *P. solvayi*, further corroborating previous work on the subject (Konishi et al. 2011). However, nearly as many differences were also reported, including the greater degree of robustness of the skull and dentition relative to the more gracile form of *P. solvayi*, a horizontally oriented retroarticular process, and absence a of strongly procumbent teeth combined with the presence of a short predental rostrum. These findings support the tentative removal of *P. overtoni* from *Prognathodon*, and that it instead likely constitutes a separate, albeit likely closely related taxon. Its omission from the genus further questions the notion that *Prognathodon* represents a group of uniquely massively built mosasaurs.

Figure 5.1. Whole skeleton of TMP 2018.042.0005 in separate blocks (1-4, from right to left). Image by H. Sharpe.

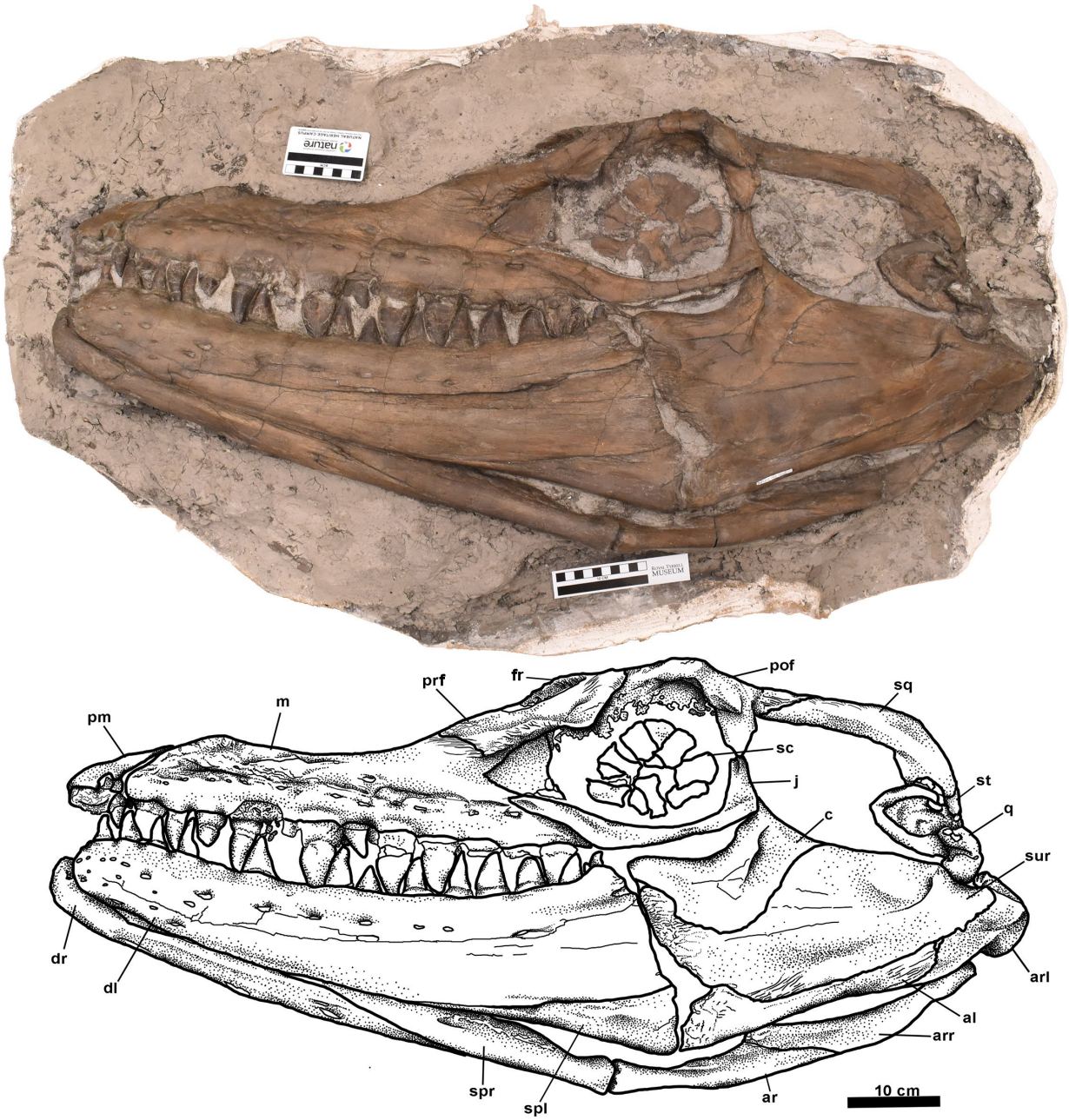

Figure 5.2. Skull of TMP 2018.042.0005 (block 1) in lateral view. Abbreviations: al, angular (left); ar, angular (right); arl, articular (left); arr, articular (right); c, coronoid; dl, dentary (left); dr, dentary (right); j, jugal; m, maxilla; pof, postorbitofrontal; pm, premaxilla; pr, q, quadrate; sc, sclerotic ossicles; spl, splenial (left); spr, splenial (right); sq, squamosal; st, supratempiral; sur, surangular. Black arrow indicates triangular depression on the prefrontal.

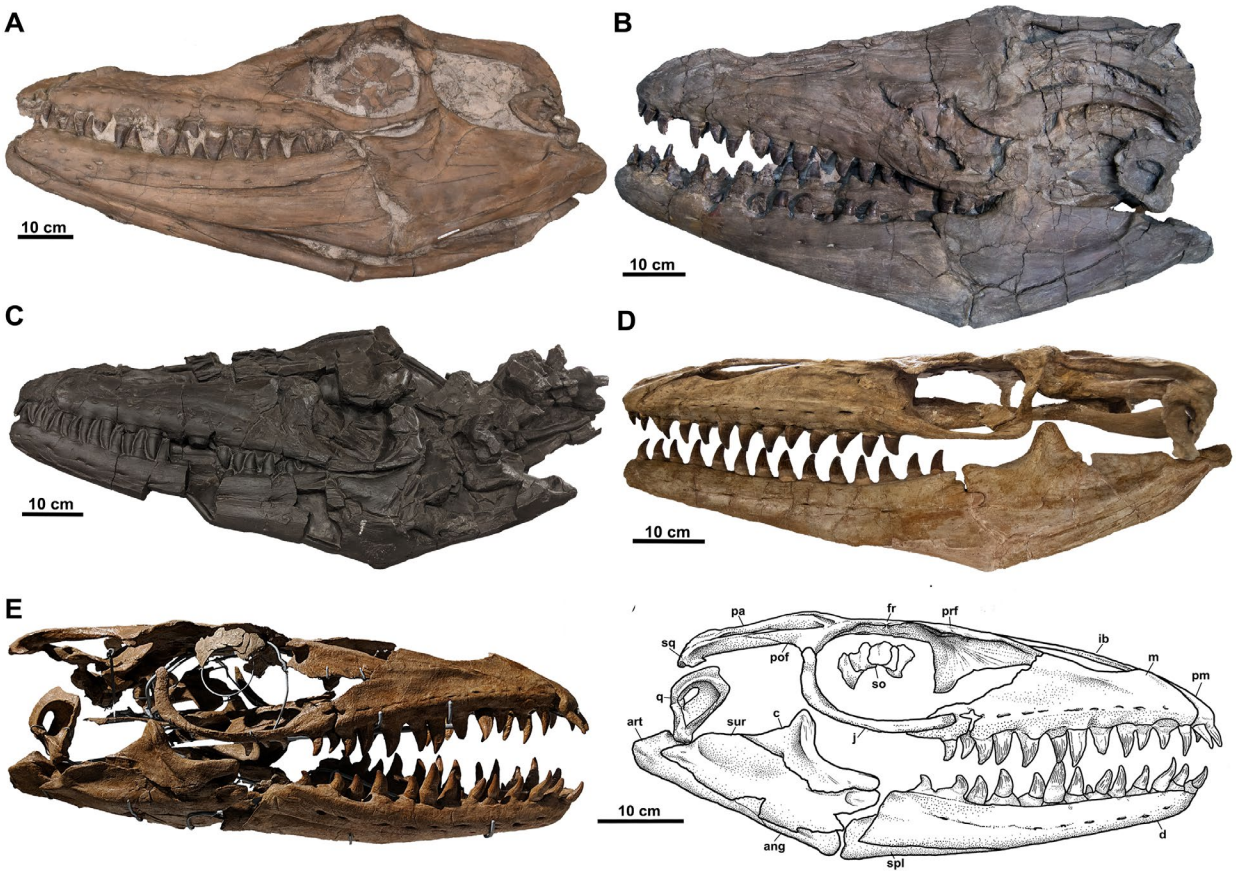

Figure 5.3. Skulls of (A) TMP 2018.042.0005, (B) TMP 2002.400.0001 (cast), (C) TMP 2007.034.0001, (D) SDSMT 3393; and (E) the skull and reconstruction of the holotype of *P. solvayi* (IRSNB R33). TMP 2002.400.0001, TMP 2007.034.0001, and SDSMT 3393 have been scaled up to match TMP 2018.042.0005 in length and mirrored to display the skulls in left lateral view.

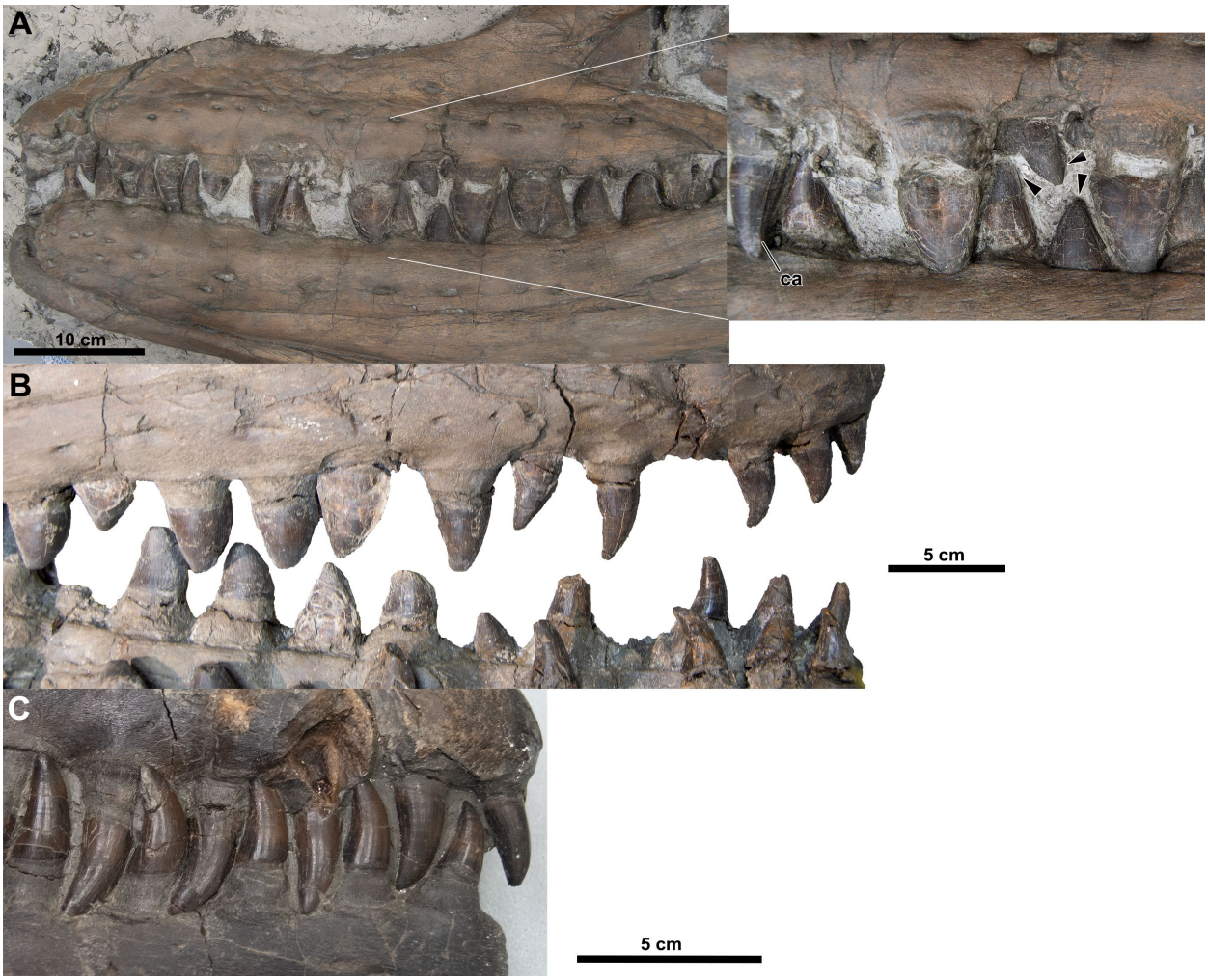

Figure 5.4. Marginal dentition of TMP 2018.042.0005 in (A) lateral view, with close-up of broader crowns from the midsection of the dentary; Anterior teeth of TMP 2002.400.0001 in (B) lateral view; Anterior teeth of TMP 2007.034.0001 in (C) lateral view. Abbreviations: ca, carina. Black arrows in (A) indicate well-preserved examples of anastomosing texture on tooth crowns.

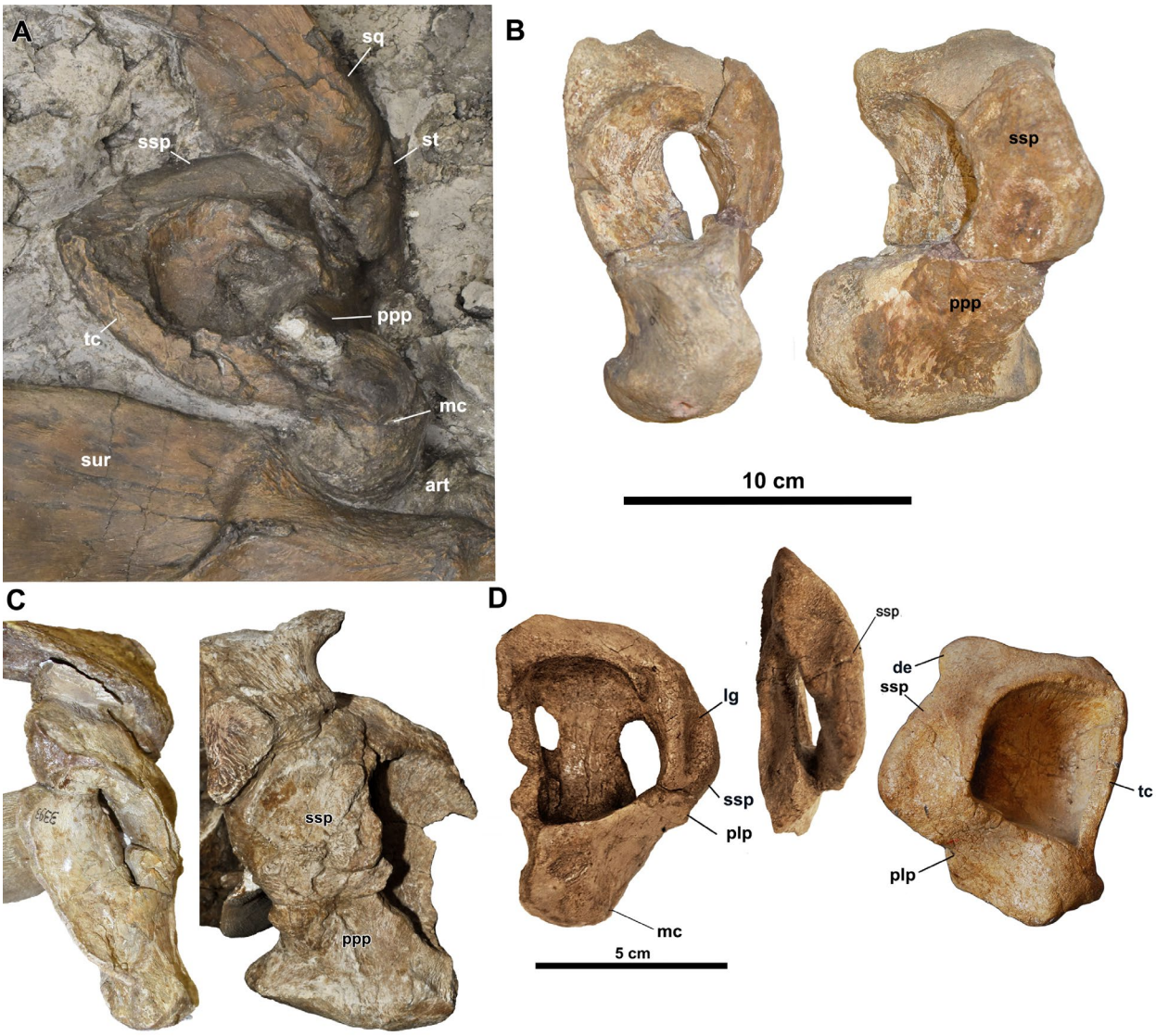

Figure 5.5. Left quadrate of TMP 2018.042.0005 in (A) lateral view; left quadrates of KU 590 in (B) lateral and posterior views; left quadrate and right quadrate of SDSMT 3393 in (C) lateral and posterior views, respectively; right quadrate of *P. sovayi* (IRSNB R33) and left quadrate in (D) dorsal and lateral views, respectively. (A), (B), and (C) are all scaled for the 10 cm bar. Abbreviations: art, articular; de, dorsal eminence; lg, lateral groove; mc, mandibular condyle; plp, posterolateral process; ppp, posterior pillar-like process; sq, squamosal; st, supratemporal; tc, tympanic crest. (isp) refers to the structure usually referred to as the infrastapedial process.

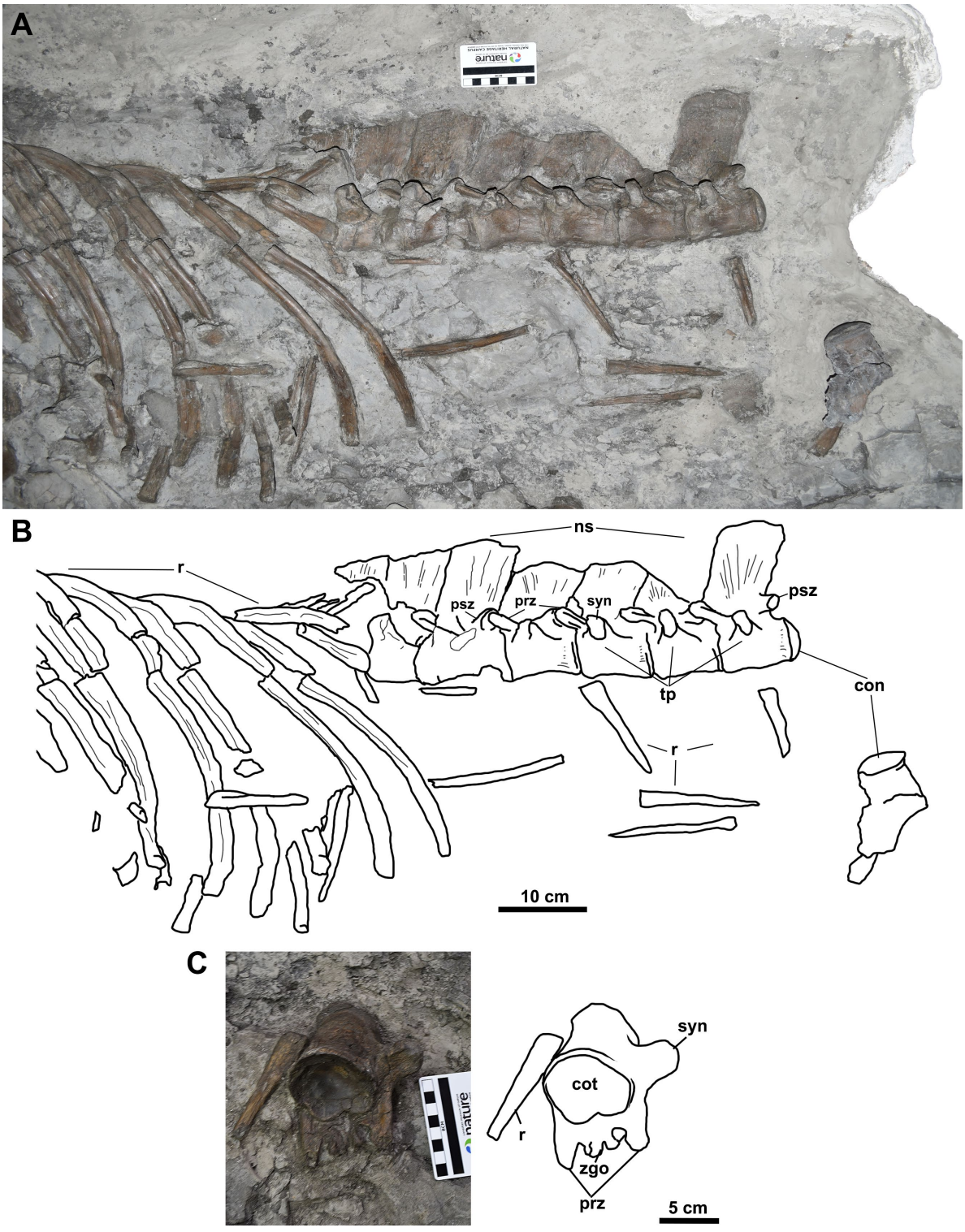

Figure 5.6. Midsection of TMP 2018.042.0005 (block 2), including ribcage and partial dorsal vertebral series in (A) lateral view; (B) simplified line drawing. Abbreviations: con, condyle; cot, cotyle; ns, neural spines; prz, prezygapophyses; psz, postzygapophyses; r, ribs; syn; synapophyseal process; tp, transverse process; zgo, zygosphene.

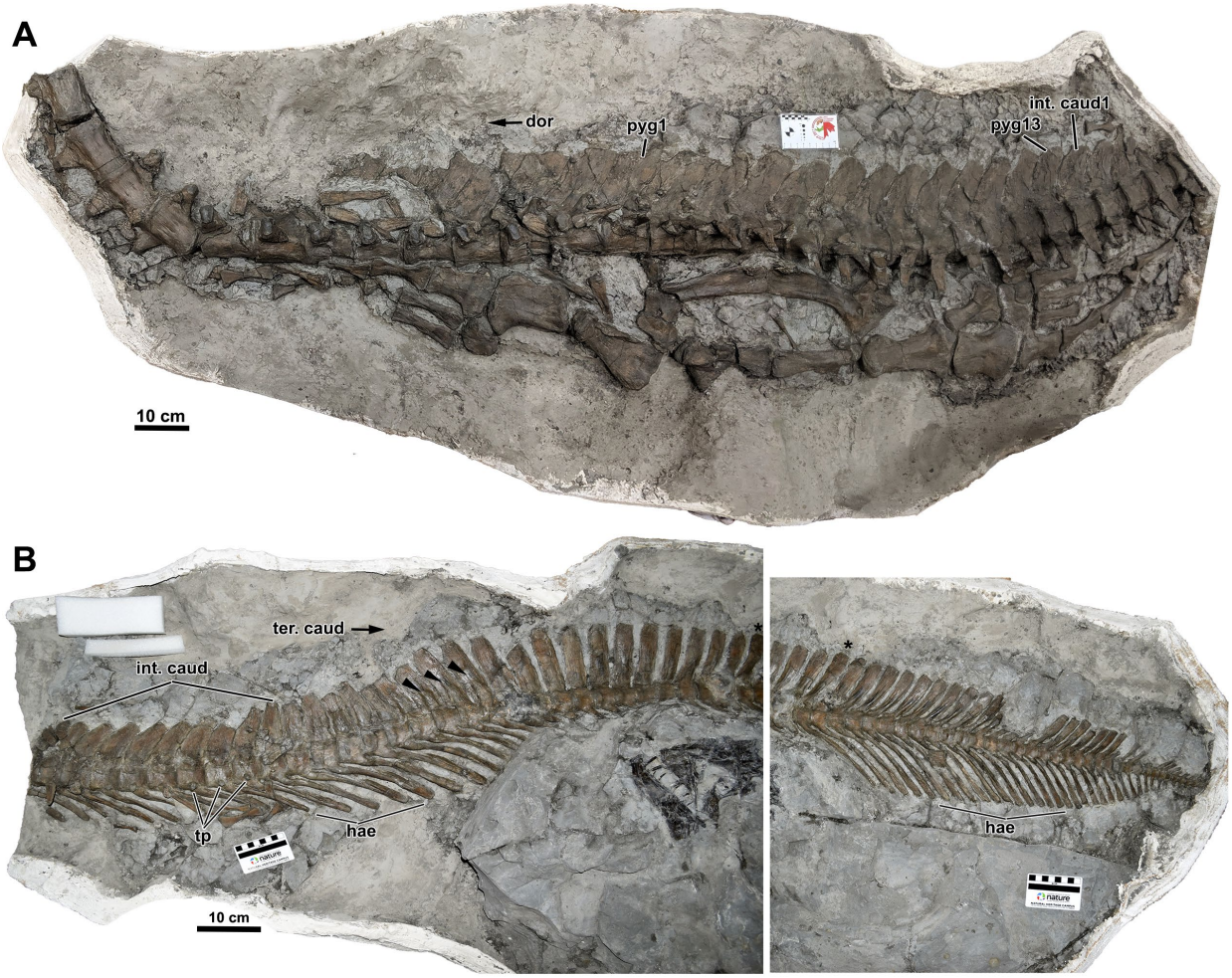

Figure 5.7. Pelvic region of TMP 2018.042.0005 including dorsal and pygal vertebrae in (A) lateral view; caudal fin in (B) lateral view. The block is split into two images. Abbreviations: dor; dorsal vertebrae, hae, haemal arches; int. caud, intermediate caudals; pyg, pygals; ter. caud, terminal caudals, tp; transverse processes. Black arrows in (B) indicate thickened centers of caudal neural spines. Black asterisks indicate the same caudal vertebrae on image one and two.

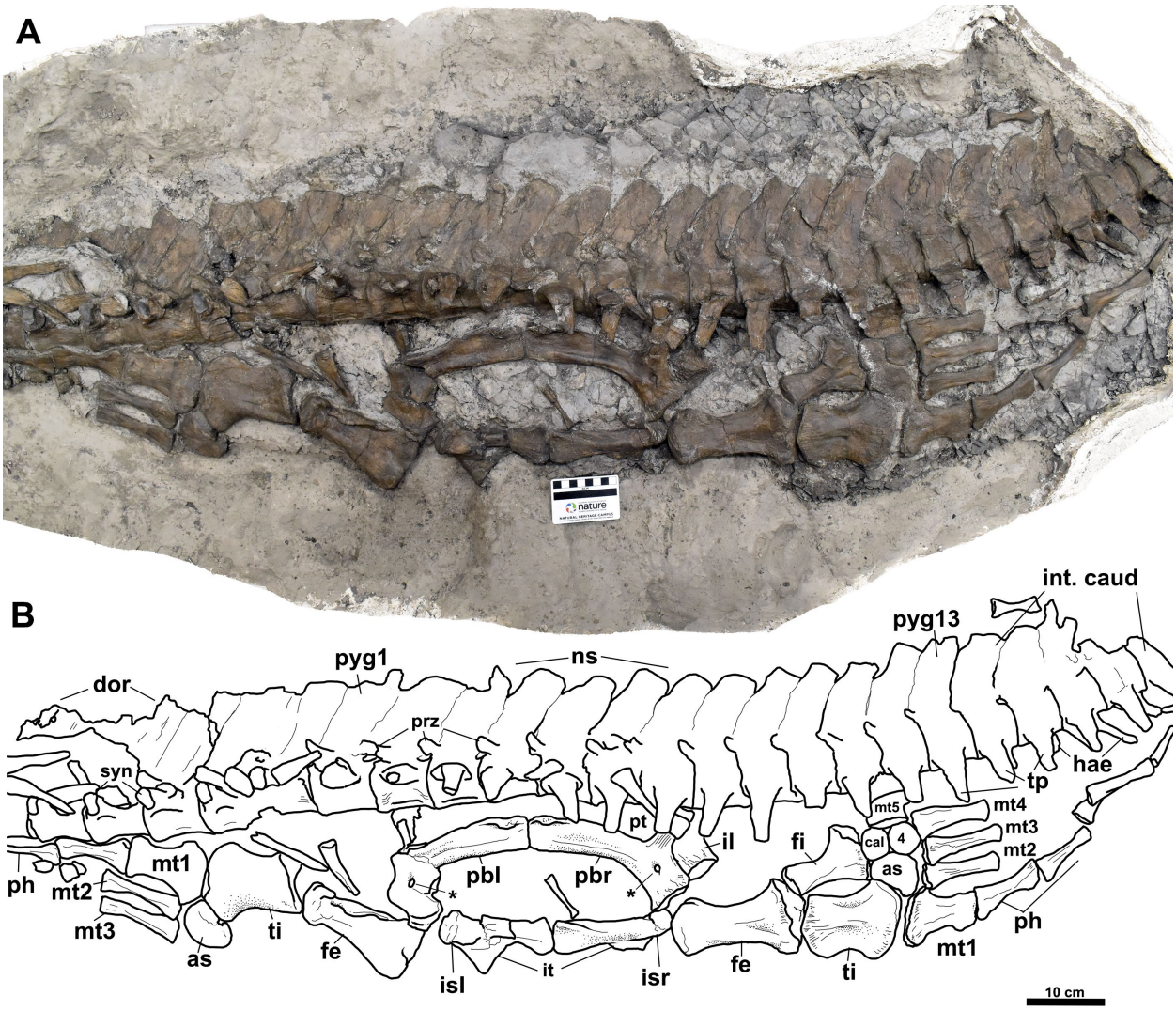

Figure 5.8. Closeup of Pelvic region of TMP 2018.042.0005. Abbreviations: as, astragalus; cal, calcaneum; dor, dorsal vertebrae; fe, femur; fi, fibula; il, ilium; int. caud; hae, haemal arches; intermediate caudals; isl, ischium (left); isr, ischium (right); mt, metarsal; ph, phalanges; pbl, pubis (left); pbr, pubis (right); ns, neural spine; prz, prezygapophyses; pt, pubic tubercle; pyg, pygal; ti, tibia; syn, synapophyseal processes; tp, transverse processes; 4, tarsal 4. Asterisks indicate the obturator foramen on the pubes.

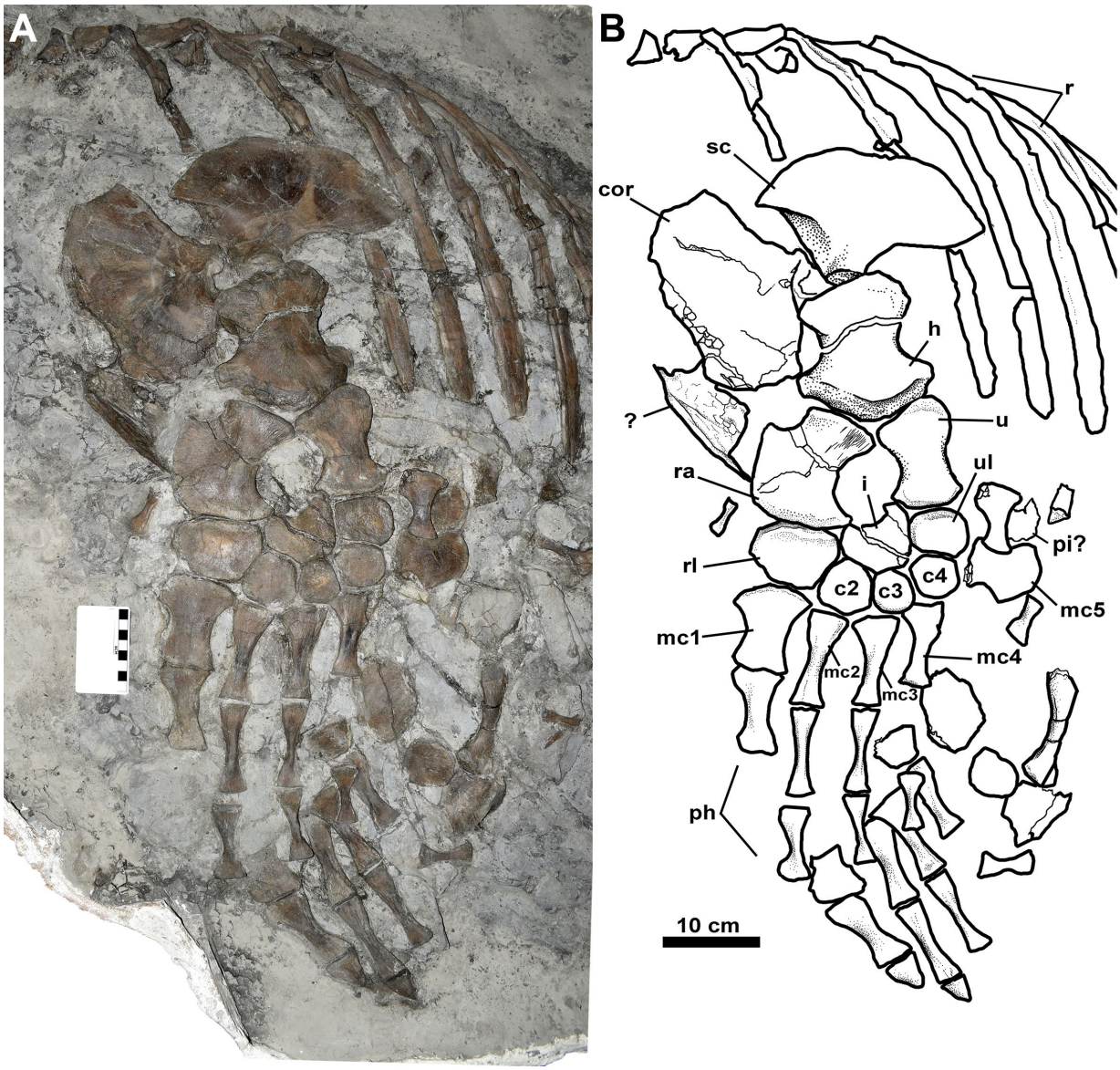

Figure 5.9. Pectoral girdle and left forelimb of TMP 2018.042.0005 in left lateral view. Abbreviations: c2-4, distal carpals 2-4; cor, coracoid; h, humerus; i, intermedium; mc1-5, metacarpals 1-5; ph, phalanges; pi?, possible pisiform; r, radius; rl, radiale; sc, scapula; u, ulna; ul, ulnare. '?' indicates fragment of possible interclavicle and/or right coracoid.

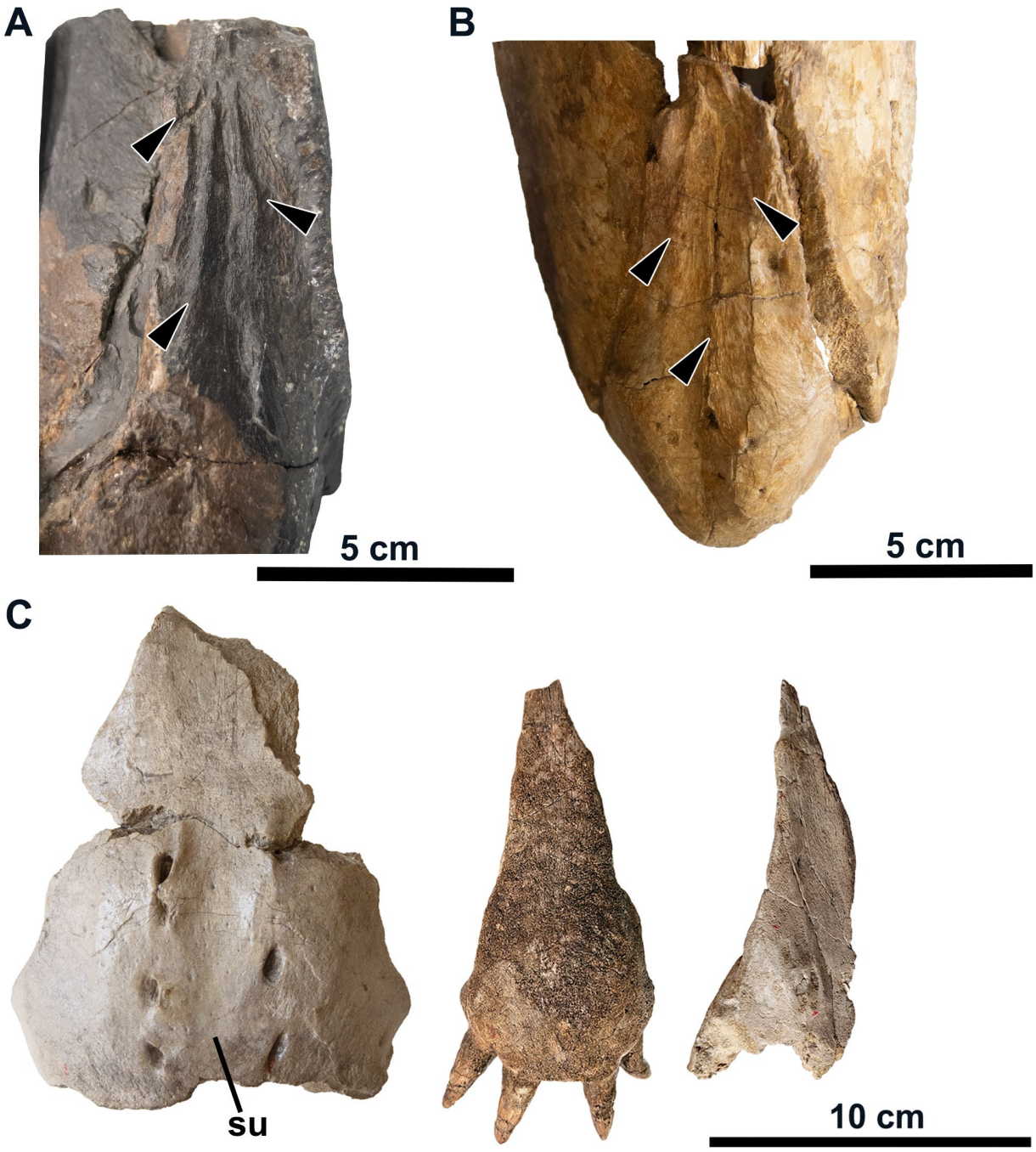

Figure 5.10. Dorsal views of premaxillae of (A) TMP 2002.400.0001, (B) SDSMT 3393 and (C) *P. solvayi* (IRSNB 0106, R33, and 0107). Abbreviations: su, sulcus. Black arrows in (A) and (B) indicate lateral and central ridges bordering the sulci.

Specimen #	Max. skull length (cm)	Max. dent. Length (cm)	Max. sur. Length (cm)
TMP 2018.042.0005	110	71	44
TMP 2007.034.0001	84	54	35.5
TMP 2002.400.0001	85-90(?)	53.5	34-39(?)
SDSMT 3393	83	52	33.5

Table 5.1. Measurements of the skull and PMU bones of TMP 2018.042.0005, TMP 2007.034.0001, TMP 2002.400.0001, and SDSM 3393.

CHAPTER 6. REDESCRIPTION AND REASSESSMENT OF *LIODON*

INTRODUCTION

The genus *Liodon* (=*Leiodon*) was established by Owen (1841), who named the type specimen "*Leiodon" anceps* (BMNH 41639) based on several teeth and an associated jaw element. Later better-preserved additions to the genus, including *L. compressidens* Gaudry (1892), *L. mosasauroides* Gaudry (1892), and *L. sectorius* Cope (1871), also consist only of jaw fragments and teeth. The respelling "*Liodon*" first appeared in Cope (1869-1870) in reference to Agassiz (1846) who noted the name was preoccupied; Lingham-Soliar (1993) recommended the restoration of *Leiodon* though today, as per Agassiz (1846) *Liodon* is the preferred term (e.g., Schulp et al. 2008).

The precise affinities of these taxa have been debated at great length. Several workers at the time found the validity of *Liodon* dubious, some suggesting the genus was likely synonymous with *Mosasaurus* (Lingham-Soliar, 1993). Dental and cranial features shared between *Liodon* and *Mosasaurus* were noted early on, and this view has persisted into recent times. Russell (1967) suggested that *Liodon* was included with the Mosasaurini based on similarities between the rostra of *Mosasaurus*, *L. compressidens*, and *L. mosasauroides*. Additionally, "*Liodon*" means "smooth tooth", although referred specimens of *Liodon anceps* and possible candidates of the now separated holotype reportedly show slight faceting on the enamel surfaces (Lingham-Soliar, 1993). *Liodon compressidens* was also described as having striated teeth, and as a result Lingham-Soliar (1993) proposed it should instead be referred to *Mosasaurus*. Additionally, Russell (1967) and Lingham-Soliar (1993) considered the suggestion by some researchers that the type species *L. anceps* should be referred to the Tylosaurine

mosasaur *Hainosaurus*, but neither author found sufficient evidence to support the notion. Despite separating *L. compressidens* and *L. mosasauroides* from *Hainosaurus*, Russell (1967) nevertheless only considered the original description of the American *L. sectorius* and did not comment further on the European examples, including the type species *L. anceps*. Largely owing to its highly fragmentary nature, little attention has been paid to *L. anceps* since its description, with the issue now compounded as Lingham-Soliar (1993) reported that the diagnostic teeth of the holotype had become separated from the jaw. Since the specimen could no longer be assessed with any certainty, Schulp et al. (2008) declared *Liodon* a *nomen dubium*. Following this, *L. compressidens, L. mosasauroides,* and *L. sectorius* were reassigned to *Prognathodon* based largely on comparisons of the aspect ratio of individual tooth crowns on the lower jaw of *Liodon sectorius* and *Prognathodon kianda*. Other members of *Prognathodon*, including the type species, were not included. However, Leblanc et al. (2012) and Palci et al. (2014) found greater similarity between *Liodon* and *Mosasaurus* than with *Prognathodon*, citing the elongate premaxillary-maxillary suture and absence of procumbent anterior teeth. Despite agreeing with multiple previous researchers, the authors were nevertheless cautious on drawing any systematic conclusions based on isolated and poorly preserved material. Hornung and Reich (2015) also cited the lack of procumbent teeth and advised caution in assigning *Liodon* to *Prognathodon*, although stated that the latter was usually typified by rounded and robust teeth.

Given the paucity and fragmentary nature of *Liodon* materials, and following the rediagnosis of *P. solvayi*, the question of the validity of *Liodon* and the referral of multiple members to the genus *Prognathodon* remains unanswered and requires extensive review. A combined evaluation of the recent literature, as well as a direct comparison and diagnosis of the

three referred species of *Liodon* with the cranium of the type species of *P. solvayi* may serve to clarify at least some aspects of the longstanding confusion surrounding these difficult taxa.

MATERIALS AND METHODS

MNHN-Z-C-1878-5 (*L. compressidens*), MNHN 1891-4 (*L. mosasauroides*), NHMM 004104 (referred specimen, *L. sectorius*), IRScNB R33 (4672), IRScNB 0106, IRScNB 0107, IRScNB 0108 (*Prognathodon solvayi*), UALVP (*Eremiasaurus heterodontus*) were photographed using a Nikon D500 camera with a Nikkor AF-S 50 mm lens. Photographs were processed and figures produced in Adobe Photoshop CS6 and Adobe Photoshop 24.6.0. Only the medial surface of NHMM 004104 (referred specimen, *L. sectorius*) was observable at the time, and references to the lateral surface were derived from Lingham-Soliar (1993). Assessments of *L. sectorius* (AMNH 1401) were performed with permission using photographs taken by other colleagues. Line drawings were traced from photographs and stippled using a Wacom Intuos pro pen tablet.

DESCRIPTION AND COMPARISON OF *LIODON SECTORIUS*

Russell (1967) reported that much of the holotype material (AMNH 1401) for *L. sectorius* is broken or lost, such that it currently isn't immediately clear whether the attribution of the referred specimens can be confidently verified at this stage. The proposed material from Europe also consists of partial fragments (Kuypers et al. 1998; Bardet et al. 2014), and diagnostic features are largely imperceptible on the skull and vertebral elements of the holotype. NHMM 004104 was recovered from the Upper Maastrichtian Maastricht Formation in The Netherlands and was central to the eventual reassignment of *Liodon* to *Prognathodon* (Schulp et al. 2008).

Dentary—NHMM 004104 consists of a single left dentary with a partial tooth row. In accordance with Lingham-Soliar and Nolf (1993) the dentary is elongate and narrow with largely straight dorsal and ventral margins, contrasting with the slightly deeper, less tapering, and bowed dentary of *P. solvayi* (Fig. 6.2A, B). Lingham-Soliar (1993) described a groove that extends from the fourth to the eleventh tooth positions along the dorsomedial surface of dentary, although this structure may be better described as a low shelf formed by the ventral margin of the slightly thickened bone along the tooth row (Fig. 6.2A). This feature is absent in *P. solvayi* but present in *P. kianda* (Schulp et al. 2008: fig. 8). Interdental pits are situated on the anterolateral surface between the anterior teeth, beginning at the posterior edge of the first tooth to roughly the seventh or eighth tooth position (Lingham-Soliar, 1993: fig. 7B). This is also absent in *P. solvayi*, and only IRScNB 0106 preserves interdental pits on the dorsal surface of the tooth row between more posteriorly positioned non-procumbent teeth (Fig. 2.6D). NHMM 004104 also lacks the continuous row of enlarged foramina that extends across the lateral surface of the dentary in multiple examples of *P. solvayi* (Fig. 2.7), although the.

NHMM 00414 preserves sixteen tooth positions as opposed to thirteen to fifteen in *P. solvayi* (Fig. 2B, Lingham-Soliar, 1993: fig. 7;). The overall shape of the marginal tooth crowns does not differ remarkably between NHMM 00414, AMNH 1401, *P. kianda,* and *P. solvayi* (Fig. 2A-C, F). Generally, teeth are narrower anteriorly and broaden posteriorly. The strongly hooked posterior-most teeth in *P. solvayi* are either not present or not preserved in NHMM 00414 and AMNH 1401. The anterior edges of the crowns are convex, and the posterior edges are straight to slightly concave in most members of *Liodon*, whereas the posterior crown edges in *P. solvayi* are more strongly concave. Teeth in *P. solvayi*, AMNH 1401, and NHMM 00414 are also slightly splayed with a lingual curvature to the apex, although this is more pronounced in the

former (Fig. 2D, Lingham-Soliar, 1993: fig: 7A, fig. 11). Comparing the degree of curvature in the apices of the anterior teeth between the two taxa is difficult as the curvature of the teeth in *P. solvayi* differ slightly between the right and left dentaries, likely due to preservation (Fig. 2B, Fig. 3B). Although the anterior three teeth are very weakly inclined in NHMM 00414, they do not extend beyond the dentary tip as they do in *P. solvayi* (Fig. 2A, B, Fig 3B). Cope (1871) noted that the anterior teeth in AMNH 1401 are circular in cross-section and become progressively more compressed posteriorly, although this is no longer apparent in the remaining material. However, Lingham-soliar (1993: fig. 8) also reported this in NHMM 00414 and observed that the first three crowns lack carinae altogether, while the fourth and fifth have only carinae on the distal edge near the apices. Further posteriorly the distal carinae extend the whole length of the crown edge. Hornung and Reich (2015) also noted that the teeth in NHMM 00414 are symmetrical in cross-section (see Lingham-Soliar, 1993: fig. 7A). In contrast, all teeth in *P. solvayi* are asymmetrical and labiolingually compressed in cross-section, as well as have both mesial and distal carinae (with the possible exception of the last one or two crowns). The remaining crowns in AMNH 1401 appear to only have posterior carinae (Fig. 2D-F). Lingham-Soliar (1993) does not mention serrations, but they are present in AMNH 1401 in some examples (Cope, 1971) (Fig. 2D). The trenchant or excavated appearance of the carinae in NHMM 00414 also occurs in *P. solvayi* (Lingham-Soliar, 1993), but not in the remaining teeth in AMNH 1401.

The broad, blunt, and squat examples in AMNH 1401 likely represent posterior teeth, although it is difficult to determine if they are directly comparable to those in NHMM 00414 (Fig. 2A, E). Some of the enamel surfaces in AMNH 1401 were described as “ribbed” but lacking facets (Cope, 1871), and three examples are heavily ornamented with fine and irregular ridges extend from the base to the apex of the crowns (Fig. 2E). These appear mostly consistent

with the structures termed striations by Street et al. (2021), although they occur on both labial and lingual faces of the crown. They do not resemble the broader troughs and regularly spaced ridges (i.e. fluting) on the marginal dentition of *P. solvayi*. Notably, NHMM 00414 lacks striations and flutes but weak faceting is present in some posterior teeth (Linham-Soliar, 1993: fig. 7B, C). Faint horizontal ribbing is present on an isolated tooth of AMNH 1401 on both the lingual and labial faces and on the lingual surface on a posterior crown of NHMM 00414 (we could not view the labial side) (Fig. 2A, C). Cope (1871) also described a maxillary and dentary tooth with a longitudinal groove extending centrally along the labial surface of the crowns. However, this is not immediately apparent in any of the remaining teeth in the holotype and does not seem to be present in NHMM 00414.

Discussion

There are few features shared between either the holotype or examined referred material of *L. sectorius* and *P. solvayi*. With the exception of similar crown shape in lateral view and the presence of trenchant carinae, important diagnostic features of *Prognathodon* including a bowed dentary and procumbent anterior teeth that extend beyond the dentary bone are absent in *L. sectorius*. The presence of carinae and the cross-sectional shape also differ between the two taxa. Bardet et al. (2012) differentiated OIGM - LU 799 from most members of *Prognathodon* primarily by tooth morphology but found the most resemblance with *P. kianda* and other former members of *Liodon*. The multitude of differences in both the dentary and dentition support the removal of *L. sectorius* from *Prognathodon*. There are also some small differences between AMNH 1401 and NHMM 00414, namely the presence of striations and lingual curvature in the former, although Palci et al. (2014) noted that intraspecific variation in the dentition is not

uncommon in modern squamate reptiles. Although there is little remaining evidence to support the referral of NHMM 00414 to *L. sectorius*, the overall poor preservation of the holotype precludes any concrete conclusions regarding the taxonomic status of the referred specimens at the present time.

The issue is further compounded by the mention of Hornung and Reich (2015) that there are strong similarities in the dentition of *L. sectorius* and *P. kianda*. The authors also questioned the validity of *P. kianda* based on its tendency to fall outside of the genus in multiple phylogenetic analyses. *L. sectorius* lacks a bowed dentary, but this element is slender in both taxa, as is the low shelf extending along the dorsomedial surface. Schulp et al. (2008) also noted multiple dental similarities between the two but distinguished them primarily by the greater labiolingual compression of the teeth in *P. kianda*.

DESCRIPTION AND COMPARISON OF *LIODON COMPRESSIDENS*

Derived from Campanian chalks in northern France, the holotype and only existing specimen of *L. compressidens* (MNHN-Z-C-1878-5) was initially described briefly by Gaudry (1892) alongside *L. mosasauroides*. Neither Russell (1967) or Lingham-Soliar (1993) provided a detailed description of *L. compressidens,* despite the latter assigning it to *Mosasaurus*. Schulp et al. (2008) provided a brief description and reassigned *Liodon* to *Prognathodon* based on similarities with *P. kianda*, although Hornung and Reich (2015) suggested *L. compressidens* belonged within the Mosasaurini and was instead more similar to *Clidastes*. Although preserving two dentaries, maxilla, and the premaxilla, the teeth and bone surfaces are both weathered and reconstructed in various areas relative to *L. sectorius* and *L. mosasauroides* and features are more difficult to observe (Fig. 6.3A).

Premaxilla—In articulation with the right maxilla, the premaxilla in MNHN-Z-C-1878-5 features a short predental rostrum in lateral view with a dorsal margin that slopes ventrally above the first tooth position (Fig. 6.3A). Dorsally, the rostrum is conical in shape with a relatively pointed tip that is roughly half a tooth position in length (Fig. 6.3B). A distinct, prominent notch or constriction on the lateral margins forms the anterior extent of the premaxillary-maxillary suture, posterior to which the premaxilla tapers abruptly towards the internarial bar. The premaxillary-maxillary suture is long and extends roughly five tooth positions. This contrasts strongly with the short, broad, and blunt premaxilla of *P. solvayi* that lacks the predental rostrum, has more gradually tapering anterolateral margins, and a short suture extending only three tooth positions (Fig. 6.3A-C). A dorsal median sulcus is present on some specimens of *P. solvayi* (IRScNB 0106, 0108; Fig. 2.1) is absent in MNHN-Z-C-1878-5.

Only the second premaxillary teeth and tips of the replacement teeth are preserved, and both are oriented vertically rather than inclined. The crowns are narrow and curve posteriorly but are proportionately smaller than those of *P. solvayi* and lacking the distinct flutes. Whereas the anterior teeth in *P. solvayi* are bicarinate, Schulp et al. (2008) described only distal carinae in the premaxillary teeth of MNHN-Z-C-1878-5, and only a faint cutting edge on the anterior margin is observable.

Maxilla—The maxilla in MNHN-Z-C-1878-5 is slender and elongate in lateral view with medially oriented anterodorsal and posterodorsal processes, differing strongly from the short maxillae in *P. solvayi* with tall, dorsally oriented processes (Fig. 6.3A, B). The slightly concave ventral margin of the maxilla in *P. solvayi* is reduced or absent in MNHN-Z-C-1878-5, as is the

distinct, arched row of large foramina extending across the lateral surface and above the tooth row. MNHN-Z-C-1878-5 preserves a possible fragment of the prefrontal that has been reattached along the posterior margin of the maxilla, but is too damaged to observe any diagnostic features, including to what extent it may have contributed to the external nares.

Roughly thirteen maxillary tooth positions are preserved in MNHN-Z-C-1878-5 (although there was likely at least one more), contrasting with twelve in *P. solvayi*. The first seven teeth are broken or missing and only the remaining five preserve discernable features. Compared to the curved, narrow premaxillary teeth, the posterior crowns are broader with curved anterior and straighter posterior edges. The anterior-most teeth (including the premaxillary tooth crowns) are circular in cross-section, whereas the teeth are labiolingually compressed from approximately the sixth tooth position onwards (Gaudry, 1892: Pl. 1). Schulp et al. (2008) also noted in general the teeth in MNHN-Z-C-1878-5 are fairly small and reported only distal carinae on the fourth and fifth teeth, partial carinae restricted to the apical section on the fifth and sixth teeth, and bicarinate crowns from the seventh position onwards. Although missing most anterior maxillary teeth, these observations were likely combined from the maxillary and dentary teeth, and the pattern holds true for the posterior crowns in the maxilla. In *P. solvayi*, the marginal teeth are larger and longer in comparison, labiolingually compressed throughout the tooth row, and both anterior and posterior crowns are bicarinate (Fig. 6.3C). Both taxa lack serrations on their mature teeth, which coincides with Gaudry's (1892) initial observations.

Dentary—Both the left and right dentaries are present in MNHN-Z-C-1878-5. Partial splenials are attached, but diagnostic features are largely not preserved (Fig. 6.3A, D). Like *P. solvayi* the dentaries of MNHN-Z-C-1878-5 are bowed and a row of large foramina extends across the

lateral surface. The anterior tip of the dentary protrudes beyond the first tooth position. Although the bone surface is weathered, interdental pits on the anterolateral surface are absent, likely because the apices of the relatively smaller teeth would not impact the bone on the tooth row. A faint predental pit is likely present (Lingham-Soliar, 1993: fig. 7B). *Liodon sectorius* and MNHN-Z-C-1878-5 share a thickened section of bone along the tooth row forming a low shelf, but in the latter this is positioned nearer to and nearly merging with the fossa for the splenial.

MNHN-Z-C-1878-5 preserves fifteen dentary tooth positions. The tooth row in the right dentary in particular is more complete than in the maxilla, better illustrating the transition between the narrower conical anterior and broader compressed posterior crowns (Fig. 3A, D; Schulp et al. 2008). The first four crowns are broken at or near their bases, but similar to the maxilla they are circular in cross-section. As the premaxillary teeth are not procumbent, the anterior dentary teeth were not likely strongly inclined and may have resembled the condition in *L. sectorius* and *P. kianda* (Fig. 6.2). Also, like *L. sectorius*, the crowns midway and posterior in the jaw of MNHN-Z-C-1878-5 have convex anterior edges and nearly straight posterior edges. Unlike *P. solvayi*, the teeth in MNHN-Z-C-1878-5 are oriented vertically as opposed to splayed (Fig. 6.3E), although the apices in both taxa curve posterolingually. The posterior curvature of the apices is slightly more pronounced than in *L. sectorius* (Fig. 6.2A). The posterior-most teeth in MNHN-Z-C-1878-5 are small and short with more strongly concave posterior margins, although they are less strongly hooked in appearance compared to *P. solvayi* (Fig. 6.3C, D). Hornung and Riech (2015) described the crowns as asymmetrical in apical view with a larger lingual surface, although there are few a notable difference between the labial and lingual faces (Lingham-Soliar, 1993: fig. 3; Fig. 6.3E).

While MNHN-Z-C-1878-5 lacks the prominent fluting in *P. solvayi*, Lingham-Soliar (1993) reported striations on its enamel surface, whereas Hornung and Reich (2015) described weak facets. The striations are interpreted here as variations in enamel preservation as opposed to intrinsic ornamentation, and instead agree that very faint faceting is present on some crowns. The distribution of the faceting across the tooth row is not clear, as several teeth are damaged and others appear largely smooth. As per Schulp et al. (2008), the dentary crowns are bicarinate midway in the jaw and posteriorly and have only partial apical carinae on the fifth and sixth crowns. The bicarinate posterior crowns are trenchant in both MNHN-Z-C-1878-5 and *L. sectorius*, a feature that is present in most teeth in *P. solvayi*. As in the maxilla, serrations are not visible (Gaudry, 1892). However, they seem to also be absent in replacement teeth in MNHN-Z-C-1878-5, although only a few small portions of the crown are visible.

Discussion

This assessment agrees with previous authors that there are few cranial or dental similarities shared between *L. compressidens* and *Prognathodon* (Palci et al. 2014; Hornung and Reich, 2015). Although the dentary is bowed and the teeth are weakly heterodont with some having trenchant carinae, *L. compressidens* lacks the large, fluted dentition, procumbent teeth extending anteriorly to the premaxilla and dentary, bicarinate and labiolingually compressed anterior teeth, short premaxillary-maxillary suture, and a short, tall maxilla with dorsally oriented processes. The dentition is arguably more comparable with *L. sectorius*, which also has smaller teeth, similar tooth counts, weak faceting on some crowns, broad posterior crowns with convex anterior and straight posterior edges, and circular anterior teeth that become compressed

posteriorly. However, serrations are absent in *L. compressidens*, as is the straight dentary and the clearly defined shelf on its dorsomedial surface.

Although Lingham-Soliar (1993) designated MNHN-Z-C-1878-5 as *Mosasaurus comrepessidens*, this was not carried forward into the more recent literature (Schulp et al. 2008; Palci et al. 2014). On initial appearance, the smaller tooth size and slender maxilla are reminiscent of *Clidastes*, as was suggested by Hornung and Riech (2015). The presence of weak faceting and lack of serrations has also been described in *Clidastes* (Lindgren and Siverson, 2004), as well as constricted lateral margins of the premaxilla (Caldwell and Diedrich, 2005: fig. 3C). However, the maxilla and dentary of *Clidastes* tend to be markedly slenderer than those of *L. compressidens* (Lively, 2019), and distal margins of the marginal teeth are more concave (Lindgren and Siverson, 2004). *Clidastes* is also typically smaller in size than MNHN-Z-C-1878-5, and Hornung and Reich (2015) could only conclude that *L. compressidens* likely belongs within the Mosasaurini as a result.

The multiple characters shared with other genera, while having little in common with *P. solvayi,* suggests that *L. compressidens* does not belong within *Prognathodon*. This agrees with other authors that concluded *L. compressidens* is likely a mosasaurine mosasaur (Lingham-Soliar, 1993; Palci et al. 2014, Hornung and Reich, 2015), and are also hesitant to refer MNHN-Z-C-1878-5 to a specific taxon in the absence of additional and better-preserved material.

DESCRIPTION AND COMPARISON OF *LIODON MOSASAUROIDES*

Liodon mosasauroides (MNHN 1891-4) is a Late Cretaceous (possibly Maastrichtian) taxon from southwestern France and consists of a relatively well-preserved anterior portion of the skull, including partial maxillae, dentaries, premaxilla, and associated marginal dentition

(Fig. 6.4). The left side is generally poorly preserved except for the teeth. There are currently no other referred specimens since Hornung and Reich (2015) recommended referring the German specimen GZG.V.10024 to *Hainosaurus*.

Following the original description of MNHN 1891-4 by Gaudry (1892), little mention was made of the taxon beyond its proposed synonymization with *Hainosaurus* (Deperet and Russo, 1925), which was subsequently rejected by Russell (1967). No further comments were made beyond the tooth form of *L. mosasauroides* relative to *L. compressidens* and *L. sectorius*. Lingham-Soliar's (1993) redescription provided a stronger basis for comparison and found numerous similarities in the morphology of the snout and tooth count with *Mosasaurus hoffmannii*. However, *L. mosasauroides* was subsequently placed within *Prognathodon* despite its exclusion from the dental aspect ratio analysis and not receiving further detailed examination (Schulp et al. 2008). Following this conclusion multiple other authors have since documented similarities between *L. mosasauroides* and *Mosasaurus* and questioned its inclusion in *Prognathodon* (LeBlanc et al. 2012; Palci et al. 2014; Hornung and Reich, 2015).

Premaxilla—The premaxilla of MNHN 1891-14 is articulated with the maxilla and in occlusion with the dentary (Fig. 6.4A). Contrasting sharply with the absence of a predental extension in *P. solvayi*, the rostrum of MNHN 1891-14 extends slightly less than one tooth length from the first tooth position (Fig. 6.4A-D). The predental rostrum is short and tapered in lateral view, slightly larger than in *L. compressidens*. A single large interdental pit is exposed on the lateral surface between the first and second tooth positions, formed by the contact of the apex of the corresponding dentary tooth (Figs. 6.4B, 6.5E). Interdental pits are absent in most specimens of *P. solvayi* except in IRScnB 0106 where a small number are present along the dorsal margin of

the tooth row (Fig. 2.6D). A deep, elongate healed injury is present on the rostrum tip of MNHN 1891-14, slightly distorting the bone surface. In dorsal view, the rostrum is conical in shape, tapering anteriorly to a rounded point. The lateral margins of the premaxillary/maxillary suture are relatively straight and narrow gradually towards the internarial bar. These features differ strongly from the broad, blunt-tipped rostrum in *P. solvayi*, which indents and tapers towards the internarial bar more abruptly relative to MNHN 1891-14. This forms a shorter premaxillary-maxillary suture that extends to only the third tooth position as opposed to the fifth (Fig. 6.4). Two raised ridges split by a shallow groove run parallel along the posterodorsal surface of the premaxilla and anterior portion of the internarial bar, converging slightly anterior to where the bar constricts midway within the narial opening (Fig. 6.5B). The internarial bar is triangular in cross-section, and a median dorsal keel is present on the wide, flattened posterior half of the bar. *P. solvayi* lacks the posterodorsal ridges, instead only sometimes showing a broad sulcus positioned anteriorly near the rostrum (Fig. 2.1). A median dorsal keel is either not present or not preserved.

Most notably, the four premaxillary teeth in MNHN 1891-14 are not procumbent and instead oriented near vertically (Fig. 6.5D, E). Enamel ornamentation is also absent, although both crowns in MNHN 1891-14 and *P. solvayi* are long, narrow, and bicarinate.

Maxilla—Most of the left maxilla is damaged or missing, but the right element is largely well-preserved. The maxillae in MNHN 1891-14 are long and relatively deep. In addition to the elongate premaxillary-maxillary suture, the anterodorsal process is oriented medially and forms a straight dorsal margin of the maxilla in lateral view. Although not well-preserved, the trajectory of the posterior margin of the maxilla relative to the anterodorsal process suggests the

posterodorsal process was likewise oriented medially (Fig. 6.4A, B). In *P. solvayi*, both processes are oriented dorsally and visible in lateral view (Fig. 6.4C). In MNHN 1891-14, a shallow depression directly adjacent to the anterodorsal process extends from the anterior tip of the narial opening to midway along the premaxillary-maxillary suture. The same region in *P. solvayi* is somewhat concave but lacks a depression at the anterodorsal process. Posteriorly, the expanded region of the narial opening is slightly shorter in *P. solvayi* and extends roughly two and a half tooth positions rather than three. Both taxa have a row of nutritive foramina situated above the tooth row, slightly arching dorsally in the center of the maxilla. Unique to MNHN 1891-14, a dense network of irregular grooves is situated on the anterolateral surface of the maxilla (Figs. 6.4A, B, 6.5A; Hornung and Riech, 2015). Some of these grooves terminate in a foramen within the network itself or on the ventral row. Leblanc et al. (2012) also described interdental pits on the lateral surface of the maxilla between individual tooth crowns that accommodate the apices of the corresponding dentary crowns in both *Mosasaurus hoffmanni* and *L. mosasauroides* (Fig. 6.4; Fig. 6.5E). In the latter, these pits are most pronounced anteriorly and visible until the tenth tooth position. This feature is absent in *P. solvayi*.

MNHN 1891-14 preserves four isolated teeth in the matrix in the right narial opening. Leblanc et al. (2012) noted that Gaudry (1892) had (likely) described these teeth as pterygoid teeth that were smaller than the marginal dentition, a condition also more similar to *Mosasaurus* than to *Prognathodon*. Gaudry (1892) related that the teeth were strongly hooked with small crenulations on the enamel surface. The enamel surfaces are largely hidden or damaged, but one tooth appears to be embedded in the maxillary bone, suggesting at least one of the teeth is from a different individual that had at some time bitten the snout of MNHN 1891-14 (Fig. 6.4D). Other

large pathologies are also preserved on the lateral surface midway above the tooth row on the maxilla and on the tip of the premaxilla (Figs. 6.4A, B, 6.5A).

Thirteen to fourteen teeth are preserved in the right maxilla, although the posterior end is poorly preserved, and more were likely present (Fig. 6.4). The left maxilla is damaged and only ten teeth are preserved. Only twelve teeth are present in the maxillae of *P. solvayi*. The tooth crowns are noticeably heterodont with narrower anterior crowns broadening posteriorly. The narrower anterior crowns tightly interdigitate with the dentary teeth until roughly the seventh tooth position, where the broader crowns prevent a strongly interlocking configuration. Unlike *L. compressidens* and *L. sectorius*, the posterior margins of the tooth crowns in MNHN 1891-14 are more concave as opposed to straight, and the teeth in general are proportionately larger in size. Multiple workers have observed the crowns are strongly labiolingually compressed (Gaudry, 1892; Russell, 1967; Lingham-Soliar, 1993; Hornung and Reich, 2015). These observations appear to hold true save for the more circular anterior three teeth, a condition also present in *L. sectorius*. Although not figured by Lingham-Soliar (1993: fig.10), Hornung and Reich (2015) identified asymmetrical crowns in cross-section with flatter labial and convex lingual faces, as well as D-shaped rostral teeth. The splayed orientation in the teeth of *P. solvayi* is also difficult to observe in MNHN 1891-14, although all the crowns appear to be oriented vertically. The crown apices in both taxa orient posteriorly and slightly lingually, although this is more exaggerated in *P. solvayi*. All preserved crowns are bicarinate with minute serrations visible most clearly on the tooth crowns midway and posteriorly on the jaw, but the crowns are not trenchant as they are in other *Liodon* taxa and *P. solvayi* (Palci et al. 2014). Contrasting strongly with *P. solvayi*, the enamel surfaces are entirely smooth and lack fluting and anastomosing texture.

Dentary—The dentaries of MNHN 1891-14 are in occlusion with the maxilla and premaxilla and are well-preserved anteriorly (Fig. 6.4A, B). Posteriorly, the bone surface is either missing or damaged, particularly midway on the right dentary. Like the maxilla, the dentary is relatively long and slender. Unlike the bowed dentary of *P. solvayi*, both dentaries are straight in lateral view (Fig. 6.4C). The anterior tip is roughly equal in length to the premaxillary rostrum, extending beyond the tooth row by slightly less than one tooth length. A predental pit on the dentary tip and interdental pits are visible posteriorly to at least the tenth tooth position on the left dentary (Fig. 6.5E), both of which have been also observed in *Mosasaurus hoffmanni* (Leblanc et al. 2012). A row large of foramina is present on the ventrolateral surface in MNHN 1891-14 and *P. solvayi*.

The right dentary preserves fifteen tooth positions, and ten teeth in the left, although Lingham-Soliar (1993) reported sixteen. Like the maxillary teeth, the dentary teeth are heterodont with anterior crowns that are rounded in cross-section and broaden and compress posteriorly. The anterior dentary crowns are not procumbent, interfinger strongly with the premaxillary and maxillary crowns, and have concave posterior margins. All crowns are bicarinate (but not strongly trenchant) with small serrations.

DISCUSSION

Like *L. sectorius* and *L. compressidens*, this study agrees with previous authors that there are few characters shared between *L. mosasauroides* and *P. solvayi* that warrant its inclusion in the genus *Prognathodon* (Leblanc et al. 2012; Palci et al. 2014; Hornung and Reich, 2015). Most notably, the strongly procumbent anterior teeth extending beyond the bony rostrum are absent, as well as the trenchant carinae and fluted marginal tooth crowns. In addition to the elongate

premaxillary and maxillary suture (Palci et al. 2014), the laterally positioned interdental pits, textured anterolateral surface of the maxilla, medial orientation of the dorsal processes in *L. mosasauroides*, and straight dentary also separates it from *Prognathodon*. Despite the scant material, there also appears to be little evidence to link MNHN 1891-14 to *Liodon*: the larger, smooth tooth crowns, non-trenchant carinae, and different shape of the teeth in effectively separate it from *L. anceps*, *L. sectorius* and *L. compressidens.* Additionally, the premaxillary rostrum is more elongate than in *L. compressidens* and lacks a constriction on its lateral margins (Figs. 6.3C, 6.5A). Multiple comparisons of the dental and cranial morphology of *L. mosasauroides* have instead been drawn with *Mosasaurus*: both taxa share numerous features, namely an elongate premaxillary-maxillary suture (Palci et al. 2014), non-procumbent anterior teeth with premaxillary and dentary rostra extending beyond the first tooth position (Leblanc et al. 2012; Palci et al. 2014), asymmetrical crowns in cross-section and a network of grooves and foramina on the anterolateral surface of the maxilla (Hornung and Reich, 2015). Lingham-Soliar (2003) also noted that the tooth count and shape and size of the cranial elements were overall reminiscent of *M. hoffmanni*.

Comments on aspect ratios of mosasaur dentition

Schulp et al. (2008: fig. 10) compared the aspect ratio (crown height/crown basal width) of dentary teeth of *Prognathodon kianda*, *L. sectorius* and *L. compressidens*, plotting the ratios of individual teeth against tooth position to illustrate the distribution of varying crown height and width (i.e. degree of heterodonty) between the respective taxa. The resulting curves were used as further support for keeping the two *Liodon* separate from *P. kianda*. However, the measurements of crown height and crown basal width (CBW) accounts for tooth shape in lateral view only,

omitting potentially important variables on the respective width in basal or apical view of each crown. Use of this measurement would have been consistent with the inclusion of varying labiolingual compression along the tooth row as diagnostic features for all members of *Liodon* (Russell, 1967; Lingham-Soliar, 1993; Schulp et al., 2008). The exclusion of *L. mosasauroides* from the analysis also casts doubt on its reassignment to *Prognathodon*. Finally, the variation in tooth shape in different dentaries of the same individual (see plot of *P. kianda*, Schulp et al. 2008: fig. 10), as well as the possibility of interspecific variation in tooth morphology due to various factors such as differences in diet (Palci et al. 2014), potentially limit accurate interpretation of the variability present in any given taxon. For these reasons, caution is recommended in deriving information and making taxonomic inferences using aspect ratio analyses of mosasaur dentition.

Comments on *Liodon anceps*

Lingham-Soliar (1993) reported that individual elements from the holotype BMNH 42939 had gone missing and/or been separated, although the author was confident they had identified at least some of the teeth. Basing the description largely on referred specimens (BMNH 48937, 1227-8, 48939-40), the teeth were characterized by a smooth enamel surface, broadly elliptical in cross-section and less labiolingually compressed crowns relative to other members of *Liodon*, and weak faceting on some of the referred crowns (contra Palci et al. 2014) (Fig. 6.1)). The anterior and posterior margins were also described as strongly trenchant, indicating enlarged, sharp carinae with hollowed edges that resemble the condition in *L. sectorius* (Lingham-Soliar (1993: fig. 5, 6). Lingham-Soliar (1993) providing an albeit short diagnosis; however, even if the separate pieces of the holotype were at some point recombined, the sparse original material

arguably does not provide sufficient diagnostic information, supporting the designation of *L. anceps* as a *nomen dubium* (Fig. 6.1; Owen, 1841; Schulp et al. 2008). Barring the discovery of better-preserved specimens, this conclusion echoes those made by Palci et al. (2014) in this instance and cautions against drawing taxonomic conclusions based only on teeth.

Comparison of *Liodon mosasauroides* and *Eremiasaurus heterodontus*

Whereas previous workers demonstrated a close resemblance between *L. mosasauroides* and *Mosasaurus* (LeBlanc et al. 2012; Palci et al. 2014; Hornung and Reich, 2015), there are several similarities with the mosasaurine mosasaur *Eremiasaurus heterodontus* (Leblanc et al. 2012). The conical rostrum that extends a short distance beyond the first tooth position and the elongate premaxillary-maxillary suture in *L. mosasauroides* is likewise observable in *Eremiasaurus heterodontus* (Fig. 5, Fig. 6). In dorsal aspect, the rostrum in both *P. mosasauroides* and *E. heterodontus* narrows to a point at the tip and narrows gradually posteriorly to the internarial bar (Fig. 5A, C). These features are also present in *Mosasaurus hoffmanni* (Leblanc et al. 2012). The premaxillary-maxillary suture is slightly shorter in *E. heterodontus*, extending only to the fourth tooth position rather than the fifth (Fig. 6A, B). A dorsal median ridge of the internarial bar is present in both taxa but only partially preserved in *E. heterodontus* (Fig. 5B, C). Notably, a shallow groove bordered by two parallel posterodorsal ridges is also visible in *E. heterodontus*, although this is less pronounced than in *L. mosasauroides* (Fig. 5A, C). In contrast, *Mosasaurus* lacks this feature (Lingham-Soliar, 1995: fig. 6A, fig. 7; Street and Caldwell, 2017). The shape of the premaxilla of *L. mosasauroides* and *E. heterodontus* also more closely resemble each other than either resembles *Mosasaurus* (Fig. 6A, C), which has a more prominent constriction posterior to the second tooth positions and

gently convex lateral margins anterior to the internarial bar (Street and Caldwell, 2017: fig. 2B; Lingham-Soliar, 1995: Fig. 6A, fig. 7).

The maxilla and dentary are slenderer in *E. heterodontus*, but there are numerous other features in common with *L. mosasauroides* (Fig. 6). The dentaries are straight with little variation in depth across their length. Like the premaxillary rostrum, the anterior-most tip of the dentaries extends nearly one tooth length beyond the tooth row. The anterodorsal process of the maxilla is oriented medially in both *L. mosasauroides* and *E. heterodontus*; the posterodorsal processes are poorly preserved in both taxa but were also likely oriented medially (Fig.6A, B, compare with 6C). The network of grooves and foramina on the anterolateral surface of the maxilla is present in *L. mosasauroides*, *E. heterodontus*, and *Mosasaurus* (Hornung and Reich, 2015; Fig. 7C). All three taxa also share interdental pits along the tooth row on the lateral surfaces of both the maxilla and dentary (Fig. 6, extending from the premaxilla to roughly the seventh maxillary tooth position where the crowns are shorter and do not contact the bone along the tooth row. A predental pit is also present anterior to the first tooth position of the dentary in both *L. mosasauroides* and *E. heterodontus* (Fig. 5E).

Tooth morphology is also similar in *L. mosasauroides* and *E. heterodontus.* Both taxa have heterodont dentition with slender, conical crowns positioned anteriorly and broad, labiolingually compressed crowns occurring midway and posteriorly along the jaw (Fig. 6). All crowns have a sharp, pointed apex that points posteriorly and convex anterior and concave posterior margins, although this is less pronounced in the straighter anterior crowns in *E. heterodontus*. The long, narrow teeth in the premaxilla and anterior teeth in the maxilla interdigitate tightly with the anterior dentary teeth (Fig. 5E, Fig. 6). Although the premaxillary teeth are damaged or missing in *E. heterodontus*, the predental pit and anterior interdental pits on

the dentary indicate they would have been oriented vertically, as they are in *L. mosasauroides*. The first three dentary and first two maxillary teeth in *E. heterodontus* possess a carina on the anterior margin only. In contrast, the anterior dentition is bicarinate in *L. mosasauroides*. Teeth midway in the jaw and posteriorly are bicarinate in both taxa, and no teeth have trenchant carinae. The fourth to ninth maxillary teeth in *E. heterodontus* are also comparatively shorter and overlap the dentary teeth in lateral view (Fig. 6; Leblanc et al. 2012). The same teeth in *L. mosasauroides* are best observed on the left side but instead insert between the dentary crowns without any significant overlap (Fig. 4A). Although the enamel surfaces are generally smooth in *L. mosasauroides* and *E. heterodontus*, weak facets are present on the fourth to ninth teeth in the latter. The posterior-most teeth are missing or broken in *L. mosasauroides* and cannot be analyzed alongside those of *E. heterodontus*.

Relative to the other members of *Liodon*, *L. mosasauroides* represents one of the better-preserved examples with a greater number of discernable and more easily comparable diagnostic features in both the cranium and dentition. Whereas *L. mosasauroides* has little in common with *Prognathodon* and other members of *Liodon*, there is sufficient evidence to warrant referring *L. mosasauroides* to *Eremiasaurus*. Numerous similarities with *Mosasaurus* are clearly present (Lingham-Soliar, 1993; Leblanc et al. 2012; Palci et al. 2014; Hornung and Reich, 2015), but this is consistent with phylogenetic analysis typically recovering a close relationship between the two genera (Leblanc et al. 2012; Simoes et al. 2017; Lively, 2020). A stronger association between *L. mosasauroides* and *Eremiasaurus* is indicated by a similarly shaped premaxilla with paired dorsal ridges, pronounced heterodonty of the tooth row, strongly interdigitating anterior teeth, and smooth enamel surfaces on most tooth crowns. Differences based primarily on the dentition

nevertheless suggest the two taxa are not synonymous, and the reassignment of *Liodon mosasauroides* to *Eremiasaurus mosasauroides* is proposed.

CONCLUDING STATEMENTS

Based on our previous redescription of *P. solvayi*, this revaluation confirms neither of the members of *Liodon* share a sufficient number of diagnostic traits with *Prognathodon*, and we therefore recommend its removal from the genus. Both the level of preservation and the present state of the type species *L. anceps* indicates that *Liodon* should remain designated as *nomen dubium*. While it is possible to draw strong comparisons with other members of the Mosasaurinae, such as *Mosasaurus* and *Clidastes*, the fragmented nature of the specimens prevents a sound referral. As much as this study underscores the challenges in interpreting poorly preserved material based largely on dental characters, it nevertheless aims to provide an updated and comprehensive review to assist in assessing fragmentary material associated with *Liodon* as well as provide partial resolution to a set of historically and continuously problematic mosasaur taxa.

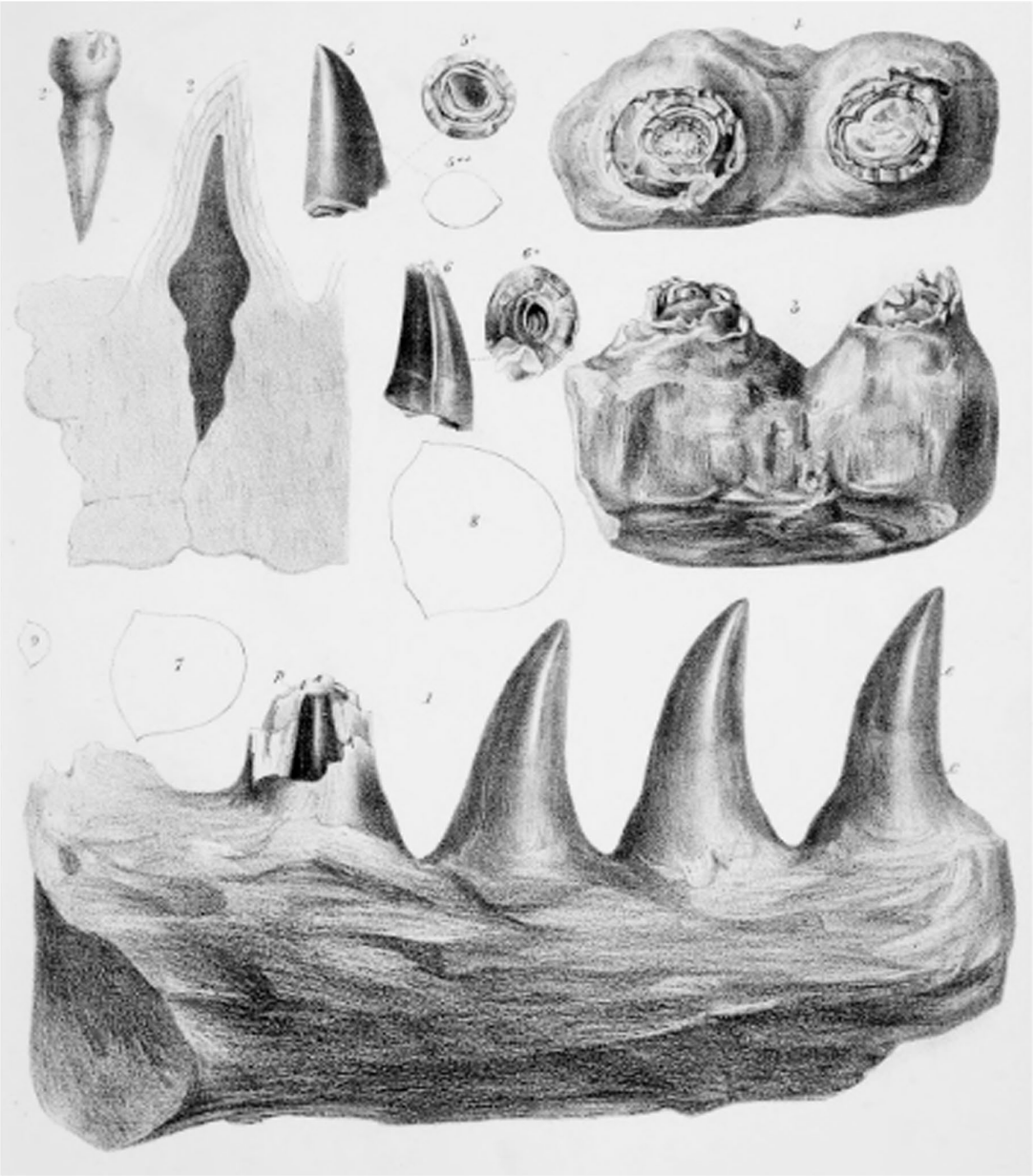

Figure 6.1. Holotype of *Liodon anceps*, from Owen, 1851.

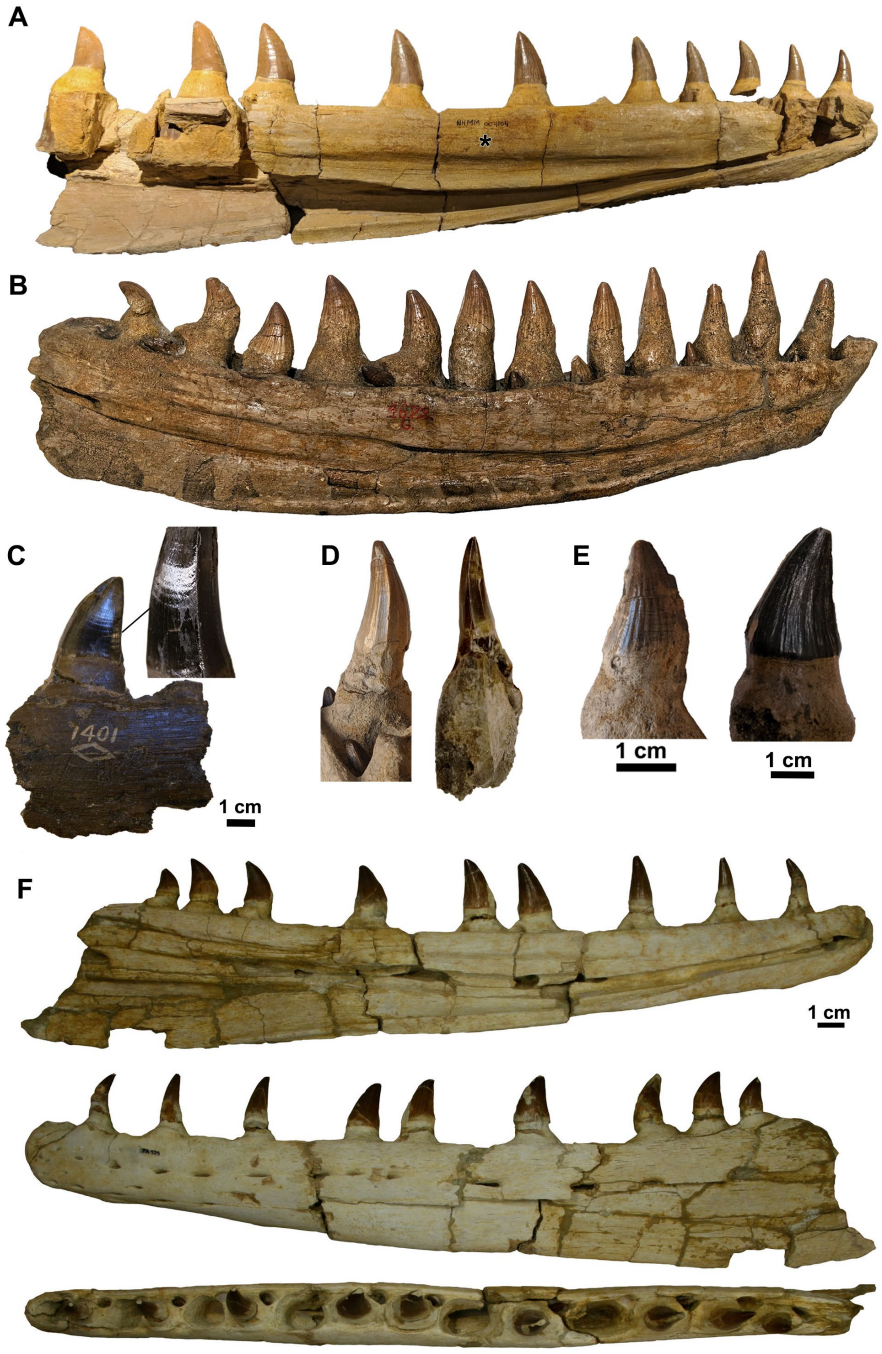

Figure 6.2. Left dentary of *L. sectorius* (NHMM 004104) in (A) medial view; left dentary of *P. solvayi* (IRScNB R33) in (B) medial view; marginal tooth of *L. sectorius* in (C) lateral view with close-up of serrations; comparison of marginal teeth of *P. solvayi* (IRScNB 0107) and holotype of *L. sectorius* (AMNH 1401) in (D) posterior view; comparison of marginal teeth of *P. solvayi* (IRScNB 0108) and *L. sectorius* (AMNH 1401) in (E) lateral view; right dentary of *P. kianda* (MGUAN PA 129) in (F) medial, lateral, and dorsal views, modified from Schulp et al. (2008: fig. 7A-C). Dentaries in (A) and (B) are not to scale as *L. sectorius* could not be accurately measured. Asterisk in (A) indicates the low shelf along the tooth row.

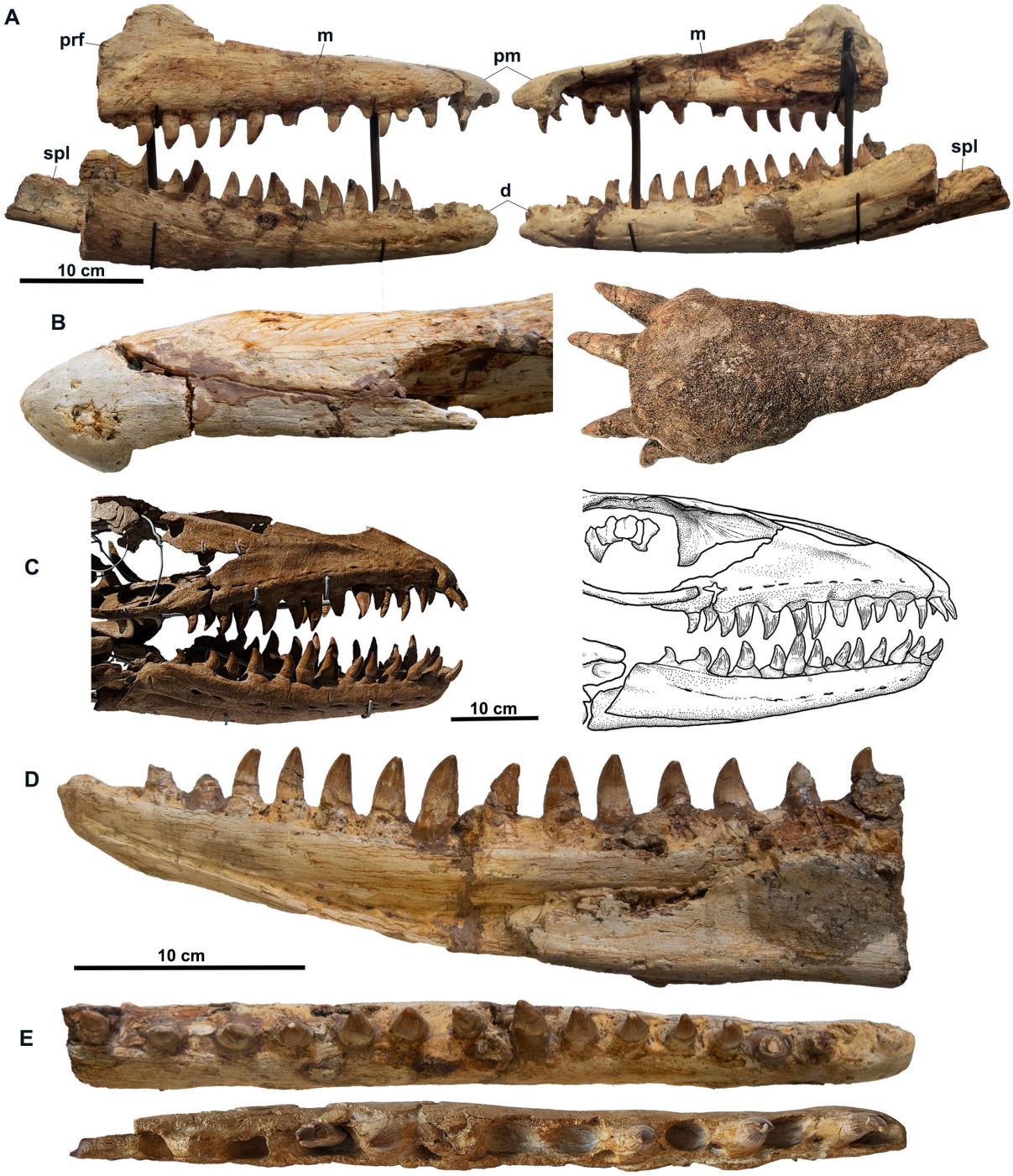

Figure 6.3. Jaws of *L. compressidens* (MNHN-Z-C-1878-5) from (A) right and left aspect; comparison of the premaxillae of *L. compressidens* (left) and *P. solvayi* (IRScNB R33) (right) in (B) dorsal view; jaws of *P. solvayi* (IRScNB R33) in (C) lateral view; right dentary of *L. compressidens* in (D) medial view; comparison of the dentaries of *L. compressidens* and *P. solvayi* (IRScNB 0108) in (E) dorsal view. Abbreviations: d, dentary; m, maxilla; pm, premaxilla; prf, prefrontal; spl, splenial.

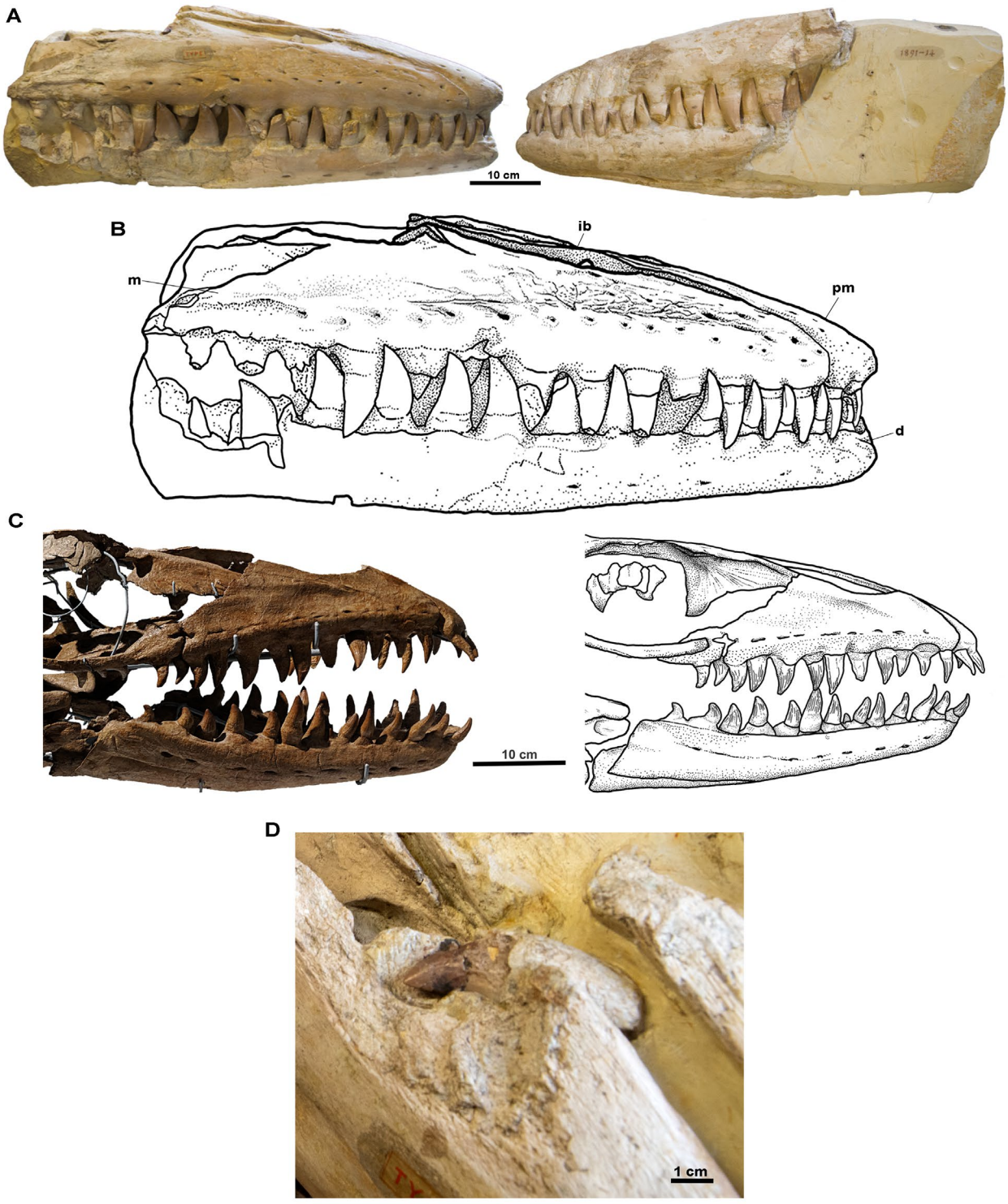

Figure 6.4. Jaws of *L. mosasauroides* (MNHN 1891-14) in (A) lateral and medial view; (B) labeled lateral view; jaws of *P. solvayi* (IRScNB R33) in (C) lateral view; isolated tooth embedded in right maxillae of *L. mosasauroides* (MNHN 1891-14) in (D) anterodorsal view. Abbreviations: d, dentary; ib, internarial bar; m, maxilla; pm, premaxilla.

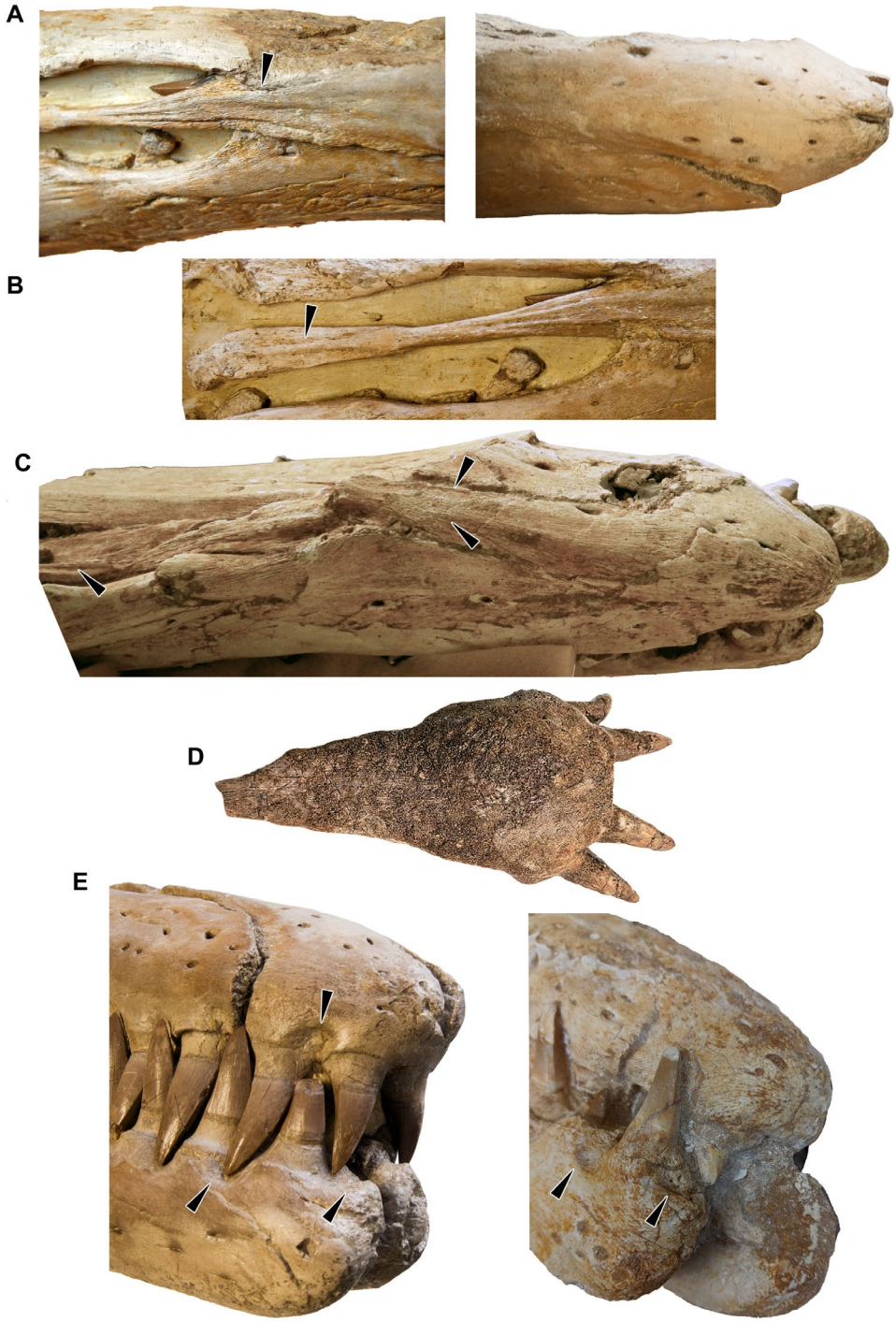

Figure 6.5. Anterior and posterior premaxilla of *L. mosasauroides* in (A), (B) dorsal view; premaxilla of *Eremiasaurus heterodontus* (UALVP 51744) in (C) dorsal view; premaxilla of *P. solvayi* (IRScNB R33) in (D) dorsal view; rostra of *L. mosasauroides* (MNHN 1891-4) and *Eeremiasaurus heterodontus* (UALVP 51744) in (E) anterolateral view. Arrows in (A) and (C) indicate ridges on dorsal surface of posterior premaxilla. Arrow in (B) and (C) (posterior) indicate dorsal median ridge on internarial bar. Arrows in (E) indicate predental and interdental pits on premaxilla and dentary. Images not to scale.

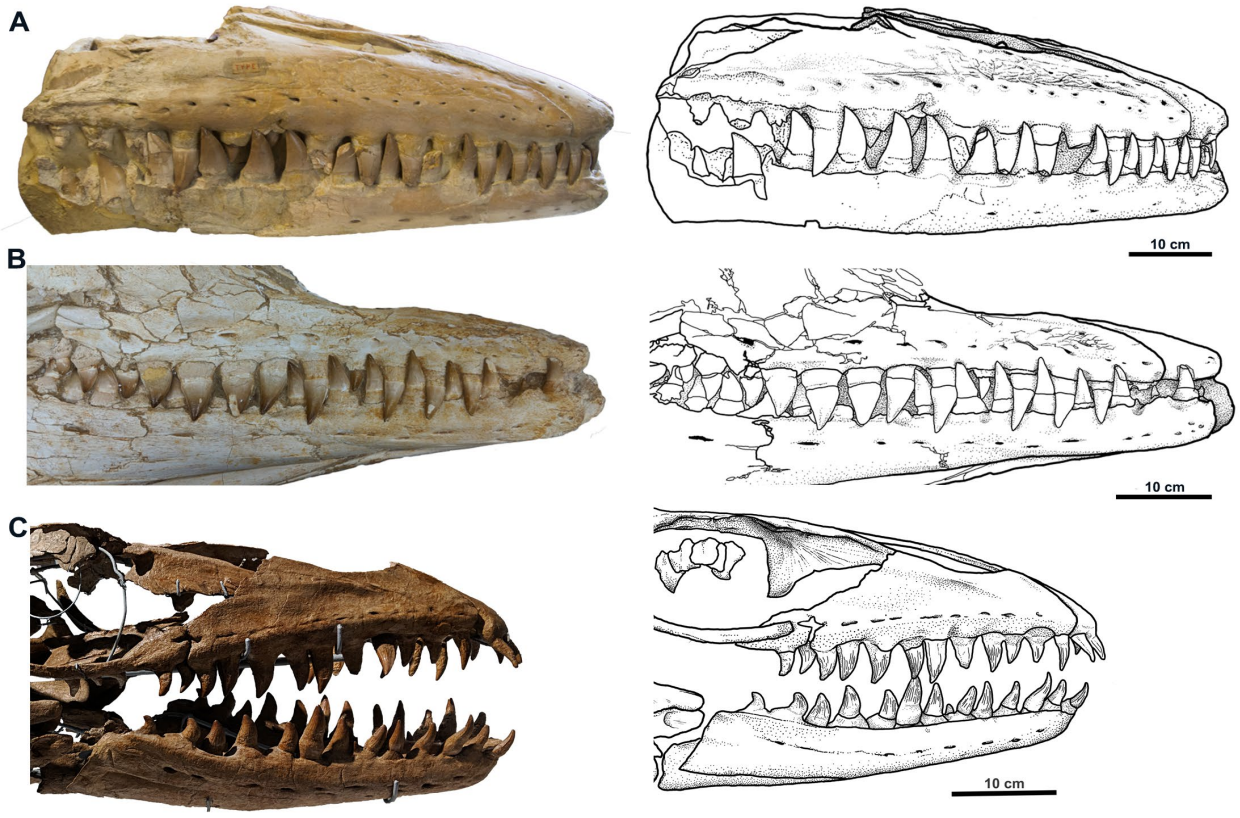

Figure 6.6. Jaws of *L. mosasauroides* (MNHN 1891-4) in (A) lateral view; jaws of *Eremiasaurus heterodontus* (UALVP 51744) in (B) lateral view; jaws of *P. solvayi* (IRScNB R33) in (C) lateral view.

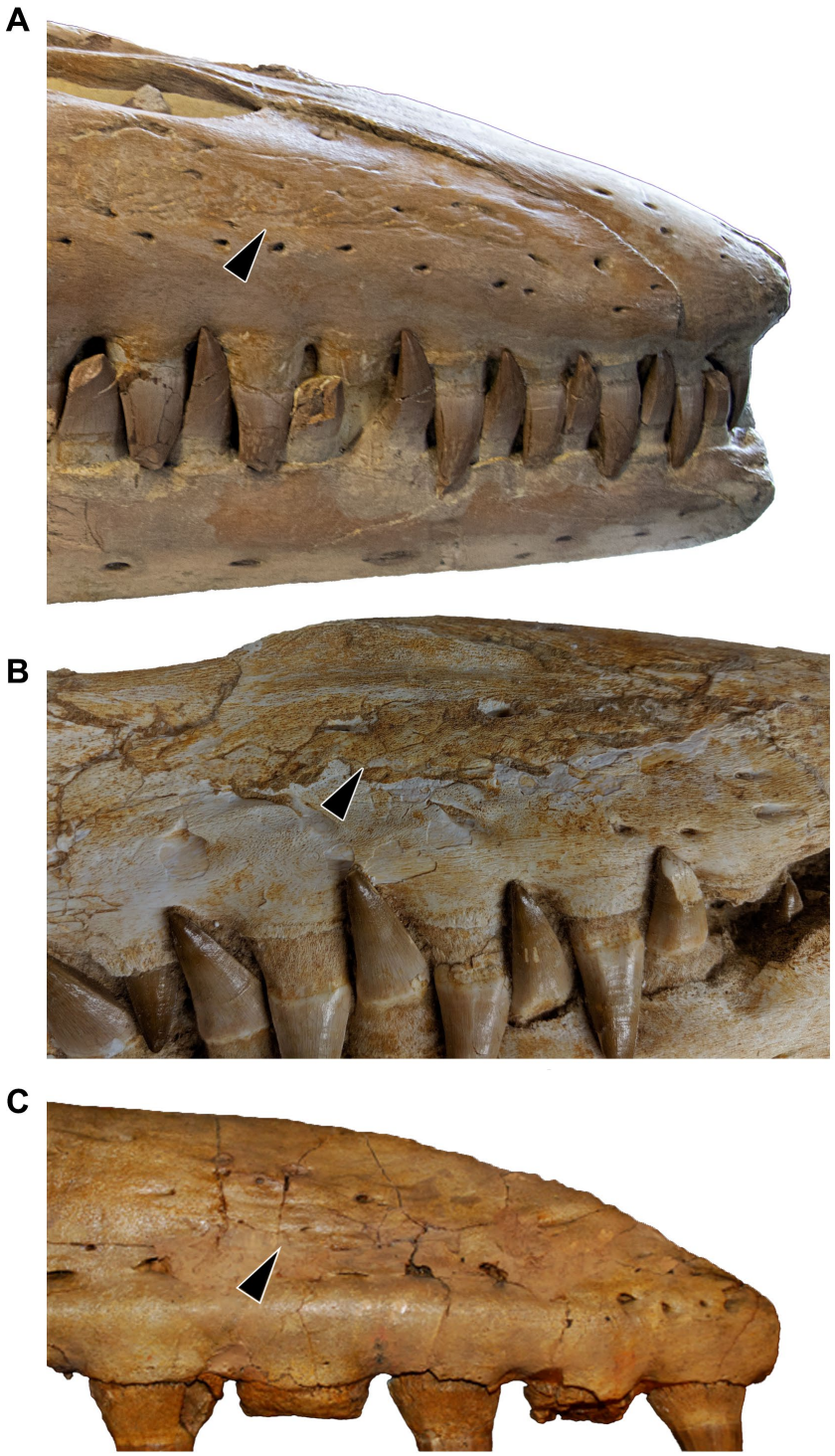

Figure 6.7. Maxilla of *L. mosasauroides* (MNHN 1891-4) in (A) lateral view; maxilla of *Eremiasaurus heterodontus* (UALVP 51744) in (B) lateral view; maxilla of *Mosasaurus hoffmanii* (IRScNB 1483) in (C) lateral view. Black arrows indicate network of irregular grooves on anterolateral surface of maxillae. Images not to scale. Photo of *Mosasaurus hoffmanii* courtesy of Hallie Street.

CHAPTER 7. A PHYLOGENETIC REVIEW OF THE GENUS *PROGNATHODON*

INTRODUCTION

The systematic relationships of the genus *Prognathodon* has persisted as a long-standing and contentious issue (Russell, 1967; Lingham-Soliar, 1989; Bell, 1997; Bell and Polcyn, 2005; Conrad, 2008; Leblanc et al. 2012; Grigoriev, 2013; Madzia and Cau, 2017; Simões et al.; Strong et al. 2020; Lively 2022; Longrich et al. 2022; Zietlow et al. 2023). Initially included within the Plioplatecarpinae (Russell, 1967), a pivotal study by Bell (1997) using phylogenetic analysis instead recovered *Prognathodon* within the Mosasaurinae, specifically in the Globidensini alongside *Globidens* and *Plesiotylosaurus*. Following this major shift in mosasaur taxonomy, the precise interrelationships of the group has remained elusive and unstable; even at the time *Prognathodon* was paraphyletic with respect to *Plesiotylosaurus* (Bell, 1997). As discussed previously (Chap. 2), these issues may have arisen at least in part from the initial exclusion of the type species, *P. solvayi*, from earlier analyses which instead only included *P. overtoni* and *P. rapax* (Bell, 1997; Bell and Polcyn, 2005), in addition to inconsistencies in the character state coding of *P. solvayi* and other *Prognathodon* taxa (Christiansen and Bonde 2002; Dortangs et al. 2002; Conrad, 2008). Numerous studies, some of which apply multiple different phylogenetic methods, nevertheless result in *Prognathodon* consistently forming a paraphyletic clade, occasionally in the form of a polytomy or Hennigian comb (Leblanc et al. 2012; Simões et al. 2017a, Strong et al. 2020, Zietlow et al. 2023). Recently, Longrich et al. (2022) recovered the robust mosasaurine *Thalassotitan* in a clade with *Prognathodon* and re-erected the Prognathodontini Russell, 1967 under a new definition, although the author stated this may

indicate *Prognathodon* is not monophyletic, and both *P. kianda* and *P. waiparaensis* were excluded from this grouping. Prognathodontini also formed formed an unresolved clade alongside a monophyletic Globidensini, composed primarily of *Globidens*.

The volatility of *Prognathodon* and closely related groups such as *Globidens* and *Plesiotylosaurus* has long indicated that the current paradigm surrounding these taxa requires significant revision. Several corrections and modifications to character codings and the addition of new characters based on the redescription of *Prognathodon* attempts to resolve these recurrent problems. The following analysis tests the recommended synonymization of the type species *P. solvayi* and *P. giganteus* and the suggested removal of *P. saturator* and *P. overtoni* from the genus. The resulting tree topologies will also be used to evaluate the validity of other referred taxa including *P. currii*, *P. kianda*, and *P. waiparaensis*, as well as the status of the Globidensini (Bell, 1997; Dortangs et al. 2002; Longrich et al. 2022). Finally, this study addresses the implications for those characters often used to diagnose *Prognathodon*, namely the fused processes of the quadrate (see Palci et al. 2022).

MATERIALS AND METHODS

Dataset Selection and Modifications

This analysis utilized the contingent character matrix modified by Strong et al. (2020) and originally derived from Simões et al. (2017a) (Appendix A). There are advantages and disadvantages to both contingent and multistate coding involving character and characters state dependency versus independency (Sereno, 2007; Simões et al. 2023); however, the contingent dataset was selected as contingent coding schemes are a more effective means by which to

reduce the issues associated with hierarchical characters (Sereno, 2007; Simões et al. 2017a; Simões et al. 2023).

The updated matrix from Strong et al. (2020) contains 47 taxa, 129 characters, and incorporates recoded taxa and eliminated or revised poorly constructed characters (Simões et al. 2017b). Additionally, the inclusion of *Prognathodon* within the Plioplatecarpinae for much of its history necessitates the use of a broad sampling of taxa included within the dataset to test the placement of the genus relative to other major groups of mosasaurs (Russell, 1967; Lingham-Soliar and Nolf, 1989; Bell, 1997). This study also maintains the outgroup choice of Strong et al. (2020) and Simoes et al. (2017a), the mosasauroid *Adriosaurus suessi* Seeley, 1881, which replaced the commonly used operational taxonomic unit (OTU) devised from a hypothetical combination of varanid characters. An unweighted maximum parsimony analysis was selected as means of comparison with previous studies using the same methods (Simoes et al. 2017a), and despite the possibility of greater accuracy, the use of this source dataset under different techniques nevertheless found generally similar patterns within the Mosasaurinae and recovered *Prognathodon* as a paraphyletic clade (Simões et al. 2017a; Strong et al. 2020).

Further modifications to the characters, character coding, and taxon list of this dataset results from the conclusions drawn in Chapters 2 through 6 (Appendix B). A single taxon, *P. giganteus,* was added to the matrix in accordance with the synonymization of the type species *P. solvayi* (Chap. 3), primarily as a means to verify its relatedness *P. solvayi*. Conversely, *Prognathodon rapax* Hay, 1902 was omitted from the taxon list due to the highly fragmentary nature of both the holotype (consisting of two right quadrates) and referred material (Lucas et al. 2005). No representatives of *Liodon* were included for similar reasons (Chap. 6). *Prognathodon currii*, *P. kianda, P. waiparaensis*, are comparatively fragmentary specimens that for a variety of

reasons were not personally observed. As a result, previous codings were instead cross-referenced with the original description, photographs taken by colleagues, and other related publications in order to ensure as much accuracy as possible (Welles and Gregg, 1971; Christiansen and Bonde 2002; Schulp et al. 2008; Street, 2017).

Three new characters (130-132) were added based on the redescription of *P. solvayi*. These include the presence or absence of a ventral ridge connecting the synapophysis to the lateral edge of the cotyle in the cervical vertebrae (130), the presence or absence of an anterodorsal process on the maxilla (131), and the dorsal or medial orientation of the anterodorsal process of the maxilla (132). Other diagnostic features present in *P. solvayi*, such as the dorsal eminence of the quadrate (Fig. 2.14B, G), were not included in the present dataset due to the broad range of differing morphologies and iterations of this feature in various other taxa (Palci et al. 2021: figs. 2-3). The disparity of shape in this structure (as well as the ambiguity of its presence in certain examples, e.g. Palci et al. (2021): fig. 3A, H) limits presumptions of homology and the construction of cogent character states. As a result, it is currently recommended that this is treated only as a diagnostic character.

Multiple character scorings were also corrected or added for included *Prognathodon* taxa. For *P. solvayi*, character 39 was corrected to ‘0’ from ‘1’, as the pterygoid teeth erupt from the main pterygoid platform rather than on a pronounced ridge. Character 42 accounts for the presence of absence of a constricted suprastapedial process. The left and right quadrate of the holotype of *P. solvayi* differ somewhat in appearance due to deformation, and it is recommended that this feature be coded as ‘?’ as opposed to present (‘0’). Character 49 was changed from ‘?’ to ‘0’ to reflect the triangular shape of the pterygoid basisphenoid process. Although the mandibular condyle is tilted anteriorly, a deflection on the anterior surface is not evident on any

quadrate, and the state coding was changed for character 52 from ‘1’ to ‘0’ as a result. *P. solvayi* possesses only a single basioccipital canal (character 55) and the character state score was changed to ‘2’. Character 60 was coded as ‘1’ as the splenial-angular articulation is laterally compressed in anteroposterior view. Character 64 coding for the presence or absence of contact between the angular and medial wing of the coronoid was corrected to absent (‘0’). A coronoid buttress is absent, changing the score of character 66 from ‘1’ to ‘0’. Character 78 describes the size of the atlas synapophysis, which is *P. solvayi* fairly prominent and therefore as ‘1’. Character 103 was changed to ‘1’, as the scapular neck tapers fairly gradually to a narrower base. The caudals of *P. solvayi* are no longer with the specimen, and with the addition of *P. giganteus* to the character matrix, character 85 coding for the fusion of the haemal arches to the centrum was scored as present ‘1’ for *P. giganteus*, but ‘?’ for *P. solvayi*. Should the referral of *P. giganteus* to *P. solvayi* hold true, it is recommended *P. solvayi* be coded as haemal arches fused in future iterations.

The greatest number of coding changes were made to *P. saturator*. Although damaged, the anterolateral extensions and weakly concave anterior margins of the frontal between the internarial bar indicate character 10 should be coded as having a small emargination (‘1’ rather than ‘0’). The descending processes broadly contact and enclose the olfactory canal, indicating character 13 should be coded as ‘1’ instead of ‘0’. A posterior extension of the maxilla overlaps the prefrontal, excluding it from the external nares (character 35, ‘1’ to ‘0’), and the anterior projection of the ectopterygoid inserting against the maxilla is visible in the right orbit (character 37, ‘?’ to ‘0’). Character 40 addressing pterygoid tooth size was coded as ‘?’ from ‘1’, as the alveoli and pterygoid teeth themselves are well enough preserved to ascertain their size relative to the marginal dentition. *Prognathodon saturator*, *P. kianda* (Schulp et al. 2008, fig. 7C-E), and

P. waiparaensis (Palci et al. 2021: fig. 3G) were all rescored as having a prominent, laterally-produced tympanic rim (character 46, '2'). *Prognathodon saturator* was originally coded as having a basioccipital canal (character 55), and this was changed to absent ('0'). Regarding dentary tooth count (character 56), the dentaries are either damaged or incomplete and the precise number of teeth is ambiguous as a result, suggesting the character state is best scored as '?' rather than '3'. Character 63 coding for the posteromedial process of the coronoid was rescored as present ('0'), as was character 64 for contact between the angular and medial wing of the coronoid ('1'). The medial surface of the posterior wing is not exposed on either coronoid, resulting in the recoding of character 65 to '?'. The state coding for character 67 was corrected from '0' (surangular contacting articular behind the condyle) to '1' (at the center of the condyle). Although the posterior-most tooth position is missing (character 74), the adjacent teeth are conical ('0') as opposed to swollen at the base ('1'). Character 99 coding the width of the scapula was originally scored as '?', and this was changed to fan-shaped widening ('1'). The degree of concavity along the poster margin of the scapular (character 101) is reduced in comparison to the deeply emarginate scapula of *P. overtoni* and more similar to the condition in *P. solvayi*, and was coded as ('1') as a result. A small amount of interdigitating suture between the scapula and coracoid appears to be preserved, similar to the condition in *P. overtoni*, and the state for character 102 was changed to '1' to reflect this morphology. The coracoid neck is broad and tapers abruptly (character 103, '1'), and character 104 (coracoid emargination on its medial margin) was scored as absent ('1').

Several characters were also changed for *P. overtoni* following the description by Konishi et al. 2011, and new osteological information on the forelimb provided by the new specimen TMP 2018.0042.0001. Character 55 was scored as '2' as SDSM 3393 and KU 950 preserve a

single, blind ended basioccipital canal. Character 79 was recoded from '?' to '1' to account for the presence of zygosphenes and zygantra on the vertebrae, as well as a dorsal ridge connecting the synapophysis to the prezygapophysis on the posterior trunk vertebrae (character 88).

Three characters codings were corrected for *P. currii*: Characters 57/58 were rescored from '1' to '0' and '-' to '0', respectively, reflecting the presence of a short dentary projection beyond the first tooth position as shown and described in the original taxon description (Christiansen and Bonde, 2002). Character 69 was changed from '0' to '1', as per the author's comments regarding the strong horizontal inflection of the retroarticular process, which is also evident in figures of the skull.

Phylogenetic analysis

Traditional (unweighted) Maximum Parsimony: Adhering to the methods used by Strong et al. (2020) and Simões et al. (2017a), the analysis was performed for the contingent character matrix in TNT v. 1.6 using the heuristic 'Traditional Search' with 1000 replicates, followed by tree bisection and reconnection (TBR) (Goloboff & Morales, 2023).

Character mapping: Synapomorphies were mapped onto all most-parsiomonious trees (MPTS) using TNT v. 1.6 (Goloboff & Morales, 2023). The resulting trees were processed through Mesquite v. 3.81 (Maddison & Maddison, 2023), then further refined in Adobe Illustrator v. 28.5.

RESULTS

Unweighted maximum parsimony analysis of the contingent character matrix (Co-UMP) generated 22 MPTs with lengths of 479 steps (CI=0.34511435; RI=0.69476744). This set of optimal trees was then used to produce strict consensus and 50% majority rule consensus trees (Fig. 7.1). Both the strict consensus tree (TL=492, CI=0.33739837, RI=0.68410853) and majority rules tree (TL=482, CI=0.34439834, RI=0.69379845) recovered a monophyletic Mosasaurinae with the inclusion of the Halisaurinae and *Dallasaurus*, similar to the Co-UMP tree of Simões et al. (2017a) and Street (2017). The current findings deviated in finding the Tethysaurinae as sister to all other mosasaurs, whereas *Komensaurus* Caldwell & Palci, 2007 was recovered within a polytomy alongside Yaguarasaurinae, Tylosaurinae, and Plioplatecarpinae. Although a monophyletic Russellosaurina Polcyn and Bell, 2005 was not recovered (Simões et al. 2017a, Street, 2017; Strong et al. 2020), internal resolution was greater for each of these groups, and Tylosaurinae was represented as the sistergroup to the Plioplatecarpinae in both trees. Similar to Street (2017), Halisaurinae forms a stepwise sister grouping with *Dallasaurus* to a monophyletic Mosasaurinae in both consensus trees. Both trees also recovered *Clidastes* as the most basal group amongst mosasaurines but did not resolve it internally. *Globidens* and *Mosasaurus* form monophyletic clades in the majority rules tree, although the latter is unresolved in the strict consensus tree.

Neither a monophyletic Globidensini or Prognathodontini were recovered in the majority rules consensus tree, as most members of *Prognathodon* formed a Hennigian comb leading to more derived mosasaurines (contra Russell, 1967; Bell, 1997; Christiansen and Bonde, 2002; Dortangs et al., 2002; Bell and Polcyn, 2005). The exception to the pattern of successive, single-taxon clades is *P. solvayi*, which was recovered as the sister taxon to *P. giganteus* in a position

more derived than *P. kianda* (occupying the most basal position), and *P. waiparaensis*. The position of *P. kianda* is consistent with both Co-UMP trees and other parsimony-based methods implemented by other researchers (Leblanc et al. 2012; Simões et al. 2017a, Street, 2017; Strong et al. 2020), whereas *P. waiparaensis* often places nearer to *Mosasaurus* in other analyses (Street, 2017; Simões et al. 2017a; Strong et al. 2020; Zietlow et al. 2023). *Prognathodon overtoni* is recovered as more derived than *P. solvayi* and *P. giganteus*, followed by *P. currii.* An unresolved clade is formed by *P. saturator*, *Globidens* and taxa typically associated with the Mosasaurini (i.e. *Eremiasaurus*, *Plotosaurus*, *Mosasaurus*), although the group containing *Mosasaurus* was fully resolved internally. *Plesiotylosaurus* was recovered between *Globidens* and *Eremiasaurus*, and is more closely associated with *Mosasaurus* than *Prognathodon*, similar to the findings of Street (2017). The strict consensus tree found largely similar results as far as the position of taxa is concerned (Fig. 1), and the group containing *P. solvayi* and *P. giganteus* was maintained, although it formed an unresolved clade alongside *P. kianda* and *P. waiparaensis*.

The synapomorphies forming the base of the *Prognathodon* comb in the majority rules tree includes (9) sinusoidal edges of the frontal anterior to the orbit, the posteroventral ascending tympanic rim of the quadrate extremely produced laterally (45) (reversed in *P. solvayi* and *P. giganteus*), swollen base of the posterior marginal teeth (74), and dorsal orientation of the anterolateral process of the maxilla (132). Five apomorphies support the clade including *P. solvayi* and *P. giganteus* in both Co-UMP trees: a short, obtuse rostrum (1), a broadly arcuate rostrum (3), projection of the dentary anterior to the first tooth position absent (57), coronoid buttress of surangular low and roughly parallel to ventral margin of mandible (66), and laterally elongate syanopophyses of the trunk vertebrae (83). A sixth apomorphy, the presence of a ventral

synapophyseal crest on the cervical vertebrae (130) also supported the clade in the majority rules tree. In both trees, the characters supporting the clade that includes *P. overtoni*, *P. currii*, *P.saturator*, *Globidens*, *Plesiotylosaurus* and putative members of the Mosasaurini are presence of a median ridge on the frontal (11), short posterior median flange of the frontal (18), contact between the prefrontal and postorbitofrontal at edge of the frontal (28), coronoid medial wing contacts the angular (64), excavation on medial surface of coronoid posterior wing (65), extreme inflection of the retroarticular process (69), and presence of a coarsely-textured tooth surface (72). *Prognathodon saturator*, *Globidens*, *Plesiotylosaurus*, and the Mosasaurini are further differentiated by the premaxillary suture extending to between the fourth and ninth tooth positions (33), and presence of a posterolateral process of maxilla excluding the prefrontal from the dorsolateral margin of the nares (35).

DISCUSSION

Despite the substantial modification to the character state scores of multiple members of *Prognathodon* and the addition of three new characters, the analysis generated trees generally in line with those produced by previous researchers, with the exception of the recovery of the Russellosaurina (Simões et al. 2017, Street, 2020; Strong et al. 2020). The formation of a paraphyletic *Prognathodon* is also consistent with the findings of numerous studies, regardless of whether parsimony-based or Bayesian analyses were implemented (Leblanc et al. 2013; Madzia and Cau, 2017; Simões et al. 2017a: fig. 1C; Street, 2017, Lively, 2020; Zietlow et al. 2023). Defined as all species nearer to *Prognathodon solvayi* than to *Globidens alabamensis* and *Mosasaurus hoffmanni*, the Prognathodontini was re-erected with the caveat that *Prognathodon* itself may not be monophyletic due to the inclusion of *Thalassotitan* within the clade (Longrich

et al. 2022). Based on phylogenetic inference alone, there is little evidence to indicate that *Prognathodon* as it is currently understood represents a monophyletic group.

The positions of the different *Prognathodon* species have typically varied relative to each other within Mosasaurinae itself, producing few persistent patterns of relationship. For example, *P. solvayi* has been recovered as the sister taxon to both *P. currii* and *P. saturator* (Dortangs et al. 2002; Schulp et al. 2006; Lively 2020; Zietlow et al. 2023), as well as *P. lutugini* (Grigoriev, 2013; Longrich et al. 2022). However, of the scoreable characters discernable in *P. giganteus*, all were identical to those of *P. solvayi.* In the majority rules tree (Fig. 7.1A), the newly added character 130 (presence of a ventral synapophyseal crest on the cervical vertebrae) was one of six characters found to support the clade including *P. solvayi* and *P. giganteus*, demonstrating the importance of rigorous osteological comparisons in identifying features of both diagnostic and phylogenetic relevance. The resulting recovery of *P. giganteus* as the sister taxon to *P. solvayi* in the current analysis supports the initial hypothesis based on morphological comparison that the two taxa are synonymous, with *P. giganteus* representing a large individual of *P. solvayi*.

Comments on the validity of other *Prognathodon* species

All other referred members of *Prognathodon* were resolved as single-taxon clades, although like *P. solvayi*, their relative positions with respect to one another has varied considerably in the past (Leblanc et al. 2012; Grigoriev, 2013; Madzia and Cau, 2017; Simões et al. 2017a; Strong et al. 2020; Lively 2022; Longrich et al. 2022; Zietlow et al. 2023). Leblanc et al. (2013) attributed much of the issue at least in part to the comparatively poor preservation of several globidensine taxa, including *P. currii*, *P. kianda*, and *P. waiparaensis*, all of which lack large or nearly entire portions of their postcrania. Additionally, both *P. kianda* and *P.*

waiparaensis are currently represented by highly fragmented skulls, eliminating a large amount of important datapoints. Although the skull of *P. currii* is articulated, the condition of the bone itself is such that diagnostic features are very difficult to discern, resulting in most cranial characters being scored as unknown. In contrast, the plethora of observed morphological differences between *P. saturator*, and to a lesser extent *P. overtoni*, is reflected in their recovery as separate from the type species. *P. saturator* in particular formed an unresolved group alongside *Globidens* and a clade including other more derived mosasaurines. This calls the validity of other referred taxa included within the analysis into question.

Prognathodon kianda is typically placed separately and positioned more basally relative to its congenerics (Leblanc et al. 2022; Madzia and Cau, 2017; Simões et al. 2017; Longrich et al. 2022; Zietlow et al. 2023). Although sharing weakly procumbent anterior teeth and fused processes of the quadrate with *P. solvayi* (Schulp et al. 2007), several diagnostic features differ considerably between the two taxa, including the presence of a short, tapered predental rostrum on the premaxilla and dentary, comparatively smaller pterygoid teeth, eruption of pterygoid teeth from a ventrally descending narrow ridge, absence of fluted marginal dentition, a broad dorsally expanded dorsal margin of the surangular, a rotated retroarticular process, a medioloterally broad fusion of the suprastapedial and a posterior pillar-like processes, and presence of a large, posteriorly-expanded tympanic ala (Schulp et al. 2008: fig. 7). *Prognathodon waiparaensis* shares the short predental rostra, weakly procumbent anterior teeth, the eruption of pterygoid teeth from a ventrally descending narrow ridge, and a markedly similar quadrate with *P. kianda* (Welles and Gregg, 1971; Schulp, 2006; pers. obs. from photographs). *Prognathodon waiparaensis* differs further from *P. solvayi* in having a posteroventral process of the jugal and broadly expanded quadrate process of the pterygoid. The similarities between *P. waiparaensis*

and *P. kianda* may account for their occurrence in similar positions on both Co-UMP trees (Fig. 7.1); however, Street (2017) instead recovered *P. waiparaensis* closer to the Mosasaurini than to *Prognathodon*, prompting its referral to new a genus, *Marichimaera waiparaensis*. Street (2017) noted that the vertebrae, phalanges, and aspects of the skull, such as the predental rostrum, more closely resembled those of *Mosasaurus*. Although it was suggested this taxon may display an intermediate set of conditions, the possibility of the holotype instead representing more than one individual due to the collection of the specimen spanning over a few years may complicate interpretation of its morphology and any taxonomic inferences as a result.

Unlike *P. kianda* and *P. waiparaensis*, *P. currii* more strongly resembles robust examples such as *P. saturator*, as well as the recently described *Thalassotitan* (Longrich et al. 2022), likely effecting its recovery between *P. overtoni* and the unresolved group containing *P. saturator* and *Globidens*. The initial referral of *P. currii* to *Prognathodon* was supported by similarities in shape of the frontal alae and transverse processes of the cervical vertebrae with *P. solvayi*, as well as the fused processes of the quadrate (this element is not well enough preserved to determine whether *P. currii* had a posterior pillar-like process) (Christiansen & Bonde, 2002). The authors distinguished *P. currii* from the type species by the differences in the marginal dentition (lacking procumbent anterior dentition and flutes; smaller, rounded and stout teeth throughout), presence of a short predental rostrum on the premaxilla and dentary, the invasion of the frontal by the external nares, and the presence of a medial dorsal ridge on the frontal. It can be further distinguished by its rotated retroarticular process and comparatively large, rounded mandibular condyle. Similar to *P. overtoni* and *P. saturator*, the skull of *P. currii* is also remarkably more massively built than that of *P. solvayi*. Although Christiansen & Bonde (2002)

recovered *P. solvayi* as the sister taxon to *P. currii*, the authors nevertheless acknowledged that the two taxa were not very similar.

The degree of resemblance between *P. currii*, *P. kianda*, and *P. waiparaensis* and the type species relative to *P. overtoni* and *P. saturator* is more difficult to assess due to the lack of data for comparison. Nevertheless, several distinguishing characteristics are recognizable in each and neither of these species grouped with *P. solvayi* in the resulting Co-UMP trees, supporting their removal from the genus *Prognathodon*.

Comments on the "globidensine" quadrate

Both the propensity for quadrates to preserve in the fossil record and the broad range of differing morphologies have resulted in the mosasaur quadrate playing a key role in the determination of taxonomic relationships (Palci et al. 2021). Similarly, the fusion of the suprastapedial and posterior pillar-like and/or posterolateral processes of the quadrate has persisted as a principal factor in the concept of *Prognathodon* as a whole. However, the quadrate of *P. solvayi* is otherwise generally distinct from those of other referred species of *Prognathodon* and disputed members of the Globidensini (Fig. 7.2; Bell, 1997): *Prognathodon solvayi* and *P. overtoni* lack the greatly expanded tympanic rim present in *P. kianda*, *P. waiparaensis*, and *P. saturator*. The quadrates of *P. kianda*, *P. waiparaensis*, *P. saturator* and *P. overtoni* are broad in anteroposterior aspect (Fig. 7.2B), and have a mediolaterally broad fusion of the suprastapedial and poster-pillar like processes (Palci et al. 2021). This contrasts sharply with the narrow, anteroposteriorly oriented fusion in *P. solvayi*, wherein a small, narrow posterolateral process primarily occupies the lateral face of the quadrate. Some examples, including the robust taxa, also exhibit a steeply inclined suprastapedial process at its anterior point of origination, whereas

it extends horizontally prior to descending ventrally in *P. solvayi* (Fig. 7.2A). *Prognathodon solvayi* also lacks the generally much larger, more rounded and convex, and upturned anterior surface present in the mandibular condyle of other referred taxa (Fig. 7.2A). The exceptions to these observations are *Globidens dakotensis* and *Globidens schurmmani* (Fig. 7.2), both of which have a small mandibular condyle.

Palci et al. (2020) attributed the broad range of quadrate morphology in squamates to ecological as opposed to phylogenetic factors. In mosasaurs, this disparity may be a consequence of external influences associated with diet, large body size, rapid evolution, and an aquatic lifestyle (Palci et al. 2021). The question then arises as to precisely how informative the quadrate is to mosasaur taxonomy.

The current results agree with numerous previous studies that recovered the Globidensini as paraphyletic (Russell, 1967; Leblanc et al. 2013; Simões et al. 2017a; Zietlow et al. 2023). Although numerous analyses found that fused processes of the quadrate was characteristic of a monophyletic Globidensini (Bell, 1997; Dortangs et al. 2002; Christiansen and Bonde, 2002; Schulp, 2006; Polcyn et al., 2010), Leblanc et al. (2013) instead found that this feature occurred basally with *P. kianda* and was therefore plesiomorphic with respect to the Mosasaurinae, to the exclusion of both *Clidastes* and *Dallasaurus*. This led Leblanc et al. (2013) to point out that the quintessential globidensine quadrate is not exclusive to the Globidensini. The authors reported fused processes of the quadrate in *Eremiasaurus heterodontus*, in addition to large pterygoid teeth, inflated bases of the marginal tooth crowns, a lower tooth count, all of which were also attributed to *P. solvayi* and have been considered characteristic of globidensines (Lingham-Soliar and Nolf, 1989). However, *Eremisasaurus* also possesses plotosaurine characters, including an alar groove on the quadrate, and in subsequent analyses is typically associated with the more

derived *Plotosaurus* and *Mosasaurus* than to either *Prognathodon* or *Globidens* (Leblanc et al. 2013; Simões et al. 2017a; Street, 2017; Lively, 2020). The occurrence of a suite of both basal and derived mosasaurine characteristics within a single taxon is evidently not unusual for some mosasaurines. The presence of features typical of both *Prognathodon* and *Mosasaurus* in *P. waiparaensis* may be borne out if the holotype was confirmed as a single individual (Street, 2017). *Plesiotylosaurus*, has placed both with the Globidensini (Bell, 1997, Polcyn & Bell, 2005; Leblanc et al. 2013; Lively 2020), and nearer to *Mosasaurus* (Simões et al. 2017a; Street, 2017; Strong et al. 2020; Longrich et al. 2022; Zietlow et al. 2023), and also exhibits a mix of features, such as a higher tooth count, a conical predental rostrum, weakly procumbent anterior teeth, and fused processes of the quadrate (Lindgren, 2009). As a result, both the poorer preservation of numerous of purportedly globidensine species and the broad distribution of traditionally globidensine characters likely play a pivotal role in the inconsistent placement of *Prognathodon*, *Globidens*, and *Plesiotylosaurus* within the Mosasaurinae.

This study found that fused processes of the quadrate (character 44) did not support or provide further clarity on any of the more inclusive groups within the Mosasaurinae (Fig. 7.1B). The quadrate alone accounts for 12 characters within the current analysis, a relatively high number compared to other individual elements, although 20 out of 142 characters were coding for the quadrate in Bell's (1997) analysis (Palci et al. 2021). The variability within the quadrate across taxa would appear to necessitate this in order to accommodate its structural complexity (Palci et al. 2021: figs. 2, 3); however, more characters will not necessarily achieve more accurate results, and the potential effects and influences of such characters on the outcomes of an analysis has yet to be widely addressed (Simões et al. 2017b; Palci et al. 2021). Hypothetically, an overabundance of quadrate characters may artificially add character weighting within the

dataset, introducing bias with the potential to effectively form a ‘tree within a tree”. Palci et al. (2021) addressed this in part by introducing a much-needed set of new terminology to reflect the subtle differences present in the infrastapedial process across mosasaur groups, and proposed that incorporating these changes into future analyses would accurately capture the variation present without exacerbating the possible issues caused by an excess of quadrate characters. Nevertheless, the broad distribution of fused processes of the quadrate across multiple mosasaurine taxa (Leblanc et al. 2013) indicate that fusion on its own as a quadrate character has limited utility for defining clades or diagnosing mosasaur taxa. The various other morphological differences between the quadrate of *P. solvayi* and related taxa underscores the importance of considering gross quadrate anatomy when diagnosing and referring specimens.

CONCLUDING STATEMENTS

The current findings support previous work that recovered *Prognathodon* as paraphyletic. Combined with the rediagnosis of the type species, *P. solvayi,* and the morphological reassessment of referred species, this analysis indicates major taxonomic revisions are necessary to provide further resolution within the group. *Prognathodon solvayi* and *P. giganteus* received essentially identical character state scores and were recovered as sister taxa, indicating they likely represent the same taxon. Based on the resulting tree topologies and a review of the shared diagnostic traits between the type species and *P. overtoni*, *P. saturator*, *P. currii*, *P. kianda*, *P. waiparaensis*, there is little evidence to support their inclusion within the genus. *Prognathodon*, as it is currently understood, is unsupported as a generic concept. Following these findings, the amended diagnosis of the type species, morphological comparisons with referred taxa, and the

results of this analysis will be incorporated and applied to a comprehensive taxonomic revision of the genus *Prognathodon*.

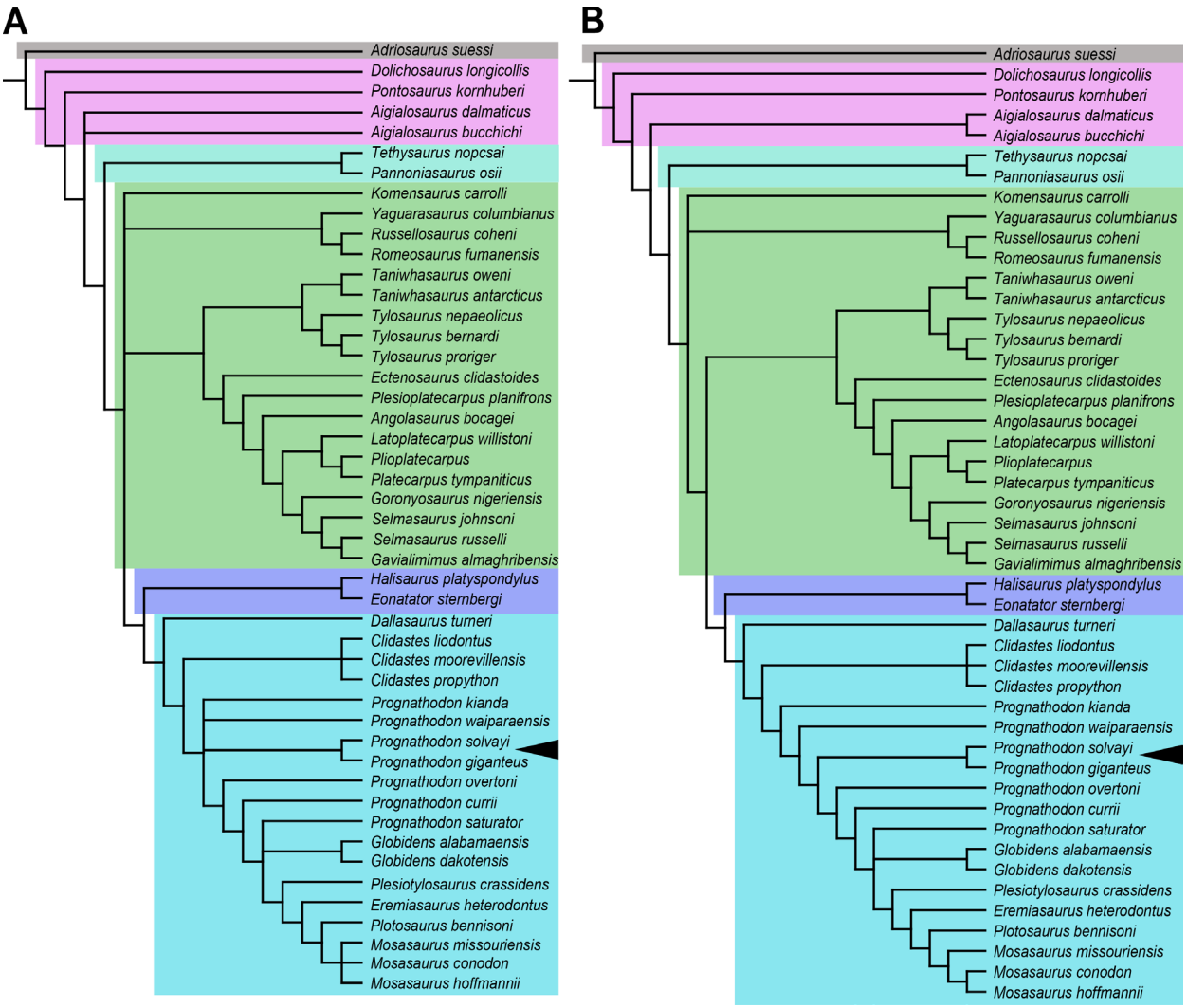

Figure 7.1. Consensus trees generated using unweighted maximum parsimony analysis of the dataset utilizing contingent character coding (Co-UMP). (A) Strict consensus tree of 22 most parsimonious trees (MPTs) of 479 steps (CI=0.337, RI=0.684); (B) 50% majority rule consensus tree of these 22 MPTs (CI=0.344, RI=0.694). Mosasaur subfamily colours: gray = outgroup, pink = Dolichosauridae + Agialosauridae, teal = Tethysaurinae, green = Russellosaurinae + *Komensaurus*, purple = Halisaurinae, light blue = Mosasaurinae. Black arrow indicates position of *Prognathodon solvayi*.

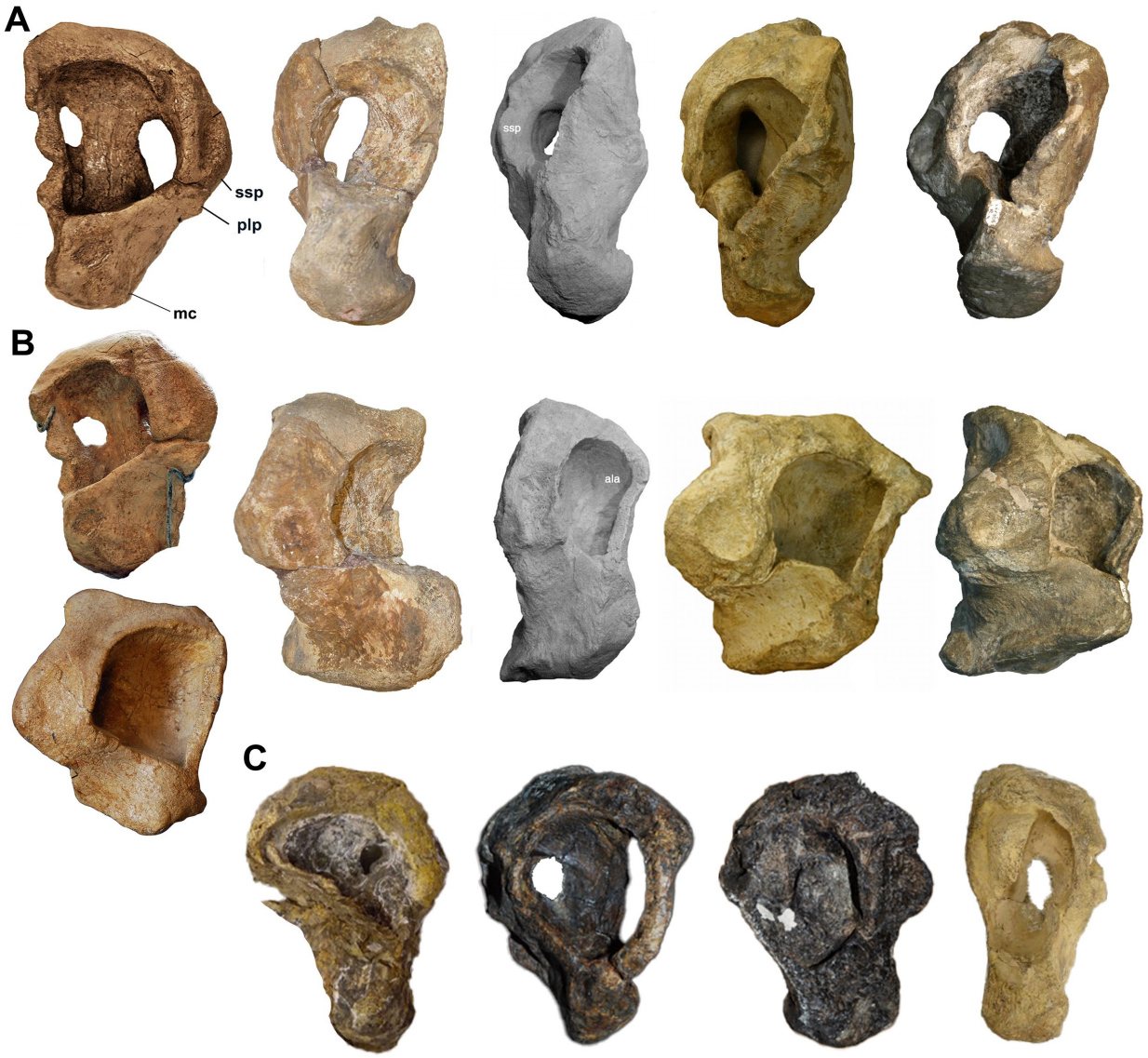

Figure 7.2. Comparison of quadrates of *Prognathodon*, *Globidens*, and *Plesiotylosaurus*. (A) From left to right, left quadrate of *P. solvayi* (IRcNB R33) in lateral view, left quadrate of *P. overtoni* (KU 950) mirrored for comparison, left quadrates of *P. saturator* (NHMM 1998141), *P. kianda* (MGUAN PA 129) (modified from Schulp et al. 2008: fig. 7D), and *P. waiparensis* (CM Zfr-108) in lateral view. (B) Left quadrate of *P. solvayi* (IRSNB R33) in posteroventral view (above) and right quadrate in posterolateral view, left quadrate of *P. overtoni* (KU 950) mirrored for comparison left quadrates of *P. saturator* (NHMM 1998141), *P. kianda* (MGUAN PA 129) (modified from Schulp et al. 2008: fig. 7D), and *P. waiparensis* (CM Zfr-108) in posterior view. (C) left quadrate of *Plesiotylosaurus crassidens* (UCMP 137249), *Globidens dakotensis* (PR 846), *Globidens schurmmani* (SDSM 74764), and right quadrate of *Globidens alabamensis* (PV 1985.0017) mirrored for comparison. Abbrevations: mc, mandibular condyle, plp, posterolateral process; ssp, suprastapedial process. Not to scale.

CHAPTER 8. SYSTEMATIC AND TAXONOMIC REVISION OF *PROGNATHODON*

INTRODUCTION

Following the redescription of the type species, the previous chapters have focused primarily on comparing and contrasting the diverse array of morphological features within *Prognathodon* with the revised generic diagnosis in order to form inferences of which taxa represent valid members of the genus. The incorporation of these findings alongside the results of the phylogenetic analysis allows for a comprehensive systematic and taxonomic revision of the genus *Prognathodon*.

The strict consensus and majority rules trees were in agreement with multiple studies that have found *Prognathodon* to represent a paraphyletic grouping. The two trees deviated little from each other in terms of relative positions of the various species of *Prognathodon*, with the degree of resolution being the primary difference. In both analyses, *P. giganteus* was recovered as a sister taxon to the type species, *P. solvayi*, amongst a Hennigian comb of separate taxa, with *P. kianda* forming its base. The more robust members, namely *P. overtoni*, *P. curri*, and *P. saturator* were recovered as more derived and the latter formed an unresolved clade containing *Globidens* and a second group comprising of derived mosasaurines. This chapter combines these results with the morphological-based hypotheses which together suggest most of the currently assigned species within *Prognathodon* should be considered invalid.

The following section first addresses the amendment in taxonomic status of those species that were included within the phylogenetic analysis (*P. solvayi*, as well as *P. currii, P. giganteus, P. kianda, P. overtoni, P. saturator*, and *P. waiparensis*). Those taxa which were excluded from

the analysis due to issues in accessibility or state of preservation are then likewise amended (*Liodon*, *P. hudae*, *P. hashimi*, *P. lutugini, P. rapax*), thereby achieving a complete systematic and taxonomic review of the genus *Prognathodon*.

Systematic Paleontology

SQUAMATA Oppel, 1811

MOSASAURIDAE Gervais, 1852

MOSASAURINAE Gervais, 1852

PROGNATHODON Dollo, 1889a

Prognathodon Dollo, 1889a:214.

Prognathosaurus Dollo, 1889b:293, pl. 9 figs. 4–5, pl. 10 figs. 8–9.

Brachysaurus Williston, 1897:96, pl. 8 (preoccupied Hallowell, 1856).

Dollosaurus Iakovlev, 1901, p. 518.

Ancylocentrum Schmidt, 1927: 59.

Prognathodon Dollo, 1889a: Russell, 1967, p. 123. (reversed)

Type species—*Prognathodon solvayi* Dollo, 1889a

Diagnosis—As for species

PROGNATHODON SOLVAYI Dollo, 1889a

Prognathodon solvayi Dollo, 1889a: 214.

Prognathosaurus solvayi Dollo, 1889b: 293, pl. 9 figs. 4–5, pl. 10 figs. 8–9. (new combination)

Prognathodon solvayi (Dollo, 1889a): Russell, 1967:162 (reversed)

Holotype—IRSNB R33

Locality—Solvay quarries near Ciply, Mesvin, and Spiennes, Belgium; Houzeau quarry near Spiennes, Belgium

Referred Specimens—IRSNB 0106, IRSNB 0107, IRSNB 0108

Revised Diagnosis—Modified from Russel (1967), Lingham-Soliar and Nolf (1989), and Konishi et al. (2011). Posterior region of skull broad and short in dorsal view, short mandible tapering anteriorly; premaxilla blunted and lacking a predental rostrum; dorsal surface of premaxilla broad and flat with shallow median sulcus (visible on referred specimen IRSNB 0106, 0107); premaxillary and anterior dentary teeth strongly procumbent; no extension of anterior dentary beyond first tooth position; median ridge of frontal absent; faint ridge on the lateral surface of the maxilla; anterodorsal and posterodorsal process of maxilla oriented dorsally, the latter greater in height than the former; large, elongate parietal foramen; borders of prefrontal and postorbitofrontal in close proximity but not in contact; prefrontal forms large portion of posterior narial border; smooth posterior border of jugal lacking posteroventral process; pterygoid lacking large, ventrally descending tooth-bearing ridge; pterygoid teeth large, similar in size to marginal teeth; six pterygoid teeth; base of the supratemporal processes originating at posterior margin of postorbital process of parietal and oriented horizontally along their entire length; bowed dentary; retroarticular process vertically oriented and angled posteriorly; medially deflected coronoid process; suprastapedial and posterolateral processes of quadrate fused; suture between suprastapedial and posterolateral processes of the quadrate narrow and oriented anteroposteriorly; single blind-ended basioccipital canal penetrating dorsal surface of occipital condyle; marginal dentition weakly splayed outwards and heterodont with

short, strongly hooked posterior teeth, more exaggerated in the dentary; teeth elongate, conical, laterally compressed and bicarinate teeth with prominent fluting on labial and lingual surfaces; zygosphenes and zygantra present on cervical and dorsal vertebral series, 12 maxillary teeth; 13-15 dentary teeth, ventral synapophyseal crest extending anteriorly to connect with lateral rim of cotyle in cervical vertebrae. Referable to the Mosasaurinae based on triangular supraorbital process of prefrontal overhanging the orbit and haemal arches fused to caudal vertebrae (IRSNB 0106).

Differential Diagnosis—Differs from *P. kianda, P. overtoni, P. saturator, P. waiparensis* in having a vertically oriented retroarticular process and basioccipital canal, and differs in lacking a predental rostrum on the premaxilla and dentary, a large dorsal expansion of the surangular with a coronoid buttress, an enlarged tympanic crest extending anteriorly and enclosing the ala, and a ventrally descending tooth-bearing ridge of the pterygoid. With the exception of *P. giganteus*, differs from all other referred taxa in having strongly procumbent premaxillary and anterior dentary teeth and lacking a predental rostrum, and well-developed fluting on the marginal dentition. Differs from *P. currii, P. overtoni*, *P. saturator* in having long, narrow, and labiolingually compressed marginal teeth; anterior teeth slightly splayed with crown apex curving lingually and posteriorly. Differs from *Globidens* in having long, narrow, labiolingually compressed, and fluted teeth. Differs from *Plesiotylosaurus* in having a shorter, deeper maxilla, strongly procumbent anterior teeth, and lacking a predental rostrum.

Remarks—Despite its larger size and having a slightly more robust mandible, as well as a dorsal median sulcus of the premaxilla, few major differences were observed between *P. giganteus* (IRSNB 0106) and the holotype of referred specimens of *P. solvayi*. The erupted teeth of *P. giganteus* lack the extensive fluting characteristic of *P. solvayi*, however, flutes were

observed in the unerupted replacement teeth in the dentary. The dorsal median sulcus is also observed on the referred specimen of *P. solvayi* (IRSNB 0107), and may therefore represent an ontogenetic feature, as with the increased robusticity of the jaw elements in the consecutively larger specimens. The otherwise strong resemblance between the two taxa and their recovery as sister taxa in the current phylogenetic analysis support the referral of *P. giganteus* to *P. solvayi*, indicating that *Prognathodon* represents a monotypic genus.

Age—Early Maastrichtian

SQUAMATA Oppel, 1811

MOSASAURIDAE Gervais, 1852

MOSASAURINAE Gervais, 1852

BRACHYSAURANA Strand, 1926

Prognathodon Dollo, 1889a, p. 214

Prognathosaurus Dollo, 1889b, 293, pl. 9 figs. 4–5, pl. 10 figs. 8–9.

Brachysaurus Williston, 1897:96, pl. 8 (preoccupied Hallowell, 1856).

Brachysaurana Strand, 1926:54.

Ancylocentrum Schmidt, 1927:59.

Prognathodon Russell, 1967: 165. figs. 89–90

Type species— *Brachysaurana overtoni*

Diagnosis—As for species

BRACHYSAURANA OVERTONI Strand, 1926:54

comb. nov., transferred from *Prognathodon*

Brachysaurus overtoni Williston, 1897 (preoccupied Hallowell, 1856).

Ancylocentrum overtoni (Williston, 1897): Schmidt, 1927:59 (new combination).

Prognathodon overtoni (Williston, 1897): Russell, 1967:165, figs. 89–90 (new combination).

Holotype—KU 950

Locality—Cheyenne River, South Dakota, USA; upper Pierre Shale, upper Campanian.

Referred specimens—SDSMT 3393, TMP 1983.164.0001, TMP 2002.400.0001, TMP 2007.034.0001, TMP 2018.042.0005

Revised Diagnosis—Modified from Williston (1897), Russell (1967), and Konishi et al. (2011). Medium to large sized mosasaur with large, massively built skull; larger individuals 7-8 meters long; small predental rostrum present; low median dorsal ridge present on internarial bar anteriorly; premaxillary-maxillary suture extending to between third and fourth maxillary teeth; naris elongate, posteriorly ending above mid-section of the 10th maxillary tooth; median dorsal keel on frontal well developed; fine, short longitudinal grooves concentrated on dorsal frontal surface between orbits; parietal foramen small, entirely enclosed within parietal; distinct triangular depression on anterolateral surface of prefrontal; prefrontal and postorbitofrontal overlapping each other and forming dorsal margin of orbit; ectopterygoid extremely robust, transversely as thick as horizontal ramus of jugal; quadrate stapedial pit oblong, with a broader dorsal border; dorsal border of surangular long, approximately two-thirds as long posterior to coronoid and only slightly expanded dorsally, appearing nearly horizontal; 12–13 maxillary teeth; 14–15 dentary teeth; marginal teeth subcircular in basal cross-section, tooth crown surface

ornamented with anastomosing texture concentrated on the apices; up to seven teeth on pterygoid; 10 anterior-most dorsal vertebrae with long, curved ribs; 11–13 pygal vertebrae; 22 intermediate caudal vertebrae; neural spines of dorsal and first-second pygal vertebrae anteroposteriorly broad and tightly contacting along their length; center of terminal caudal neural spines supported by an elongate, thickened section of bone; antebrachial foramen bordered by radius, ulna, and intermedium; hind limb phalangeal formula 4-5-5-3-1.

Differential Diagnosis—Differs from *Prognathodon* in having a more robust skull, short predental rostrum, strongly procumbent anterior teeth, broader, rounder more robust marginal dentition with well-developed anastomosing texture and lacking flutes, overlapping contact between prefrontal and postorbitofrontal, median frontal ridge on frontal, and a rotated retroarticular process. Differs from *Globiden*s in lacking low, rounded, crushing-style marginal teeth. Differs from *Thalassotitan* in having more strongly heterodont dentition, a broader parietal table, dorsal sulcus of the premaxilla, a less dorsally exapanded surangular. It lacks invasion of the external naries on the the anterior margin of the frontal. Further differs in having a less broad and shorter coronoid process, broader anterior portion of frontal, shallower dentary, and less robust jugal (Longrich et al. 2022).

Remarks—*"Prognathodon" overtoni* resembles *Prognathodon* in having a short premaxillary-maxillary suture extending to the third tooth position, a single, blind-ended basioccipital canal, and the prefrontal forming large posterolateral border of the nares. Both taxa also lack an extended tympanic crest of the quadrate. In contrast, it shares a robust skull, short predental rostrum, more blunted dentition lacking flutes, and a rotated retroarticular process with other former species of *Prognathodon*, as well as *Thalassotitan*. As *Prognathodon* was found to be paraphyletic and *"P." overtoni* formed a sister clade with the group containing *Thalassotitan*,

Longrich et al. (2022) tentatively suggested that the name *Brachysaurana* Strand, 1926:54 be considered. The current analyses likewise support this recommendation and therefore refer *Prognathodon overtoni* to *Brachysaurana overtoni*.

Age—upper Campanian

SQUAMATA Oppel, 1811

MOSASAURIDAE Gervais, 1852

MOSASAURINAE Gervais, 1852

THALASSOTITAN Longrich et al. 2022

Mosasaurus (*Leiodon*) cf. *anceps*, Arambourg, 1952

Mosasaurus (*Leiodon*) cf. *anceps*", Machalski et al., 2003

Prognathodon sp., Bardet et al., 2004

Prognathodon sp. nov., Bardet et al., 2008

Prognathodon sp. nov., Bardet et al., 2010

Prognathodon sp. nov., Bardet, 2012

Prognathodon sp., Cappetta et al., 2014

Prognathodon sp. nov., Bardet et al., 2015

Prognathodon sp. nov., Bardet al., 2017

Prognathodon aff. *saturator*, Longrich et al., 2021a

Prognathodon aff. *saturator*, Longrich et al., 2021b

Type species—*Thalasstitan atrox*

Revised Diagnosis—Modified from Longrich et al. (2022). Large mosasaur exceeding 9 meters in length with a robustly-built cranium. Predental rostrum short and blunt on both premaxilla and dentary, interdigitating along premaxillary-maxillary suture, anterodorsal process of maxilla oriented dorsally, ventral margin of maxilla convex, prefrontal broadly overlaps onto frontal; prefrontal contact laterally postorbitofrontal and excluding frontal from orbital margin; narrow dorsolateral surface of postorbitofrontal; frontal short, broad, strongly constricted anteriorly and anteriorly concave at contact with parietal postorbital wings; postorbital processes displaced anteriorly; large posteromedial processes of frontal invading parietal and enclosing small, circular parietal foramen; narrow parietal table constricting in center and with broad posterolateral flanges overhanging the supratemporal fenestrae; horizontal ramus of jugal anteriorly expanded, pterygoid teeth similar in size and shape to marginal dentition; robust quadrate with large fused supra- and posterior pillar-like processes below middle of the shaft; bowed dentary short and deep; tall, anteroposteriorly broad coronoid process triangular in shape, dorsally expanded surangular forming large coronoid buttress; excavation along posterolateral surface of surangular; retroarticular process rotated horizontally relative to the PMU (posterior mandibular unit), 12 maxillary teeth, 14 dentary teeth, marginal dentition massive, conical, and weakly curved posteriorly, anastomosing ridges on crown apex and serrated mesial and distal carinae; humerus short and robust; radius with large anterior process extending to distal facet; short phalanges with broad epiphyses.

Differential Diagnosis—Differs from *Prognathodon* in having a large, robust skull, short blunted predental rostra, marginal teeth shorter, broader and lacking flutes, lacking procumbent anterior tooth crowns, narrower postorbitofrontal, greatly expanded dorsal margin of the

surangular, and horizontally rotated retroarticular process. Also has a longer, narrower parietal table (Longrich et al. 2020).

Age—late Maastrichian

THALASSOTITAN SATURATOR Dortangs et al. 2002

comb. nov., transferred from *Prognathodon*

Prognathodon saturator, Dortangs et al. 2002

Holotype—NHMM 1998141

Locality— ENCI-Maastricht B. V. quarry, 3 km S of Maastricht, The Netherlands

Revised Diagnosis—Modified from Dortangs et al. (2002). Massive, robustly built mosasaur with a large cranium. Median ridge on anterodorsal surface of the frontal; prefrontal excluded from the posterolateral border of the external nares by posterodorsal tongue of maxilla, and also possibly by anterolateral extensions of frontal; triangular supraorbital process of prefrontal overhanging the orbit; prefrontal overlapping postorbitofrontal in ventral view; elongate, large parietal foramen encased in parietal and bounded by elongate posteromedian flanges of the frontal; postorbital processes of parietal broadly exposed in dorsal view; pterygoid bearing thickened ventrally descending tooth-bearing expansion; pterygoid teeth large, similar in size to marginal teeth; six pterygoid teeth; flutes on pterygoid tooth enamel surface; posterior region of skull long and narrow in dorsal view; base of the supratemporal processes originating at posterior margin of postorbital process of parietal and oriented vertically at base; tall, bowed dentary; broad, dorsal expansion of the surangular with a coronoid buttress; retroarticular process oriented obliquely relative to the PMU; suprastapedial and posterior pillar-like processes of

quadrate fused; mediolaterally oriented suture between expanded supra- and posterior pillar-like processes; tympanic crest extending posteriorly from well-developed tympanic ala; robust, circular marginal teeth lacking enamel ornamentation with the exception of anastomosing texture near the crown apex; very weakly heterodont dentition with posterior marginal teeth decreasing in size; vertebrae massively built with large, robust extremities; large zygosphene and zygantra present on cervical and dorsal vertebral series; tightly contacting neural spines of the posterior dorsal vertebrae; haemal arches fused to caudal centra.

Differential Diagnosis—Differs from *Thalassotitian atrox* in having a considerably narrower and more elongate frontal lacking constricted anterior borders, a longer and narrower temporal arcade, a larger, oval parietal foramen, a large anterior fossa on surangular accommodated by the margin of the lateral wing of the coronoid, greater lateral exposure of the splenial and angular at the intramandibular joint, and comparatively larger and more robust cervical and dorsal vertebrae, including the pre- and postzygapophyses, centra, and synapophyseal processes (Longrich et al. 2022; fig. 6). Differs from *Prognathodon* in having a generally more robust skull and skeleton, larger, more robust dentition that is rounded in cross-section and lacks flutes, a narrower, elongate frontal with a dorsal medial ridge, exclusion of the prefrontal from the border of the external nares, overlapping prefrontal and postorbitofrontal, dorsally expanded surangular margin, rotated retroarticular process, and a large quadrate with a broadly expanded tympanic crest enclosing the ala. Differs from *Globidens* in lacking low, rounded, and blunt dentition.

Discussion—Longrich et al. (2020) recovered *Thalassotitan atrox* in a clade alongside "*P." saturator* and *P. currii* and stated that the latter two could either form distinct genera or be referred to *Thalassotitan*. The authors state Thalassotitan differs from *"P." saturator* in having

anterolateral processes of the frontal that extend around the border of the external nares, but this feature is also present in *"P." saturator*. Based on the specimens included in Longrich et al. (2020), it is unclear if the prefrontal is excluded from the border of the external nares, a feature present in *"P." saturator*. There are few major characteristics distinguishing these species; however, with the level of preservation in both species and the removal of the *"P." saturator* from *Prognathodon*, it is recommended that *"P." saturator* be included within *Thalassotitan* due to both its position in the phylogenetic tree produced by Longrich et al. (2020) and the morphological similarities demonstrated here. However, the discovery of better preserved cranial and postcranial material could easily result in any of these robust forms being synonymized.

Age—late Maastrichtian

THALASSOTITAN CF. ATROX (Christiansen & Bonde, 2002)

comb. nov., transferred from *Prognathodon*

Prognathodon currii, Christiansen & Bonde, 2002

Holotype—HUJ.OR 100

Locality— Main Phosphate-Bed IV, Oran Phoshmate Plant, Negev desert, Israel

Diagnosis—Modified from Christiansen & Bonde (2002). Large mosasaur with a massively built cranium. Predental rostra short, internarial bar slender, anterior portion of internarial bar short and bifurcate, frontal wider than long, fronto-parietal suture posteriorly triangular and lateral sides straight, external naris invades posterior part of frontal, prefrontal forms large portion of posterolateral margin of external, prefrontal contacts postorbitofrontal and excludes frontal from orbital rim, horizontal ramus of jugal expands anteriorly, quadrate processes fused,

dentary weakly bowed, anterior section of quadrate ala thin, marginal dentition short and robust with anastomosing texture at the crown apices, teeth bicarinate and conical with blunt apices, serrations variably preset, 11 maxillary teeth, 12 dentary teeth, posterior horizontal inflection on mandibular retroarticular process.

Differential Diagnosis—Differs from *Prognathodon* in having a massively built cranium, short predental rostrum, very weakly procumbent anterior teeth that do not extend beyond the rostrum, short, blunted teeth lacking flutes, and a horizontally oriented retroarticular process. May differ slightly form *Thalassotitan atrox* and *Thalassotitan saturator* in having a shorter parietal and temporal arcade, as well as comparatively smaller and more blunted teeth, fewer teeth in the maxilla and dentary.

Discussion—The preservation of the bone surface in *"P". currii* is such that there are few diagnostic features discernible. The triangular frontoparietal suture that invades the parietal posteriorly may simply be an artefact of taphonomy, and the posterior region of the nares is badly crushed, despite Christiansen & Bonde (2002) stating that the prefrontal forms the posterolateral borders of the external nares. The diagnosable traits *"P". currii* does preserve are nearly identical to those of *Thalassotitan* but are largely distinct from *Prognathodon*. With few to no characteristics that can conclusively distinguish it between *Thalassotitan atrox* and *Thalassotitan saturator*, it is recommended "*P." currii* instead be referred to *Thalassotitan cf. atrox*, which is consistent with its recovery as a sister taxon to *Thalassotitan atrox* in the phylogenetic analysis performed by Longrich et al. (2022). This renders *Prognathodon currii nomen dubium*, barring the discovery of more complete material with which to differentiate it from its congeners.

Age—Late Campanian

SQUAMATA Oppel, 1811

MOSASAURIDAE Gervais, 1852

MOSASAURINAE Gervais, 1852

MARICHIMAERA Street, 2017

Type species—*Marichimaera waiparaensis* (Welles and Gregg, 1971)

Diagnosis—Modified from Street (2017). Blunt-tipped conical edentulous rostrum on premaxilla; jugal with tall dorsal process, robust anterior ramus, and distinct posteroventral process; eight pterygoid teeth; anterior pterygoid teeth similar in size to marginal teeth, erupting from a narrow descending ridge; quadrate process of pterygoid broadly expanded; ectopterygoid with broad medial process and posterior eminence on posterior margin of medial process; robust extension of tympanic ala tightly encloses quadrate conch; deep tympanic ala; quadrate suprastapedial process moderately long, fusion to robust posterior pillar-like process is mediolaterally broad; stapedial pit small, circular; V-shaped splenial/angular articulation with distinct vertical tongue and groove; angular lateral exposure wedge-shaped, but shorter than splenial lateral exposure; coronoid with tall dorsal process and large, tapering posterior wing; dentary with at least 14 teeth; teeth tall, narrow, and laterally compressed, as well as bicarinate, and posteriorly curved; tooth enamel generally smooth, with occasional subtle lingual fluting; atlas centrum long dorsally; elongate posterior process on axis intercentrum; axis peduncle and hypapophysis massive; robust vertebrae; dorsal vertebrae transverse processes without ventral flange but with strong posterior buttress; carpals well ossified; short, hourglass-shaped phalanges.

Differential diagnosis—Similar to *Eremiasaurus Globidens*, *Plesiotylosaurus, Prognathodon*, and *Thalassotitan* in having fused supra- and posterior pillar-like processes of the quadrate, although differs from *Prognathodon* in having a mediolaterally broad fusion, expanded tympanic ala, and large mandibular condyle, as well as a predental rostrum and proportionately more robust vertebrae. Differs from *Globidens* in lacking robust, rounded marginal teeth with well-deleloped anastomosing texture. Differs from *Eremiasaurus* in lacking heterodonty of marginal teeth. Differs from *Plesiotylosaurus* in having expanded tympanic ala of quadrate, a shorter, conical premaxillary rostrum and fewer but larger dentary teeth. Differs from Mosasaurini in the presence of fusion of the supra- and pillar-like processes of the quadrate.

Age—Maastrichtian (Haumurian)

MARICHIMAERA WAIPARAENSIS (Welles and Gregg, 1971)

comb. nov., transferred from *Prognathodon*

Prognathodon waiparaensis Welles and Gregg, 1971

Holotype—CM Zfr-108

Diagnosis—As for genus

Locality/Stratigraphy—Middle Waipara River, South Island, New Zealand/ Maastrichtian (Haumurian) Ladimore Formation

Remarks—The referral of *P. waiparensis* to the comb. nov. *Marichimaera* by Street (2017) is affirmed here, in accordance with its separation from the type species in phylogenetic analysis and lack of features relative to the revised diagnosis of *P. solvayi*. According to Street (2017), *Marichimaera* possess features typical of both *Mosasaurus* and *Prognathodon*. It

resembles *Prognathodon* in having large anterior pterygoid teeth and fused processes of the quadrate, although the overall topology of the quadrate is largely distinct from that of *P. solvayi*. Street (2017) likewise attributes the tapering posterior wing of the coronoid and an abruptly tapered lateral exposure of the angular to *Prognathodon,* although the latter feature is not seen in *P. solvayi*, which has a broader and more gradually tapering exposure of the angular. The conical predental rostrum is more similar to that of *Mosasaurus,* as are the size of the vertebrae and shorter length of the phalanges, although this is more difficult to assess in *P. solvayi*, as large portions of its postcranium are not preserved. Street (2017) also notes that the holotype specimen was collected during separate ventures over several years, and it is possible that it represents more than one individual, and possibly more than one taxon.

MARICHIMAERA SP., Schulp et al. 2008

comb. nov., transferred from *Prognathodon*

Prognathodon kianda, Schulp et al. 2008

Holotype - MGUAN PA 129

Referred Material - MGUAN PA 128, MGUAN PA149, MGUAN PA 150, MGUAN PA 151.

Locality—Bentiaba site 05, 07, Namibe Province, Angola

Diagnosis— Modified from Schulp et al. 2008. Medium-sized mosasaurine mosasaur characterized by a dorsal keel of the internarial bar, short, tapered predental rostrum on the premaxilla and dentary, premaxillary teeth weakly procumbent, comparatively smaller pterygoid teeth, eruption of pterygoid teeth from a ventrally descending narrow ridge, absence of fluted

marginal dentition, marginal teeth weakly heterodont, narrow anterior teeth broadening posteriorly slightly, with posterior-most teeth reduced in size and more strongly hooked, anterior teeth unicarinate and posterior teeth bicarinate, a dorsally expanded dorsal margin of the surangular, a horizontally rotated retroarticular process, presence of a mediolaterally broad fusion between the suprastapedial and posterior pillar-like processes, and presence of a large, expanded tympanic crest, slender, slightly bowed dentary, 15 dentary teeth.

Differential Diagnosis—Differs from *Prognathodon* in the presence of predental rostra lacking fluting on the marginal teeth, mediolaterally broad fusion of the suprastapedial and pillar-like processes of the quadrate, enlarged tympanic crest, comparatively small pterygoid erupting from thin ventrally descending ridge, dorsally expanded surangular, rotated retroarticular process, and higher tooth count. Differs from *Marichimaera waiparensis* in having smaller pterygoid teeth, but lacking facets and/or flutes, although the teeth of *Marichimaera waiparensis* are also mostly smooth.

Remarks—Discernable diagnostic features on the available material of *"P". kianda* is currently very limited, and only some features, such as fused processes of the quadrate and dorsally oriented processes of the maxillae are shared with *Progmathodon*. In contrast, several of these traits are instead shared with *Marichimaera waiparensis.* The Co-UMP analyses resolved *"P". kianda* and *Marichimaera waiparensis* as closely related but separate taxa, although the latter is occasionally found in a more derived position (Street, 2017). Longrich et al. 2020 recovered *"P". kianda* as the sister taxon to *Eremiasaurus heterodontus* alongside *"P". waiparensis* in a clade separate from *Prognathodon*, although the dentition and shape of the maxilla and dentary of *Eremiasaurus* is very different from that of *P. kianda* (Leblanc et al. 2013). The inconsistency in their taxonomic positions is very likely due to their highly

fragmented cranial and sparse postcranial material (i.e., virtually undescribed in *"P". kianda"*). Nevertheless, the quadrates of *"P". kianda* and *Marichimaera waiparensis* are remarkably similar (Fig. 7.2), both possessing large, robust quadrates with a mediolaterally broad fusion and extended tympanic crest enclosing the alae. The jugals are also similar in possessing a curved horizontal ramus and a broad-based and vertically oriented vertical ramus. The remnants of a small posteroventral process may also be present in *"P". kianda*. Both also share a short, conical predental rostrum and weakly procumbent premaxillary teeth. Apart from its removal from *Prognathodon*, the comparatively poor preservation in both taxa precludes other well-supported conclusions regarding its taxonomy, therefore it is tentatively referred to *Marichaemera*. This is likely to change with the description of more complete specimens.

Age—Campanian-Maastrichtian (Piripauan-Haumurian)

EREMIASAURUS MOSASAUROIDES, LeBlanc et al., 2012

comb. nov., transferred from *Prognathodon*

Liodon mosasauroides Gaudry, 1892

Leiodon mosasauroides Lingham-Solar, 1993

Prognathodon mosasauroides Schulp et al. 2008

Liodon mosasauroides Longrich et al. 2020

Holotype—MNHN 1891-14

Locality—Cardess, France

Revised Diagnosis—Modified from Lingham-Soliar (1993). Medium-sized mosasaurine mosasaur with an elongate snout and short conical rostrum; paired parallel ridges on

posterodorsal surface of premaxilla; dorsal keel on internarial bar; network of grooves and foramina on anterolateral surface of maxilla; deep interdental pits on anterior maxilla and dentary; predental pit preceding first tooth position on dentary; dentary with straight dorsal and ventral margins; slender anterior marginal teeth, broad, labiolingually compressed teeth midway and posteriorly in jaw; interdigitating anterior marginal teeth; non-trenchant carinae; serrations on carinae.

Differential diagnosis—Differs from *Eremiasaurus heterodontus* in having a comparatively larger maxilla and dentary, longer premaxillary-maxillary suture extending five tooth positions rather than four, interdental pits occurring further posteriorly, bicarinate anterior teeth, slightly less pronounced heterodonty, shearing fourth to ninth maxillary teeth that do not overlap those on the dentary, and smooth enamel surfaces. Differs from *Prognathodon* in having a predental rostrum on premaxilla and dentary, medially oriented anterodosral of the maxilla, long premaxillary-maxillary suture, straight anterior teeth, and smooth enamel surfaces.

Age—Late Cretaceous (Marnes de Nay Formation, Maastrichtian?)

MOSASAURINAE INCERTAE SEDIS

Leiodon compressidens Gaudry 1892

Mosasaurus compressidens Lingham-Soliar, 1993

Prognathodon compressidens Schulp et al. 2008

Mosasaurinae incertae sedis

Holotype—MNHN-Z-C-1878-5

Locality—Michery, France

Revised Diagnosis—Mosasaurine mosasaur with slender jaws and small teeth. Premaxilla with short, conical rostrum and constricted lateral margins; slender, long maxilla with premaxillary-maxillary suture extending five tooth positions; narrow, bowed dentary; slender, anterior teeth that broaden posteriorly, anterior margins of crowns convex, posterior margins straight; anterior teeth circular in cross-section, labiolingually compressed middle and posterior teeth; weak faceting may be present on posterior crowns; middle crowns with partial carinae; posterior teeth bicarinate and trenchant; serrations on carinae absent.

Differential Diagnosis—Differs from *Prognathodon* in having a conical predental rostrum, a long premaxillary-maxillary suture, elongate and slender maxilla, and smaller, smooth marginal teeth. Lacks procumbent anterior teeth.

Age—Campanian

Leiodon sectorius Cope, 1871: 41

Tylosaurus sectorius Cope: Merriam, 1894: 25

Leiodon sectorius Lingham-Soliar, 1993

Prognathodon sectorius Schulp et al. 2008

Mosasaurinae incertae sedis

Holotype—AMNH 1401

Locality—Pemberton Marl Company pit (Navesink), Navesink Formation, New Jersey

Referred Material—NHMM 00414(?), NHMM LV 150 (?), OIGM – LU 799(?)

Revised Diagnosis—Modified from Cope (1871) and Lingham-Soliar (1993). Straight, slender dentary; low shelf on medial surface of dentary ventral to the tooth row; interdental pits on lateral surface of dentary from the first to seventh tooth position; sixteen, possibly more,

dentary teeth; heterodont dentition with anterior narrow, curved crowns that broaden posteriorly; anterior teeth slightly procumbent but dentary extends anterior to first tooth position; anterior dentary tooth crowns circular in cross-section and lacking carinae, posteriorly become compressed and elliptical in shape; central longitudinal groove may be present in anterior maxillary and dentary crowns; crowns midway on dentary with convex anterior and straight posterior margins; faint facets and/or horizontal ribbing on some posterior crowns.

Differential Diagnosis—Differs from *Prognathodon* in having a narrower, unbowed dentary, predental rostrum on dentary, and marginal teeth lacking prominent flutes.

Age—Maastrichtian

Clidastes (?) *lutugini* sp. n.: Yakovlev, 1901

Dollosaurus lutugini: Yakovlev, 1905

Prognathodon lutugini: Lingham-Soliar, 1989

Mosasaurinae incertae sedis

Holotype—CCMGE 818

Locality— Krymskoe village, Slavyanoserbsk District, Lugansk Province of Ukraine

Referred Material—NHMM 00414(?), NHMM LV 150 (?), OIGM – LU 799(?)

Revised Diagnosis—Modified from Russell (1967) and Grigoriev (2013). Bowed dentary lacking predental rostrum; ventrally descending tooth-bearing ridge on ptergygoid; pterygoid teeth large in size; distinct horizontal tongues and grooves on splenial-angular facets; 13 dentary teeth; condyles of anterior trunk vertebrae slightly depressed; cervical vertebrae nearly equal in size to the longest vertebrae in the column; haemal arches fused to caudal vertebrae.

Differential Diagnosis— Differs from *Prognathodon* in having a ventral tooth-bearing ridge on the pterygoid and smooth tooth crowns.

Remarks—Russell (1967) stated that the premaxilla of CCMGE 818 lacked a predental rostrum and no dentary extension beyond the first tooth position. Grigoriev (2013) reported on a description that also noted the base of the first premaxillary tooth was inclined, although the premaxilla is currently lost. Coupled with the large pterygoid teeth, CCMGE 818 could conceivably represent a valid species within *Prognathodon*. However, because other mosasaurines have been shown here to have large pterygoid teeth (e.g. *Thalassotitan*) and the specimen is very sparce and fragmented, there are not enough diagnostic traits present to definitively refer this specimen to any lower-level taxon.

Age—upper Campanian

Marcosaurus laevis in part, Leidy, 1865

Liodon validus Cope, 1869-1870

Tylosaurus rapax Hay, 1902

Ancylocentrum hungerfordi Chaffee, 1939

Prognathodon rapax Russell, 1967

Mosasaurinae incertae sedis

Holotype—AMNH 1490

Locality—Navesink Formation, New Jersey

Remarks—AMNH 1490 consists of only two right quadrates. Lucas et al. (2005) stated a second referred specimen comprised of a similar quadrate, isolated teeth, fragments of the jaw, and isolated trunk vertebrae. Other referred specimens also only consist of fragmentary and

partial skeletons. Although having fused processes of the quadrate, the left quadrate of the holotype has a mediolaterally broad fusion consistent with the posterior pillar-like process and a mediolaterally expanded mandibular condyle (Russell, 1967: fig. 91; Palci et al. 2021), which is present in many mosasaurine genera, but not *Prognathodon*. There is currently not enough material containing clear diagnostic characters to refer this taxon with any confidence.

Age—Maastrichtian

Tenerasaurus hashimi Kaddumi, 2009

Prognathodon hashimi Lindgren et al. 2013

Mosasaurinae incertae sedis

Holotype—ERMNH HFV 197

Locality—Muwaqqar Chalk Marl Formation (MCMF), Harrana, Jordan

Remarks—ERMNH HFV 197 consists of an articulated postcranial skeleton and was referred to *Prognathodon* based on similarities of the postcranium. The revised model of *Prognathodon* is not based on extensive postcranial features as only isolated vertebrae, ribs and fragmented pectoral girdle elements are represented. *Brachysaurana overtoni* preserves the best most comparable postcranial material; however, the description of TMP 2018.042.0005 in Chapter 5 and Konishi et al. (2011) noted that the hindlimb morphology in particular was strongly reminiscent of *Clidastes*. A lack of diagnostic features results from the high potential for ambiguity and the lack of a cranium, indicating this specimen cannot be confidently referred to a specific taxon at this time.

Age—Maastrichtian

Prognathodon hudae Kaddimi, 2009

Mosasaurinae incertae sedis

Holotype—ERMNH HFV 277

Locality—Muwaqqar Chalk Marl Formation (MCMF), Harrana, Jordan

Remarks— ERMNH HFV 277 consists of a fragmented left and right dentary with teeth. The diagnosis included weakly heterodont marginal dentition, with narrow anterior crowns becoming progressively blunter, and large mesial and distal carinae. Neither of these features are specifically indicative of *Prognathodon* to the exclusion of other mosasaurine taxa. The dentary also appears straight rather than bowed and extends beyond the first tooth position. Beyond this, ERMNH HFV 277 is deemed too fragmentary to be diagnostic.

Age—Maastrichtian

CHAPTER 9. SUMMARY AND CONCLUDING STATEMENTS

For much of its history, the taxonomic status of *Prognathodon* has fluctuated greatly with respect to its ingroup relationships as well as amongst other well-established mosasaur clades. The primary focus of this study has therefore been to address the multitude of issues that have carried forward and prevented a clear understanding of what defines the genus, what species it contains, and where and how it is situated within the Mosasaurinae.

To do so, the holotype of type species, *Prognathodon solayi* Dollo, 1889a underwent a thorough redescription that both refined previous characters and identified new diagnostic traits with which an expanded and concise generic and species diagnosis was formulated. Two referred specimens were also compared, finding no difference between the generic and species diagnosis. An assessment of the features that led researchers to initially assign the genus to the Plioplatecarpinae determined these were likely homoplastic and confirmed the conclusions of later studies that referred *Prognathodon* to the Mosasuarinae. A historical review of the earliest descriptions of *P. solvayi* found recurring issues in terms of accuracy in subsequent descriptions as new taxa were added over time, as well as revealed numerous inconsistencies in how the type species was interpreted within a phylogenetic framework. This set of observations cast doubt on the notion that *Prognathodon* represents a group of uniquely large, massively built mosasaurs.

A systematic survey of six referred taxa that were compared against the type species and the revised generic diagnosis of *Prognathodon* recovered the following results: (1) *Prognathodon giganteus* Dollo, 1904 with a few exceptions, was largely indistinguishable from the type species, rectifying previous interpretations that described them as distinct. The synonymization of these taxa is further supported by their occurrence within the same

stratigraphic assemblage. Based on amended the interpretation of certain osteological features from previous descriptions, the addition of previously undescribed elements from the braincase and postcranium, and newly identified diagnostic features, (2) *Prognathodon saturator* Dortangs et al., 2002 was readily distinguishable from *P. solvayi*, and recognized as a likely invalid member of the genus. (3) Although it shares some features in common with *Prognathodon, P. overtoni* Williston, 1897 is likely also not assignable to the genus. The comparison with *P. solvayi* was combined with a description of a new, exceptionally well-preserved specimen of *P. overtoni* that preserves the first articulated forelimb described within the genus, as well as a simple assessment using ratios of the skull that uncovered little osteological variation between the new specimen and its conspecifics in spite of its larger size, finding no significant indicator of any major ontological variation. (4) The removal of four taxa originally attributed to *Liodon* Owen, 1841 from *Prognathodon* was based on a lack of evidence of similarity that primarily stemmed from the fragmentary nature of the specimens. Although most specimens are too fragmented to confidently assign to a specific taxon, *Liodon mosasauroides* was assigned to genus *Eremiasaurus* due to its strong resemblance with *Eremiasaurus heterodontus*.

The data garnered from these detailed morphological comparisons was subsequently incorporated into a broad-scale phylogenetic analysis, resulting in substantial changes to the character state codings of several taxa, as well as the addition of new characters. In agreement with numerous studies that reported similar results (Leblanc et al. 2012; Simões et al. 2017a, Street, 2017; Strong et al. 2020; Longrich et al. 2022; Zietlow et al. 2023), *Prognathodon* was recovered as a paraphyletic group, as was the Globidensini; historically considered to be a monophyletic group containing *Prognathodon* and other purportedly closely related taxa. *P. solvayi* and *P. giganteus* were recovered as sister taxa alongside other *Prognathodon* species

within a Hennigian comb comprising of single taxon clades, ultimately agreeing with the morphology-based hypotheses regarding the affinities of the referred members within the genus. The following taxonomic revision of *Prognathodon* resulted in the exclusion of most referred species, including *Prognathodon currii* Christiansen & Bonde, 2002*, Prognathodon kianda* Schulp et al. 2008, *Prognathodon overtoni, Prognathodon saturator*, and *Prognathodon waiparensis* Welles and Gregg, 1971, and their assignment to different genera. More poorly preserved taxa that lack diagnostic features, namely *Liodon*, *Prognthadon hudae* Kaddumi 2009, *P. hashimi* Kaddumi 2009, *Prognathodon lutugini* Yakovlev, 1901*, Prognathodon rapax* Hay, 1902 were summarily reassigned or rendered as *incertae sedis*. This analysis also demonstrated that key features traditionally considered as characteristic of *Prognathodon,* such as the fused processes of the quadrate, are less informative than previously thought due to its widespread occurrence in numerous another mosasaurine mosasaurus.

This broadscale systematic and taxonomic revision ultimately demonstrates that the current concept of *Prognathodon* as a diverse clade of large, robust mosasaurs is unsupported. The recognition of *P. giganteus* as a synonym of *P. solvayi* establishes *Prognathodon* as a monotypic genus consisting solely of *Prognathodon solvayi*.

REFERENCES

Bardet, N., Cappetta, H., Suberbiola, X.P., Mouty, M., Maleh, A., Ahmad, M., Khrata, O., Gannoum, N. 2000. The marine vertebrate faunas from the Late Cretaceous phosphates of Syria. Geological Magazine. 137. 269-290. 10.1017/S0016756800003988.

Bardet, N., Suberbiola, X.P., Corral, J.C., Baceta, J., Torres, J., Botantz, B., Gorka, M. 2012. A skull fragment of the mosasaurid *Prognathodon cf. sectorius* from the Late Cretaceous of Navarre (Basque-Cantabrian Region). Bulletin de la Societe Geologique de France. 183. 117-121.

Bell, G.L. Jr. A phylogenetic revision of North American and Adriatic Mosasauroidea In: editors: Callaway JM, Nicholls EL. Ancient Marine Reptiles. San Diego: San Diego: Academic Press; 1997. pp. 293–332.

Bell, G.L., Jr, and M.J. Polcyn. 2005. Dallasaurus turneri, a new primitive mosasauroid from the Middle Turonian of Texas, and comments on the phylogeny of Mosasauridae (Squamata). Netherlands Journal of Geosciences 84: 177– 194.

Caldwell, M.; Diedrich, C. 2005. Remains of Clidastes Cope, 1868, an unexpected mosasaur in the upper Campanian of NW Germany. Netherlands Journal of Geosciences 84. 10.1017/S0016774600020990.

Christiansen, P.; Bonde, N. 2002. A new species of gigantic mosasaur from the Late Cretaceous of Israel. Journal of Vertebrate Paleontology, 22 (3): 629.

Conrad, J. L. 2008. Phylogeny and systematics of Squamata (Reptilia)based on morphology. Bulletin of the American Museum of Natural History 310:1–182.

Cope, E. D. 1871a. Supplement to the “Synopsis of the Extinct Batrachia and Reptilia of North America.” Proceedings of the American Philosophical Society, 12 (86): 41–52.

Cope, E.D. 1871b. Catalogue of the Pythonomorpha found in the Cretaceous strata of Kansas. Proceedings of the American Philosophical Society (separate): 1-24.

Cuthbertson R, Maddin HC, Holmes R, Anderson JS. The braincase and endosseous labyrinth of *Plioplatecarpus peckensis* (Mosasauridae, Plioplatecarpinae), with functional implications for locomotor behaviour. Anat Rec. 2015; 298 (9):1597–611.

Deperet, C. Russo, P. 1925. Les phosphates de Melgou (Maroc) et leur faune de mosasuariens et de crocodiliens. Bull. Soc. geol. Fr. 4 (5): 329–346.

Dortangs, R.W.; Schulp, A.S.; Mulder, E.W.A.; Jagt, J. W. M.; Peeters H. H. G.; Graaf. D.T. 2002. A large new mosasaur from the Upper Cretaceous of the Netherlands. Netherlands Journal of Geosciences/Geologie en Mijnbouw, 81(1):1–8.

Dollo L. 1889*a*. Note sur les Vertébrés fossiles récemment offerts au Musée de Bruxelles par M. Alfred Lemonnier. Bulletin de la Société belge de Géologie, de Paléontologie et d'Hydrologie, 3: 181–182.

Dollo L. 1889*b*. Première note sur les mosasauriens de Mesvin. Mémoires De La Société belge de Géologie, de Paléontologie et D'Hydrologie, 3: 271–304.

Dollo, L. 1904. Les mosasauriens de la Belgique**.** Bulletin de la Société Belge de Géologie, de Paléontologie et Hydrologie.18, mémoires: 207-216.

Dollo, L. 1909. The fossil vertebrates of Belgium. Annals of the New York Academy of Sciences, 19: 99-119.

Gaudry, A., 1892. Les Pythonomorphes de France. Mémoires de la Société géologique de France (Paléontologie) 3 (3)(10): 1–13

Gervais, P. 1852. Zoologie et Paléontologie Françaises (Animaux Vertébrés), First. ed. Libraire de la Société de Géographie.

Goloboff, P.A. and Morales, M.E. 2023. TNT version 1.6, with a graphical interface for MacOS and Linux, including new routines in parallel. Cladistics 39: 144-153.

Grigoriev, D. V. 2013. Redescription of Prognathodon lutugini (Squamata, Mosasauridae). 1. Proceedings of the Zoological Institute RAS, 317: 246–261.

Hallowell, E. 1856. Notes on the reptiles in the collection of the Academy of Natural Sciences of Philadelphia. Proceedings. Academy of Natural Sciences of Philadelphia, 8: 221–238.

Hay. 1902. Bibliography and catalogue of the fossil Vertebrata of North America. United States Geological Survey Bulletin, 179: 1-868.

Holmes, R. 1996. *Plioplatecarpus Primaevus* (Mosasauridae) from the Bearpaw Formation (Campanian, Upper Cretaceous) of the North American Western Interior Seaway. Journal of Vertebrate Paleontology. 16 (4): 673–687.

Hornung JJ, Reich M. 2015. Tylosaurine mosasaurs (Squamata) from the Late Cretaceous of northern Germany. Netherlands Journal of Geosciences - Geologie en Mijnbouw. 94 (1): 55–71.

Ikejiri, T., Lucas, S.G. 2014. Osteology and taxonomy of *Mosasaurus conodon* Cope 1881 from the Late Cretaceous of North America. Netherlands Journal of Geosciences. 94 (1): 39-54.

Kaddumi, H. F. 2009. A new species of *Prognathodon* (Squamata: Mosasauridae) from the Maastrichtian of Harrana. In: Fossils of the Harrana Fauna and the adjacent areas. Eternal River Museum of Natural History, Amman, pp 65-71.

Kaddumi, H.F. 2009. Fossils of the Harrana Fauna and the Adjacent Areas. Publications of the Eternal River Museum of Natural History, Amman. 324 pp.

Kass, M. 1999. *Prognathodon stadtmani* (Mosasauridae): a new species from the Mancos Shale (lower Campanian) of western Colorado; pp. 275–294 in D. D. Gillette (ed.),

Vertebrate Paleontology in Utah. Utah Geological Survey Miscellaneous Publication 99-1. Utah Geological Survey, Salt Lake City, Utah.

Kuhn, O., 1939. Squamata: Lacertilia et Ophidia. Fossilium Catalogus. I: Animalia., pars 86. *Dr. W*.

Kuypers, M.M.M., Jagt, J.W.M., Peeters, H.H.G. & de Graaf, D.T., 1998. Laat-kretaceische mosasauriers uit Luik-Limburg: nieuwe vondsten leiden tot nieuwe inzichten. Publicaties van het Natuurhistorisch Genootschap in Limburg XLI(1): 5–48.

Konishi, Takuya. (2008). A new specimen of *Selmasaurus sp., cf. S. russelli* (Mosasauridae: Plioplatecarpini) from Greene County, western Alabama, USA.

Konishi, T., Brinkman, D., Massare, J.A., Caldwell, M.W. 2011. New exceptional specimens of *Prognathodon overtoni* (Squamata, Mosasauridae) from the upper Campanian of Alberta, Canada, and the systematics and ecology of the genus. Journal of Vertebrate Paleontology 31: 1026–1046. doi:10.1080/02724634.2011.601714

Konishi, Takuya & Caldwell, Michael. (2009). New Material of the Mosasaur *Plioplatecarpus nichollsae*, Clarifies Problematic Features of the Holotype Specimen. Journal of Vertebrate Paleontology. 29: 417-436. 10.1671/039.029.0225.

Konishi, T., Caldwell, M.W., Bell, G.R. 2010. Redescription of the holotype of *Platecarpus tympaniticus* Cope, 1869 (Mosasauridae: Plioplatecarpinae), and its implications for the alpha taxonomy of the genus. Journal of Vertebrate Paleontology. 30 (5): 1410–21.

Konishi, T., & Caldwell, M. W. 2011. Two New Plioplatecarpine (Squamata, Mosasauridae) Genera from the Upper Cretaceous of North America, and a Global Phylogenetic Analysis of Plioplatecarpines. Journal of Vertebrate Paleontology, 31 (4): 754–783.

Leblanc, A.R.H.; Caldwell, M.W.; Bardet, N. 2012. A new mosasaurine from the Maastrichtian (Upper Cretaceous) phosphates of Morocco and its implications for mosasaurine systematics". Journal of Vertebrate Paleontology 32 (1): 82–104.

Leblanc, A. R. H., Caldwell, M. W., & Lindgren, J. 2013. Aquatic adaptation, cranial kinesis, and the skull of the mosasaurine mosasaur *Plotosaurus bennisoni*. Journal of Vertebrate Paleontology, **33** (2), 349–362.

LeBlanc, A.; Mohr, S.; Caldwell, M. 2019. Insights into the anatomy and functional morphology of durophagous mosasaurines (Squamata: Mosasauridae) from a new species of Globidens from Morocco. Zoological Journal of the Linnean Society (186) 4: 1026–1052.

Leidy, J. 1865a. Memoir on the extinct reptiles of the Cretaceous formations of the United States. Smithsonian Inst. Contrib. Knowl. 14 (6): 1-165

Lindgren, J., Siverson, J. 2004. The first record of the mosasaur *Clidastes* from Europe and its palaeogeographic implications. Acta Palaeontologica Polonica 49 (2): 219–234.

Lindgren, J. 2005. Dental and vertebral morphology of the enigmatic mosasaur *Dollosaurus* (Reptilia, Mosasauridae) from the lower Campanian (Upper Cretaceous) of southern Sweden. Bulletin of the Geological Society of Denmark 52 (1): 17–25.

Lindgren, J., Jagt, J.W.M. and Caldwell, M.W. 2007. A fishy mosasaur: the axial skeleton of *Plotosaurus* (Reptilia, Squamata) reassessed. Lethaia 40: 153–160.

Lindgren, J. 2009. Cranial osteology of the giant mosasaur *Plesiotylosaurus* (Squamata, Mosasauridae). Journal of Paleontology. 83 (3): 448–456.

Lindgren, J.; Caldwell, M.W.; Konishi, T.; Chiappe, L.M. (2010). Farke, Andrew Allen (ed.). Convergent Evolution in Aquatic Tetrapods: Insights from an Exceptional Fossil Mosasaur". PLOS ONE. 5 (8): e11998.

Lindgren J., Everhart M.J., Caldwell M.W. 2011. Three-Dimensionally Preserved Integument Reveals Hydrodynamic Adaptations in the Extinct Marine Lizard *Ectenosaurus* (Reptilia, Mosasauridae). PLoS ONE 6 (11): e27343.

Lingham-Soliar, T., Nolf, D. 1989. The mosasaur *Prognathodon* from the Upper Cretaceous of Belgium (Reptilia, Mosasauridae). Bulletin de l'Institut Royal des Sciences Naturelles de Belgique. 59, 137–190.

Lingham-Soliar, T. 1991. Locomotion in mosasaurs. Modern Geology 16:229-248.

Lingham-Soliar, T. 1991. Predation in mosasaurs - A functional approach. In Natural Structures, Principles, Strategies in Models in Architecture. Sondersforschunbereif. 230 (6): 169-177.

Lively, J.R. 2018. Taxonomy and historical inertia: *Clidastes* (Squamata: Mosasauridae) as a case study of problematic paleobiological taxonomy, Alcheringa: An Australasian Journal of Palaeontology, 42 (4): 516-527.

Lively, J. R. 2020. Redescription and phylogenetic assessment of *'Prognathodon' stadtmani*: implications for Globidensini monophyly and character homology in Mosasaurinae. *Journal of Vertebrate Paleontology*: e1784183.

Longrich, N.R.; Jalil, N-E.; Khaldoune, F.; Yazami, O.K.; Pereda-Suberbiola, X; Bardet, N. 2022. *Thalassotitan atrox,* a giant predatory mosasaurid (Squamata) from the Upper Maastrichtian Phosphates of Morocco. Cretaceous Research. 140: 105315.

Maddison, W. P. and D.R. Maddison. 2023. Mesquite: a modular system for evolutionary analysis. Version 3.81. http://www.mesquiteproject.org

Madzia, D. 2020. Dental variability and distinguishability in *Mosasaurus lemonnieri* (Mosasauridae) from the Campanian and Maastrichtian of Belgium, and implications for taxonomic assessments of mosasaurid dentitions, Historical Biology, 32:10, 1340-1354,

Madzia, D.; Cau, A. 2017. Inferring "weak spots" in phylogenetic trees: application to mosasauroid nomenclature. *PeerJ*: 3782.

Martin, J. E. 2007. A new species of the durophagous mosasaur, *Globidens* (Squamata: Mosasauridae) from the Late Cretaceous Pierre Shale Group of central South Dakota, USA. Pages 167-176 in Martin, J. E. and

Mulder, Eric. 1999. Transatlantic latest Cretaceous Mosasaurs (Reptilia, Lacertilia) from the Maastrichtian type area and New Jersey. Geologie en Mijnbouw. 78. 10.1023/A:1003838929257.

Oppel, M. 1811. Die Ordnungen, Familien, und Gattungen der Reptilien als Prodrom Einer Naturgeschichte Derselben. Joseph Lindauer. 86 pp.

Osborn, H. F. (1900). Intercentra and Hypapophyses in the Cervical Region of Mosasaurs, Lizards, and Sphenodon. The American Naturalist, 34 (397), 1–7.

Owen, R. 1841. Odontography, or a Treatise on the Comparative Anatomy of the Teeth; Their Physiological Relations, Mode of Developement, and Microscopic Structure, in the Vertebrate Animals. London, H. Baillière, 1840-45.

Owen, R. 1851. A monograph of the fossil Reptilia of the Liassic formations. Palæontographical society, London.

Palci, A., Caldwell, M. W., Papazzoni, C. A., & Fornaciari, E. (2014). Mosasaurine mosasaurs (Squamata, Mosasauridae) from northern Italy. Journal of Vertebrate Paleontology, 34 (3), 549–559.

Palci, A., M.W. Caldwell, M. N. Hutchinson, T. Konishi, and MS. Y. Lee. 2020. The morphological diversity of the quadrate bone in squamate reptiles as revealed by high-

resolution computed tomography and geometric morphometrics. Journal of Anatomy 236:210–227.

Palci, Alessandro, Takuya Konishi, and Michael W. Caldwell. 2020. A Comprehensive Review of the Morphological Diversity of the Quadrate Bone in Mosasauroids (Squamata: Mosasauroidea), with Comments on the Homology of the Infrastapedial Process. Journal of Vertebrate Paleontology 40 (6).

Parris D. C. (eds.), The Geology and Paleontology of the Late Cretaceous Marine Deposits of the Dakotas. Geological Society of America, Special Paper 427.

Polcyn, M.J., and G.L. Bell, Jr. 2005. *Russellosaurus coheni n. gen., n. sp.*: a 92 million-yearold mosasaur from Texas (USA), and the definition of the parafamily Russellosaurina. 158 Bulletin American Museum of Natural History NO. 310. Netherlands Journal of Geosciences 84: 321–333.

Polcyn, M. J., and Everhart, M. J., 2008, Description and phylogenetic analysis of a new species of *Selmasaurus* (Mosasauridae: Plioplatecarpinae) from the Niobrara Chalk of western Kansas: In: Proceedings of the Second Mosasaur Meeting, edited by Everhart, M. J, Fort Hays Studies, Special Issue number 3, p. 13-28.

Polcyn, M. J., L. L. Jacobs, A. S. Schulp, and O. Mateus. 2010. The North African mosasaur *Globidens phosphaticus* from the Maastrichtian of Angola. *Historical Biology* 22:175–185.

Ritter, D. 1996: Axial muscle function during lizard locomotion. *Journal of Experimental Biology* 199, 2499–2510.

Robaszynski, F. & Christensen, W.K.. 1989. The Upper Campanian-Lower Maastrichtian chalks of the Mons Basin, Belgium: a preliminary study of belemnites and foraminifera in the Harmignies and Ciply areas. Geologie en Mijnbouw, 68 (4) : 391-408.

Russell, D.A. 1967. Systematics and morphology of American mosasaurs. Bulletin of the Peabody Museum of Natural History, Yale University. 23, 1–240.

Schmidt, K. 1927. New reptilian generic names. *Copeia* 163: 58-59.

Schulp, Anne S., et al. 2006. New mosasaur material from the Maastrichtian of Angola, with notes on the phylogeny, distribution and palaeoecology of the genus Prognathodon. On Maastricht Mosasaurs. Publicaties van het Natuurhistorisch Genootschap in Limburg 45 (1): 57-67.

Schulp, A.S., Polcyn, M.J., Mateus, O., Jacbs, L.L., Morais, M.L. 2008. A new species of *Prognathodon* (Squamata, Mosasauridae) from the Maastrichtian of Angola, and the affinities of the mosasaur genus *Liodon*. Proceedings of the Second Mosasaur Meeting: 1–12.

Seeley, HG. 1881. On Remains of a small Lizard from the Neocomian Rocks of Comén, near Trieste preserved in the Geological Museum of the University of Vienna. *Quarterly* Journal of the Geological Society, 37: 52–6.

Simões, T.R., Vernygora, O., Paparella, I., Jimenez-Huidobro, P., Caldwell, M.W. 2017a. Mosasauroid phylogeny under multiple phylogenetic methods provides new insights on the evolution of aquatic adaptations in the group. *PLOS ONE* 12 (5): e0176773.

Simões, T.R., Caldwell, M.W., Palci, A. and Nydam, R.L. 2017b. Giant taxon-character matrices: quality of character constructions remains critical regardless of size. *Cladistics* 33: 198–219.

Simões, T.R., Vernygora, O.V.; de Medeiros, B.A.S., Wright, A.M. 2023. Handling Logical Character Dependency in Phylogenetic Inference: Extensive Performance Testing of

Assumptions and Solutions Using Simulated and Empirical Data. *Systematic Biology* 72 (3): 662–680.

Strand, E. 1926. Miscellanea nomenclatorica zoologica et palaeontologia. Archiv für Naturgeschichte Abt. A. Original-Arbeiten, 92: 30–75.

Street, H.P. 2016. A re-assessment of the genus *Mosasaurus (Squamata: Mosasauridae)* (PDF) (PhD). University of Alberta.

Williston, S. W. 1897. The Kansas Niobrara Cretaceous. University Geological Survey of Kansas. 2: 235-246.

Willman, A.J.; Konishi, T.; Caldwell, M.W. (2021). A new species of *Ectenosaurus* (Mosasauridae: Plioplatecarpinae) from western Kansas, USA, reveals a novel suite of osteological characters for the genus. Canadian Journal of Earth Sciences: 741–755.

Wright, K.R; Shannon, S.W..1988.A new plioplatecarpine mosasaur (Squamata, Mosasauridae) from Alabama. Journal of Vertebrate Paleontology, 8 (1): 102–107.

Yakovlev N.N. 1901. Remains of the Late Cretaceous mosasaur from the south of Russia. Izvestiya Geologicheskogo Komiteta, 20: 507–522.

Yamashita, M., Konishi, T., Sato, T. 2015. Sclerotic Rings in Mosasaurs (Squamata: Mosasauridae): Structures and Taxonomic Diversity. Structures and Taxonomic Diversity. PLOS ONE 10(2): e0117079.

Zietlow, A.R.; Boyd, C.A.; Van Vranken, N.E. 2023. *Jormungandr walhallaensis*: a new mosasaurine (Squamata: Mosasauroidea) from the Pierre Shale Formation (Pembina Member: Middle Campanian) of North Dakota. Bulletin of the American Museum of Natural History (464).

Appendix A. Character descriptions for contingent character coding matrix, modified from Simões et al. (2017b), Konishi & Caldwell (2011), and Strong et al. (2020).

Character list applying contingent coding

(1) Premaxilla predental rostrum I: total lack of a bony rostrum (0); or presence of any predental rostrum (1). In lateral profile, the anterior end of the premaxilla either exhibits some bony anterior projection above the dental margin, or the bone recedes posterodorsally from the dental margin. State 1 produces a relatively taller lateral profile with an obvious ‘bow’ or ‘prow.’

(2) Premaxilla predental rostrum II: rostrum very short and obtuse (0); or distinctly protruding (1); or very large and inflated (2). In *Clidastes* a short, acute, protruding rostrum (state 1) produces a ‘V’-shaped dorsal profile and, as far as is known, is peculiar to that genus. An alternative condition, described as ‘U’- shaped, includes those taxa whose rostral conditions span the whole range of states of characters 1 and 2. Hence, the descriptive character is abandoned in favor of a more informative structure-based series.

(3) Premaxilla shape: bone broadly arcuate anteriorly (0); or relatively narrowly arcuate or acute anteriorly (1). In virtually all lizards the premaxilla is a very widely arcuate and lightly constructed element, and the base of the internarial process is quite narrow as in *Aigialosaurus bucchichi*. All other mosasaurids have a very narrowed premaxilla with the teeth forming a tight curve and the internarial process being proportionally wider (state 1).

(4) Premaxilla internarial bar width: narrow, distinctly less than half of the maximum width of the rostrum in dorsal view (0); or wide, being barely narrower than the rostrum (1).

(5) Premaxilla internarial bar base shape: triangular (0); or rectangular (1). A vertical cross-section through the junction of the internarial bar and the dentigerous rostrum produces an inverted triangle in most taxa. But in state 1, this cross-section is transversely rectangular because the broad ventral surface of the bar is planar.

(6) Premaxilla internarial bar dorsal keel: absent (0); or present (1). In state 1 a ridge rises above the level of a normally smoothly continuous transverse arch formed by the bones of the anterior muzzle.

(7) Premaxilla internarial bar venter: with entrance for the fifth cranial nerve close to rostrum (0); or far removed from rostrum (1). The conduit that marks the path of the fifth cranial nerve from the maxilla into the premaxilla is expressed as a ventrolateral foramen within the premaxillo-maxillary sutural surface at the junction of the internarial bar and the dentigerous rostrum. State 1 includes a long shallow groove on the ventral surface of the bar. Anteriorly, this groove becomes a tunnel entering the bone at an extremely shallow angle, but disappearing below the surface at least 1 cm behind the rostrum.

(8) Frontal shape in front of the orbits: sides sinusoidal (0); or bone nearly triangular and sides relatively straight (1). In state 1, the area above the orbits is expanded and an isosceles triangle is formed by the rectilinear sides. In certain taxa, a slight concavity is seen above the orbits, but anterior and posterior to this, there is no indication of a sinusoidal or recurved edge.

(9) Frontal width: element broad and short (0); intermediate dimensions (1); or long and narrow (2). Mosasauroid frontals can be separated into a group that generally has a maximum length to maximum width ratio greater than 2:1 (state 2), between 1.5:1 and 2:1 (state 1), or equal to or less than 1.5:1 (state 0).

(10) Frontal narial emargination: frontal not invaded by posterior end of nares (0); or distinct embayment present (1). In some mosasauroids, the posterior ends of the nares are concomitant with the anterior terminus of the frontal-prefrontal suture and, therefore, there is no marginal invasion of the frontal by the opening. However, in other mosasauroids this suture begins anterior and lateral to the posterior ends of the nares, causing a short emargination into the frontal.

(11) Frontal midline dorsal keel: absent (0); or low, fairly inconspicuous (1); or high, thin, and well-developed (2).

(12) Frontal ala shape: sharply acuminate (0); or more broadly pointed or rounded (1). In state 0, the anterolateral edge of the ala is smoothly concave, thus helping to form the sharply pointed or rounded and laterally oriented posterior corners. In some forms the anterolateral edge of the ala may be concave, but the tip is not sharp and directed laterally.

(13) Frontal olfactory canal embrasure: canal not embraced ventrally by descending processes (0); or canal almost or completely enclosed below (1). In state 1, very short descending processes from the sides of the olfactory canal surround and almost, or totally, enclose the olfactory nerve.

(14) Frontal posteroventral midline: tabular boss immediately anterior to the frontal-parietal suture absent (0); or present (1). A triangular boss with a flattened ventral surface at the posterior end of the olfactory canal is represented by state 1.

(15) Frontal-parietal suture: apposing surfaces with low interlocking ridges (0); or with overlapping flanges (1). In state 0, an oblique ridge on the anterior sutural surface of the parietal intercalates between a single median posterior and a single lateral posterior ridge from the frontal. In state 1, these ridges are protracted into strongly overlapping flanges. The dorsal trace of the suture can be

quite complex with a portion of the parietal embraced by the posterior extension of these frontal flanges.

(16) Frontal-parietal suture overlap orientation: suture with oblique median frontal and parietal ridges contributing to overlap (0); or with all three ridges almost horizontal (1). In state 0, the median ridge from the frontal and the single parietal ridge are oriented at a distinct angle to the upper skull surface while the outer, or lateral, frontal ridge appears to be nearly horizontal. In *Tylosaurus nepaeolicus* and T. *proriger* (state 1), the obliquity of the intercalating ridges is reclined almost to the horizontal, greatly extending the amount of lateral overlap.

(17) Frontal invasion of parietal I: lateral sutural flange of frontal posteriorly extended (0); or median frontal sutural flange posteriorly extended (1); or both extended (2); or suture straight (3). In all mosasaurines the oblique median frontal sutural ridge extends onto the dorsal surface of the parietal table and embraces a portion of the anterior table within a tightly crescentic midline embayment. In *Plioplatecarpus* and *Platecarpus*, the lateral oblique sutural ridge from the frontal is greatly protracted posteriorly to cause a large, anteriorly convex embayment in the dorsal frontal-parietal suture. In this case the entire posterolateral corner of the frontal is extended backwards to embrace the anterolateral portion of the parietal table on both sides. Consequently, the pineal foramen is very widely embraced laterally and the oblique anterior sutural ridge of the parietal occupies a position inside the embayment within the frontal.

(18) Frontal medial invasion of parietal II: if present, posteriorly extended median sutural flange short (0); or long (1). The median oblique sutural flange is either short, not reaching back to the pineal foramen (state 0), or tightly embraces the foramen while extending backwards to a position even with or beyond its posterior edge (state 1).

(19) Parietal length: dorsal surface relatively short with epaxial musculature insertion posterior, between suspensorial rami only (0); or dorsal surface elongate, with epaxial musculature insertion dorsal as well as posterior (1).

(20) Parietal table shape: generally rectangular to trapezoidal, with sides converging, but not meeting (0); or triangular, with sides contacting in front of suspensorial rami (1); or parietal table elongate, triangular to subrectangular, and highly medially constricted, with a distinct mid- or parasagittal crest anterior to the divergence of the suspensorial rami (2).

(21) Pineal foramen size: relatively small (0); or large (1). If the foramen is smaller than or equal to the area of the stapedial pit, it is considered small. If the foramen is significantly larger or if the distance across the foramen is more than half the distance between it and the nearest edge of the parietal table, the derived state is achieved.

(22) Pineal foramen position I: foramen generally nearer to center of parietal table, well away from frontal-parietal suture (0); or close to or barely touching suture (1); or huge foramen straddling suture and deeply invading frontal (2). Generally in state 1, the distance from the foramen to the suture is about equal to or less than one foramen's length.

(23) Pineal foramen ventral opening: opening is level with main ventral surface (0); or opening surrounded by a rounded, elongate ridge (1).

(24) Parietal posterior shelf: presence of a distinct horizontal shelf projecting posteriorly from between the suspensorial rami (0); or shelf absent (1). In some mosasauroids, a somewhat crescent-shaped shelf (in dorsal view) lies at the posterior end of the bone medial to, and below, the origination of the suspensorial rami.

(25) Parietal suspensorial ramus compression: greatest width vertical or oblique (0); or greatest width horizontal (1). In *Tylosaurus*, the anterior edge of the ramus begins very low on the lateral wall of the descending process, leading to formation of a proximoventral sulcus, but the straps are horizontal distally.

(26) Parietal union with supratemporal: suspensorial ramus from parietal overlaps supratemporal without interdigitation (0); or forked distal ramus sandwiches proximal end of supratemporal (1).

(27) Prefrontal supraorbital process: process absent, or present as a very small rounded knob (0); or a distinct, to large, triangular, or rounded overhanging wing (1).

(28) Prefrontal contact with postorbitofrontal: no contact at edge of frontal (0); elements in contact there (1). State 1 is usually described as the frontal being emarginated above the orbits. Often this character can be evaluated by examining the ventral surface of the frontal where depressions outline the limits of the sutures for the two ventral elements.

(29) Prefrontal-postorbitofrontal overlap: prefrontal overlapped ventrally by postorbitofrontal (0); or prefrontal overlapped laterally (1). Postorbitofrontal ventral overlap of the prefrontal is extreme in *Platecarpus tympaniticus* and *Plioplatecarpus*, such that there is even a thin flange of the frontal interjected between the prefrontal above and the postorbitofrontal below. In *T. proriger*, the postorbitofrontal sends a long narrow process forward to fit into a lateral groove on the prefrontal. In *Plesiotylosaurus*, the overlap is relatively short and more oblique, and there is no groove on the prefrontal.

(30) Postorbitofrontal shape: narrow (0); or wide (1). In *Clidastes* and the *Globidensini*, the lateral extent

of the element is almost equal to half of the width of the frontal and the outline of the bone is basically squared.

(31) Postorbitofrontal transverse dorsal ridge: absent (0); or present (1). In state 1, an inconspicuous, low, and narrowly rounded ridge traces from the anterolateral corner of the parietal suture across the top of the element to disappear behind the origin of the jugal process.

(32) Maxilla tooth number: 20–24 (0); or 17–19 (1); or 15–16 (2); 12–14 (3).

(33) Maxillo-premaxillary suture posterior terminus: suture ends above a point that is anterior to or level with the midline of the fourth maxillary tooth (0); or between the fourth and ninth teeth (1); or level with or posterior to the ninth tooth (2). These somewhat arbitrary divisions of the character states are meant to describe in more concrete terms those sutures that terminate far anteriorly, those that terminate less anteriorly, and those that terminate near the midlength of the maxilla, respectively.

(34) Maxilla posterodorsal process: recurved wing of maxilla dorsolaterally overlaps a portion of the anterior end of the prefrontal (0); or process absent (1).

(35) Maxilla posterodorsal extent: recurved wing of maxilla prevents emargination of prefrontal on dorsolateral edge of external naris (0); or does not (1).

(36) Jugal posteroventral angle: angle very obtuse or curvilinear (0); or slightly obtuse, near 120^{o} (1); or 90^{o} (2).

(37) Jugal posteroventral process: absent (0); or present (1).

(38) Ectopterygoid contact with maxilla: present (0); or absent (1).

(39) Pterygoid tooth row elevation: teeth arise from robust, transversely flattened, main shaft of pterygoid (0); or teeth arise from thin pronounced vertical ridge (1). In state 0, the teeth emanate from the relatively planar surface of the thick, slightly dorsoventrally compressed main shaft of the pterygoid. In state 1, a tall, thin dentigerous ridge emanates ventrally from a horizontal flange that forms the base of the quadratic ramus and the ectopterygoid process, thus causing the main shaft to be trough-shaped. Although the outgroup we selected (*Varanus*) does not possess pterygoid teeth we decided to code the primitive condition as state 0 because that is the condition observed in fossil varanoids like *Ovoo gurval* and basal anguimorphs like *Ophisaurus apodus*.

(40) Pterygoid tooth size: anterior teeth significantly smaller than marginal teeth (0); or anterior teeth large, approaching size of marginal teeth (1). As per the argument discussed for character 40 we coded the outgroup as having state 0.

(41) Quadrate suprastapedial process length: process short, ends at a level well above midheight (0); or of moderate length, ending very near midheight (1); or long, distinctly below midheight (2); suprastapedial process absent (3).

(42) Quadrate suprastapedial process constriction: distinct dorsal constriction (0); or virtually no dorsal constriction (1). Lack of constriction results in an essentially parallel-sided process in posterodorsal view, but can also include the tapering form characteristic of some *Tylosaurus*.
Remarks: This character refers to whether the sides of the suprastapedial process are parallel or not in posterodorsal view. State 0 occurs when there is a localized narrowing or 'pinching' of the suprastapedial process near its attachment with the quadrate shaft, causing the sides of the process to be non-parallel. This is generally typical of mosasaurines (see *Clidastes* as an exemplar). In some

other taxa (e.g., *Selmasaurus*, *Gavialimimus*), the suprastapedial process is 'dorsally constricted' in terms of being broadly medially excavated; however, this is different from the morphology to which the present character is referring. Rather than being 'pinched in' at the junction of the suprastapedial process and quadrate shaft, the sides of the suprastapedial process remain continuous/parallel throughout its length in these taxa (see holotypes of *Gavialimimus* or *Selmasaurus* as exemplars). Based on the above criterion that a parallel-sided process reflects lack of constriction, these taxa would fall under state 1 (dorsal constriction – i.e., the narrowed base of the suprastapedial process – not present).

(43) Quadrate suprastapedial ridge: if present, ridge on ventromedial edge of suprastapedial process indistinct, straight and/or narrow (0); or ridge wide, broadly rounded, and curving downward, especially above stapedial pit (1).

(44) Quadrate suprastapedial process fusion: no fusion present (0); or process fused to, or in extensive contact with, elaborated process from below (1). A posterior rugose area may be inflated and broadened mediolaterally to partially enclose the ventral end of a broad and elongate suprastapedial process as in *Halisaurus*. In *Globidens*, *Prognathodon*, and *Plesiotylosaurus*, the process is fused ventrally to a narrow pedunculate medial extension of the tympanic rim. A similar condition is present in *Ectenosaurus*, except that the tympanic rim is not medially extended and has a short projection that overlaps a portion of the suprastapedial process posteriorly.

(45) Quadrate stapedial pit shape: pit broadly oval to almost circular (0); or relatively narrowly oval (1); or extremely elongate with a constricted middle (2). In state 0, the length to width ratio is less than 1.8:1; in state 1 it ranges from 1.8:1 to 2.4:1; and in state 2, it is greater than 2.4:1.

(46) Quadrate posteroventral ascending tympanic rim condition: ascending ridge small or absent (0); or a

high, elongate triangular crest (1); or a crest extremely produced laterally (2). In state 1, this extended rim causes a fairly deep sulcus in the ventral portion of the intratympanic cavity. In *Plioplatecarpus*, the entire lower tympanic rim and ala are expanded into a large conch (state 2), which tremendously increases the depth of the intratympanic cavity. *In some examples of Prognathodon, the tympanic rim is robust and projects posteriorly.*

(47) Quadrate ala thickness: ala thin (0); or thick (1). In state 0, the bone in the central area of the ala is only about 1 mm thick in medium-sized specimens and that area is usually badly crushed or completely destroyed. Alternatively, the ala extends from the main shaft with only minor thinning, providing a great deal of strength to the entire bone.

(48) Quadrate conch: ala and main shaft encompassing a deeply bowled area (0); or alar concavity shallow (1). A relatively deeper sulcus in the anterior part of the intratympanic cavity and more definition to the ala and the main shaft are features of state 0.

(49) Basisphenoid pterygoid process shape: process relatively narrow with articular surface facing mostly anterolaterally (0); or somewhat thinner, more fan- shaped with a posterior extension of the articular surface causing a more lateral orientation (1).

(50) Quadrate ala groove: absent (0); or long, distinct, and deep groove present in anterolateral edge of ala (1); or groove along dorsal margin of quadrate ala (2).

(51) Quadrate median ridge: single thin, high ridge, dorsal to ventral (0); or ridge low and rounded with divergent ventral ridges (1).

(52) Quadrate anterior ventral condyle modification: no upward deflection of anterior edge of condyle (0);

or distinct deflection present (1). A relatively narrow bump in the otherwise horizontal trace of the anterior articular edge is also supertended by a sulcus on the anteroventral face of the bone.

(53) Quadrate ventral condyle: condyle saddle-shaped, concave in anteroposterior view (0); or gently domed, convex in any view (1).

(54) Basioccipital tubera size: short (0); or long (1). Long tubera are typically parallel-sided in posterior profile and protrude ventrolaterally at exactly 45° from horizontal. Short tubera have relatively large bases that taper distally, and emanate more horizontally.

(55) Basioccipital canal: absent (0); or present as a pair separated by a median septum (1); or present as a single bilobate canal (2).

(56) Dentary tooth number: 20–24 (0); 17–19 (1); 15–16 (2); 14 (3); 13 (4); 12 (5). It is easy to assume this character is correlated with the number of maxillary teeth, except that is not the case in *Ectenosaurus clidastoides*, which has 16 or 17 maxillary teeth and only 13 dentary teeth.

(57) Dentary anterior projection: projection of bone anterior to first tooth present (0); or absent (1).

(58) Dentary anterior projection length: short (0); or long (1). In state 1, the projection of bone anterior to the first tooth is at least the length of a complete tooth space.

(59) Dentary medial parapet: parapet positioned at base of tooth roots (0); or elevated and strap-like, enclosing about half of height of tooth attachment in shallow channel (1); or strap equal in height to lateral wall of bone (2); or medial parapet taller than lateral wall of bone (3). States 1,2, and 3 are possible sequential stages of modification from a classically pleurodont dentition to the typical

mosasaur ‘sub-thecodont’ dentition.

(60) Splenial-angular articulation shape: splenial articulation in posterior view almost circular (0); or laterally compressed (1).

(61) Splenial-angular articular surface: essentially smooth concavoconvex surfaces (0); or distinct horizontal tongues and grooves present (1).

(62) Coronoid shape: coronoid with slight dorsal curvature, posterior wing not widely fan-shaped (0); or very concave above, posterior wing greatly expanded (1).

(63) Coronoid posteromedial process: small but present (0); or absent (1).

(64) Coronoid medial wing: does not reach angular (0); or contacts angular (1).

(65) Coronoid posterior wing: without medial crescentic pit (0); or with distinct excavation (1). In state 1, there is a posteriorly open, ‘C’-shaped excavation in the medial side of the posterior wing of this element.

(66) Surangular coronoid buttress: low, thick, about parallel to lower edge of mandible (0); or high, thin, rapidly rising anteriorly (1). A rounded dorsal edge of the surangular remains almost parallel to the ventral edge as it approaches the posterior end of the coronoid, meeting the latter element near its posteroventral edge in state 0. In state 1, the dorsal edge rises and thins anteriorly until meeting the posterior edge of the coronoid near its apex, producing a triangular posterior mandible in lateral aspect.

(67) Surangular-articular suture position: behind the condyle in lateral view (0); or at middle of glenoid on lateral edge (1); anterior to condyle (2). In state 1, there is usually an interdigitation in the dorsal part of the suture.

(68) Surangular-articular lateral suture trace: suture descends and angles or curves anteriorly (0); or is virtually straight throughout its length (1). In state 1, the suture trails from the glenoid posteriorly about halfway along the dorsolateral margin of the retroarticular process, then abruptly turns anteriorly off the edge and strikes in a straight line for the posterior end of the angular.

(69) Articular retroarticular process inflection: moderate inflection, less than 60^{o} (0); or extreme inflection, almost 90^{o} (1).

(70) Articular retroarticular process innervation foramina: no large foramina on lateral face of retroarticular process (0); or one to three large foramina present (1).

(71) Tooth surface I: teeth finely striate medially (0); or not medially striate (1). In "Russellosaurinae," medial tooth striations are very fine and groups of tightly spaced striae are usually set apart by facets, leading to a fasciculate appearance.

(72) Tooth surface II: teeth not coarsely textured (0); or very coarsely ornamented with bumps and ridges (1). In both species of *Globidens* and in *Prognathodon overtoni*, the coarse surface texture is extreme, consisting of thick pustules, and vermiform or anastomosing ridges. Teeth in *P. rapax* are smooth over the majority of their surface, but usually a few widely scattered, large, very long, sharp-crested vermiform ridges are present.

(73) Tooth facets and/or flutes: absent (0); or present (1). *Halisaurus* teeth are smoothly rounded except

for the inconspicuous carinae. *Clidastes* is described in numerous places as having smooth unfaceted teeth, but many immature individuals and some larger specimens have teeth with three distinct facets on the medial faces. *Mosasaurus* has taken this characteristic to the extreme. This character was combined with former character (74) which coded for the presence of absence of flutes, following the recommendations of Street et al. (2023).

(74) Tooth inflation: crowns of posterior marginal teeth conical, tapering throughout (0); or crowns of posterior marginal teeth swollen near the tip or above the base (1). The rear teeth of *Globidens* and *Prognathodon overtoni* are distinctly fatter than other mosasauroid teeth.

(75) Tooth carinae I: absent (0); or present but extremely weak (1); or strong and elevated (2). *Halisaurus* exhibits the minimal expression of this character (state 1) in that its marginal teeth are almost perfectly round in cross-section; the carinae are extremely thin and barely stand above the surface of the teeth.

(76) Tooth carinae serration: absent (0); or present (1).

(77) Atlas neural arch: notch in anterior border (0); or no notch in anterior border (1).

(78) Atlas synapophysis: extremely reduced (0); or large and elongate (1). In state 1, a robust synapophysis extends well posteroventral to the medial articular surface for the atlas centrum, and it may be pedunculate (*Clidastes*) or with a ventral ‘skirt’ that gives it a triangular shape (*Mosasaurus*). A very small triangular synapophysis barely, if at all, extends posterior to the medial articular edge in state 0.

(79) Zygosphenes and zygantra: absent (0); or present (1). This character assesses only the presence of

zygosphenes and zygantra, not their relative development. Nonfunctional and functional are considered as present. Although the outgroup we selected (*Varanus*) does not possess zygosphene and zygantra we decided to code the primitive condition as present because these structures can be observed in primitive varanoids like *Saniwa*.

(80) Zygosphene and zygantra number: present on many vertebrae (0); or present on only a few (1). As per the argument discussed for character 84 we coded the outgroup as having state 0.

(81) Hypapophyses: last hypapophysis occurs on or anterior to seventh vertebra (0); or on eight or posteriorly (1).

(82) Synapophysis height: facets for rib articulations tall and narrow on posterior cervicals and anterior trunk vertebrae (0); or facets ovoid, shorter than the centrum height on those vertebrae (1).

(83) Synapophysis length: synapophyses of middle trunk vertebrae not laterally elongate (0); or distinctly laterally elongate (1). The lateral extension of the synapophyses from the middle of the trunk is as much as 70–80% of the length of the same vertebra is represented by state 1.

(84) Synapophysis ventral extension: synapophyses extend barely or not at all below ventral margin of cervical centra (0); or some extend far below ventral margin of centrum (1). In state 1, two or more anterior cervical vertebrae have rib articulations that dip well below the centrum, causing a very deeply concave ventral margin in anterior profile.

(85) Vertebral condyle inclination: condyles of trunk vertebrae inclined (0); or condyles vertical (1).

(86) Vertebral condyle shape I: condyles of anterior-most trunk vertebrae extremely dorsoventrally

depressed (0); or essentially equidimensional (1). In state 0, posterior height: width ratios of anterior trunk vertebrae are close to 2:1. In state 1, they are between to 4:3 and 1:1.

(87) Vertebral condyle shape II: condyles of posterior trunk vertebrae not higher than wide (0); or slightly compressed (1). In state 1, the posterior condylar aspect reveals outlines that appear to be higher than wide and even perhaps slightly subrectangular, due to the slight emargination for the dorsal nerve cord.

(88) Vertebral synapophysis dorsal ridge: sharp ridge absent on posterior trunk synapophyses (0); or with a sharp-edged and anteriorly precipitous ridge connecting distal synapophysis with prezygapophysis (1). In state 0, the ridge in question, if present, may be incomplete or it may be rounded across the crest with the anterior and posterior sides about equally sloping.

(89) Vertebral length proportions: cervical vertebrae distinctly shorter than longest vertebrae (0); or almost equal or are the longest (1).

(90) Presacral vertebrae number I: relatively few, 32 or less (0); or numerous, 39 or more (1). Here, presacral vertebrae are considered to be all those anterior to the first bearing an elongate transverse process.

(91) Presacral vertebrae number II: if few, then 28 or 29 (0); 30 or 31 (1).

(92) Sacral vertebrae number: two (0); or less than two (1). Numerous well preserved specimens of derived mosasauroids have failed to show any direct contact of the pelvic girdle with vertebrae in the sacral area. Certainly, no transverse processes bear any type of concave facet for the ilium, and so it is generally assumed that a ligamentous contact was established with only one transverse process.

Depending on one's perspective, it could be said that derived mosasauroids have either no or one sacral vertebra.

(93) Caudal dorsal expansion: neural spines of tail all uniformly shortened posteriorly (0); or several spines dorsally elongated behind middle of tail (1).

(94) Haemal arch length: haemal arches about equal in length to neural arch of same vertebra (0); or length about 1.5 times greater than neural arch length (1). This ratio may be as great as 1.2:1 in state 0. Comparison is most accurate in the middle of the tail and is consistent even on those vertebrae in which the neural spines are also elongated.

(95) Haemal arch articulation: arches articulating (0); or arches fused to centra (1).

(96) Tail curvature: no structural downturn of tail (0); or tail with curved posterior portion (1).

(97) Body proportions: head and trunk shorter than or about equal to tail length (0); or head and trunk longer than tail (1).

(98) Scapula/coracoid size: both bones about equal (0); or scapula about half the size of coracoid (1).

(99) Scapula width: no anteroposterior widening (0); or distinct fan-shaped widening (1); or extreme widening (2). In state 0, the anterior and posterior edges of the scapula encompass less than one quarter of the arc of a circle, but in state 1, the arc is increased to approximately one third. In state 2, the distal margin encompasses almost a half-circle and the anterior and posterior borders are of almost equal length.

(100) Scapula dorsal convexity: if scapula widened, dorsal margin very convex (0); or broadly convex (1). In state 0, the anteroposterior dimension is almost the same as the proximodistal dimension. In state 1, the anteroposterior dimension is much larger.

(101) Scapula posterior emargination: posterior border of bone gently concave (0); or deeply concave (1). In state 1, there is a deeply arcuate emargination on the posterior scapular border, just dorsal to the glenoid. It is immediately bounded dorsally by a corner, which begins a straight-edged segment that continues to the dorsal margin.

(102) Scapula-coracoid suture: unfused scapula-coracoid contact has interdigitate suture anteriorly (0); or apposing surfaces without interdigitation (1).

(103) Coracoid neck elongation: neck rapidly tapering from medial corners to a relatively broad base (0); or neck gradually tapering to a relatively narrow base (1); coracoid neck absent (2). In state 1, this character describes an outline of the bone, which is nearly symmetrical and gracefully fan-shaped, with gently concave, nearly equidistant sides.

(104) Coracoid anterior emargination: present (0); or absent (1).

(105) Humerus length: humerus distinctly elongate, about three or more times longer than distal width (0); or greatly shortened, about 1.5 to 2 times longer than distal width (1); or length and distal width virtually equal (2); or distal width slightly greater than length (3).

(106) Humerus postglenoid process: absent or very small (0); or distinctly enlarged (1).

(107) Humerus glenoid condyle: if present, condyle gently domed and elongate, ovoid in proximal view (0); or condyle saddle-shaped, subtriangular in proximal view and depressed (1); or condyle highly

domed or protuberant and short ovoid to almost round in proximal view (2). In some taxa, the condylar surfaces of the limbs were finished in thick cartilage and there was no bony surface of the condyle to be preserved. This condition is scored as not represented. In some taxa, the glenoid condyle extends more proximally than does the postglenoid process (state 2), and it is not ovoid as state 0.

(108) Humerus deltopectoral crest: crest undivided (0); or split into two separate insertional areas (1). In state 1, the deltoid crest occupies an anterolateral or anterior position confluent with the glenoid condyle, while the pectoral crest occupies a medial or anteromedial area that may or may not be confluent with the glenoid condyle. The deltoid crest is often quite short, broad, and indistinct, being easily erased by degradational taphonomic processes.

(109) Humerus pectoral crest: located anteriorly (0); or medially (1). In state 1, the pectoral crest is located near the middle of the flexor (or medial) side on the proximal end of the bone.

(110) Humerus ectepicondylar groove: groove or foramen present on distolateral edge (0); or absent (1).

(111) Humerus ectepicondyle: absent (0); or present as a prominence (1). A radial tuberosity is reduced in size in *Prognathodon*, but very elongated in *Plesiotylosaurus*.

(112) Humerus entepicondyle: absent (0); or present as a prominence (1). The ulnar tuberosity protrudes posteriorly and medially from the posterodistal corner of the bone immediately proximal to the ulnar facet, causing a substantial dilation of the posterodistal corner of the humerus.

(113) Radius shape: radius not expanded anterodistally (0); or slightly expanded (1); or broadly expanded (2).

(114) Ulna contact with centrale: broad ulnare prevents contact (0); or ulna contacts centrale (1). In state 1, the ulnare is omitted from the border of the antebrachial foramen. There is usually a well-developed faceted articulation between the ulna and the centrale (or intermedium, as used by Russell, 1967).

(115) Radiale size: large and broad (0); or small to absent (1).

(116) Carpal reduction: carpals number six or more (0); or five or less (1).

(117) Pisiform: present (0); or absent (1).

(118) Metacarpal I expansion: spindle-shaped, elongate (0); or broadly expanded (1). The broad expansion is also associated with an anteroproximal overhanging crest in every case observed.

(119) Phalanx shape: phalanges elongate, spindle-shaped (0); or blocky, hourglass-shaped (1). *Mosasaurus* and *Plotosaurus* have phalanges that are slightly compressed and anteroposteriorly expanded on both ends.

(120) Ilium crest: crest blade-like, articulates with sacral ribs (0); or elongate, cylindrical, does not articulate with sacral ribs (1).

(121) Ilium acetabular area: arcuate ridge supertending acetabulum (0); or acetabulum set into broad, short ‘V’-shaped notch (1). The primitive ilium has the acetabulum impressed on the lateral wall of the bone, with a long narrow crest anterodorsally as the only surrounding topographic feature. In state 1, the acetabular area is set into a short, broadly ‘V’-shaped depression that tapers dorsally. The lateral walls of the ilium are therefore distinctly higher than the rim of the acetabulum.

(122) Pubic tubercle condition: tubercle an elongate protuberance located closer to the midlength of the shaft (0); or a thin semicircular crest-like blade located close to the acetabulum (1).

(123) Ischiadic tubercle size: elongate (0); or short (1). In state 0, the tubercle is as long as the shaft of the ischium is wide, but it is only a short narrow spur in state 1.

(124) Astragalus: notched emargination for the crural foramen, without pedunculate fibular articulation (0); or without notch, pedunculate fibular articulation present (1). For state 0, the tibia and fibula are of equal length about the crural foramen and the astragalus contacts both to about the same degree. The form of the latter element is symmetrical and subcircular with a sharp proximal notch. In state 1, the outline of the element is basically reniform and the tibial articulation is on the same line as the crural emargination. The fibula is also shortened and its contact with the astragalus is narrow.

(125) Appendicular epiphyses: formed from ossified cartilage (0); or from thick unossified cartilage (1); or epiphyses missing or extremely thin (2). Ends of the limb bones show distinct vascularization and rugose surfaces indicating an apparently thick non-vascularized, unossified cartilage cap. Extremely smooth articular surfaces suggest the epiphyses were excessively thin or perhaps even lost.

(126) Hyperphalangy: absent (0); or present (1). Hyperphalangy is defined as presence of one or more extra phalanges as compared to the primitive amniote formula of 2-3-4-5-3.

(127) Posterior thoracic vertebra: not markedly longer than anterior thoracic vertebrae (0); or are markedly longer (1).

(128) Ectopterygoid process of pterygoid: distal portion of process not offset anterolaterally and/or

lacking longitudinal grooves and ridges (0); distal portion of process is offset anterolaterally and bears longitudinal grooves and ridges (1).

(129) Quadrate mid-shaft lateral deflection: absent (0); present (1). In state 1, the quadrate shaft is bent laterally such that the suprastapedial process is deflected dorsolaterally relative to the main shaft of the quadrate.

NB: the wording of this character has been modified from Konishi and Caldwell (2011). The original character was phrased as "Quadrate mid-shaft medial bending," referring to the bend itself projecting medially, resulting in the ventromedial/dorsolateral deflection of the quadrate. The wording was changed to avoid confusion, as the original phrasing gave the impression of the dorsal quadrate shaft and suprastapedial process being deflected medially, when in reality they are deflected laterally [e.g., see amended diagnosis of quadrate in Konishi (2008); see also specimens GSATC 221 (*S. russelli* holotype) and ALMNH PV 995.4.1 (*Selmasaurus* quadrate, cf. *S. russelli*)].

(130) Ventral synapophyseal crest of the cervical vertebrae: absent (0); present (1). In state 1, a thin crest or ridge connects the ventral margin of the synapophyses to the lateral margin of the centrum.

(131) Anterodorsal process of the maxilla: absent (0); present (1). When present, the anterodorsal process forms a peak where it meets the junction at the dorsal extent of the premaxillary-maxillary suture and anterior margin of the external nares.

(132) Anterodorsal process orientation: dorsally (0); medially (1). In state 0, the anterodorsal process is oriented so that it is visible in lateral view. In state 1, the process is folded medially and therefore hidden in lateral view.

Appendix B. Character matrix modified from Strong et al. (2020)

Adriosaurus suessi

0 - 0 0 ? ? ? 1 0 1 0 1
? ? 0 0 0 0 ? ? 1 0 ? 0
? ? 1 0 ? 0 ? ? ? 0 0 ?
? 0 ? ? ? ? ? ? ? ? ? ?
? ? ? ? ? ? ? ? ? ? ? ?
? ? ? ? ? 0 ? 0 ? ? ? ?
? ? ? ? ? ? 1 ? 1 ? 0 ?
? ? ? 0 1 1 - 0 1 0 0 0
0 ? ? ? ? ? ? 0 1 0 ? ?
? ? ? ? 1 ? ? ? ? 1 0 0
0 ? ? ? 1 0 0 ? ? ? ? ?

Dolichosaurus longicollis

? ? ? ? ? ? ? ? ? ? ? ?
? ? ? ? ? ? ? ? ? ? ? ?
? ? ? ? ? ? ? ? ? ? ? ?
? ? ? ? ? ? ? ? ? ? ? ?
? ? ? ? ? ? ? ? ? ? ? ?
0 0 ? ? ? ? ? ? ? ? ? ?
? ? ? ? ? ? 1 0 1 1 0 0
0 0 0 0 1 1 - 0 ? ? 0 0
? 1 0 - ? 0 0 1 1 ? ? ?
? ? ? ? 1 ? ? ? ? ? ? 0
? ? ? ? 2 ? 0 ? ? ? ? ?

Pontosaurus kornhuberi

0 - 0 0 1 0 1 0 1 1 0 1
? ? 0 - 3 - 0 0 0 0 ? 1
1 ? 1 0 - 1 0 ? 0 1 - 1
0 ? ? ? ? ? ? ? ? 0 1 0
? 0 ? 0 ? ? ? ? 1 - ? ?
? ? ? ? ? 0 ? ? 0 0 ? 0
1 0 ? ? 1 0 1 0 1 0 0 ?
? ? ? 0 1 1 - 0 0 0 0 0
0 0 0 - 0 1 2 ? 0 ? ? ?
? ? 1 1 0 ? 0 ? ? 0 0 0
0 1 ? 1 0 0 0 ? 0 ? ? ?

Aigialosaurus dalmaticus

? ? ? ? ? 0 ? 1 2 1 0 0
? ? 0 - 3 - 0 0 0 0 ? 1
1 0 0 0 - 1 0 ? ? 0 0 1
0 ? ? ? 3 - - - ? 0 1 1

?	0	?	?	?	0	0	?	?	?	?	?
0	0	?	?	?	0	2	0	0	1	?	0
0	0	?	?	1	0	?	?	?	0	0	0
?	?	?	0	1	0	0	0	?	?	?	?
?	?	?	?	?	?	?	?	0	?	?	?
?	0	0	0	0	0	0	0	0	0	0	0
0	1	?	1	0	0	0	?	0	1	?	?

Aigialosaurus bucchichi

0	-	0	?	?	1	?	1	2	?	0	0
?	?	0	-	3	-	0	0	0	0	?	1
1	0	0	0	-	1	0	?	?	?	-	1
0	0	0	0	1	?	0	0	?	0	0	1
0	0	0	0	1	0	0	3	1	-	0	?
0	0	?	0	0	1	1	0	?	?	0	0
0	0	0	-	1	?	?	?	0	?	0	0
?	?	?	?	1	0	?	?	0	0	0	0
?	0	1	0	0	0	0	0	0	0	-	?
?	?	0	0	0	0	0	0	0	0	0	?
?	?	?	1	?	?	0	0	0	?	?	?

Komensaurus carrolli

?	?	?	?	?	?	?	?	?	?	?	?
?	?	?	?	?	?	?	?	?	?	?	?
?	?	?	?	?	?	?	?	?	?	?	?
?	?	?	?	2	0	?	0	?	0	0	0
?	0	?	?	?	?	?	?	?	?	?	?
?	?	?	?	?	0	0	0	0	?	?	?
?	?	?	?	?	?	1	?	?	?	0	?
0	1	?	?	0	0	?	0	?	0	0	?
?	?	?	?	?	?	?	?	?	?	?	?
?	?	0	0	0	0	?	0	0	0	?	0
0	1	1	?	0	0	0	?	0	?	?	?

Halisaurus platyspondylus

1	0	1	0	0	0	0	0	2	1	1	0
0	0	0	0	3	?	1	0	1	0	1	?
0	?	0	0	?	?	?	?	1	1	-	?
?	?	1	?	2	0	0	1	0	0	0	0
?	0	0	0	1	?	?	?	?	?	?	1
0	1	?	0	0	0	1	0	0	0	1	0
0	0	1	0	?	?	0	?	?	?	?	?
0	0	?	?	?	?	?	?	?	?	1	?
?	?	?	?	?	?	?	?	?	?	?	?
?	?	?	?	?	?	?	?	?	?	?	?
1	?	?	?	?	?	0	0	0	?	?	?

Eonatator sternbergi

0	-	1	0	0	?	0	0	2	1	0	0
0	0	0	0	3	?	0	0	1	0	1	0
0	0	0	0	?	?	?	0	2	1	-	?
?	?	0	0	2	0	?	1	?	0	0	0
?	0	?	0	1	?	0	?	1	?	1	1
0	1	?	0	?	0	1	0	0	0	1	0
?	0	1	0	?	1	0	?	?	0	0	1
0	0	?	?	0	0	1	1	1	0	1	0
1	1	1	1	1	1	0	0	1	0	0	1
0	0	0	0	1	0	1	1	1	0	0	1
1	1	1	?	0	1	0	?	0	?	?	?

Dallasaurus turneri

?	?	?	?	?	?	?	0	?	?	0	?
?	?	1	?	?	0	?	?	?	?	?	?
?	?	?	?	?	?	?	?	?	?	?	?
?	?	0	?	?	?	?	?	?	?	?	?
?	?	?	?	?	?	?	?	0	0	0	1
0	?	?	0	?	1	?	?	?	?	1	0
0	0	2	?	?	1	1	?	?	0	0	1
1	1	1	1	0	?	?	?	?	?	1	?
?	?	0	-	0	?	?	?	0	1	0	0
0	0	0	0	?	?	?	?	?	?	?	?
0	?	?	?	0	?	1	?	?	?	?	?

Clidastes liodontus

1	1	1	0	0	0	?	0	2	0	0	1
0	?	1	0	1	0	1	0	0	1	1	1
1	?	1	0	-	1	0	2	1	0	0	2
?	?	1	0	1	0	?	0	0	0	0	0
0	0	0	1	0	1	0	2	0	0	2	1
?	1	0	0	0	1	0	0	0	?	1	0
1	0	2	0	0	1	1	0	0	0	0	0
1	1	0	1	0	1	?	1	1	1	1	0
1	0	1	1	0	0	0	0	2	1	0	1
0	1	1	1	2	1	0	0	0	1	0	1
0	0	0	1	2	1	1	?	0	?	?	?

Clidastes moorevillensis

1	1	1	0	0	0	0	0	2	0	0	1
0	0	1	0	1	0	1	0	0	1	1	1
1	?	1	0	-	1	0	2	1	?	0	2
0	?	1	0	1	0	?	0	0	0	1	0
0	0	0	1	0	1	0	2	0	0	2	1

0	1	0	0	0	1	0	0	0	0	1	0
1	0	2	0	0	1	1	0	0	0	0	0
1	1	?	1	0	1	?	1	1	1	1	?
?	0	1	1	0	0	0	0	2	1	0	1
0	1	1	1	2	1	0	0	0	1	0	1
0	0	0	1	2	1	1	?	?	?	?	?

Clidastes propython

1	1	1	0	0	0	?	1	2	0	0	1
0	0	1	0	1	0	1	0	0	1	1	1
?	?	1	0	-	1	0	2	1	?	0	?
?	?	1	0	1	0	?	0	0	0	1	0
0	0	0	1	0	1	0	1	0	0	2	1
0	1	?	1	0	1	0	0	0	0	1	0
1	0	2	0	0	1	1	0	0	0	0	0
1	1	?	1	0	?	?	?	1	?	1	?
?	?	?	?	?	0	0	0	2	1	0	1
0	1	1	1	2	1	0	?	0	?	?	?
?	?	?	?	2	?	1	0	0	0	?	0

Prognathodon overtoni

1	0	1	0	0	0	?	1	0	0	1	1
0	0	1	0	1	1	1	0	0	1	?	1
1	1	1	1	0	1	0	3	0	0	1	2
0	0	1	1	1	0	1	1	0	1	1	0
?	0	0	1	0	1	2	3	0	0	2	1
0	1	0	1	1	1	0	0	1	0	1	1
0	1	2	1	?	?	1	?	0	?	0	?
1	1	0	1	1	1	-	?	1	1	1	1
1	0	1	1	1	0	0	1	2	1	2	1
0	1	1	1	2	1	0	1	?	1	0	1
0	0	0	0	2	1	1	?	0	?	1	1

Prognathodon solvayi

0	-	0	0	0	0	0	1	0	0	0	1
0	0	1	0	1	0	1	0	1	1	1	1
1	1	1	0	-	0	0	3	0	?	1	1
0	?	01	1	1	?	0	1	0	1	0	0
0	0	0	01	1	1	2	4	1	-	2	1
0	1	0	0	0	0	?	0	0	0	1	0
1	1	2	1	0	1	1	0	0	0	1	0
1	1	?	1	?	?	?	?	?	?	?	?
?	0	1	?	0	1	1	?	?	?	?	?
?	?	?	?	?	?	?	?	?	?	?	?
?	?	?	?	?	?	?	?	0	1	1	1

Prognathodon giganteus

0 - 0 ? ? ? ? ? ? ? ? ?
? ? ? ? ? ? ? ? ? ? ? ?
? ? ? ? ? ? ? ? ? ? ? ?
? ? 0 1 ? ? ? ? ? ? ? ?
? ? ? ? ? ? ? ? 1 - 2 1
? ? ? ? ? 0 ? ? 0 ? 1 0
1 ? 2 1 ? ? 1 ? ? 0 1 0
1 1 ? 1 ? ? ? ? ? ? 1 ?
? ? ? ? ? ? ? ? ? ? ? ?
? ? ? ? ? ? ? ? ? ? ? ?
? ? ? ? ? ? ? ? ? 1 ? ?

Prognathodon currii

1 0 0 0 ? ? ? ? 0 1 1 1
? ? ? ? ? ? 1 0 ? ? ? 1
1 ? 1 1 0 0 0 3 0 ? 1 2
0 ? ? 1 ? ? ? ? ? ? ? 0
? ? ? ? 1 ? ? 5 0 0 ? ?
? ? ? ? ? ? 0 0 1 ? ? 1
0 ? 2 0 ? ? ? ? ? ? ? ?
? ? ? ? ? ? ? ? ? ? ? ?
? ? ? ? ? ? ? ? ? ? ? ?
? ? ? ? ? ? ? ? ? ? ? ?
? ? ? ? ? ? ? ? ? 1 ? ?

Prognathodon waiparaensis

1 0 1 0 0 0 0 ? ? ? ? ?
? ? ? ? ? ? ? ? ? ? ? ?
? ? ? ? ? ? ? ? ? ? ? 2
1 ? 1 1 1 ? ? 1 0 2 1 0
? 0 0 1 0 ? ? 3 ? ? ? 1
0 1 ? ? ? ? ? ? ? ? 0 0
? 1 2 1 ? ? ? ? ? ? ? ?
? ? ? ? ? ? ? ? ? ? ? ?
? ? ? ? ? ? ? ? ? ? ? ?
? ? ? ? ? ? ? ? ? ? ? ?
? ? ? ? ? ? ? 0 ? ? ? ?

Prognathodon saturator

? ? ? 0 0 ? ? 1 0 1 1 1
1 0 1 0 1 1 1 0 1 1 1 ?
? ? 1 1 0 0 0 ? ? ? 0 2
0 0 1 ? 1 ? 0 1 0 2 1 0
0 0 0 1 0 1 0 ? ? ? 2 1

0 1 0 1 ? 1 1 0 1 0 1 1
0 0 2 1 0 ? 1 0 ? 0 1 0
1 1 1 1 0 ? ? ? ? 0 1 ?
? 0 1 1 0 0 0 1 ? ? ? ?
? ? ? ? 2 ? ? ? ? ? ? ?
? ? ? ? ? ? ? ? 0 0 ? ?

Globidens alabamaensis

? ? ? ? ? ? ? 1 0 ? 1 1
1 0 1 0 1 ? ? ? ? ? ? ?
? ? 1 0 ? 1 0 ? 1 ? ? ?
? ? 1 0 1 0 ? 1 1 1 ? 0
? ? 0 1 0 ? ? ? ? ? ? 1
0 1 0 ? 1 1 0 0 0 0 1 1
0 1 1 0 0 1 1 ? ? 0 ? 0
1 1 ? ? 0 ? ? ? ? ? ? ?
? ? ? ? ? 0 ? ? 2 1 0 1
0 1 1 1 ? ? ? ? ? ? ? ?
? ? ? ? 2 ? 1 ? ? 1 1 1

Globidens dakotensis

1 1 1 0 ? 0 ? 1 0 1 1 1
? ? 1 0 1 0 1 0 0 1 ? 1
1 ? 1 1 ? 1 0 3 1 0 0 2
0 ? 1 0 1 0 ? 1 0 1 1 0
? 0 ? 1 0 1 0 ? ? ? ? ?
? ? ? ? ? ? ? ? ? ? 1 1
0 1 1 0 0 1 1 ? 0 0 ? 0
1 1 ? 1 0 ? ? ? ? ? ? ?
? ? ? ? ? ? ? ? ? ? ? ?
? ? ? ? ? ? ? ? ? ? ? ?
? ? ? ? ? ? 1 0 ? ? 1 1

Mosasaurus conodon

? ? ? ? ? ? ? ? ? ? ? ?
? ? ? ? ? ? ? ? ? ? ? ?
? ? ? ? ? ? ? ? ? ? ? ?
? ? ? ? ? ? ? ? ? ? ? ?
? ? ? ? ? ? ? 1 ? ? 2 1
0 1 ? ? ? ? 0 0 0 0 1 0
1 0 2 1 0 1 1 1 0 0 1 0
1 1 0 1 1 ? ? ? ? ? 1 ?
? ? 1 ? 0 0 1 0 3 1 1 1
0 1 1 1 ? 1 ? ? ? ? ? ?
? ? ? ? 2 ? 1 ? 0 0 ? ?

Mosasaurus hoffmannii

1	1	1	0	0	1	?	0	0	0	1	1
?	?	1	0	1	1	1	0	0	2	1	1
1	?	1	1	0	0	0	3	1	?	?	2
1	?	1	0	0	0	?	0	0	1	0	1
?	1	1	0	1	1	0	3	0	0	2	1
0	1	0	?	1	1	0	1	1	0	1	0
1	0	2	1	0	1	1	1	0	1	1	0
1	1	0	?	1	?	?	1	1	1	1	1
?	0	2	1	0	0	1	1	3	1	1	1
0	1	1	1	2	1	0	0	0	1	1	1
0	0	0	1	2	1	1	0	0	0	0	-

Mosasaurus missouriensis

1	1	1	0	0	1	?	1	0	0	1	1
?	?	1	0	1	1	1	0	0	1	?	1
1	?	1	1	0	0	0	3	0	0	1	?
?	?	1	0	0	0	?	0	0	1	0	0
?	1	?	0	1	1	?	3	0	0	2	?
0	1	0	1	1	1	0	1	1	0	1	0
1	0	2	?	0	1	1	?	0	0	0	0
1	1	0	1	1	1	?	1	?	?	1	1
?	0	1	?	?	0	0	?	?	?	?	?
?	?	?	?	2	1	0	0	?	1	1	?
?	?	?	?	2	?	1	?	0	0	1	0

Plesiotylosaurus crassidens

1	1	1	0	1	?	?	1	0	?	1	1
?	?	1	0	1	1	1	0	0	1	1	1
1	?	1	1	1	0	0	3	1	?	1	?
?	0	1	1	0	0	?	1	0	1	1	0
?	0	?	1	0	1	?	2	0	0	2	1
1	1	0	1	1	1	0	0	?	?	1	0
1	0	2	1	?	?	?	?	?	0	0	0
1	1	?	1	0	?	?	?	?	?	?	?
?	0	1	1	0	0	1	1	3	1	2	1
0	1	1	1	2	1	0	0	0	1	0	?
?	?	?	?	2	?	?	?	0	?	0	-

Plotosaurus bennisoni

1	0	1	0	0	1	?	1	0	1	0	1
?	?	1	0	1	1	1	0	1	1	?	1
1	1	1	1	0	0	0	1	1	0	0	2
0	0	1	0	0	0	?	0	0	1	0	0
0	1	1	0	1	1	?	1	0	1	?	1

?	1	?	?	?	1	0	1	1	0	0	0
0	1	2	?	0	1	0	?	1	0	?	0
1	1	?	?	1	1	?	?	?	1	?	1
?	0	2	1	0	0	1	1	3	1	1	1
0	1	1	1	2	1	0	0	0	1	1	?
?	1	?	?	2	1	1	?	0	0	1	0

Tylosaurus nepaeolicus

1	2	1	1	1	1	?	0	0	1	0	1
0	1	1	1	?	?	1	0	0	1	?	1
1	0	0	1	1	0	0	3	0	0	0	2
1	1	0	0	1	1	?	0	2	1	1	1
1	0	0	1	0	0	?	4	0	1	2	1
0	0	0	0	0	0	0	0	0	0	0	0
1	0	2	1	1	0	0	?	?	0	0	0
1	0	1	0	1	?	?	?	?	0	0	?
?	?	?	?	?	?	?	?	2	0	0	0
1	0	0	0	1	0	1	1	1	0	0	?
?	?	?	?	?	?	0	0	0	0	1	0

Tylosaurus bernardi

1	2	1	1	1	1	?	0	0	1	1	1
0	?	1	1	?	?	1	0	0	1	?	1
1	0	0	1	1	0	0	3	1	0	?	2
1	?	?	0	?	?	?	?	2	0	0	0
1	0	0	1	0	0	?	4	0	1	?	1
0	0	0	0	0	0	0	0	0	0	0	0
1	0	2	1	1	0	0	?	0	0	0	0
1	0	1	0	1	0	1	1	0	0	0	1
0	1	1	0	1	1	0	1	2	0	0	0
1	0	0	0	?	0	1	1	1	0	0	?
?	?	?	0	?	1	0	0	0	0	1	0

Taniwhasaurus oweni

1	2	1	1	1	1	?	0	0	?	2	1
?	?	1	1	?	?	?	?	0	1	?	?
?	?	0	1	1	0	0	3	?	0	?	2
1	?	?	0	1	1	?	0	2	0	0	0
?	0	0	1	0	?	?	3	0	1	?	?
?	0	0	?	0	?	?	?	?	?	0	1
1	?	2	?	1	0	0	?	?	?	?	0
1	0	1	0	?	?	?	?	?	0	0	?
?	1	?	?	?	?	?	?	?	?	?	?
?	?	?	?	?	?	?	?	?	?	?	?
?	?	?	?	?	?	0	?	0	?	1	0

Taniwhasaurus antarcticus

1	2	1	1	1	1	?	0	0	?	2	1
0	?	1	1	?	?	1	0	0	1	?	1
1	?	0	1	1	0	0	?	0	?	?	2
1	?	?	?	1	1	?	0	2	0	0	0
?	0	0	1	0	?	?	?	0	1	?	1
0	0	0	?	0	0	?	0	?	?	0	1
1	0	2	1	?	0	?	?	?	?	?	?
1	?	1	?	?	?	?	?	?	0	0	?
?	?	?	?	?	?	?	?	?	?	?	?
?	?	?	?	?	?	?	?	?	?	?	?
?	?	?	?	?	?	0	?	1	0	1	0

Tylosaurus proriger

1	2	1	1	1	1	1	0	0	1	1	1
0	?	1	1	?	?	1	0	0	1	?	1
1	0	0	1	1	0	0	3	1	0	0	2
1	0	0	0	1	1	?	0	2	0	0	0
1	0	0	1	0	0	0	4	0	1	2	1
0	0	0	0	0	0	0	0	0	0	0	0
1	0	2	1	1	0	0	?	0	0	0	0
1	0	1	0	1	0	1	1	0	0	0	1
0	1	1	0	1	1	0	1	2	0	0	0
1	0	0	0	1	0	1	1	1	0	0	1
0	?	0	0	1	1	0	0	0	?	1	0

Yaguarasaurus columbianus

0	-	1	0	?	0	?	0	2	0	0	0
?	?	?	0	2	0	1	2	0	0	?	1
1	0	0	0	?	0	?	3	0	0	1	1
1	1	?	?	2	1	0	0	2	0	0	1
1	0	0	0	0	0	1	3	0	0	1	?
?	?	?	?	?	?	?	?	?	?	0	0
?	0	1	0	?	?	1	?	?	?	?	?
?	?	?	?	?	?	?	?	?	?	?	?
?	?	?	?	?	?	?	?	?	?	?	?
?	?	?	?	?	?	?	?	?	?	?	?
?	?	?	?	?	?	0	?	0	?	1	0

Eremiasaurus heterodontus

1	0	1	0	0	1	?	1	0	1	1	1
?	?	1	0	1	?	1	0	?	1	?	1
1	?	1	1	?	0	1	3	0	0	0	2
0	?	1	1	1	?	?	1	?	?	0	?
?	1	?	1	1	1	?	2	0	0	2	1

0 1 0 ? ? 1 0 1 1 ? 1 0
0 1 2 1 0 1 ? ? 0 1 0 0
1 1 0 ? 0 ? ? 1 1 1 1 1
0 0 1 ? 0 1 ? ? ? 1 0 ?
? ? ? ? ? ? ? ? ? ? 0 1
? ? 0 1 ? ? 1 ? ? 0 1 0

Prognathodon kianda

1 0 1 0 0 1 ? ? 0 0 ? 1
? ? 1 ? 1 ? 1 0 ? 1 ? 1
1 ? ? 0 ? ? ? 3 0 ? ? 2
1 1 1 ? 1 0 ? 1 0 2 1 0
0 0 0 1 0 1 ? 2 0 0 2 1
? 1 0 0 0 1 0 0 0 0 1 0
0 1 2 0 ? ? ? ? ? ? ? ?
? ? ? ? ? ? ? ? ? ? ? ?
? ? ? ? ? ? ? ? ? ? ? ?
? ? ? ? ? ? ? ? ? ? ? ?
? ? ? ? ? ? ? 0 0 ? 1 1

Russellosaurus coheni

1 0 1 ? ? 0 0 0 2 0 0 0
1 1 1 0 2 0 1 2 0 0 0 1
1 0 0 0 - 0 1 2 0 ? 1 2
1 1 0 0 2 1 0 0 2 0 0 1
1 2 0 0 0 0 1 2 1 - 1 1
0 0 0 0 0 0 1 0 0 1 0 0
0 0 1 0 ? ? ? ? ? ? ? ?
? ? ? ? ? ? ? ? ? ? ? ?
? ? ? ? ? ? ? ? ? ? ? ?
? ? ? ? ? ? ? ? ? ? ? ?
? ? ? ? ? ? ? 1 0 ? 1 0

Romeosaurus fumanensis

? ? ? ? ? ? ? ? ? ? ? ?
? ? ? ? ? ? ? ? ? ? ? ?
? ? 1 0 - ? ? 2 0 ? ? 2
1 ? 1 0 2 1 0 0 2 0 1 1
? 2 0 1 1 ? ? 2 0 0 1 ?
? 0 0 0 0 0 1 0 0 ? 1 0
0 0 1 0 ? ? ? ? ? 0 1 1
0 1 ? ? 0 ? ? ? ? ? ? ?
? ? 0 - 1 1 ? ? 0 0 ? 0
0 ? 0 0 ? ? ? ? ? ? ? ?
? ? ? ? ? ? ? 1 0 1 0 -

Ectenosaurus clidastoides

1	1	1	0	0	0	1	0	2	0	0	1
1	1	1	0	2	0	1	1	1	0	0	0
1	?	0	0	-	0	1	1	1	0	1	1
1	0	0	0	1	0	0	1	2	1	0	1
1	1	0	?	?	0	2	3	0	0	2	0
0	0	1	0	0	0	0	0	0	1	0	0
0	0	2	0	0	0	1	0	0	1	0	0
1	?	?	?	0	?	?	?	?	?	?	?
?	0	1	0	1	1	0	0	2	1	?	?
?	0	0	1	2	0	1	0	1	0	0	?
?	?	?	?	1	1	1	0	0	0	1	1

Plioplatecarpus

?	?	?	?	?	?	?	0	0	1	1	1
0	0	1	0	0	-	1	1	1	2	0	1
1	?	0	1	-	0	0	?	0	?	?	1
1	0	0	0	2	1	1	0	0	2	0	0
?	0	1	1	1	0	2	5	1	-	2/3	1
1	0	1	0	0	0	0	0	0	1	0	0
0	0	2	0	?	?	0	?	?	0	0	0
1	1	0	0	0	0	?	?	?	?	0	?
?	0	1	0	1	1	0	0	2	0	?	1
1	0	0	1	2	0	1	1	1	0	0	?
?	?	?	?	1	?	0	0	0/1	?	?	?

Plesioplatecarpus planifrons

1	0	1	0	0	0	0	0	0	1	0	1
1	?	1	0	0	-	1	1	1	0	?	1
1	?	0	0	?	?	1	3	0	0	0	?
1	0	0	0	2	1	0	0	1	0	0	0
?	0	0	1	1	0	1	5	0	0	2	1
0	0	1	0	0	0	0	0	0	1	0	0
0	0	2	0	1	0	1	0	0	0	0	0
1	1	?	?	0	?	?	?	?	?	?	?
?	0	1	0	1	1	0	0	2	0	?	1
1	0	0	?	2	0	1	1	1	0	0	?
?	?	?	?	1	?	0	0	0	?	1	1

Platecarpus tympaniticus

0	-	1	0	0	0	0	0	0	1	1	1
1	1	1	0	0	-	1	1	1	1	0	1
1	?	0	1	0	0	1	3	0	0	0	1
1	?	0	0	2	1	1	0	1	1	0	0
1	0	1	1	1	0	2	5	1	-	2	1

1 0 1 0 0 0 0 0 0 1 0 0
0 0 2 0 1 0 0 1 0 0 0 0
1 1 0 0 0 0 0 1 0 0 0 1
0 0 1 0 1 1 0 0 2 0 ? ?
1 ? 0 1 2 0 1 1 1 0 0 1
0 1 1 0 1 1 0 0 0 1 1 1

Latoplatecarpus willistoni

0 - 1 0 0 0 ? 0 0 1 2 0
1 1 1 ? 0 - 1 1 1 2 0 ?
1 ? 0 1 - 0 1 3 0 0 0 2
1 ? 0 0 2 1 0 0 1 2 0 0
1 0 1 1 1 0 2 5 1 - 2 1
1 0 1 0 0 0 0 0 0 1 0 0
0 0 2 0 1 1 1 0 0 0 1 0
1 1 ? ? 0 ? ? ? ? ? 0 ?
? ? 2 1 1 1 ? ? ? ? ? ?
? ? ? ? ? ? ? ? ? ? ? ?
? ? ? ? ? ? ? 0 0 1 1 1

Selmasaurus johnsoni

1 0 1 0 0 0 ? 1 0 0 0 1
1 1 1 0 2 0 1 2 0 0 0 1
1 ? 0 1 - 0 1 ? 0 ? ? 2
1 ? 0 0 1 1 0 1 1 1 0 0
? 0 0 0 1 0 1 5 1 - 2 1
1 1 1 0 0 0 0 0 0 1 0 0
0 0 2 0 1 0 1 0 0 0 0 0
1 1 0 0 0 ? ? ? ? ? ? ?
? ? ? ? ? ? ? ? ? ? ? ?
? ? ? ? ? ? ? ? ? ? ? ?
? ? ? ? ? ? ? ? 1 ? 1 0

Angolasaurus bocagei

1 0 1 ? ? 0 ? 0 1 ? 1 1
? ? ? 0 ? ? 1 1 0 0 ? 1
? ? 0 0 ? 0 ? 3 0 ? ? ?
? 1 ? ? 2 1 0 0 0 1 0 0
1 0 0 0 1 0 1 5 1 - 2 1
? 0 1 0 0 0 1 0 0 1 ? 0
0 0 2 ? ? ? 1 ? ? ? ? ?
? ? ? ? ? ? ? ? ? ? ? ?
? ? ? ? ? ? ? ? ? ? ? ?
? ? ? ? ? ? ? ? ? ? ? ?
? ? ? ? ? ? 0 ? 0 ? ? ?

0 - 0 0 ? 0 ? 0 2 1 1 0
? ? 1 0 2 0 1 2 0 0 ? 1
1 0 0 0 - 0 ? 0 0 ? ? 2
1 ? ? 0 0 1 0 0 2 0 0 0
1 ? 2 0 0 0 1 1 1 - ? 1
0 0 1 0 0 0 1 0 0 0 0 0
0 0 0 - ? ? 1 0 ? 1 1 1
0 0 0 ? ? ? ? ? ? ? 0 ?
? 1 1 1 0 ? 0 0 ? ? ? ?
? 0 0 0 ? ? ? ? ? ? ? 0
0 0 ? ? ? ? ? 0 0 ? ? ?

Pannoniasaurus osii

0 - 0 0 ? 0 ? ? ? ? ? ?
? ? ? ? ? ? ? ? ? ? ? ?
? ? ? ? ? 0 ? ? ? ? ? ?
? ? ? ? 0 1 0 0 2 0 0 0
? ? 2 0 0 ? ? 0 1 - 2 0
0 1 0 ? 0 0 ? ? 0 0 0 0
0 0 2 0 ? ? 1 0 ? 1 1 1
0 0 0 0 ? ? ? 0 ? ? 0 ?
? ? ? ? 0 1 ? ? ? 0 ? ?
? 0 0 0 ? ? ? ? ? ? ? 0
0 ? ? ? ? ? ? ? 0 1 1 0

Selmasaurus russelli

? ? ? ? ? ? ? 1 0 0 0 1
0 1 ? ? 0 - 1 2 1 0 1 0
? ? ? ? ? 0 1 ? ? ? ? 2
1 ? ? ? 2 1 1 1 1 0 0 ?
1 0 0 0 1 0 2 ? ? ? ? ?
? ? ? ? ? ? ? ? ? ? ? ?
? ? ? ? 1 0 ? ? ? ? ? ?
? ? ? ? ? ? ? ? ? ? ? ?
? ? ? ? ? ? ? ? ? ? ? ?
? ? ? ? ? ? ? ? ? ? ? ?
? ? ? ? ? ? ? ? 1 ? ? ?

Goronyosaurus nigeriensis

0 - 1 0 0 0 ? 1 0 ? 1 1
1 ? ? ? ? ? 1 ? 1 0 ? ?
? ? ? ? ? ? ? ? ? ? ? ?
? ? 0 0 ? ? ? ? ? ? ? ?
? ? ? ? ? ? ? 5 1 - 2 1
? ? ? ? ? ? ? ? ? ? ? ?
? 0 2 ? ? ? ? ? ? ? ? ?

? ? ? ? ? ? ? ? ? ? ? ?
? ? ? ? ? ? ? ? ? ? ? ?
? ? ? ? ? ? ? ? ? ? ? ?
? ? ? ? ? ? ? 0 ? ? ? ?

Gavialimimus almaghribensis

0 - 1 0 ? 0 ? 1 0 0 0 1
? 1 ? ? 3 - 1 2 1 1 1 1
? ? 0 1 0 1 0 3 1 1 - ?
? ? 0 0 ? 1 ? ? 1 ? 0 ?
? ? ? ? ? ? ? 5 1 - 3 ?
? ? ? ? ? ? 1 1 ? ? 1 0
0 0 2 0 ? ? 0 ? ? 1 ? 0
? ? ? ? ? ? ? ? ? ? ? ?
? ? ? ? ? ? ? ? 2 ? ? ?
? ? 1 1 ? ? ? ? ? ? ? ?
? ? ? ? ? ? ? 0 ? 0 ? ?